GEOMAR REPORT

GEOMAR
Helmholtz-Zentrum für Ozeanforschung Kiel

RV MARIA S. MERIAN Fahrtbericht / Cruise Report MSM63

PERMO

Southampton – Southampton (U.K.)
29.04.-25.05.2017

Berichte aus dem GEOMAR
Helmholtz-Zentrum für Ozeanforschung Kiel

Nr. 37 (N. Ser.)

August 2017

GEOMAR

Helmholtz-Zentrum für Ozeanforschung Kiel

RV MARIA S. MERIAN Fahrtbericht / Cruise Report MSM63

PERMO

Southampton – Southampton (U.K.)
29.04.-25.05.2017

Berichte aus dem GEOMAR
Helmholtz-Zentrum für Ozeanforschung Kiel

Nr. 37 (N. Ser.)

August 2017

GEOMAR
Helmholtz-Zentrum für Ozeanforschung Kiel

Das GEOMAR Helmholtz-Zentrum für Ozeanforschung Kiel ist Mitglied der Helmholtz-Gemeinschaft Deutscher Forschungszentren e.V.

The GEOMAR Helmholtz Centre for Ocean Research Kiel is a member of the Helmholtz Association of German Research Centres

Herausgeber / Editors:
Christian Berndt and Judith Elger with contributions from cruise participants C. Böttner, R.Gehrmann, J. Karstens, S. Muff, B. Pitcairn, B. Schramm, A. Lichtschlag, A.-M. Völsch

GEOMAR Report
ISSN Nr.. 2193-8113, DOI 10.3289/GEOMAR_REP_NS_37_2017

Helmholtz-Zentrum für Ozeanforschung Kiel / Helmholtz Centre for Ocean Research Kiel
GEOMAR
Dienstgebäude Westufer / West Shore Building
Düsternbrooker Weg 20
D-24105 Kiel
Germany

Helmholtz-Zentrum für Ozeanforschung Kiel / Helmholtz Centre for Ocean Research Kiel
GEOMAR
Dienstgebäude Ostufer / East Shore Building
Wischhofstr. 1-3
D-24148 Kiel
Germany

Tel.: +49 431 600-0
Fax: +49 431 600-2805
www.geomar.de

Prof. Dr. Christian Berndt
GEOMAR Helmholtz Centre for Ocean Research Kiel
Wischhofstr. 1-3, 24148 Kiel
Germany

Ph.: +49 431 6002273
Fax: +49 431 6002922
cberndt@geomar.de

MSM63 PERMO

Cruise Report

Southampton – Southampton
29 April 2017 – 25 May 2017

Chief Scientist Leg 1: Prof. Dr. Christian Berndt
Chief Scientist Leg 2: Dr. Judith Elger
Master: Björn Maaß

With contributions by Christoph Böttner, Romina Gehrmann, Jens Karstens, Sina Muff, Ben Pitcairn, Bettina Schramm, Anna Lichtschlag, Ann-Marie Völsch

May 2017

Table of content

1 Cruise Summary

(C. Berndt)

1.1 German

Die hydraulische Permeabilität von Sedimentbecken variiert über mehrere Größenordnungen und auf verschiedenen Skalen. Da sie schwer zu messen und daher weitgehend unbekannt ist, ergeben sich daraus ernsthafte Probleme bei der numerischen Modellierung von Fluidzirkulation in Sedimentbecken. Während des FP7-ECO2-Projektes konnten wir zeigen, dass fokussierte Fluidwege, sogenannte „Pipe“-Strukturen, erhebliche Auswirkungen auf die Fluidzirkulation haben können und dass es notwendig ist, die hydraulische Permeabilität und die zeitliche Veränderlichkeit dieser Strukturen zu bestimmen.

Innerhalb des Arbeitspakets 3 des Horizon 2020-Projektes STEMM-CCS versuchen wir nun, die Permeabilität von „Pipe“-Strukturen in einem komplexen Experiment zu bestimmen. Dieses beinhaltet Feldstudien an geologischen Aufschlüssen an Land, marine geophysikalische Datenerfassung und wissenschaftliche Bohrungen sowie neuartige numerische Modellierungsansätze. Die Expedition MSM 63 PERMO zielte darauf ab, die notwendigen geophysikalischen Daten sowie Sedimentkerne und Bohrlochdaten für die Modellierung bereitzustellen um folgende Hypothesen zu untersuchen: 1) Seismische „Pipe“-Strukturen haben eine deutlich höhere hydraulische Permeabilität gegenüber dem umgebenden Gestein, was zu einer Fokussierung der Fluidzirkulation führt. 2) Seismische „Pipe“-Strukturen bleiben für eine lange geologische Zeit nach ihrer Bildung offene Wegsamkeiten; Und 3) Seismische „Pipe“-Strukturen zeichnen sich durch kontinuierliche Fluidmigration aus.

Aufgrund der komplexen Logistik und des limitierten Stellplatzes an Deck, konnte das geophysikalische Equipment nicht zeitgleich mit dem Meeresbodenbohrgerät RockDrill2 an Bord der Maria S. Merian gebracht werden und die Expedition musste daher in zwei Fahrtabschnitte aufgeteilt werden. Der erste Fahrtabschnitt begann in Southampton am 29.04.2017 und endete in Aberdeen am 12.05.2017. Der zweite Fahrtabschnitt begann in Aberdeen am 18.05.2017 und endete in Southampton am 25.05.2017. Zu Beginn des ersten Abschnitts haben wir zwei potenzielle Ziele untersucht, um zu entscheiden, welches besser als Arbeitsgebiet geeignet sein würde. Nachdem wir uns gegen das Gebiet im norwegischen Sektor der Nordsee in der Nähe des Sleipner-Öl- und Gasfeldes entschieden hatten, konzentrierten wir uns auf die Scanner-Pockmark im U.K.-Sektor weiter westlich. Dort sammelten wir einen umfassenden geophysikalischen Datensatz bestehend aus Multibeam-, Parasound-, 2D-Seismik-, OBS- (Ozeanbodenseismometer) und Elektromagnetik-Daten (engl. Controlled Source Electromagnetic - CSEM). Leider konnten die geplanten hochauflösenden 3D-Seismikdaten nach ein paar Tagen schlechten Wetters wegen Zeitmangel nicht aufgenommen werden.

Der zweite Fahrtabschnitt widmete sich der Vermessung des zweiten Arbeitsgebiets des STMM-CSS-Projekts bei dem Goldeneye Feld. In Vorbereitung auf eine im Oktober stattfindende FS Alkor-Ausfahrt führten wir einen hochaufgelösten bathymetrischen Survey in Form eines engmaschigen Gitters durch und zeichneten zusätzlich eine hohe Zahl an Parasound-

Profilen auf, um ein geeignetes Ziel für das geplante CO_2-Austritt-Experiment zu bestimmen. Darüber hinaus wurden zahlreiche Wasserproben während der CTD Einsätze gesammelt, um den Ursprung des aus dem Meeresboden sickernden Gases zu bestimmen. Die geplanten Bohrungen mussten wegen schiffsseitiger Probleme verschoben werden. Wir beabsichtigen, die Bohrungen im Herbst 2018 nachzuholen.

Vorläufige Ergebnisse zeigen einen tief sitzenden Fluid-Migrationsweg unterhalb des Scanner-Pockmarks, der seinen Ursprung mindestens 300 m unter dem Meeresboden hat. Während der Expedition beobachteten wir einen kontinuierlichen Blasenstrom („flare“) in der Wassersäule, was darauf hindeutet, dass die Wegsamkeit zumindest auf dieser Zeitskala dauerhaft geöffnet ist. Die bathymetrischen und Parasound-Daten zeigen, dass es mindestens fünf Phasen der Pockmark Bildung gibt. Vier davon sind mit der glaziomarinen / glaziolakustrinen Witchground Formation verbunden, während nur die größten Pockmarks wie der Scanner Pockmark mit dem tiefen Untergrund verbunden sind. Die Auswertung der Ozeanbodenseismometer- und der elektromagnetischen Daten sind noch nicht abgeschlossen.

1.2 English

Hydraulic permeability in sedimentary basins varies by several orders of magnitude. As it is difficult to determine and therefore largely unknown this poses serious problems for the simulation of fluid migration in sedimentary basins. During the FP7 ECO2 project we could show that a focused fluid pathways known as pipe structures can have significant impact on fluid migration and that it is necessary to constrain their hydraulic permeability and how it varies over time.

Within work package 3 of the Horizon 2020 project STEMM-CCS we are attempting to determine the permeability of pipe structures in a complex approach reaching from onshore field studies through marine geophysical data acquisition and scientific drilling to numerical modeling. The cruise MSM 63 PERMO was aimed at providing the necessary geophysical data as well as sediment cores and downhole logging data. The objective was to provide data that helps testing the following hypotheses: 1) Seismic pipe structures have significantly higher hydraulic permeability compared to the surrounding country rock leading to focused fluid migration; 2) Seismic pipe structures remain open pathways for a long geological time after their formation; and 3) Seismic pipe structures are characterized by continuous fluid migration.

Because of the complex logistical requirements, i.e. not all the geophysical and drilling equipment could fit on Maria S. Merian at the same time, the cruise was split into two legs. The first leg commenced in Southampton on 29.04.2017 and ended in Aberdeen on 13.05.2017. The second leg started delayed in Aberdeen on 18.05.2017 and ended in Southampton on 25.05.2017. In the beginning of the first leg we investigated two potential targets to decide which one is most suitable as a study area. After having discarded a site in the Norwegian sector of the North Sea close to the Sleipner oil and gas field, we focused on the Scanner pockmark in the U.K. sector further west. There we collected a comprehensive geophysical data set consisting of multi-beam

bathymetry data, Parasound sub-bottom profiler data, 2D seismic data, ocean bottom seismometer data, and controlled source electromagnetic (CSEM) data. Unfortunately, the planned high-resolution 3D seismic data could not be collected because of a lack of time after a couple of days were lost due to bad weather.

The second leg was dedicated to surveying the second study site of the STMM-CSS project at the Goldeneye License. In preparation for an Alkor cruise upcoming in October we collected a bathymetric grid and many Parasound sub-bottom profiler lines in order to determine a suitable target for the planned CO2 release experiment. We also collected numerous water samples during CTD casts to determine the origin of gas seeping from the sea floor. The planned drilling operation had to be canceled because of technical problems with the vessel. We intend to conduct them in fall 2018 instead.

Preliminary results show a deep seated fluid migration pathway below the Scanner pockmark that rises from at least 300 m below the sea floor. During the cruise we observed continuously a gas flare in the water column suggesting that the pathway is continuously open. The multibeam bathymetry and Parasound data show that there are at least five episodes of pockmark formation. Four of these are associated with the glaciomarine or glaciolacustrine Witchground Formation whereas only the biggest pockmarks such as Scanner Pockmark can be linked to the deep subsurface. Evaluation of ocean bottom seismometer data and controlled source electromagnetic data is still ongoing.

2 Paticipants

(J. Karstens, A. Völsch)

2.1 Principal Investigators

Prof. Dr. Christian Berndt, GEOMAR
Dr. Judith Elger, GEOMAR

2.2 Scientific Party

Leg 1

1.	Prof. Dr. Christian Berndt	Chief scientist	GEOMAR
2.	Dr. Jens Karstens	Marine Geology	GEOMAR
3.	Dr. Benedict Reinardy	Marine Geology	U Stockholm
4.	Sina Muff	P-Cable	GEOMAR
5.	Bettina Schramm	OBS	GEOMAR
6.	Christoph Böttner	Hydroacoustics	GEOMAR
7.	Dr. Romina Gehrmann	CSEM	Soton
8.	Dr. Gaye Bayrakci	CSEM	Soton
9.	Gero Wetzel	P-Cable engineer	GEOMAR
10.	Florian Beeck	Airgun engineer	GEOMAR

11. Ben Pitcairn	OBEM engineer	OBIC
12. Martin Weeks	OBEM engineer	OBIC
13. Dean Wilson	OBEM engineer	OBIC
14. Laurence North	CSEM engineer	Soton
15. Tan Yee Yuan	CSEM engineer	Soton
16. Nils-Peter Finger	Watch keeper	GEOMAR
17. Michel Kühn	Watch keeper	GEOMAR
18. Bhargav Boddupalli	Watch keeper	Soton
19. Vanessa Monteleone	Watch keeper	Soton
20. Gesa Franz	Watch keeper	GEOMAR
21. Naima Karolina Yilo	Watch keeper	Soton

Leg 2

1. Dr. Judith Elger	Chief scientist	GEOMAR
2. Bettina Schramm	Marine Geology	GEOMAR
3. Christoph Böttner	Hydroacoustics	GEOMAR
4. Dr. Anna Lichtschlag	Marine Geochemistry	Soton
5. Kate Peel	Marine Geochemistry	Soton
6. Dr. Anita Flohr	Marine Geochemistry	Soton
7. Adeline Dutrieux	Marine Geochemistry	Soton
8. Ismael Falcon-Suarez	Rock Physics	Soton
9. Nils-Peter Finger	Watch keeper	GEOMAR
10. Gesa Franz	Watch keeper	GEOMAR
11. Ilena Flügge	Watch keeper	GEOMAR
12. Florian Gausepohl	Watch keeper	GEOMAR
13. Anne Völsch	Administration	GEOMAR
14. Apostolos Tsiligiannis	RockDrill2	BGS
15. Garry George McGowan	RockDrill2	BGS
16. Joseph Leo Hothersall	RockDrill2	BGS
17. Connor Richardson	RockDrill2	BGS
18. Rodrigue Akkari	RockDrill2	BGS
19. Michael Wilson	RockDrill2	BGS
20. David Baxter	RockDrill2	BGS
21. Dr. Sally Morgan	Logging	U Leicester

3.3 Affiliations

GEOMAR	GEOMAR Helmholtz Centre for Ocean Research Kiel Marine Geodynamics, Wischhofstr. 1-3, 24148 Kiel, Germany
Soton	University of Southampton, European Way, SO14 3ZH, Southampton, U.K.
BGS	British Geological Survey, The Sir George Bruce Building,

	Research Avenue South, Edinburgh, EH14 4AP, U.K.
OBIC	Ocean-Bottom Instrumentation Consortium, Department of Earth Sciences, Durham University, Science Labs, Durham DH1 3LE, U.K.
U Stockholm	Stockholms Universitet, Institutionen för Naturgeografi, Stockholm, Sweden
U Leicester	University of Leicester, Department of Geology, University Road, Leicester, LE1 7RH, U.K.

3.4 Crew

Leg 1

1. Björn Maaß	Master
2. Eberhard Stegmaier	Chief Officer
3. Ralf Peters	1st Officer
4. Sören Janssen	2nd Officer
5. Benjamin Rogers	Chief
6. Manfred Boy	2nd Engineer
7. Frank Baumann	Electrician
8. Emmerich Reize	System Operator
9. Jens Herrmann	Electronics
10. Enno Vredenborg	Bosun
11. Detlef Altmann	Ships Mechanik
12. Holger Grunert	Ships Mechanik
13. Andre Werner	Ships Mechanik
14. Detlef Etzdorf	Ships Mechanik
15. Peter Peschkes	Ships Mechanik
16. Jens Peschel	Ships Mechanik
17. Joerg Preuss	2nd Cook
18. Martina Tober	Stewardess
19. Johann Ennenger	1st Cook
20. Philipp Schwieger	3rd Engineer
21. Jürgen Sauer	Motormann
22. Helmut Friesenborg	Fitter
23. Karsten Peters	Ship's Mechanik

Leg 2

24. Björn Maaß	Master
25. Eberhard Stegmaier	Chief Officer
26. Ralf Peters	1st Officer
27. Sören Janssen	2nd Officer
28. Benjamin Rogers	Chief

29. Manfred Boy	2nd Engineer
30. Frank Baumann	Electrician
31. Emmerich Reize	System Operator
32. Joerg Walter	Electronics
33. Enno Vredenborg	Bosun
34. Detlef Altmann	Ships Mechanik
35. Holger Grunert	Ships Mechanik
36. Andre Werner	Ships Mechanik
37. Detlef Etzdorf	Ships Mechanik
38. Peter Peschkes	Ships Mechanik
39. Jens Peschel	Ships Mechanik
40. Joerg Preuss	2nd Cook
41. Martina Tober	Stewardess
42. Sebastian Matter	1st Cook
43. Philipp Schwieger	3rd Engineer
44. Jürgen Sauer	Motormann
45. Helmut Friesenborg	Fitter
46. Karsten Peters	Ship's Mechanik

3 Research Programm

(C. Berndt, J. Karstens)

3.1 Motivation

Young marine sediments may have porosities in excess of 90%. During burial sediments in marine sedimentary basins compact and porosity reduces to less than 10% in several kilometres depth releasing enormous amounts of pore fluid. The transport of fluids through marine sediments is primarily governed by pressure and permeability contrasts. The past three decades have completely overturned the way in which we think about this fluid migration. While in the past it was assumed that fluid migration is diffusive by migration through permeable beds, which can be described by Darcy's law, three-dimensional (3D) seismic data have revealed an enormous range of anomalies that can be related to focused fluid migration. This focusing occurs whenever the escape of fluids from the sediments cannot keep up with the forces driving the fluids out of the sediments, e.g. rapid loading, hydrothermal activity, or diagenetic processes and is primarily directed up to the surface of the basin. The formation of pathways is generally believed to be controlled by overpressure-induced hydro fracturing of an impermeable cap rock and fluid migration, but it is not known how long after formation they remain open and how permeable they are compared to the generally low permeability of the host sediments. By altering the integrity of sealing cap rocks and transferring pressure in the marine sedimentary overburden, vertical fluid conduits imply inter-stratigraphic hydraulic connectivity and significantly affect the migration of fluids and gases in the subsurface [Karstens & Bendt, 2015]. Emergence, architecture and mechanics of vertical fluid migration structures require a fundamental understanding as they might affect the transmission of fluids and gases from the sedimentary strata to the hydrosphere and finally to the atmosphere [Gurevich et al., 1993; Gasda

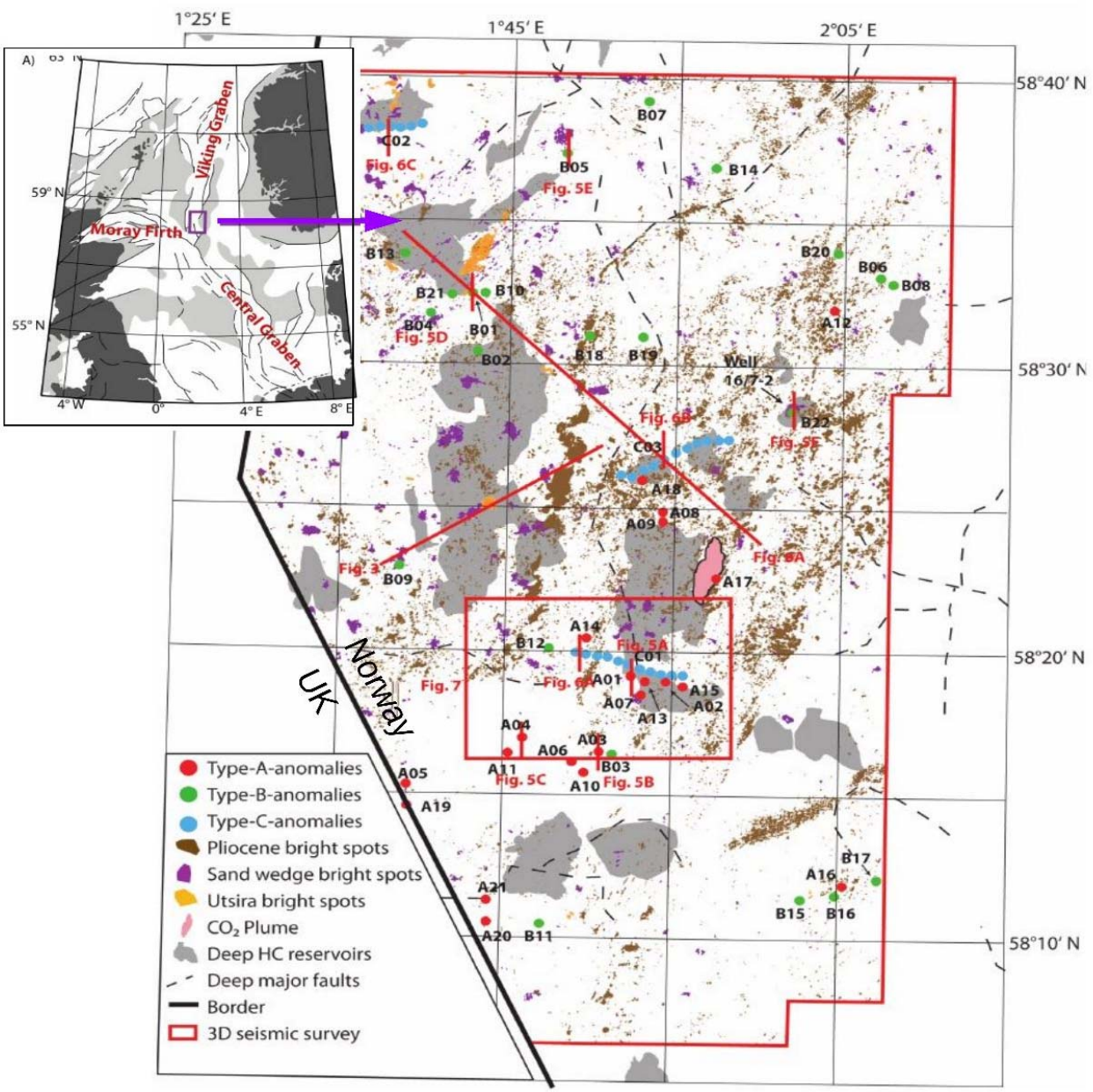

Figure 3.1.1: Map of the Sleipner area in the SVG showing the location of fluid flow manifestations and exploration type seismic profiles (red lines): bright spots beneath the top of the Utsira Formation (pale green), within the sand wedge (pale red), beneath the top Pliocene (pale blue), type-A-anomalies (red dots), type-B-anomalies (green dots), type-C-anomalies (red dots), CO2-plume (rose), deep hydrocarbon reservoirs (grey), deep faults (black lines) [Karstens, 2015]

et al., 2004]. Apart from direct geological implications, such as climate controls or slope stability, focused fluid migration affects severely safety and efficiency of exploration wellbore activities and sub-seabed CO_2 storage operations in marine sedimentary basins and thus needs to be understood in detail to minimize potential hazards.

Different studies and geophysical field programs on focused fluid flow structures have been conducted in the past and will be supplemented by the scientific objectives of this proposal. The 7th framework European Union funded research project "**ECO_2 – Sub-seabed CO_2 Storage: Impact on Marine Ecosystems**" successfully published it's summary report in April 2015 with

a new approach regarding the environmental risk assessment for sub-seabed storage sites of carbon capture and storage (CCS) projects. ECO_2 was triggered by the activities of several EU supported demonstration projects to store CO_2 at the emergence of fossil fuel power plants into either marine sub-seabed storage sites or onshore deep geological formations. Within the industrial countries CCS is regarded as a key technology to significantly reduce CO_2 emissions from new and existing industrial sources and mitigate the contribution of greenhouse gas emissions to global warming and ocean acidification. In particular the injection into oil-, gas- or water-bearing geological storage sites is regarded as a suitable option for carbon dioxide sequestration on a commercial scale [Rackley, 2010]. ECO_2 conducted a comprehensive offshore field programme at the Norwegian storage sites Sleipner and Snøvit and at several natural CO_2 seepage sites in order to identify potential pathways for CO_2 leakage through the overburden and to monitor and track their fluid flux in the seabed and water column. The key objectives addressed by ECO_2 were to investigate the likelihood of leakage from sub-seabed storage sites, understand the potential effects on benthic ecosystems and finally assess the risk of sub-seabed carbon dioxide storage sites. The objectives were followed by numerous field campaigns, research cruises, laboratory experiments and numerical modelling [ECO_2, 2015]. As one of the main results the investigations of ECO_2 revealed that a quantitative assessment of CO2 seepage rates and a reliable prediction of seep sites cannot be conducted unless the nature, and in particular the permeability of sub-seabed chimney structures is better constrained.

During his PhD thesis [Karstens, 2015] Jens Karstens of GEOMAR mapped, quantified and interpreted focused fluid conduits in the marine sedimentary basin of the Sleipner area in the North Sea Basin in the exploration type 3D seismic data set ST98M3, acquired by Statoil. Research on the Sleipner CO_2 storage site has mainly focused on the CO_2 migration within the storage formation [e.g. Chadwick et al., 2009; Arts et al., 2008], while natural fluid manifestations in the overburden have only been reported briefly by Heggland [1997] and Nicoll [2011]. The investigated industrial data cover an area of 2,000 km^2 and were processed with 12.5 m horizontal and ~10 m vertical resolution. Karstens mapped and categorised vertical seismic anomalies (Figure 3.1.1, type-A-anomalies, type-B-anomalies, type-C-anomalies). In total, 46 large-scale vertical seismic anomalies (500–800 m long and 100-1000 m wide) are present in the shallow (> 1000) subsurface of the study area and their appearance assigned to different formation processes (Figure 3.1.1). These seismically-imaged chimneys are considered to be pathways for sedimentary fluid flow, which could act as pathways for CO_2, if the plume reaches the base of the structures and if their permeability is high enough. The analyses revealed seal-weakening, formation-wide overpressure and the presence of free gas as the requirements to initiate the formation of vertical fluid conduits in the SVG [Karstens & Bendt, 2015].

Similar seismic anomalies have been recognized around the world and are generally associated with vertical fluid flow [e.g. Berndt, 2005; Cartwright et al., 2007; Løseth et al., 2009; Andresen, 2012; Gay et al., 2012]. The activity of vertical fluid conduits can be associated to blowout-like events, e.g. resulting in pipe structures offshore Nigeria [Løseth et al., 2011] or Norway [Bünz et al., 2003] or fluid flow may be continuous and long-lasting, e.g. chimney structures above North Sea salt diapirs [Hovland and Sommerville, 1985; Granli et al., 1999; Arntsen et al., 2007]. The shallow subsurface of the Central North Sea is highly affected by

focused fluid flow. The seafloor of the Fladen Ground in the British sector west of the Sleipner area is densely populated with pockmarks. Most of these pockmarks are only a few meters wide, while a few prominent structures like the Scanner pockmark have diameters of more than 100 meter [Judd and Hovland, 2007]. The Scanner pockmark emits methane, which is trapped beneath a glacial unconformity less than 80 meters below the seafloor [Judd et al., 1994]. 3D seismic data suggest that this shallow gas reservoir is charged by a vertical fluid conduit comparable to the seismic fluid flow structures identified in the Sleipner area (Figure 3.1.2 left).

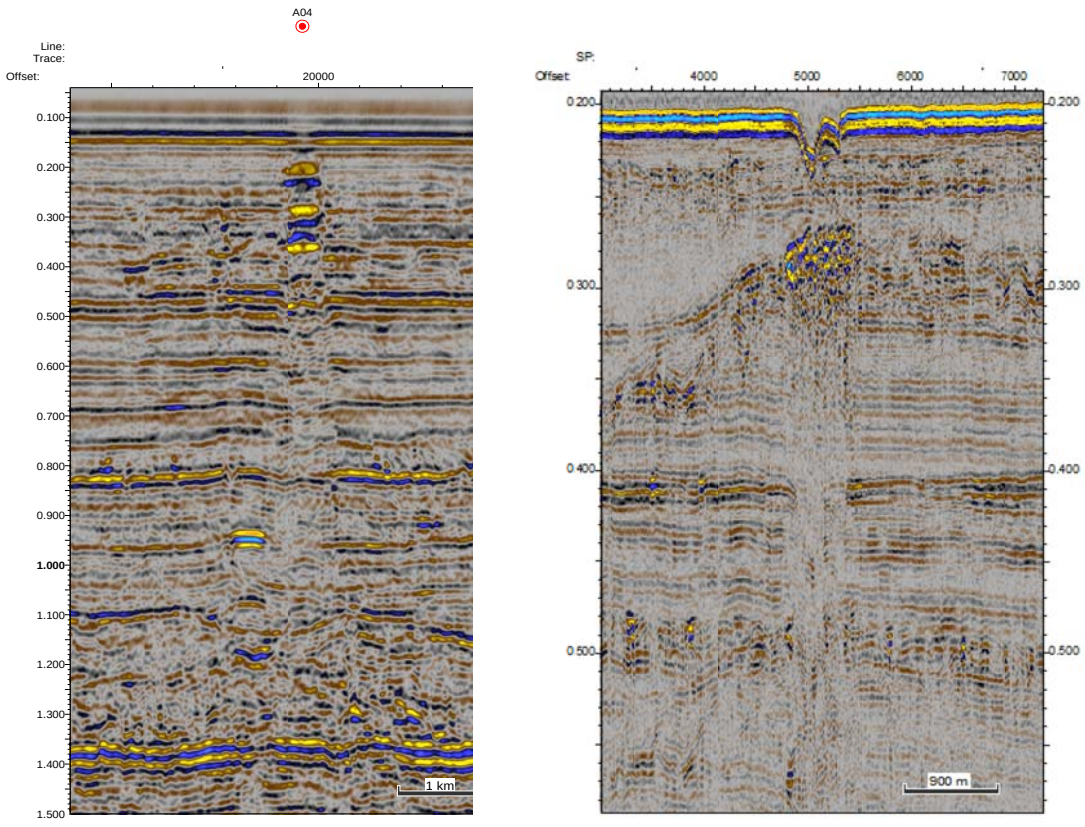

Figure 3.1.2: Seismic examples for pipe structures. The left panel shows exploration type 3D seismic data of Chimney A04 south of the Sleipner Field. The right panel shows the pipe structure underlying the Scanner pockmark in high-resolution 2D seismic data collected during MSM63.

We selected the two prominent vertical seismic fluid flow structures A04 (Sleipner area, Norway) and the Scanner pockmark (U.K.) in the Southern Viking Graben as study sites for this cruise. Both structures have been imaged previously with exploration-type 3D seismic data and were judged suitable for our experiments (Figures 3.1.2, right and left). However, the 3D seismic data could not resolve if the fluid conduit of A04 crosscuts the youngest glacial sediments and would be reachable with drilling. Therefore, the final site selection for the Scanner Pockmark Site depended on high-resolution sub-bottom profiler data, which we collected during the cruise. Alltogether we did acquire high-resolution 2D seismic data, very high-resolution sub-bottom profiler data to image small-scale fracture networks in the top 20 m of sediments, ocean bottom seismometer data for velocity analysis and controlled source electromagnetic data to assess fracture anisotropy in the subsurface [Exley et al., 2010; Key et al., 2012]. All four data sets will be combined to a geophysical model of a chimney structure and form the basis for permeability modelling after the data have been ground-truthed by drilling. These data will provide the

steppingstone from interpretation of borehole samples to exploration-type 3D seismic data. This will provide the geophysical database for assessing the permeability of a typical chimney structure. Within the STEMM-CCS project the analysis and interpretation of the borehole results will be augmented with the study of field analogues and numerical simulations.

3.2 Aims of the Cruise

Quantification of focused fluid migration through the sedimentary succession is fundamental for a large number of research themes ranging from the assessment of geological climate controls and slope stability to verify applied question such as where hydrocarbons accumulate and how safe CO_2 storage is [Berndt, 2005]. Within the ECO_2 project we have attempted to assess the integrity of the overburden, but the combination of field studies and numerical simulation has shown clearly that it is not possible to describe fluid migration in a sedimentary basin quantitatively without understanding the role of seismic chimney structures.

The main scientific goals of this project were

a) **firstly to constrain the bulk permeability of an existing chimney structure**, i.e. to assess the amount of aqueous and gassy fluids that may move through these structures over time.
b) **Secondly, we tried to constrain the temporal evolution of fluid migration through pipe structures over time,** i.e. do they transport fluids continuously or episodically and if episodically is it likely that CO_2 storage may initiate a new episode of migration.
c) **Thirdly, we set out to test the hypothesis that chimney structures in seismic data represent indeed fault networks created by hydro-fracturing** and not bulk mobilization of sediments as a diapir or subsidence of sediments in the style of a breccia pipe.

These goals will be met within the STEMM-CCS project by combining geophysical observations from two scientific cruises by GEOMAR and the National Oceanography Centre, Southampton with field samples from the Colorado Plateau and numerical simulations. The cruise proposed here will provide the required borehole samples from inside and outside the chimney structures and the necessary geophysical data with different frequency content from high-resolution sub bottom profiler data to P-Cable high-resolution data to upscale the borehole observations through a nested approach to the existing high-quality exploration-type seismic data. This will provide the required data set to achieve the three objectives above. These data will be augmented by ocean bottom seismometer data and controlled-source electro-magnetic data, which we will collect during the cruise and which will allow us determining if there is continuously linked fracture permeability inside the chimney structures from directional differences in the seismic velocities and the electric resistivity, respectively.

4 Narrative of the Cruise

(C. Berndt, J. Elger)

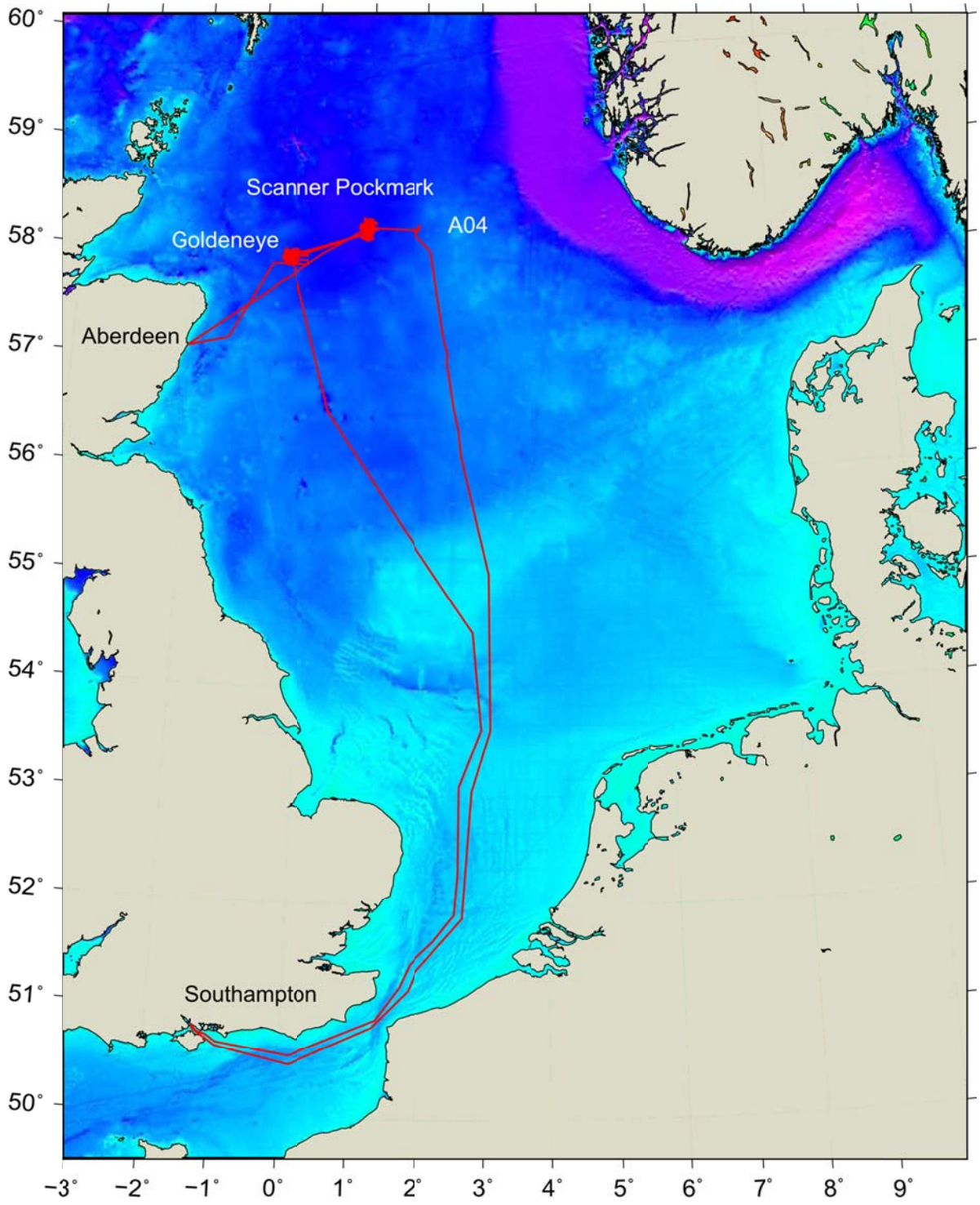

Figure 4.1: Cruise MSM63 started from Southampton, U.K. on 29.05.2017 and finished in Southampton, U.K. on 25.05.2017 after a port call in Aberdeen from 12.-18.05.2017 when the geophysical equipment was offloaded. The main study area during Leg 1 was the Scanner Pockmark, during Leg 2 it was the Goldeneye field, both located in the U.K. sector of the North Sea.

29.4. Saturday
After mobilization of OBEMs and DASI we sailed from Southampton at 17:30. We set off for the study area with a south-easterly breeze.

1.5. Monday
We arrived in the first study area south of the Sleipner Field at 22:00. We carried out releaser tests for both the OBEM and the OBS and ran a sound velocity profile.

2.5. Tuesday
In the early morning from 2 to 5 o'clock we ran several Parasound profiles to inspect if the chimney structure at site A03 reaches the surface sediments as indicated by the low-resolution 3D-seismic data. Unfortunately this is not the case also the secondary target site A04 did not show any evidence for a fluid flow anomaly within the top 30 m that could be reached by RockDrill2. Therefore, we decided to steam to the back-up location in the British sector (Scanner Pockmark). We reached that site at 08:00 and began to deploy the OBIC OBEM's. After having deployed six OBEM we continued with the deployment of the GEOMAR OBS at 14:00 to allow the OBIC team to have a break. All 17 OBS were deployed by 20:30. Then we fixed a sensor on Merian's pod drive and carried out a high-voltage test on DASI before deploying the remaining OBEMs starting at 21:30.

3.5. Wednesday
At 03:30 all OBEM were installed at the sea floor and we continued with the deployment of DASI which was up and running by 07:00. For the next two days we acquired CSEM data in good weather (N2-4).

5.5. Friday
Except for a short break to change the battery of the Posidonia receiver on DASI in the evening of the 4.5. the DASI system ran smoothly until we recovered it in the morning of the 5th between 08:00 and 09:00. Then we continued with the recovery of the OBEMs. These were on deck at 14:00. During the afternoon and early evening we deployed the P-Cable system, but there were technical difficulties. Two t-junctions caused leakage and even though the system worked for a short time after everything was deployed, more leakage occurred just before firing up the airguns and everything had to be retrieved. During the night we shot at 10 s intervals into the OBS.

6.5. Saturday
Because of poor weather forecast force 7-8 from Sunday morning, we decided not to try to deploy the P-Cable system again but continued shooting into the OBS. At 10:00 o'clock we had to stop to repair one of the pod drives. Afterwards, we continued with shooting the OBS lines but now also with a 2D streamer and a higher shooting rate in order to produce reverse shot lines and geometry information in addition to the dedicated OBS shots at 10 s intervals.

7.5. Sunday

At 08:00 we retrieved the 2D seismic system because the weather deteriorated with up to 6 m high waves. For the following two days we conducted a multibeam survey that covered 2/3 of the study area.

9.5. Tuesday

We started to recover the OBS at 06:00 and managed to retrieve all eighteen instruments by 12:00. Afterwards we redeployed the P-Cable system. The system was up and running by 18:00, but after a few shots leakage in one of the cables occurred and we had to get it back on deck. Afterwards we re-configured it in 2D mode and at 22:00 we started to acquire 2D seismic data during the night.

10.5. Wednesday

At 08:00 we repaired streamer three in which the connector broke during the night. The system was up an running again within one hour.

11.5. Thursday

In the morning the airgun float collapsed and we had to repair it before continuing shooting 2D seismic lines across the CSEM DASI profiles. At 16:00 we retrieved the 2D seismic system and ran another sound velocity profile for the calibration of the multibeam system, before starting the transit to Aberdeen.

12.5. Friday

We arrived in the prot of Aberdeen at 06:00. All instruments used on leg 1 were demobilized and unloaded by noon. The mobilization of RD2 (rock drill) started at 08:00.

18.5. Thursday

After spending the last 5 days in Aberdeen harbour because of technical problems we sailed from Aberdeen at 19:00. During that time RD2 had have to be demobilized, as the remaining time of the second leg of MSM63 does not allow to drill any cores and demobilize RD2 then in Southampton. Instead we plan to use multibeam, Parasound, CTD and water samples to study the area around the Golden Eye platform. We set off for the study area with sunshine and a south easterly breeze.

19.5. Friday

At about 01:00 we arrived in the study area the Golden Eye platform and started to acquire Parasound data. At about 13:30 we stopped to measure a CTD profile to measure salinity, pressure, temperature, oxygen and turbidity and to take water samples for further analyses in the lab at home. Afterwards we continued the Parasound measurements until 16:15 and did a second CTD. At about 17:00 we started with a multibeam survey that will image the seafloor in an area of about 10 by 10 km around the Golden Eye platform.

20.5. Saturday

We interrupted the multibeam survey to measure the water column with the CTD at three locations around the Golden Eye platform, at about 08:30, 11:30 and 13:15, and one at about 15:00 in the north-western part of the survey area. As the wind got stronger during the night, there is about 2 m of swell.

21.5. Sunday

We finished the multibeam survey at around 03:00 in the night and sailed to the
Scanner pockmark area. We turned on the Parasound until we left the area of study permission at Golden Eye, about 05:30. In the morning we started the mulitbeam survey in the Scanner pockmark area around 08:15. We took two CTD measurements in the early afternoon, one in the Scanner pockmark at the flare and one outside. The wind calmed down again and the sea is very calm.

22.5. Monday

We finished the multibeam survey shortly after midnight and headed back to the Golden Eye platform. Back there, we filled up gaps in the multibeam data until about 08:30. Afterwards, we did 8 CTD measurments (with and without water sampling) and connected them with Parasound profiles. Afterwards we did another multibeam survey in the southwestern part of the study area. In the evening, we started to measure a grid of Parasound profiles on the eastern side of the platform.

23.5. Tuesday

We finished the Parasound survey around 02:00 in the morning and set off for Southampton.

25.5. Thursday

After about 2 days of transit the pilot entered the vessel around 06:00 and we arrived in the port of Southampton at 08:00.

5 Preliminary Results

5.1 Seismic Data Acquisition and Processing

(S. Muff)

5.1.1 Method and experiment setup

The aim of the seismic survey was to map the spatial extent of the scanner pockmark. During the cruise an array of two 105/105 in3 GI-Gun's was fired as seismic source for the seismic lines. Data were recorded with GeoEel digital streamer segments. Fig. 5.1.1 gives an overview upon the seismic 2D lines during Cruise MSM63.

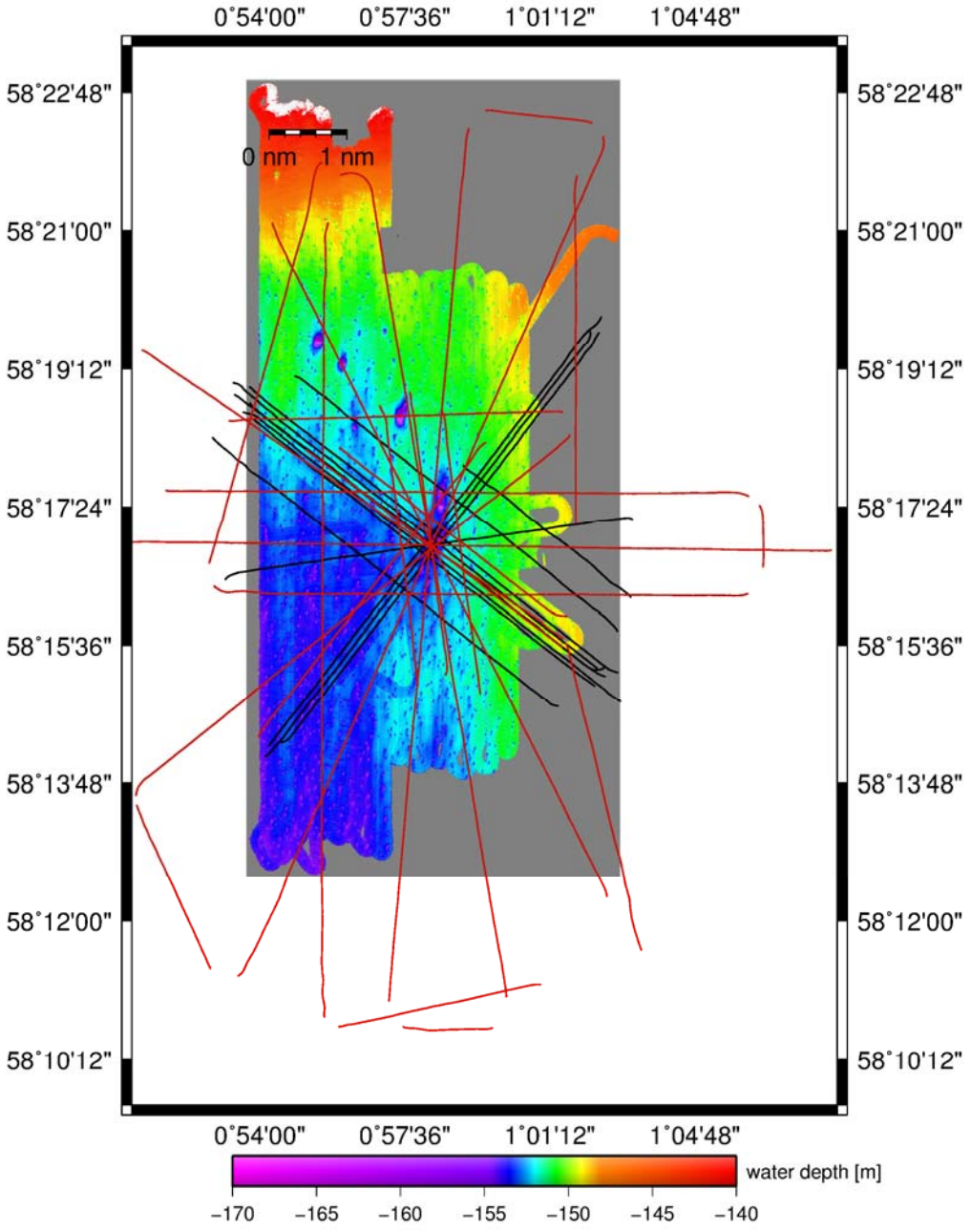

Figure 5.1.1: 2D survey lines of MSM63: Red lines show lines of P2000. Black lines show lines of P3000.

Seismic sources

During this cruise two standard GI-Guns in harmonic mode were operated as seismic source. Both guns were connected to a stringer with the GI-Guns hanging on two chains about 70 cm beneath. An elongated buoy, which stabilized the guns in a horizontal position at a water depth of ~2 m, was connected to the stringer by two rope loops (Fig. 5.1.2).

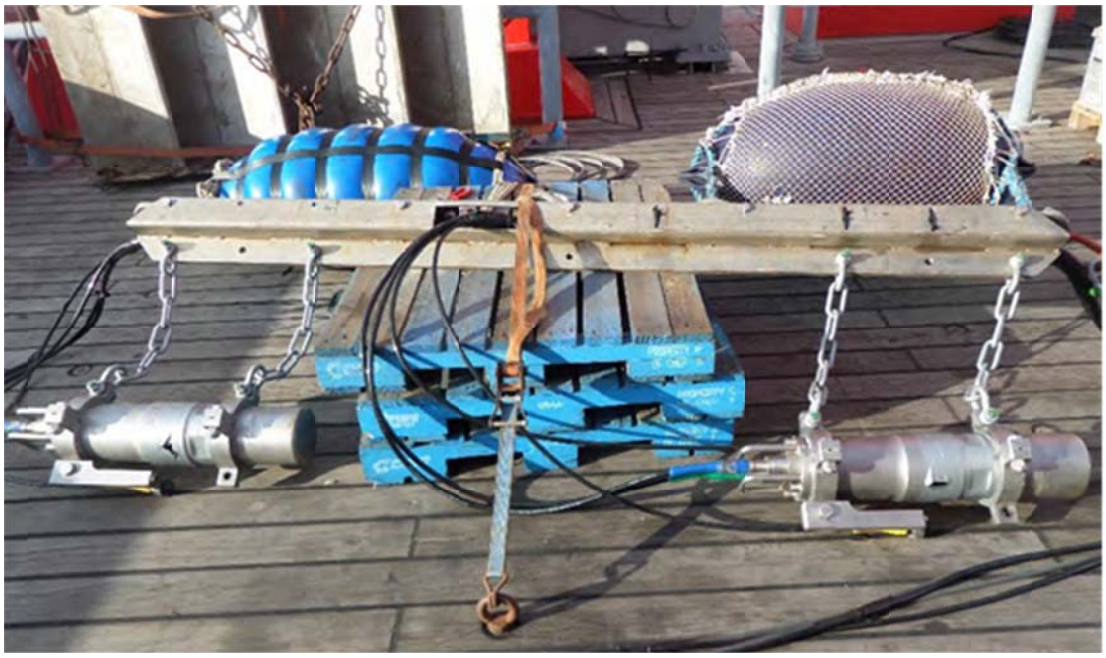

Figure 5.1.2: GI-Gun setup

Each gun had a volume of 210 in3, separated in 105 in3 for the generator and 105 in3 for the injector chamber. A gun hydrophone, which is located inside the air bubble, is supposed to provide both, the time break and the shape of the near-field signal for permanent monitoring and direct quality control of the source signal. The release of the injector pulse was triggered with a delay of 5 ms in manual mode with respect to the generator signal for all seismic surveys. This value was adjusted to the approximated source depth of 2 m and a gun pressure of 3000 psi (210 bar).

The shooting interval was adjusted to 6 seconds for survey lines P2000, resulting in a shot point distance of 10.50 - 15 m in a range of approximately 3.5 – 5 knots. For survey lines P3000 the gun was fired every 5 seconds, resulting in a shot point distance of 8.75 – 12.5 m at the same speed. The frequency range of the two-GI-Gun-array is 15 - 500 Hz.

Figure 5.1.3: GeoEel streamer segments of 12.5 m length were connected to build up the 2D streamer system.

Streamer System

Different configurations in digital streamer length (Geometrics GeoEel streamer segments) were used for recording the seismic signal. Deck geometries, streamer configuration and seismic gun setting for the 2D surveys are illustrated in Fig. 5.1.3. The entire survey P2000 and lines 3 to 10 from survey P3000 were recorded with two oil filled streamer sections (each 12.5 m) with 16 channels. Survey lines two and all lines in between eleven and thirty from survey P3000 were recorded with a 150 m long streamer and 96 channels. The last four streamers of this configuration were solid state. All streamer configurations consisted of a tow cable, one vibro stretch section of 25 m length behind the tow cable the active sections (each 12.5 m) attached behind the stretch zone. The tow cable had a length of 20 m behind the vessel's stern. Each active section contained 8 channels with a hydrophone group spacing of 1.56 m. One AD digitizer module belonged to each active section. These AD digitizer modules are small Linux computers. Communication between the AD digitizer modules and the recording system in the lab was transmitted via TCP/IP. A repeater was located between the deck cable and the tow cable (Lead-In). The SPSU managed the power supply and communication between the recording system and the AD digitizer modules. Three birds controlled and monitored the streamer depth during the survey with 96 channels. They were attached to the stretch zone, the first and the third streamer segment. A small buoy was connected to the tail swivel of the 2D streamer (Fig. 5.1.4).

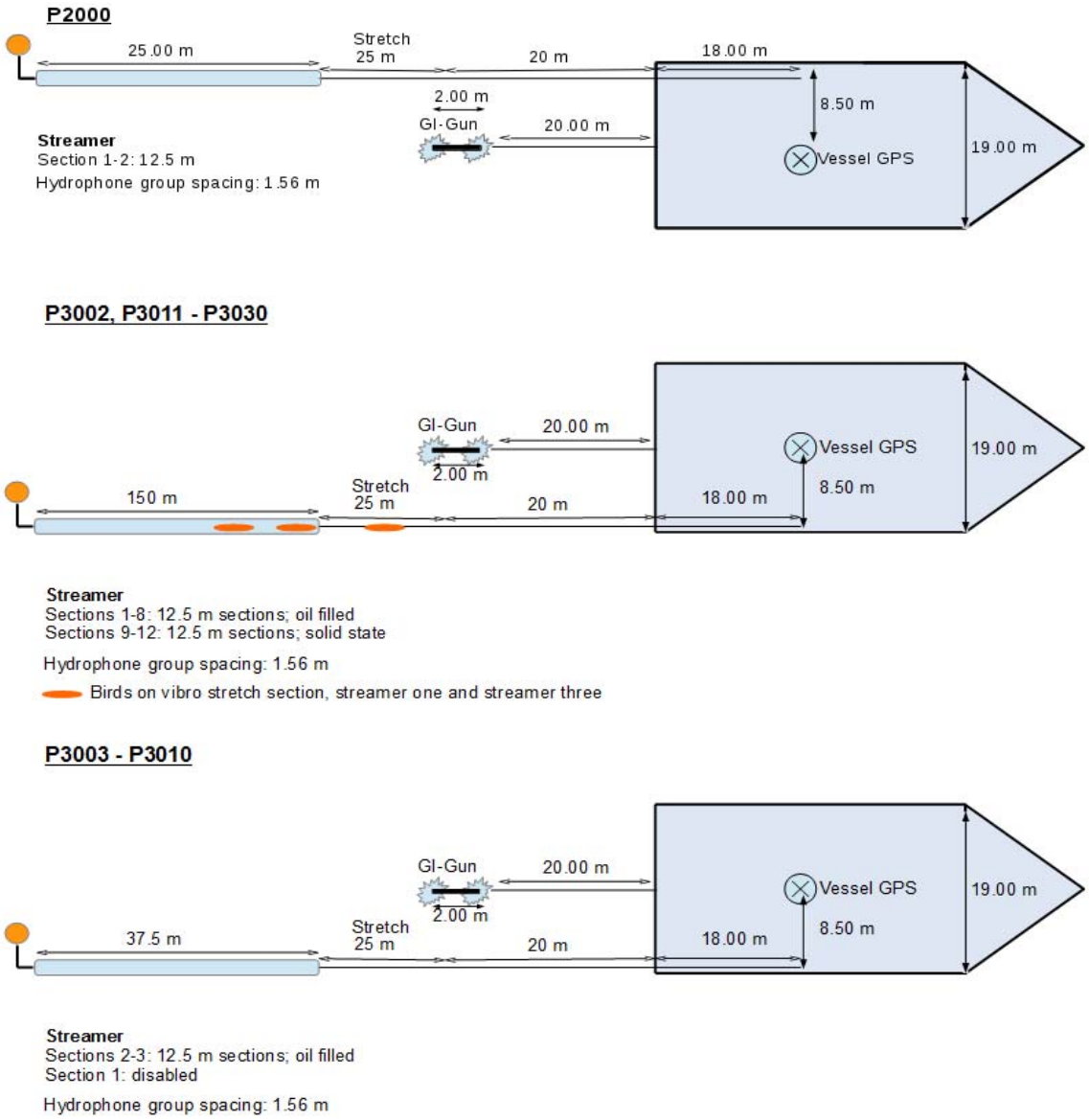

Figure 5.1.4: Geometry and streamer configuration of the 2D seismic surveys.

Bird Controller

Three Oyo Geospace Bird Remote Units (RUs) were deployed on the streamer. The locations of the birds are listed in Fig. 5.1.4. The RUs have adjustable wings. A bird controller in the seismic lab controlled the RUs. Controller and RUs communicate via communication coils nested within the streamer. A twisted pair wire within the deck cable connects controller and coils. Designated streamer depth was 2 m in accordance with good weather conditions and low swell noise. The RUs thus forced the streamer to the chosen depth by adjusting the wing angles accordingly. The birds were deployed at the beginning of a survey but no scanning of the birds was carried out during the survey because bird scans caused false triggers. However, the birds worked very reliably and kept the streamer at the designated depth.

Data Acquisition Systems
Data were recorded with acquisition software provided by Geometrics. The analogue signal was digitized with 2 kHz. The seismic data were recorded as multiplexed SEG-D. Recording length was 6 (P2000) and 5 seconds (P3000). One file with all channels within the streamer configuration was generated per shot. The corresponding Shotlog reports shot number and time information contained in the RMC string. The acquisition PC allowed online quality control by displaying shot gathers, a noise window, and the frequency spectrum of each shot. The cycle time of the shots were displayed as well. The software also allows online NMO-Correction and stacking of data for displaying stacked sections. The vessel's GPS was simultaneously logged in RMC string and logged time and position information.

Trigger Unit
A long shot was used as gun controller. The injector was triggered with a delay of 5 ms in manual mode. From seismic data analyses we determined a total delay of 18 ms for lines one to four of survey P2000 and all other lines a delay of 20 ms between triggering and real shooting time. No direct quality control of the source signal was carried out.

Processing
On-board processing included geometry calculations, delay calculations and source and receiver depth control. A ghost effect in the seismic data was not detected. The processing was performed with the Seismic Unix software. The source-receiver locations were binned on a grid with 1.5625 m by 1.5625 m cells. Survey lines P2000 were bandpass-filtered with a low-cut ramp of 55 – 65 Hz and a high-cut ramp of 350 - 500 Hz to suppress a strong bubble pulse overprint. Survey lines P3000 were filtered with bandpass corner frequencies of 25, 45, 420, 500 Hz. An NMO correction (with a constant velocity of 1488.08 m/s calculated from CTD measurements) was than applied and the data stacked. The stack was migrated with a 2D Stolt algorithm (1500 m/s constant velocity model).

5.1.2 Initial Results

(C. Boettner)

Preliminary analysis of 2D seismic lines show the overall shape of the sedimentary succession underneath the Scanner pockmark. The seismic image (see Figure 5.1.5) is centered around the Scanner pockmark and show it as a ~ 180 m wide and ~16 m deep depression at the seafloor.

The sedimentary succession is well imaged by the high-resolution 2D seismic data. The Nordland formation is clearly visible as well-stratified sediments. The multiple of the seafloor is distorting the image at ~ 440 ms.

Between the seafloor and the well-stratified sediments of the Nordland formation (200-350 ms TWT) clear indication for several stage of deposition and erosion are visible. A characteristic tunnel valley with steep flanks and several phases of deposition and erosion is located SW of the Scanner pockmark. The 2D seismic data provides higher resolution and quality than the pre-

existing 3D industry seismic data for the upper 500 ms TWT. Especially the different stages of glacial deposition and erosion can be untangled and further interpreted with the data.

A chimney-type anomaly is visible underneath the Scanner pockmark. However, our data does not enable a clear distinction between seismic artifact and real geological fluid conduit. At the topmost extent of the blanking zone, a bright spots are visible. Although the bright spots show amplitude increase by a magnitude, a single flat spot is not visible. A single flat spot would indicate large amounts of free gas and/or a single reservoir within the sedimentary succession. However, we can state that this gas reservoir underneath the Scanner pockmark is likely the source region of the flares emerging from the center of the pockmark. A conduit or fracture network between the bright spots and the Scanner pockmark is undetectable as only one wiggle trace shows anomalous behavior.

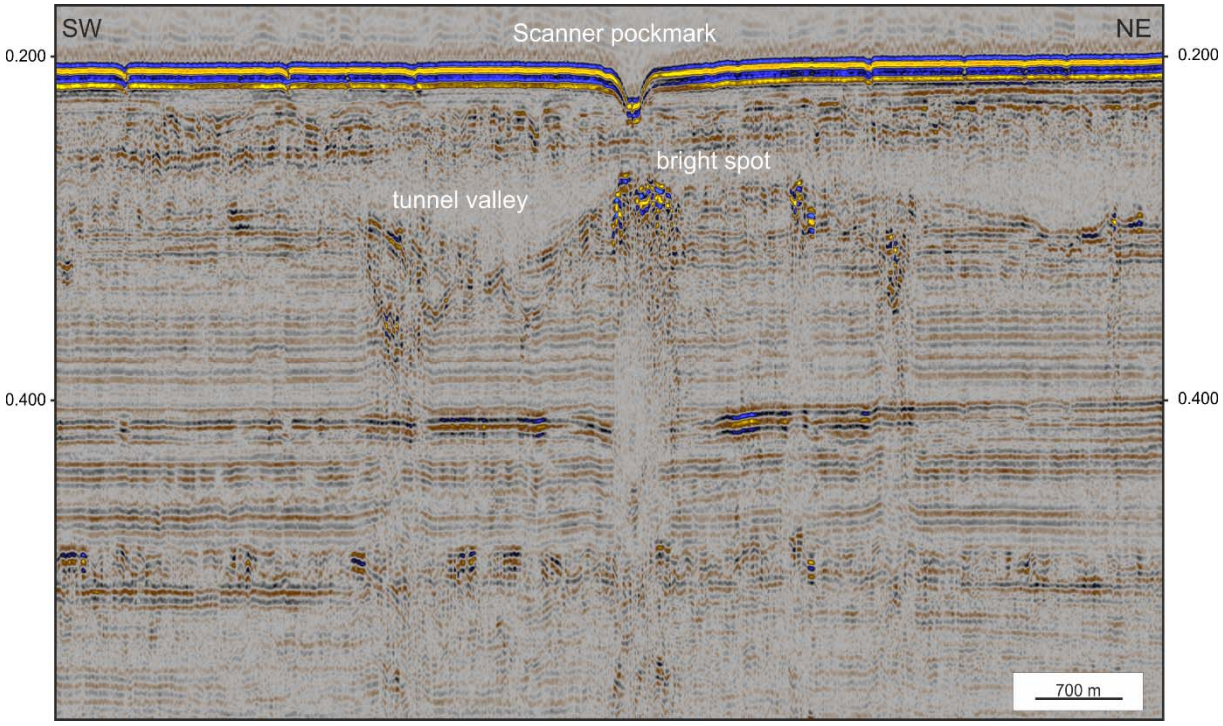

Figure 5.1.5: Seismic image of the Scanner pockmark

5.2 OBS Experiments

(B. Schramm)

The Ocean Bottom Seismometer (OBS) consists of four floats, which are connected to a frame and is generally equipped with a three-component seismometer, a hydrophone and a data recorder encased in a high-pressure tube (Fig. 5.2.1). All sensors are connected to the recording unit and continuously record the incoming signals. The system itself floats at the sea surface, so in order to deploy the device on the ocean bottom a weight is mounted to the frame and attached to a so-called releaser. This releaser has an acoustic communication unit, which can be addressed from the ship in order to disconnect the weight after the experiment. The OBS will then ascend to the surface and can be recovered. A flashlight, radio transmitter and a flag are attached to the

frame to increase the visibility of the OBS and to facilitate an easy and quick recovery. While the OBS continuously records seismic signals an additional data logger on board records the corresponding shot times and is used to correlate the results at a later stage of data processing.

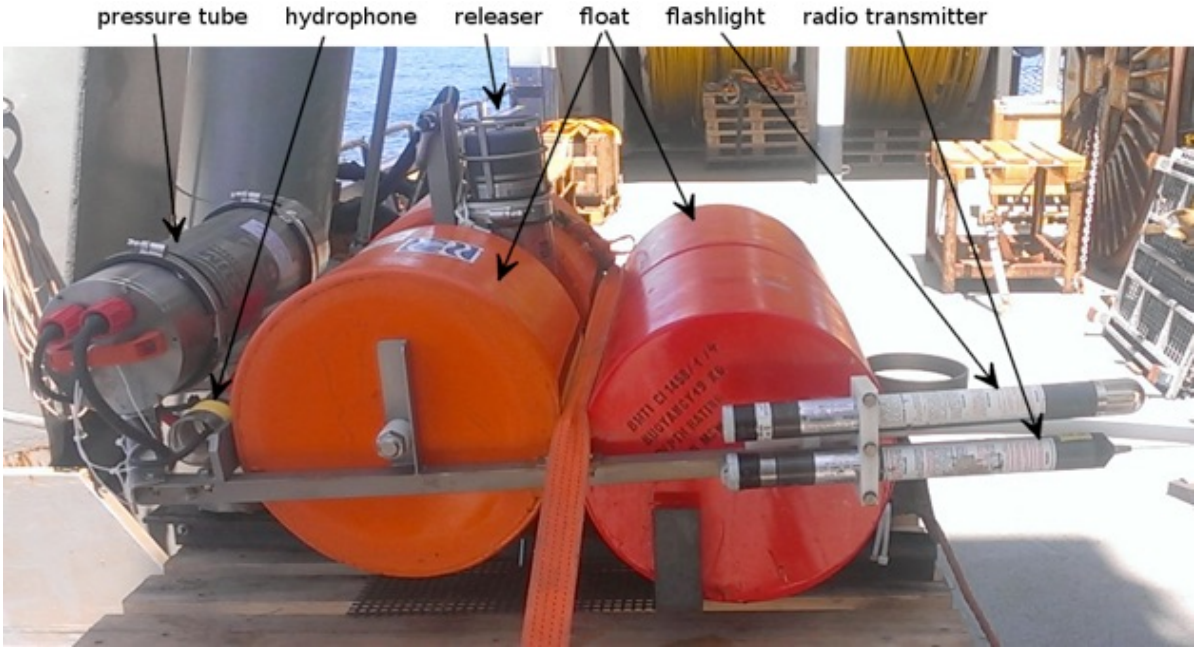

Figure 5.2.1: GEOMAR Ocean Bottom Seismometer (OBS)

The data recorders need to be programmed before the deployment of the system. The sample rate of the OBS recorders was set to 500 Hz, while the time logger had a sample rate of 1000 Hz. The gain of the input channels was set to 15 for the three geophone components and to 7 for the hydrophones. Initial tests showed some problems with the recording unit of OBS 18, so that the gain for the geophone components was increased to 31.

Each recorder was equipped with 5 GB storage space (either one 2 GB and three 1 GB or two 2 GB and two 1 GB flash memory cards). The exact recording parameters for the deployments can be found in Appendix B (OBS protocols). The recording units were synchronized with the GPS signal both before and after the recording period to correct for any time shifts within the logger's internal clock.

A total of 18 OBS were deployed around the chimney on May the 1st 2017 (Fig.5.2.2). The water depth varied between 153 and 169 m. Afterwards, the airgun was deployed and six profiles (P1001 – P1006) crossing the OBS were shot for 10 hours. The shot interval was 10 s with two GI-guns (Appendix C). In addition, a streamer was deployed on the following day and the shot interval was reduced to 6 s (P2001-P2013). Ring profiles could not be achieved due to bad weather conditions.

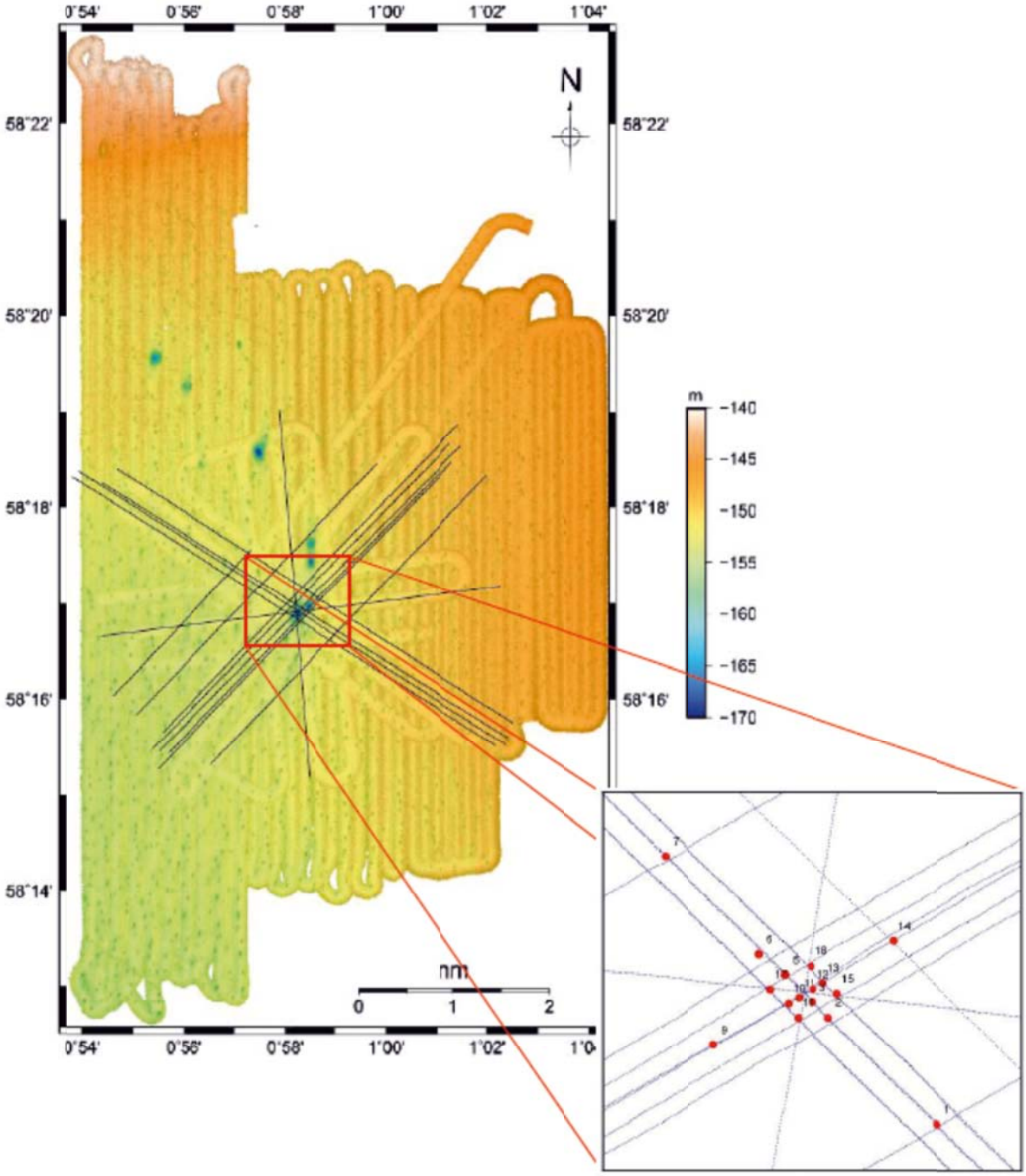

Figure 5.2.2: Bathymetric overview map of the seismic survey during the OBS operation. Black lines show profiles P1000 to P2000. The red square is displaying the OBS positions.

The main target of these profiles was to provide velocity information for 3D tomography as well as to support further 2D and 3D seismic analyses of the investigation area.

All 18 OBS were recovered successfully on May the 9th and the collected data were immediately read and copied to a processing unit. Synchronization failed with two of the recorders, because the instruments went low on battery during the operation. OBS 04 could be synchronized, but copying of the data failed. On OBS 18, two of the geophone components failed during recording.

All data were copied and converted to SEG-Y/ PASSCAL files on board. A first quick quality control showed promising data, but detailed processing will be carried out after the cruise at GEOMAR (Fig. 5.2.3).

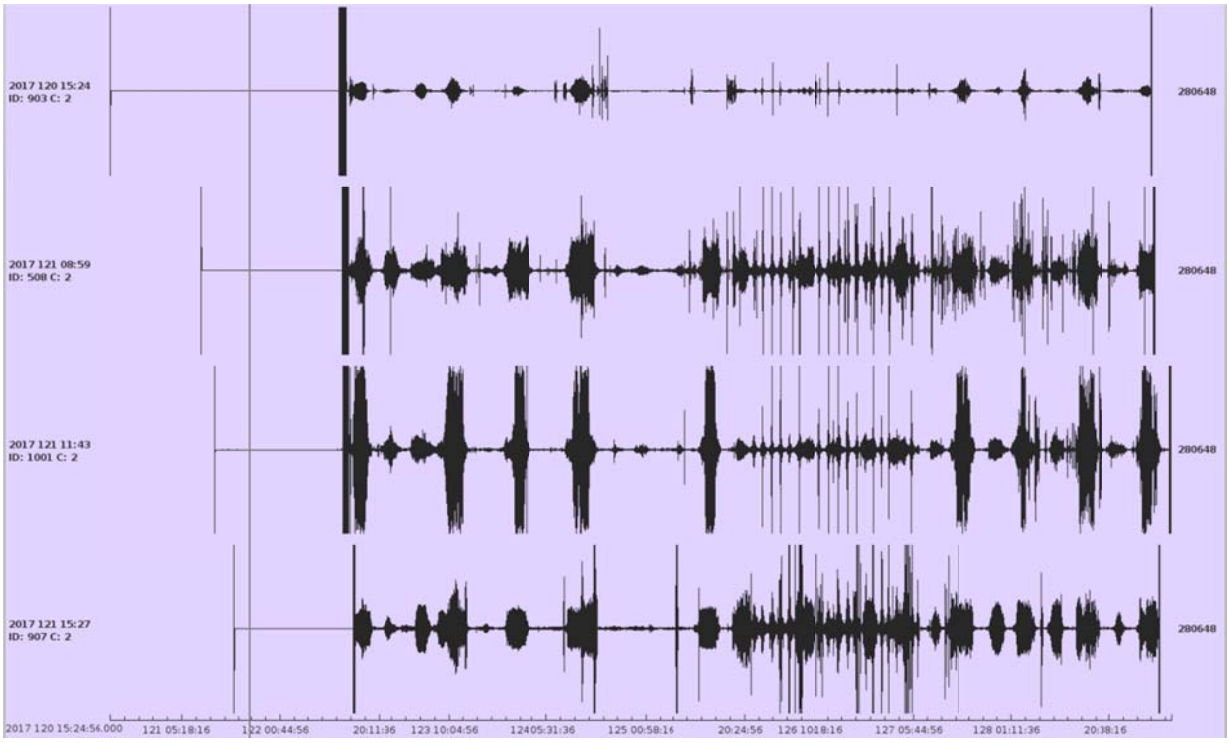

Figure 5.2.3: This figure shows the X component of OBS 01, 02, 03 and 09

5.3 Controlled Source Electromagnetic Surveys

(R. Gehrmann, B. Pitcairn)

5.3.1 Introduction to DASI and Vulcan

The deep-towed active source instrument (DASI) is powered from the ship via a conducting deep-tow cable. DASI is designed to transmit electromagnetic (EM) signals from a towed neutrally-buoyant antenna at low frequencies that penetrates the seafloor [Sinha, 1989]. The EM response of the seafloor is then measured and recorded by two towed three-axis electric field Vulcan receivers [Constable et al., 2016] and ocean bottom electromagnetic (OBEM) instruments. The amplitude and phase of the measured EM response is related to the electrical conductivity (or resistivity - the inverse of the conductivity) of the seafloor. Further information on the conductivity structure is then inferred from the responses measured at different frequencies. The instrument array is sensitive to bulk changes in electric conductivity in the seafloor and is, therefore, sensitive to the contrast between resistive and conductive seafloor layers. Figures 5.3.1 and 5.3.2 show the schematic setup of the STEMM-CCS survey during the MSM63 cruise. Figure 5.3.3 shows the instrument during deployment.

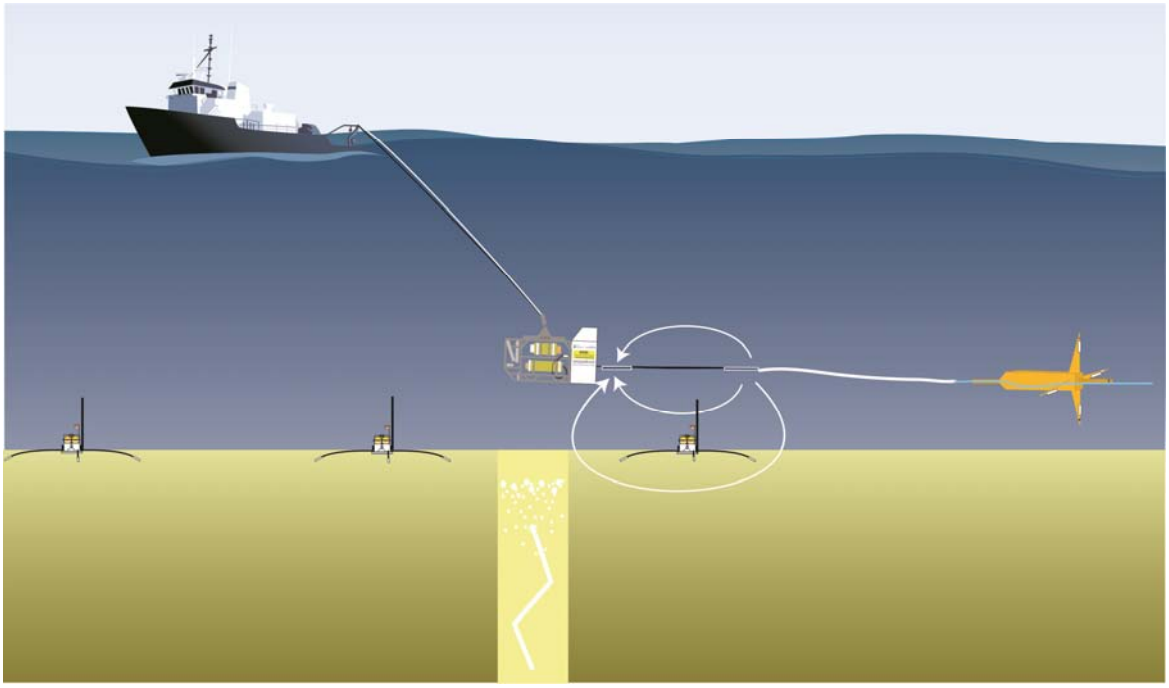

Figure 5.3.1: Sketch of the University of Southampton towed CSEM system: DASI [Sinha, 1989] towing the dipole transmitting antenna array (white lines represent current streamlines generated by the antenna), the three-axis electric field Vulcan receiver [Constable et et al., 2016] and three-axis ocean bottom electric field receivers (OBIC). Figure adapted from Weitemeyer (pers. communication)

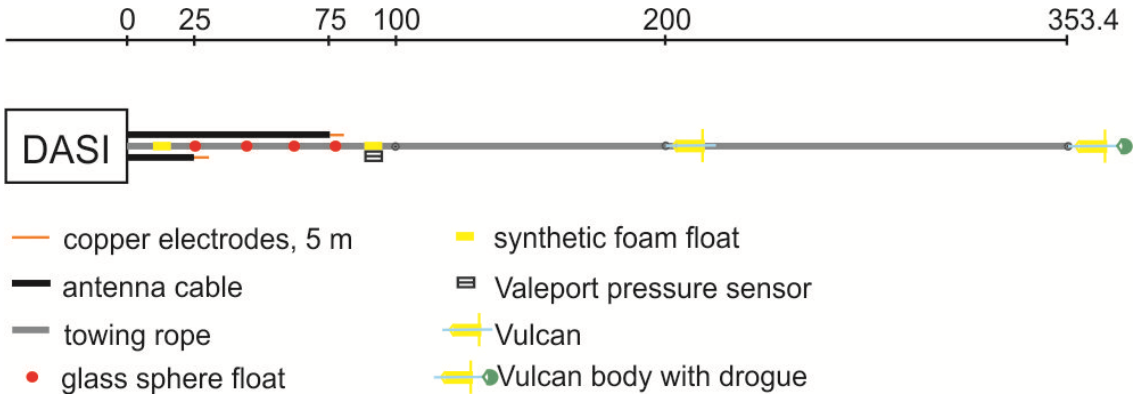

Figure 5.3.2: Details on the DASI and Vulcan dimension (scale in metres) setup for the STEMM-CCS survey.

Figure 5.3.3: a (left), b (centre) and c (right) show the DASI transmitter deployed off the aft of FS Merian and the towed EM receivers (Vulcans) used for this survey.

For this experiment, the planned EM survey gridlines (shown below which is superimposed with the location of the deployed Ocean Bottom Electric (OBE) field receivers and the amplitude of the glacial unconformity reflections from seismic data, courtesy of PGS) is indicated in the Figure 5.3.4.

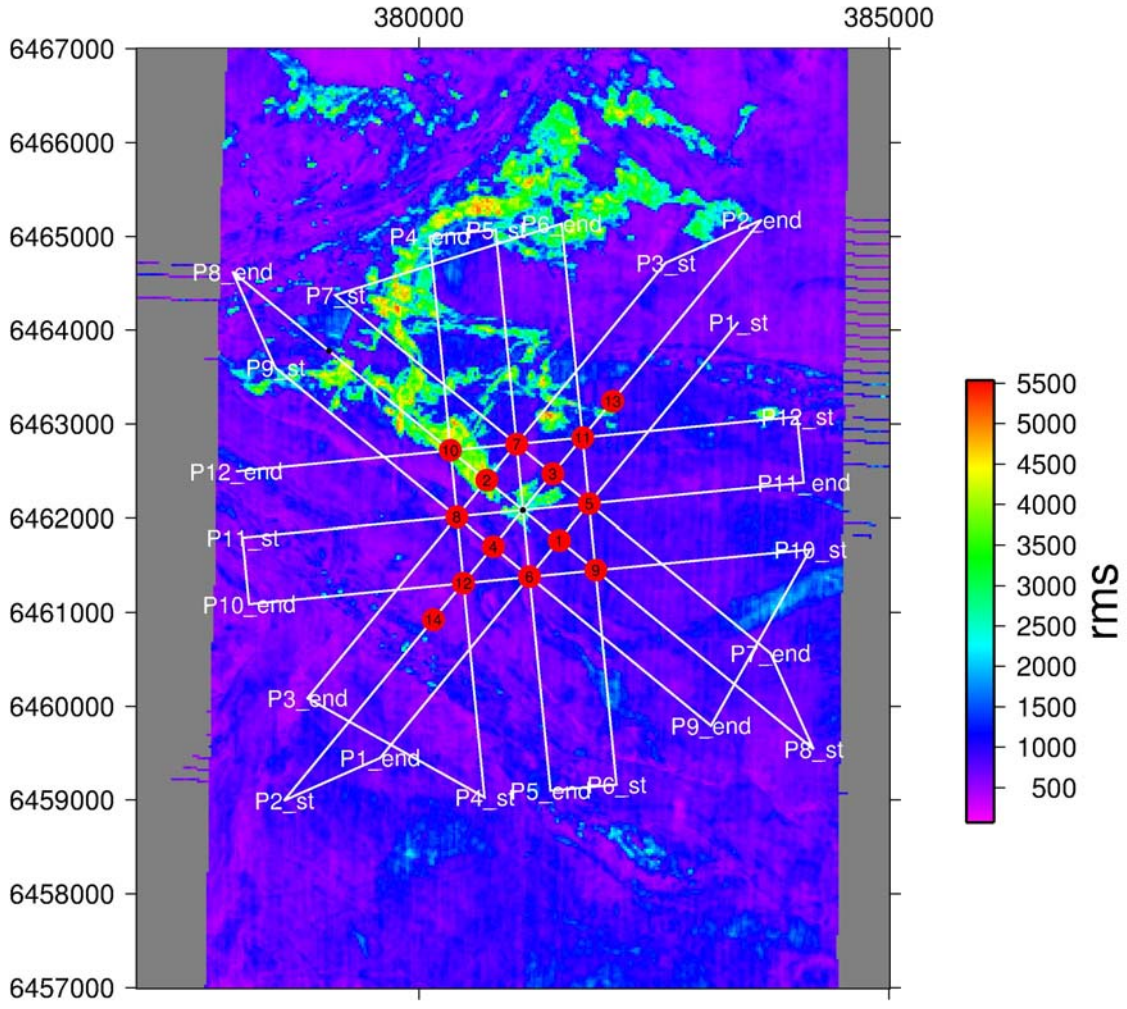

Figure 5.3.4: This figure shows the superimposed plot of the locations of deployed OBEM and seismicreflecteddata(data courtesy of PGS) and EM survey lines. The X & Y axes show UTM coordinates.

5.3.2 Ocean Bottom Electro-Magnetic (OBEM) Receivers

UK based OBIC (Ocean Bottom Instrumentation Consortium) supplied 14 OBEM (Ocean Bottom Electro-Magnetic) receivers for this STEMM_CCS work package. These instruments are based on the LCHEAPO platform and the LC2000 data logger developed by Scripps Institution of Oceanography, USA. All of the instruments were equipped with two orthogonal horizontal 12m electrode dipoles, six were equipped with a vertical 1.5m dipole in addition. Red farings are used to reduce the strumming on the pole.

All instruments were equipped with a burn-wire release system and light, VHF radio, and high-visibility flag to aid with recovery. All of the acoustic releases were tested prior to deployment using a basket lowered from the ships CTD winch.

5.3.2.1 OBEM Deployments

The instruments were lowered to 12 m from the seabed using the ship's winch, run through a pulley block on crane 3. They were then released to freefall the remaining distance using an acoustic release supplied and operated by the ship's crew. The position of release was logged by the IxBlue Posidonia receiver. After the initial setup of the winch and release system, each deployment took between 40 minutes and one hour to complete. The instruments were deployed in two shifts on the 2nd and 3rd May 2017.

Figure 5.3.5: The OBEM deployment without and with vertical electrode arm off Maria S. Merian's starboard side.

5.3.2.2 Recoveries

All the OBEM recoveries were completed on 5th May 2017. All acoustic communication was done using the ship's hull mounted transducer which worked well for all recoveries. The fast rescue boat was used to assist in locating and retrieving the instruments which sped up the time taken to position the ship and crane each instrument on board. Each instrument took between 15 and 20 minutes to recover and partially disassemble.

Table 1: Summary of OBEM deployments on MSM63. All positions are the ship position at time of deployment.

Site	Logger	Z-pole	Latitude N ship	Longitude E ship	Latitude N wire release	Longitude E wire release	deployment	recovery
EM01	SCRIPPS	Yes	58° 16.744’	0° 58.672’	58° 16.741’	0° 58.655’	02/05/17 22:05	05/05/17 11:16
EM02	SCRIPPS	Yes	58° 17.074’	0° 57.863’	58° 17.069’	0° 57.847’	02/05/17 21:33	05/05/17 11:33
EM03	SCRIPPS	Yes	58° 16.953’	0° 58.968’	58° 17.118’	0° 58.564’	02/05/17 10:56	05/05/17 12:19
EM04	SCRIPPS	Yes	58° 16.699’	0° 57.947’	58° 16.692’	0° 57.937’	03/05/17 00:37	05/05/17 10:20
EM05	SCRIPPS	No	58° 16.954’	0° 58.988’	58° 16.952’	0° 58.969’	02/05/17 09:58	05/05/17 12:36
EM06	SCRIPPS	No	58° 16.533’	0° 58.351’	58° 16.525’	0° 58.342’	02/05/17 23:47	05/05/17 10:35
EM07	SCRIPPS	Yes	58° 17.285’	0° 58.179’	58° 17.281’	0° 58.157’	02/05/17 12:06	05/05/17 12:04
EM08	SCRIPPS	Yes	58° 16.864’	0° 57.543’	58° 16.856’	0° 57.530’	03/05/17 01:18	05/05/17 10:02
EM09	OBIC	No	58° 16.583’	0° 59.072’	58° 16.575’	0° 59.061’	02/05/17 23:04	05/05/17 10:57
EM10	OBIC	No	58° 17.238’	0° 57.464’	58° 17.234’	0° 57.442’	02/03/17 12:55	05/05/17 11:46
EM11	OBIC	No	58° 17.336’	0° 58.895’	58° 17.333’	0° 58.876’	02/05/17 09:00	05/05/17 12:51
EM12	OBIC	No	58° 16.487	0° 57.633’	58° 16.478	0° 57.622’	03/05/17 02:06	05/05/17 09:34
EM13	OBIC	No	58° 17.552’	0° 59.199’	58° 17.552’	0° 59.199’	02/05/17 08:07	05/05/17 13:06
EM14	OBIC	No	58° 16.275’	0° 57.322’	58° 16.266’	0° 57.311’	03/05/17 02:46	05/05/17 09:15

5.3.3 Data

The DASI source injects a 1s square wave with a base frequency of 1 Hz and its odd harmonics, and a maximum frequency of 256 Hz.

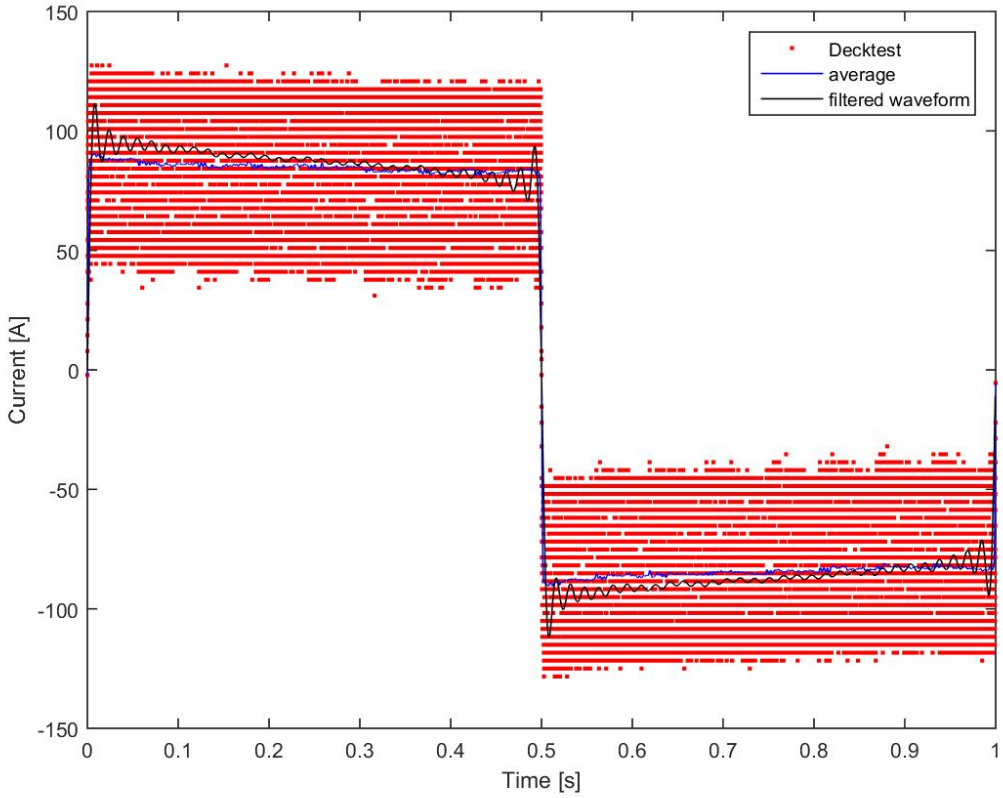

Figure 5.3.6: DASI input waveform from Deck test performed on JC138 with a current clamp (red) in Ampere, its average value (blue, note: the average is only used for display purposes) compared to the filtered waveform from the data measured with a Hall sensor inside DASI's large pressure tube from MSM63.

5.3.3.1 Vulcan Data

Vulcan 2 was 200 m behind DASI and received the strongest response. Figures 5.3.7 - 5.3.9 show the overall spectrum over frequency and time, a small window time series and a spectrum for that time series. Figures 5.3.10 – 5.3.12 show the same for Vulcan1 which was 353.4 m behind DASI. It can be observed that Vulcan 2 has more energy in the x component than Vulcan 1, indicating that it was not straight behind the transmitting dipole. It can also be observed that the energy content in the higher frequencies is lower in Vulcan 1 than in Vulcan 2 caused by the larger offset and therefore a stronger attenuation of the signal.

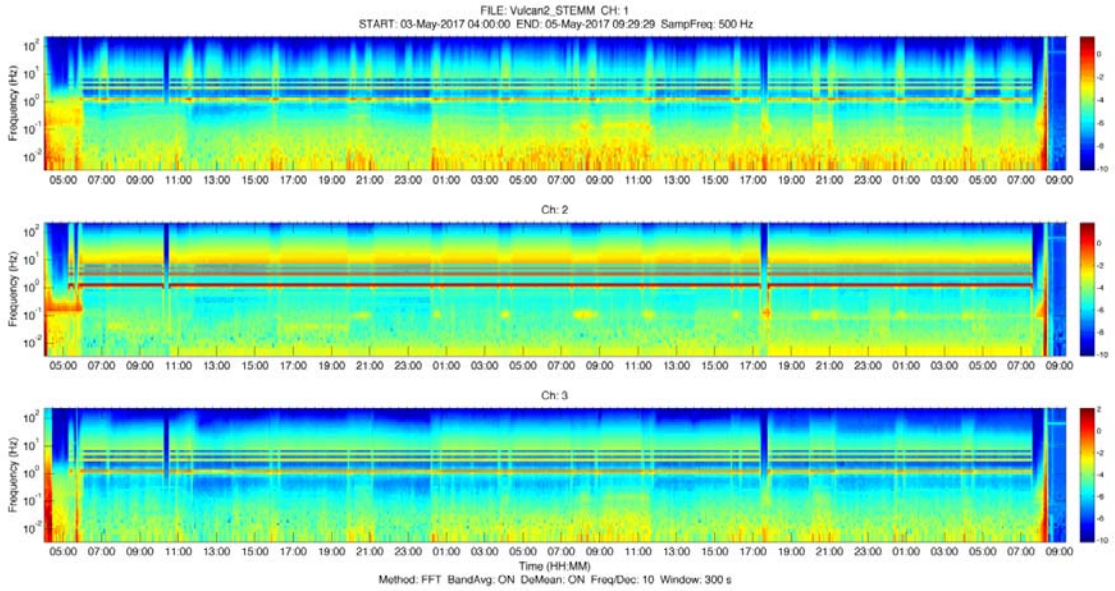

Figure 5.3.7: Spectra of the Vulcan 2 data, the electric fields Ex, Ey (inline), Ez (vertical), over a time period of two days (3rd May 4 am until 5th May 9:30 am). The base frequency of 1 Hz and the odd harmonics are the strongly visible horizontal lines.

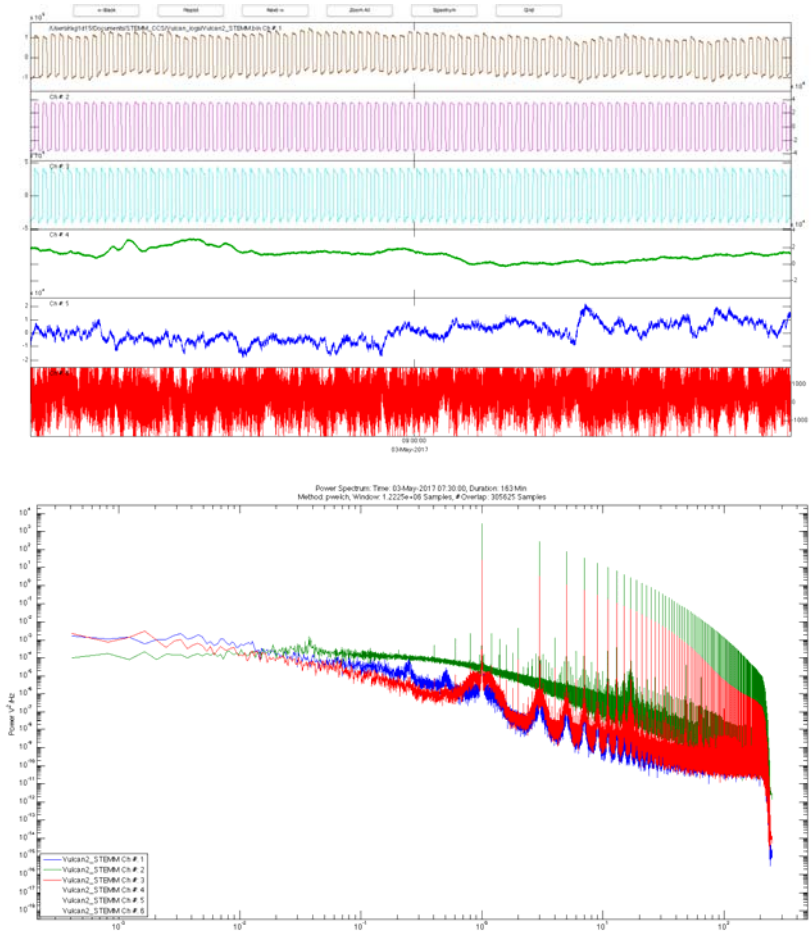

Figure 5.3.8: (Top) Electric field recording from Vulcan 2, Ex (Ch 1), Ey (Ch 2), Ez (Ch 3), and acceleration in x (Ch 4), y (Ch 5) and z (Ch 6) for a time period around 9 am May 3rd. (Bottom) Spectrum of time series in Fig. 5.3.7. The peaks at 1 Hz to 256 Hz represent the high energy in the submission frequencies.

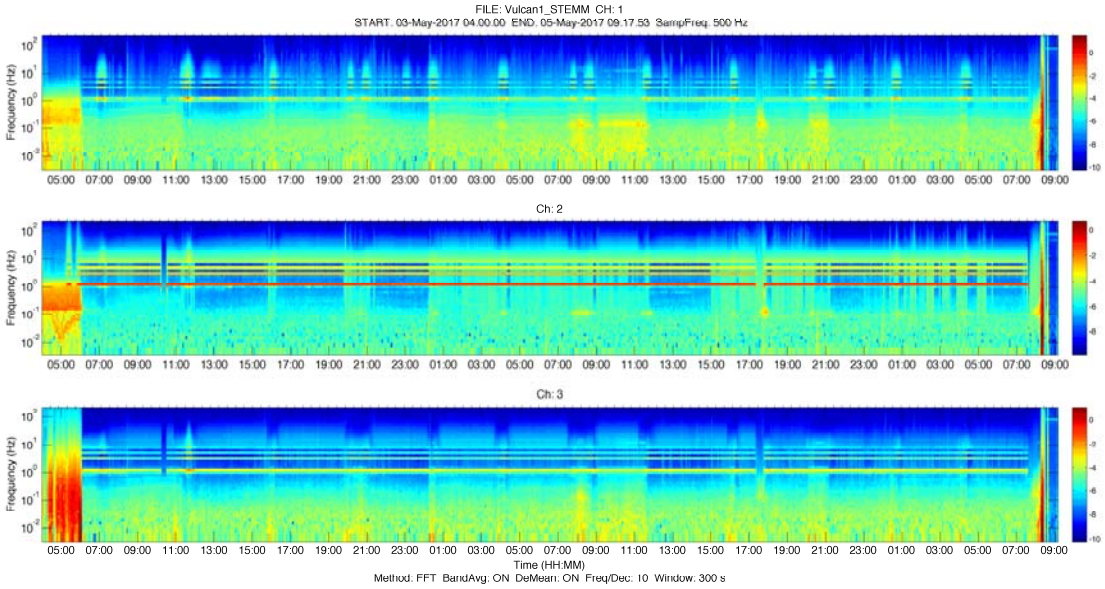

Figure 5.3.9: Spectra of the Vulcan 1 data, the electric fields Ex, Ey (inline), Ez (vertical), over a time period of two days (3rd May 4 am until 5th May 9:30 am). The base frequency of 1 Hz and the odd harmonics are the strongly visible horizontal lines.

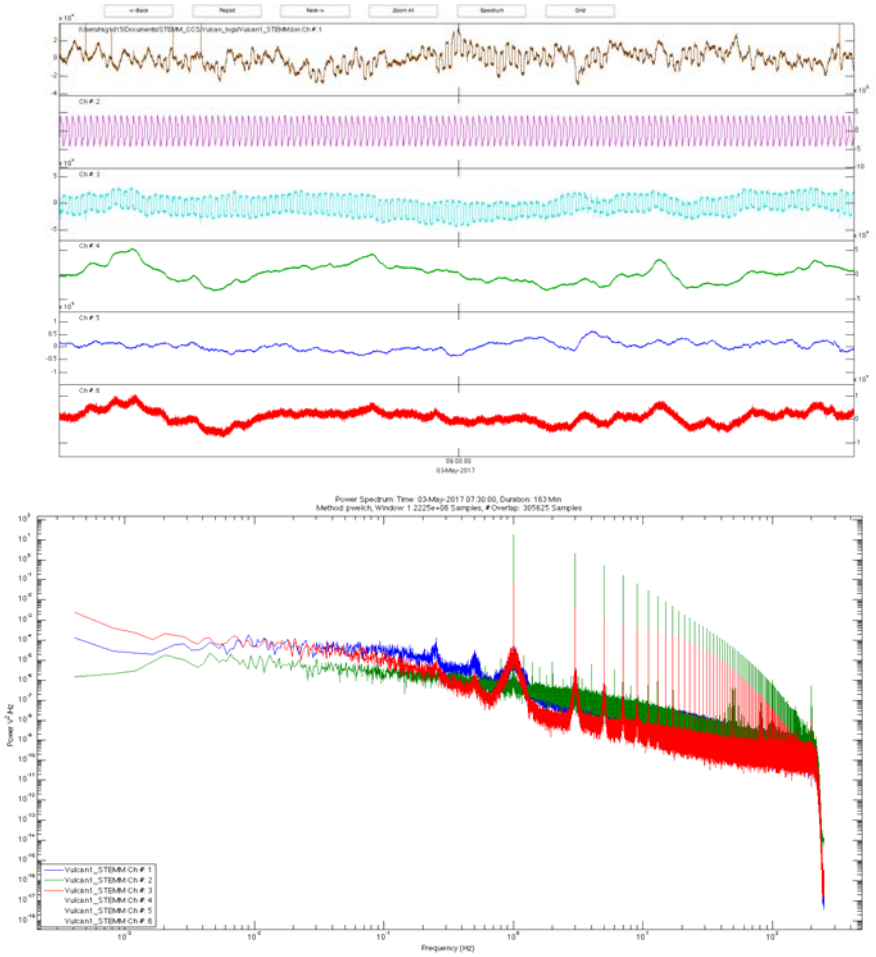

Figure 5.3.10: (Top) Electric field recording from Vulcan 2, Ex (Ch 1), Ey (Ch 2), Ez (Ch 3), and acceleration in x (Ch 4), y (Ch 5) and z (Ch 6) for a time period around 9 am May 3rd. (Bottom): Spectrum of time series. The peaks at 1 Hz to 256 Hz represent the high energy in the transmission frequencies.

5.3.3.2 OBE Data

The raw data spectra shown in show the intensity of the signal per frequency over time for EM 1 (Scripps logger, with z pole), EM 5 (Scripps logger, no z pole), and EM 11 (OBIC logger, no z-pole). The main frequency of the DASI waveform is 1 Hz and is followed by the odd harmonics (3 Hz, 5 Hz, …) which result in a tree-like image of the spectral energy over time when DASI is towed across the OBEM. Electric noise is strongest in the frequencies below 0.1 Hz and a distinct noise spectrum can be observed with in frequencies of ~0.4 Hz, 0.7, 0.8 Hz (highest energy), 1.2 Hz, 1.6 Hz, 2Hz, 2.4 Hz. Fortunately these distinct noise spectra are not overlapping with the DASI signal at 1 Hz.

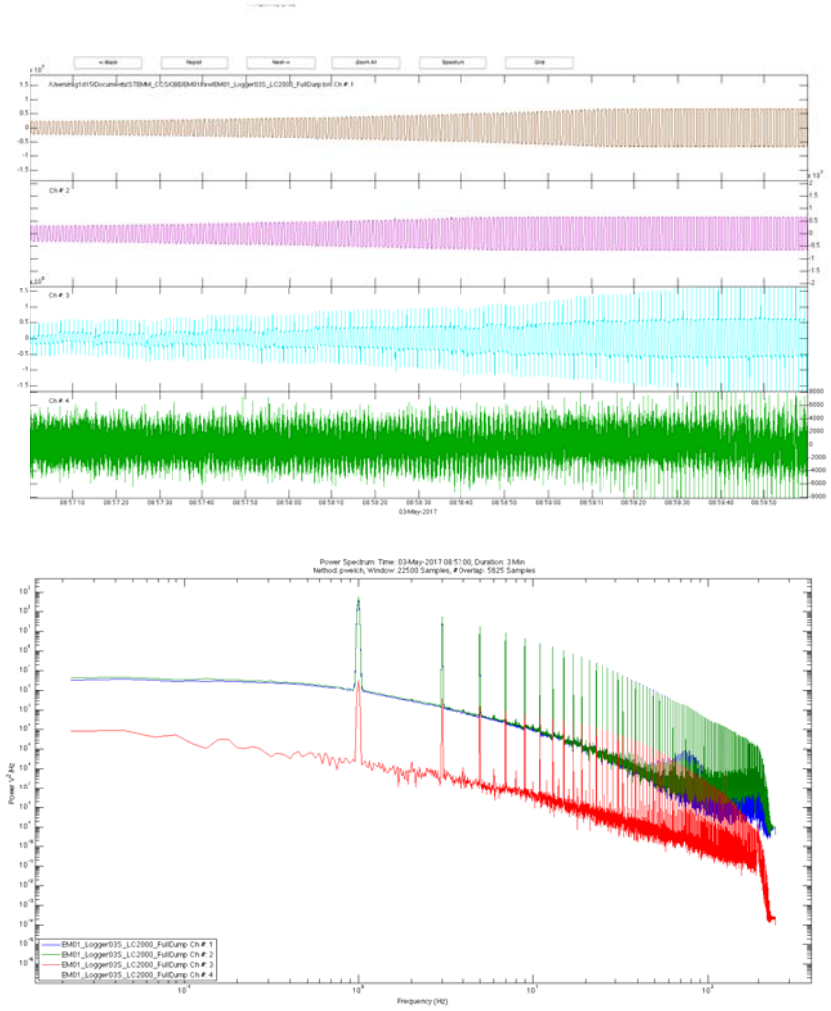

Figure 5.3.11: (Top) Time series for EM01 and profile 1 for Ex (Ch. 1), Ey (Ch. 2) and Ez (Ch. 3). The maximum range for the amplifiers is reached and the signal clipped about 150 m to the instrument. (Bottom) The spectra are shown on the right. The power decreases generally by 1/f and has significant spikes for the DASI waveform from 1 Hz up to 256 Hz.

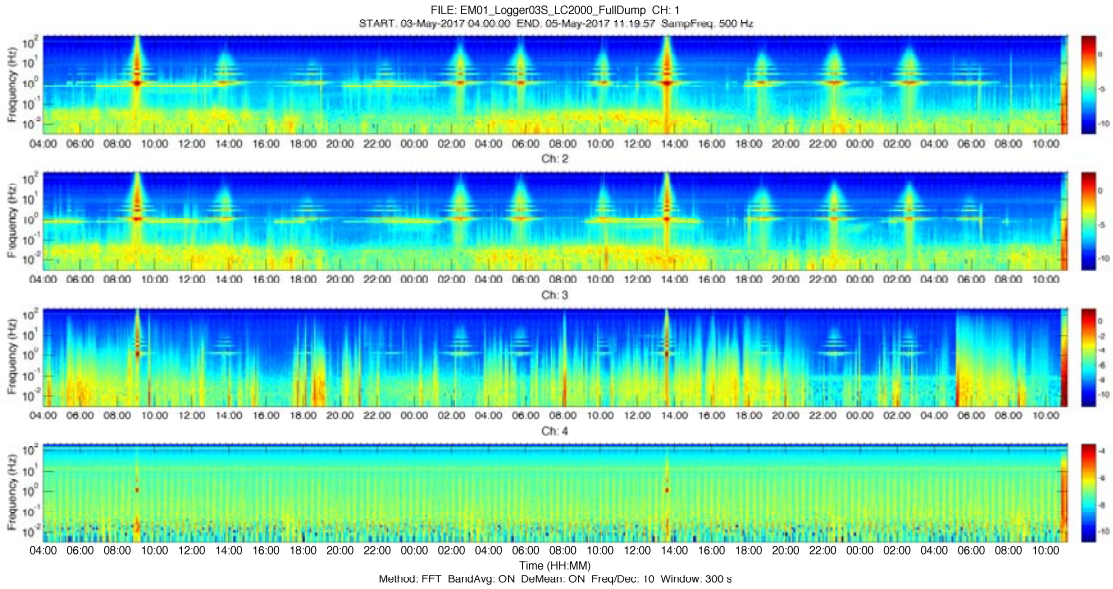

Figure 5.3.12: EM01 (Scripps data logger), which recorded Ex, Ey and Ez, was crossed by DASI on profile 1 at 9:00 May 3rd, and on profile 8 13:30 May 4th.

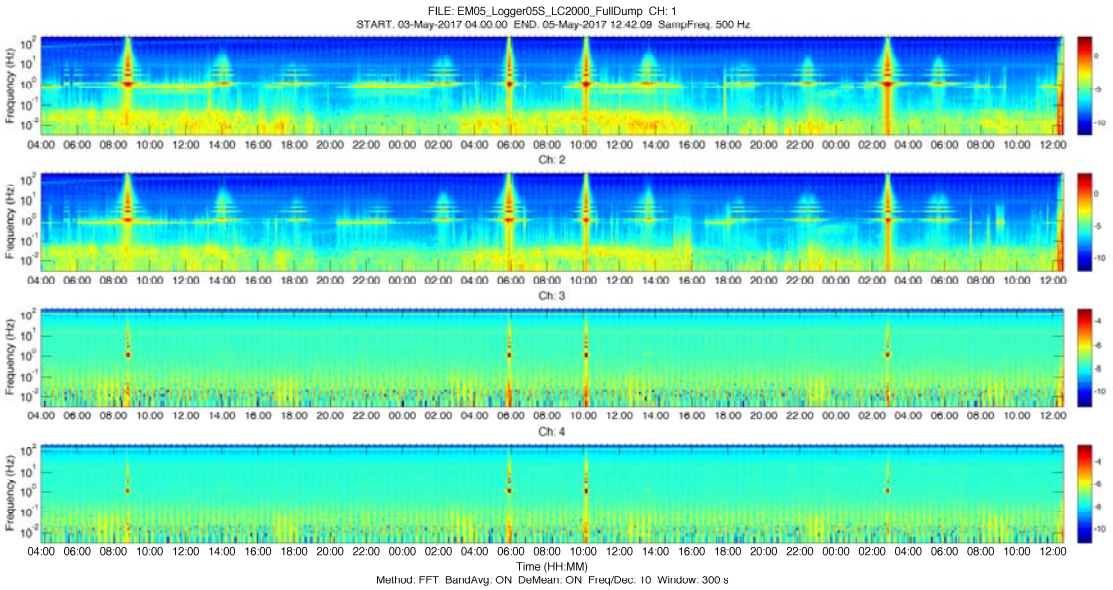

Figure 5.3.13: EM05 (Scripps data logger), which recorded Ex, Ey only, was crossed by vessel on profile 1 at 8:42 on May 3rd and on profile 6 at 5:50 on May 4th and on profile 7 at 10:10 on May 4th and on profile 11 at 02:50 on May 5th.

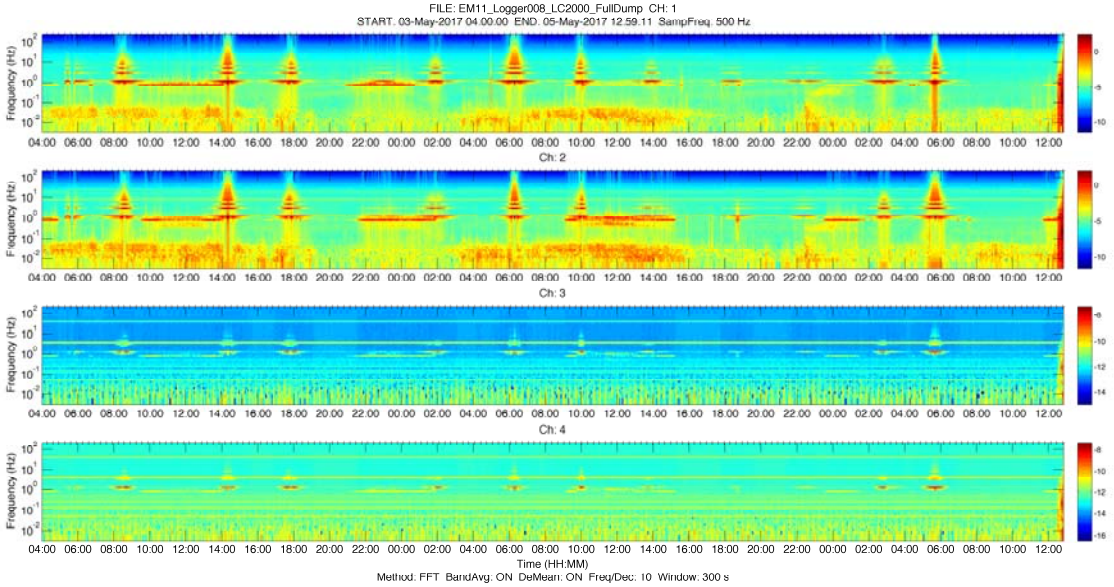

Figure 5.3.14: EM11 (OBIC data logger), which recorded Ex, Ey only, was crossed by vessel on profile 2 at 14:15 on May 3rd and on profile 6 at 6:15 on May 4th and on profile 12 at 5:36 on May 5th.

5.3.4 Conclusion

During cruise MSM63 a successful (100% recovery) marine CSEM data set was acquired with 14 OBE and 2 towed Vulcan receivers over a seismic chimney in the Scanner Pockmark site (UK waters). The electromagnetic source was towed at about 20 m above the seafloor, which increased the coupling of the signal to the seafloor compared to previous tows at 50 to 100 m altitude. Because of low-altitude tow and the shallow water (which causing a strong signal from the air interface) the observed frequencies range between 1 to 256 Hz. The OBE data shows good quality for the instruments with and without z-pole. The OBEs with the OBIC loggers use 10 times the amplification compared to the Scripps loggers and are therefore noisier, but have recorded data to an average offset of 3,7km to DASI.

5.4 Multibeam

(C. Boettner)

5.4.1 Equipment

RV MARIA S. MERIAN is equipped with two Kongsberg Maritime multibeam echosounders: The EM122 system operates at 12 kHz and covers water depths from 20 meters below the transducers up to full ocean depth, while the EM712 system uses offers three different frequency ranges (40-100 kHz, 50-100 kHz, 70-100 kHz) of signals for water depths ranging from 3 m below transducers to roughly 3500 m. Two different transmit pulses can be selected: a CW (Continuous Wave) or FM (Frequency Modulated) chirp. In case of the EM712, the latter is part of the full performance version that is installed on RV Maria S. Merian. The sounding mode can be either equidistant or equiangle, depending on operation preferences and requirements. Both systems can be operated in single-ping or dual-ping mode, where one beam is slightly tilted

forward and the second ping slightly tilted towards the aft of the vessel. The whole beam can also be inclined towards the front of the back and the pitch of the vessel can be compensated dynamically. The EM122 system produces 432 beams covering a swath angle of up to 150° while the EM712 system produces 512 beams for a maximum swath angle of 140°. The latter offers a high-density beam-processing mode with up to 800 soundings per swath. The swath angle, however, can be reduced, if required.

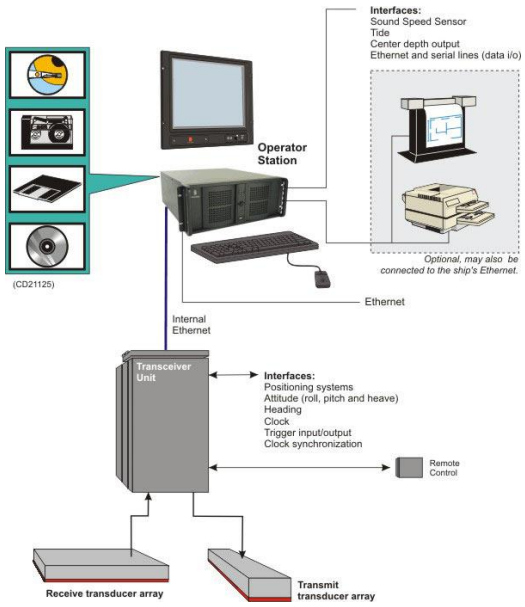

Figure 5.4.1: Configuration drawing of the EM122 system units and interfaces.

The transducers of both multibeam echosounder systems of RV MARIA S. MERIAN are mounted in a so-called Mills cross array, where the transmit array is mounted along the length of the ship and the receive array is mounted across the ship. The system on RV MARIA S. MERIAN is of a 1° x 1° design. The EM712 system installed on RV MARIA S. MERIAN is of a 0.5° x 0.5° design, but transducers are much smaller.

The echo signals detected from the seafloor go through a transceiver unit (Kongsberg Seapath) into the data acquisition computer or operator station (Fig. 5.4.1). In turn, the software that handles the whole data acquisition procedure is called Seafloor Information System (SIS). In order to correctly determine the point on the seafloor, where the acoustic echo is coming from, information about the ship's position, movement and heading, as well as the sound velocity profile in the water column are required. Positioning is implemented onboard RV MARIA S. MERIAN with conventional GPS/GLONASS plus differential GPS (DGPS) by using either DGPS satellites or DGPS land stations resulting in quasi-permanent DGPS positioning of the vessel. These signals also go through the transceiver unit (Seapath) to the operator station. Ship's motion and heading are compensated within the Seapath and SIS by using a Kongsberg MRU 5+ motion sensor. Beamforming also requires sound speed data at the transducer head, which is available from a Valeport MODUS SVS sound velocity probe. This signals goes directly into the SIS operator station. Finally, a sound velocity profile for the entire water column can be obtained from either a sound velocity probe or from a CTD (conductivity, temperature and density) probe.

The temperature (T), salinity (S) and pressure (p) data acquired by any CTD (conventional or mounted on the AUV) can be converted into sound speed by using a sound speed function C(S,T,p). During cruise MSM63 we either used direct sound velocity measurements with a special profiler or converted the sound speed from CTD data with the function by Delgrosso (1974).

In addition to bathymetric information both the EM122 and the EM712 system register the amplitude of each beam reflection as well as a sidescan signal for each beam (so-called snippets). Both systems also allow recording the entire water column. The amplitude signals correspond to the intensity of the echo received at each beam. It is registered as the logarithm of the ratio between the intensity of the received signal and the intensity of the output signal, which results in negative decibel values. For each ping EM122 records 432 backscatter intensity values while the EM712 records 800 backscatter values. The water column data correspond to the intensity of the echoes recorded from the instant the output signal is produced. All echoes coming from the water column, the seabed and even below the seabed are recorded for each beam. When the water column data of one ping is divided into a starboard and port subsets, one can produce two traces, one for each subset. Each trace is build up as a time series in which for each time the highest amplitude is selected from all beams. Then the starboard and the port traces are joint together.

5.4.2 Acquisition Parameters

During cruise MSM63 the Simrad EM122 system was not used, due to the low water depth in the central North Sea. Acquisition parameters for the EM712 system were set the following. The pulse was FM, ping mode was set to equidistant, dual ping mode was switched off, and depth mode was set to automatic. The beam angle was reduced to 130° during most of the survey, except for the survey at Goldeneye, where the maximum coverage was desired. Survey speed varied between 5 and 8 knots. Water column data were recorded throughout the survey. Data were acquired continuously, except for OBS deployment and recovery, OBEM deployment and recovery as well as during PARASOUND P70 profiles. Unfortunately, a trigger box to organize the soundings of different systems is absent on RV MARIA S. MERIAN. Therefore, we had problems with the PARASOUND P70 interfering strongly with the EM712. This made a simultaneous acquisition of data impossible. Similar interference (but not as strong as the PARASOUND) was found in combination with the ADCP38kHz system. We strongly recommend considering installing a trigger box (like on RV SONNE).

Without a CTD, we used a Levitus database' water sound profile at 0.5° E and 58.5° N. This database provides annual mean values for the water column with half-degree resolution. One SVP cast and a CTD cast were used for water sound velocity profiles: one SVP cast at the Scanner pockmark site and a CTD cast in the Goldeneye area. About 240 km^2 were mapped in detail during the cruise.

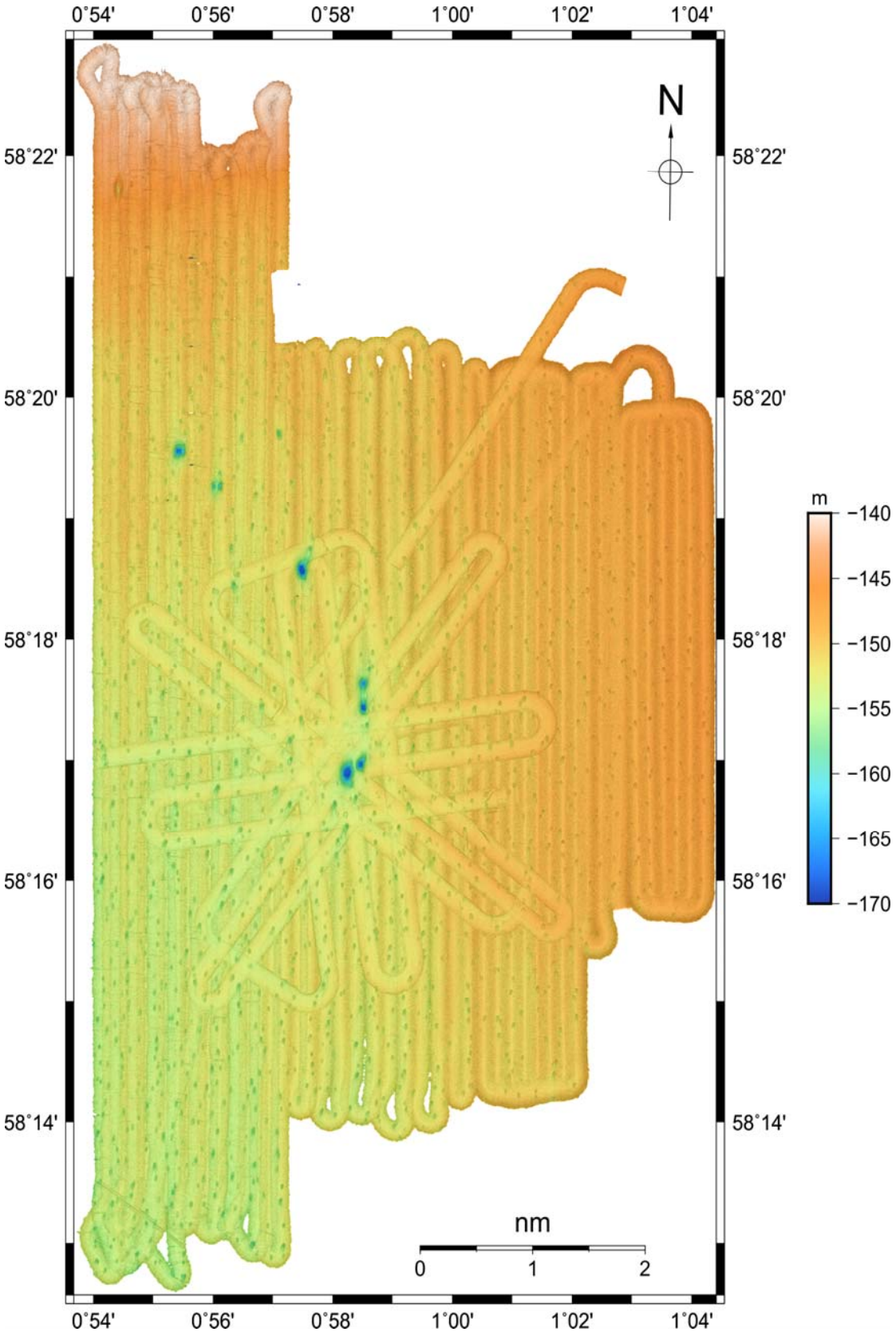

Figure 5.4.2: Multibeam map of the Scanner pockmark field mapped on research cruise MSM63

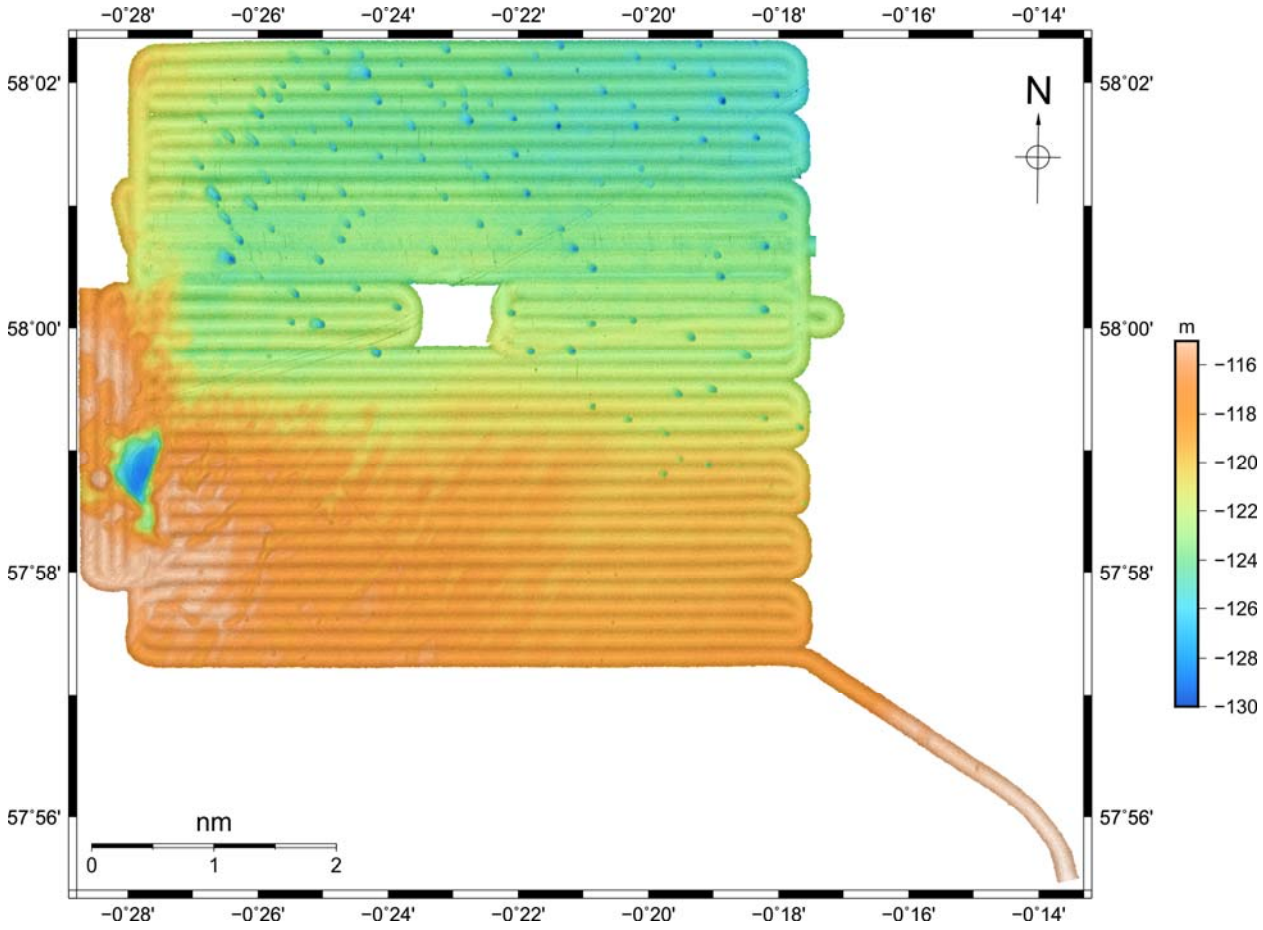

Figure 5.4.3: Multibeam bathymetrie map of the Goldeneye area mapped on the research cruie MSM63

The EM712 system was running stable throughout the cruise. Problems with the outer beams were encountered during this cruise, especially in “Dual Swath Mode”. Data obtained with the EM712 system show typical spread and increased standard deviation of the soundings with increasing distance from the nadir.

5.4.3 Data Processing

Data processing has been carried out onboard using different software packages (MB Systems, QPS Fledermaus). Within MB Systems Version 5.5.2303 (release: April 28, 2017) the processing and gridding of EM712 data took place. The soundings were preprocessed from Kongsberg all-format to an internal MB Systems format (format: 59).

The pings were cleaned in two steps (mbareaclean, mbclean). First we applied an area-filter with 3 m bin size, which flags all bad soundings with more than one standard deviation from surrounding (N=10 pings). Furthermore, we flagged all soundings with a deviation of 2% from the local (N=10 pings) median. Second we applied a swath-filter, which flags 20 outer beams (highly influenced by noise), zaps bad rails (10 m) and cleans all pings outside 10% of the mean depth for each swath. Residual bad soundings or spikes were cleaned with the manual 3D ping tool (mbeditviz).

The data were subsequently gridded with MB-Systems using a Gaußian weighted mean with a cell size of 5 m. Around the Scanner pockmark the coverage of swath data allowed 3 m cell sizes. To eliminate unwanted influence of outer beams on the grid, induced by deviation of the outer beams, we applied a spline tension with a value of 2. All data were interpolated for a maximum of 3 cell sizes to achieve good coverage for the high-resolution grid.

5.4.4 Backscatter

The backscatter (amplitude) signal is stored and preprocessed automatically by the Kongsberg software Seafloor Information System (SIS), including altitude processing, time varying gain (TVG) and angle varying gain (AVG). Backscatter data were processed onboard using FMGeocoder. The backscatter have been processed using FMGeocoder, where radiometric corrections, filtering, anagle-varying gain and anti-aliasing filters are applied to the backscatter data before outputting a georeferenced mosaic.

5.4.5 Water Column

The EM710 multibeam echosounder produces a second type of raw data files with extension *.wcd, which stores water column data. These files were imported into QPS FmMidwater. The raw multibeam echosounder data (.all format) and associated water column data (.wcd) were placed into a single folder and imported into FMMidwater. Each line was subsequently opened in Swath Editor and displayed as a curtain image (along track, viewed from starboard side) and a time-series video (across track, viewed from stern). The data were also filtered by intensity. We found evidence for gas flares at emerging from the seafloor and especially in the Goldeneye area an abundance of shoals of fish or sediment plumes in the water column.

5.4.6 Preliminary Interpretation

5.4.6.1 Scanner Pockmark

The bathymetric map of the Scanner pockmark shows a clear depression on the seafloor and a satellite pockmark towards the east. The measurements show a depression of elliptical shape with 180 m diameter in North-South direction and 160 m in East-West direction. The depth is ~16 m in comparison to the surrounding seafloor. North of the Scanner pockmark the Scotia pockmark is visible. Similar to the Scanner pockmark this feature is an elliptical shaped. Both giant pockmarks are surrounded by small scale depressions with tens of meters in diameter and only 1-3 m in depth. All pockmarks (giant and small) show sharp edges towards the northeast and smooth-out towards the southwest.

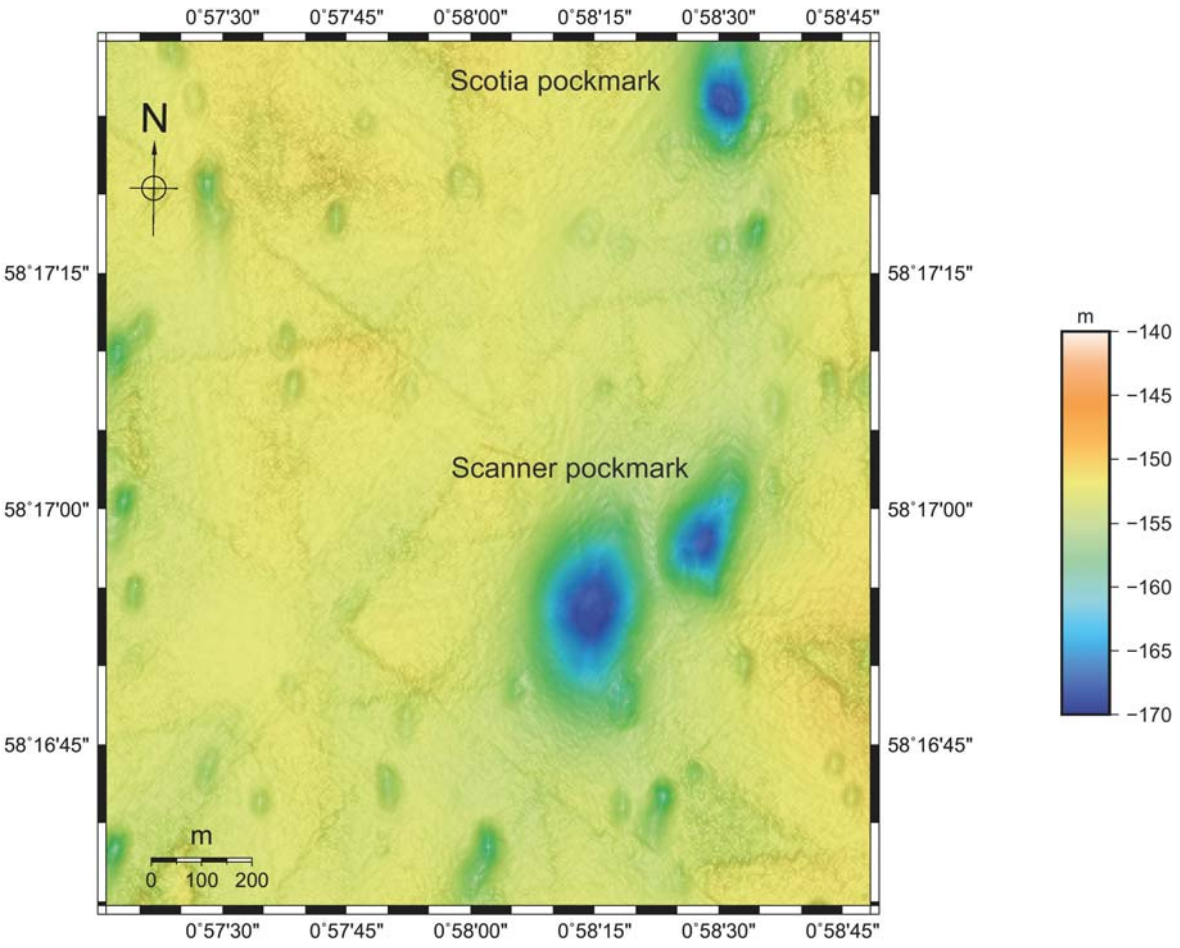

Figure 5.4.4: Bathymetric map of the Scanner pockmark, satellite pockmark and the Scotiapocokmark. The area is interspersed with numerous small-scale pockmarks.

Unfortunately, the data were not corrected for tides and the calibration (heave, roll, pitch) was not finished during the cruise. Therefore, the data shows distinct patterns of noise and unmatched boundaries of adjacent swaths.

The backscatter map shows high backscatter in bright colors and low backscatter in dark colors. Pockmarks are well resolved with the backscatter and show high values at the edges. This might be an effect of bathymetry, but could also indicate carbonates at the edges. Towards the northwest of the Scanner pockmark, a bright spot in backscatter indicates the location of the abandoned well 15/25b-01A. Plough marks govern the seafloor imagery and backscatter East of the Scanner pockmark (see Figure 5.4.5 zoom).

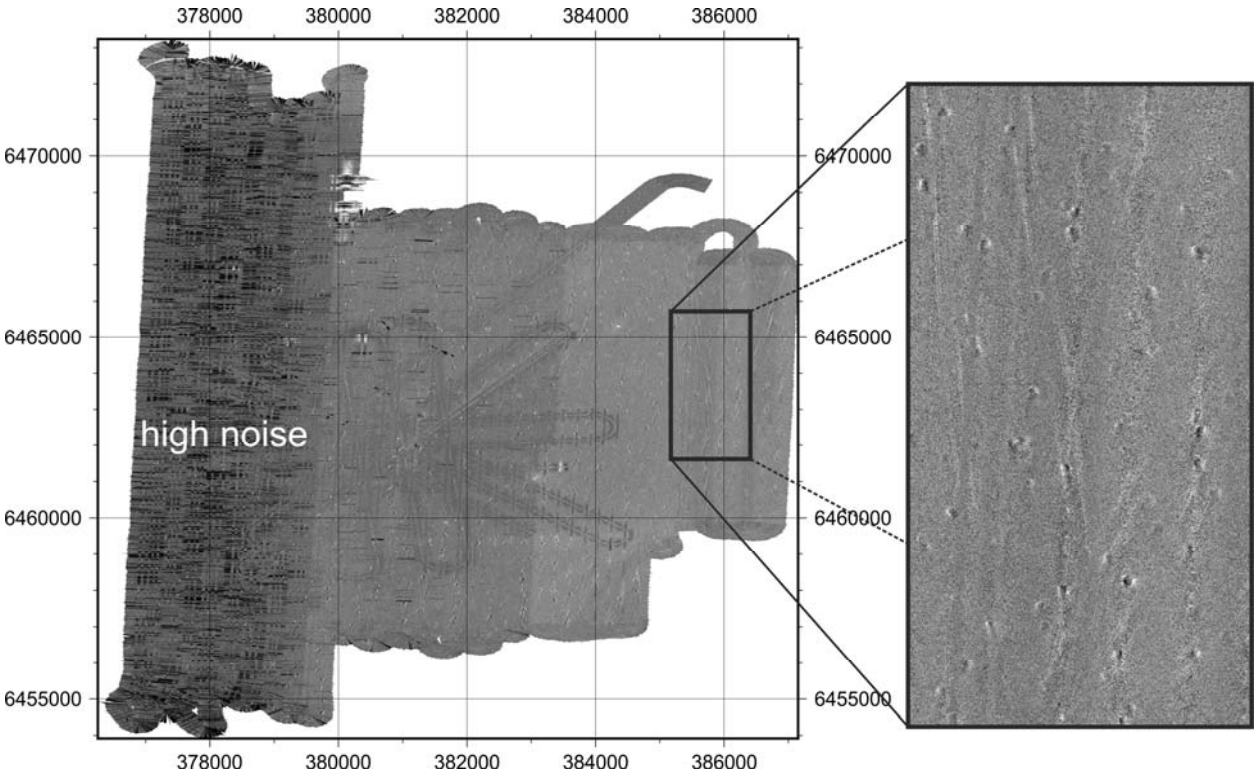

Figure 5.4.5: Backscatter of EM712 multibeam system. The map is highly influenced by noise, which a storm and subsequent heavy waves produced. The zoom shows plough marks at the seafloor.

The water-column imaging was used to identify possible seep sites. All major pockmarks in the area show distinct flares emerging from the center of the large-scale depressions. The flares (gas escape from the seafloor) reach up to 50 m above the seafloor and show indications for strong dependency on bottom currents (e.g. tidal currents).

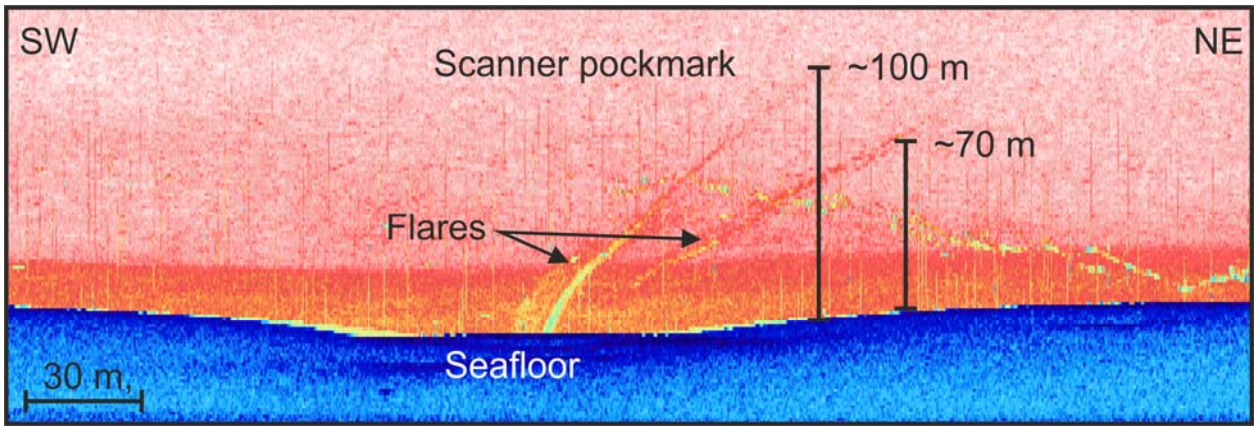

Figure 5.4.6: Range stack of watercolumn imaging showing flares above the Scanner pockmark. The flares are deviated from bottom current, but ascent up to 100 m into the water column from the seafloor. A fish shoal is visible as clear disturbance of the water column from the seafloor. A fish shoal is visible as clear disturbance of the water column in form of small Blue colors represent high backscatter and red colors low backscatter.

5.4.6.2 Goldeneye Platform

The Goldeneye platform area shows an increase in water depth towards the northwest. In the southwest of the survey area NNE-SSW trending scour marks and small pockmarks shape the seafloor. Towards the northeast, the pockmarks increase in occurrence. In general, the pockmarks in this area are small-scale depressions at the seafloor with tens of meters in diameter and 1-3 m in depth. The center data gap is a result of the 600 m minimum safety distance between the ship and the Goldeneye platform.

A several pipelines are crossing the survey from the northwest towards the northeast, of which one is directly connected to the Goldeneye platform. Southwest of our survey area, we identified a canyon-like geological feature at the seafloor. The canyon shows a small source area in the South and a fan-shaped depression towards the North.

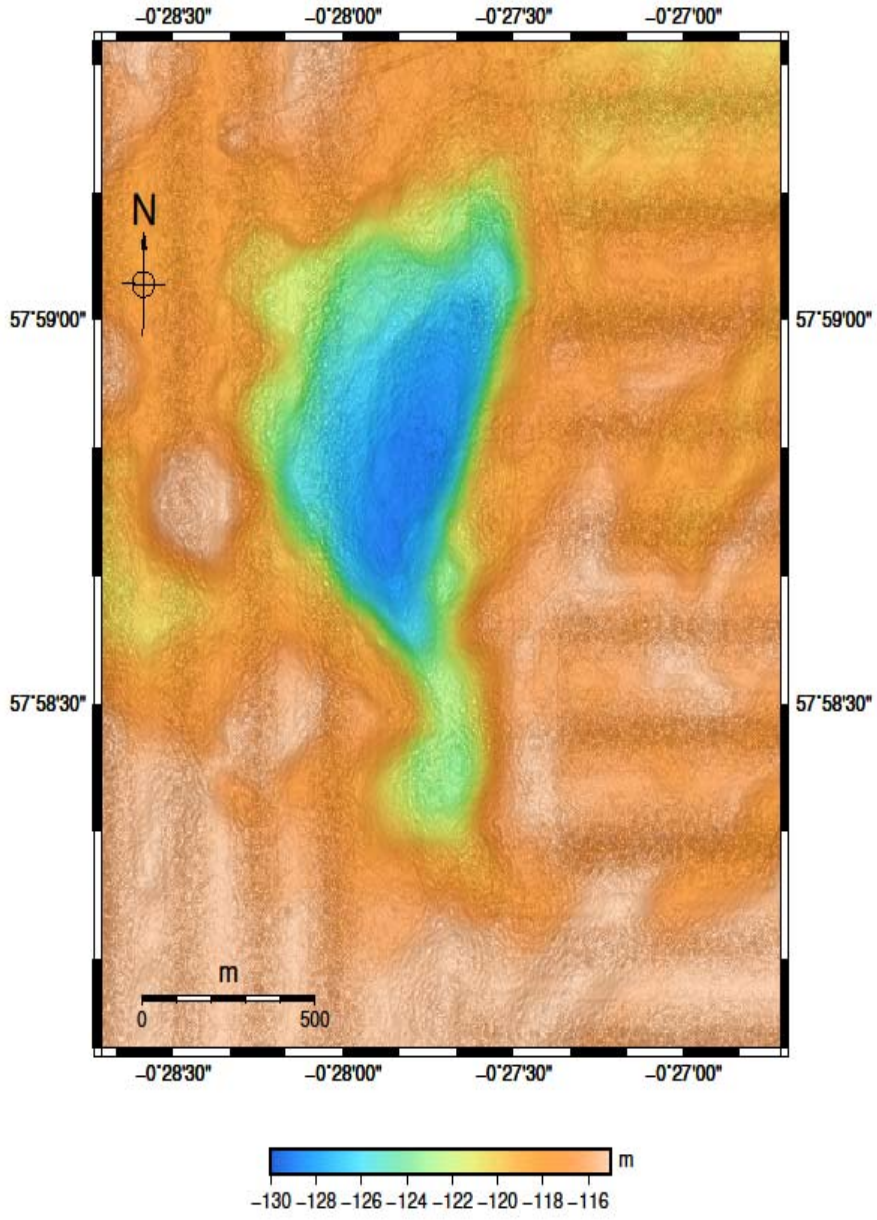

Figure 5.4.7: Bathymetric map of canyon system southwest of the Goldeneye platform. The canyon shows a small source area in the south and a fan-shaped depression towards the North.

Backscatter

The backscatter map indicates the locations of the pipelines crossing the survey area as well as the abundant pockmarks (See Figure 5.4.9, zoom 1). In the South the pockmarks show high backscatter (light color) as a result of erosion down to the glacial tills, which likely are poor sorted and therefore create high backscatter. South of the Goldeneye platform (data gap in the center) four pockmarks different pattern of backscatter as they have dark colors, indicating low backscatter (See Figure 5.4.9, zoom 1). Towards the North and East, the pockmarks show similar backscatter patterns to the Scanner pockmark area and ploughmarks are abundant (See Figure 5.4.9, zoom 2). The inner circle shows low backscatter and the edges high backscatter (See Figure 5.4.9, zoom 3).

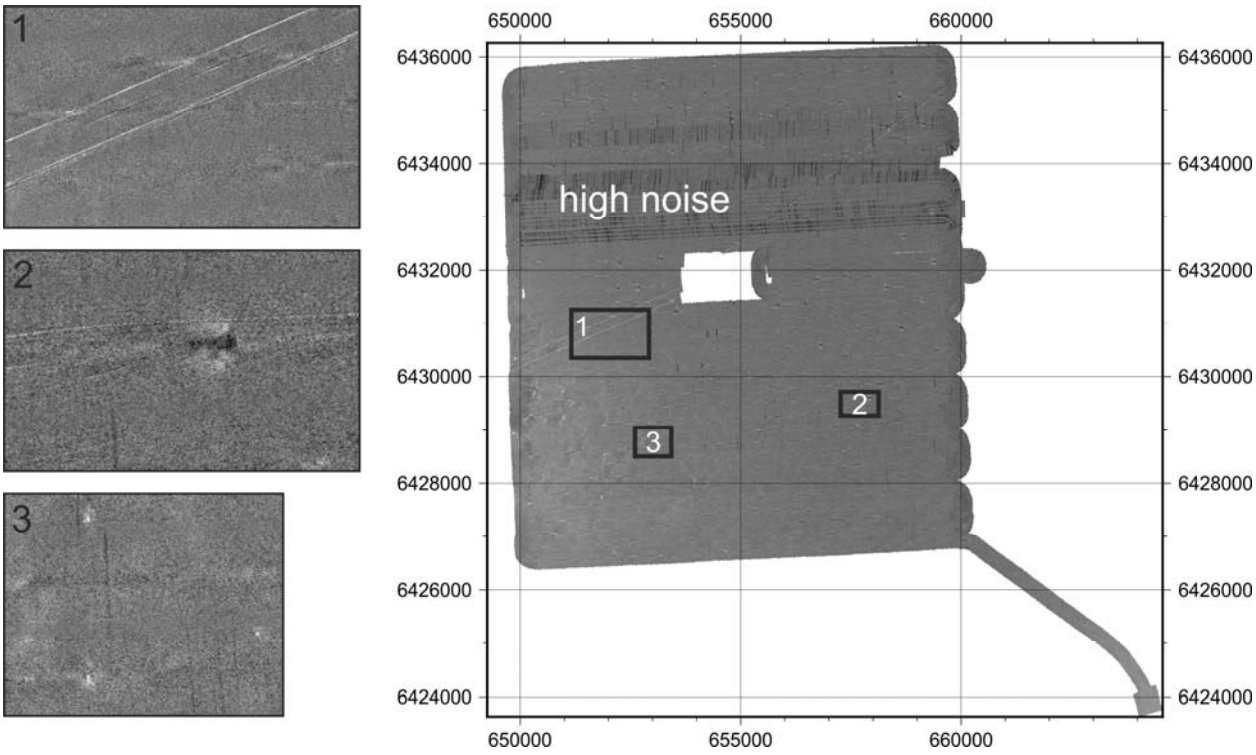

Figure 5.4.8: Multibeam backscatter map of the Goldeneye area

WCI

Indications for fluid escape from the seafloor can be observed within the Goldeneye water column images. The observed flare show heights inside the water column ranging between 15 m and ~70 m. However, the possible flares are not easy to distinguish from shoals of fish. Nevertheless, the abundance of flare within the water column and small-scale sediment plumes indicate fluid flow activity or active seepage in the Goldeneye area.

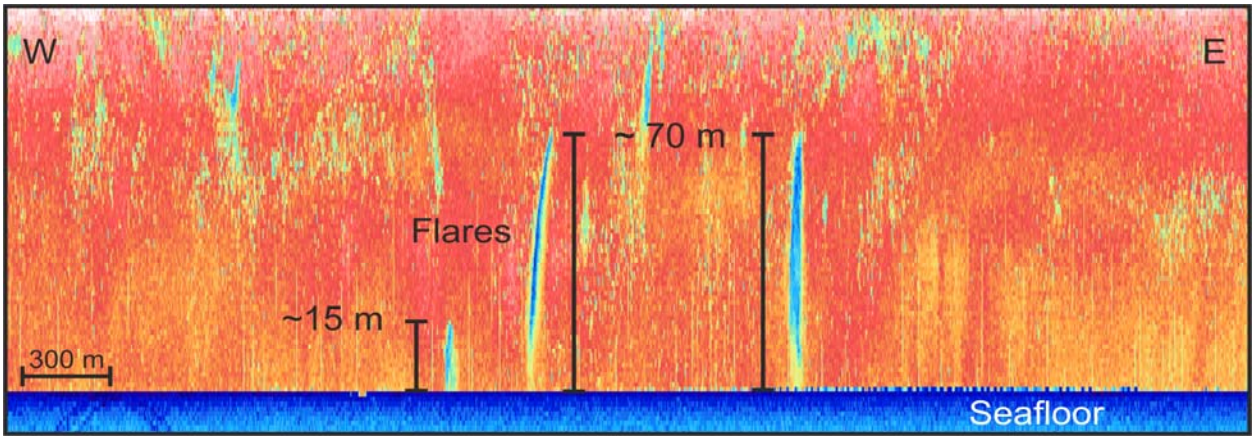

Figure 5.4.10: Range stack of watercolumn im aging showing flares within the Goldeneye platform area. The flares ascent up to 70 m into the water column from the seafloor. Blue colors represent high backscatter and red colors low backscatter.

5.5 Parasound

(Christoph Böttner)

5.5.1 Method

The hull-mounted parametric sub-bottom profiler PARASOUND P70 (Atlas Hydrographic) was operated on a 24-hour schedule for flare imaging and to provide high-resolution (less than 15cm for sediment layers) information on the uppermost 50-100 m of sediment. The system has a depth range of 10 m to > 11000 m (full ocean depth) and a maximum penetration of 200 m. This high sediment penetration is acquired through the high pulse transmission power of 70 kW.

The RV Maria S. Merian is equipped with a PARASOUND P70 system since the start in 2007. PARASOUND P70 works as a narrow beam sediment echo sounder, providing primary frequencies of 18 (PHF) and adjustable 18.5 – 28 kHz, thus generating parametric secondary frequencies in the range of 0.5 – 6 kHz (SLF) and 36.5 – 48 kHz (SHF) respectively. The secondary frequencies develop through nonlinear acoustic interaction of the primary waves at high signal amplitudes. This interaction occurs in the emission cone of the high-frequency primary signals, which is limited to a beam width of 4.5° x 5° for the PARASOUND P70. The system consists of four identical transducer modules, each about 0.3 m x 1.0 m. The P70 version includes 384 acoustic elements combined to form 128 stave channels. Therefore, the footprint size is approx. 4% of the water depth and vertical and lateral resolution is significantly improved compared to conventional 3.5 kHz echo sounder systems. The system provides features like recording of the 18 kHz primary signal and both secondary frequencies, continuous recording of the whole water column, beam steering, different types of source signals (continuous wave, chirp, barker coded) and signal shaping. Digitization takes place at 98 kHz to provide sufficient sampling rates for the high secondary frequency. A down-mixing algorithm in the frequency domain is used to reduce the amount of data and allow data distribution over Ethernet.

For the standard operation a parametric frequency of 4 kHz and a sinusoidal source wavelet of 3 periods were chosen to provide a good balance between signal penetration and vertical resolution. The 18 kHz signal was also recorded permanently.

At the survey area the system was mainly used for analysis of sedimentary processes, such as identification of different phases of glacial deposition or erosion. Due to low water depth (< 200m) at the survey area the Parasound system was operated in a single pulse mode.

Except for the first day, where the electrical unit of the Parasound did not work due to a non-closed lid, technical problems did not occur during our cruise. The system worked reliable and produced high-quality data throughout the whole time. Unfortunately, the PARSOUND P70 could not be used during multibeam surveys. The systems causes strong interference within the new installed EM712. A trigger box to organize the signals during acquisition, as it is installed on RV Sonne, is missing.

All raw data were stored in the ASD data format (Atlas Hydrographic), which contains the data of the full water column of each ping as well as the full set of system parameters. Additionally a 200 m-long reception window centered on the seafloor was recorded in the compressed PS3 and SEGY data format after mixing the signal back to a final sampling rate of 12.1 kHz. This format is in wide usage in the PARASOUND user community and the limited reception window provides a detailed view on subbottom structures.

All data were converted to SEG-Y format during the cruise using the software package ps32sgy (Hanno Keil, Uni Bremen). The software allows generation of one SEG-Y file for longer time periods, frequency filtering (low cut 2 kHz, high cut 6 kHz, 2 iterations), subtraction of mean and envelope calculation. We used the frequency filtering and loaded all data to the seismic interpretation software HIS Kingdom. The Envelope was calculated subsequently within the IHS Kingdom. If seismic data were collected simultaneously, one SEG-Y file was created for the length of each seismic profile. In all other cases 1h-long pieces were generated (e.g. during transit, long seismic lines). This approach allowed us to obtain a first impression of sea floor morphology variations, sediment coverage, sedimentation patterns along the ship’s track and imaging of glaciation phases. In addition the data was converted from time to depth domain with an average velocity of 1500 m/s to select locations for the BGS RockDrill2.

5.5.2 Initial Results

We used the PARASOUND P70 to analyze and interpret the uppermost sedimentary succession in the survey area, located in the central North Sea. Despite the expected coarse-grained material and glacial tills on the North Sea seafloor, the system showed very good penetration rates, in some cases exceeding 60 m below the seafloor.

The PARASOUND P70 provided high-resolution images of the upper 10-30 m, which we were not able to see in the industry 3D seismic volumes with 12.5 m lateral and approximately 7 m vertical resolution. We used the system to identify and verify any fluid conduits reaching to

the surface. Due to the high-frequency signal the system is highly sensitive to fluids or gases within the sedimentary succession and above the seafloor. However, the first target of the cruise A03 did not show any indications for fluid migration pathways within the upper 12 m sub-seafloor or fluid escape into the water column in form of flares. Unfortunately, the penetration depth in this survey area did not exceed 12 m due to the high impedance contrast of the underlying glacial debris unit (chaotic to transparent unit) and the water column.

The second target was the Scanner pockmark, which is located in Block UK15/25. Judd et al. [1994] describe several small pockmarks and three major pockmarks in Block UK15/25. The pockmarks are named after the vessels that were used during the expeditions (Scanner, Scotia and Challenger). The topmost sedimentary succession is composed of the Witchground member, Witchground formation and the Fladen member. The upper three units are underlain by the Coal Pit formation, which also forms the base of all major pockmarks in this area [Judd et al., 1994].

We were able to identify all three major pockmarks with the PARASOUND P70 system and map the former described composition of the sedimentary succession. The Coal Pit formation represents the acoustic basement for our PARASOUND P70 data. All major pockmarks showed flares (high backscatter in the water column), which indicate their activity in terms of fluid flow from the subsurface. Our PARASOUND P70 data shows a strong correlation of the abundant pockmarks with the Witchground formation. The numerous small pockmarks do not show recent activity in form of flares.

The overall penetration in the Scanner pockmark area is very good and in many parts up to 30 m into the subsurface. We used the very high-resolution PARASOUND P70 profiles in addition to the existing 3D seismic data, to identify possible drill targets for the second part of the cruise with the BGS's RockDrill2.

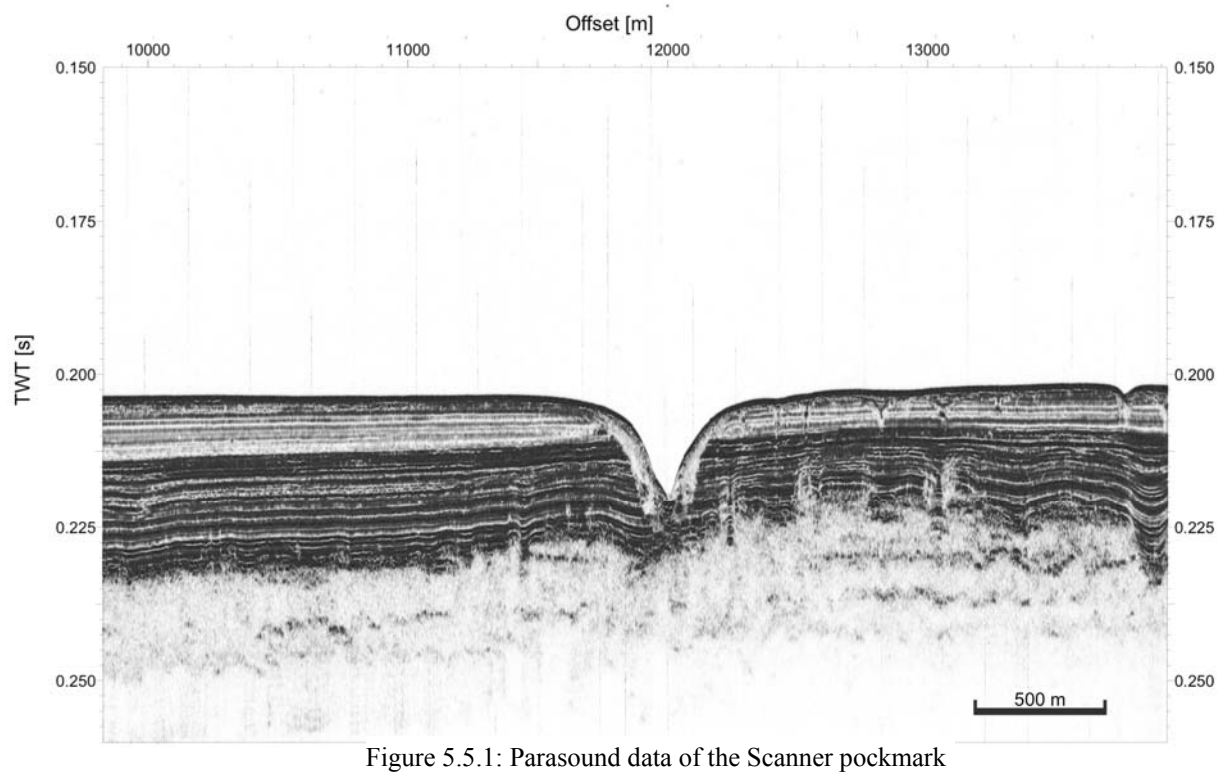

Figure 5.5.1: Parasound data of the Scanner pockmark

The second leg was originally planned to acquire sediment cores with the BGS RockDrill2. Due to unforeseen technical problems we were not able to achieve that goal. Our alternative scientific program at Goldeneye platform included a site survey for the STEMM-CCS project and other work-packages within the program. With several regional lines, we were able to trace the Witchground formation over a large area and identify geological features such as pockmarks, channels and fluid migration pathways. The Witchground formation is underlain by several glacial deposit units, that separate each other by small impedance contrasts in between. The seismic facies of glacial deposits are transparent to chaotic and give insights on the poor sorting of the glacial tills.

The Witchground formation pinches out towards the SE of our survey area and thickens towards the NE. It shows high similarity with the region around the Scanner pockmark in terms of seismic facies and shares the abundance of small-scale pockmarks. However, medium- to large-scale pockmarks are not identified. There is no clear evidence for pockmark activity (flares) around the Goldeneye platform. However, we found small-scale high-reflectivity patches, which could either be shoals of fish or sediment plumes lifted from the seabed by gas escape activity [Judd, 1990; McQuillin & Fannin, 1979].

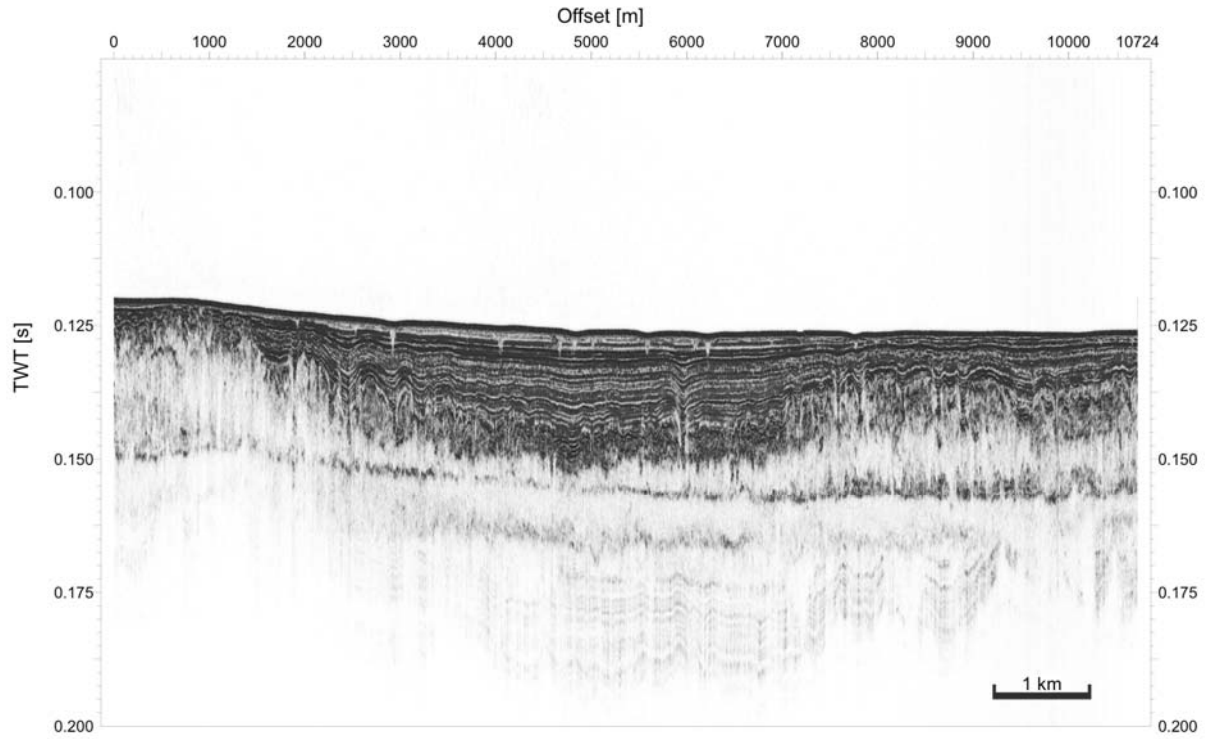

Figure 5.5.2: Parasound data of the Witchground formation

5.6. Chemistry and Hydrography

(A. Lichtschlag, A. Flohr, K. Peel, I. Falcon-Suarez, A. Dutrieux)

During the 2nd leg of the expedition we focused on water column sampling in the vicinity of the Goldeneye platform. These data will provide important insights into the hydrographical and biogeochemical characteristics of the Goldeneye region in spring/early summer. This data set

will complement the upcoming baseline cruises planned in the framework of the STEMM-CCS project for the autumn/winter period and thus will make a useful contribution to characterise the seasonal variability.

5.6.1 Water Column Sampling

The main target area extended approximately 10 x10 km around the Goldeneye platform (Fig. 5.6.1a). An additional target was the Scanner pockmark and a reference station approximately 500 m NW of the pockmark (Fig. 5.6.1b). Hydrographical profiles of temperature, salinity, turbidity, fluorescence and oxygen were acquired with a Sea-Bird SBE9plus CTD with a rosette water sampler equipped with NISKIN bottles (Table 2, Fig. 5.6.2). Conductivity, temperature and oxygen were measured with duplicate sensors.

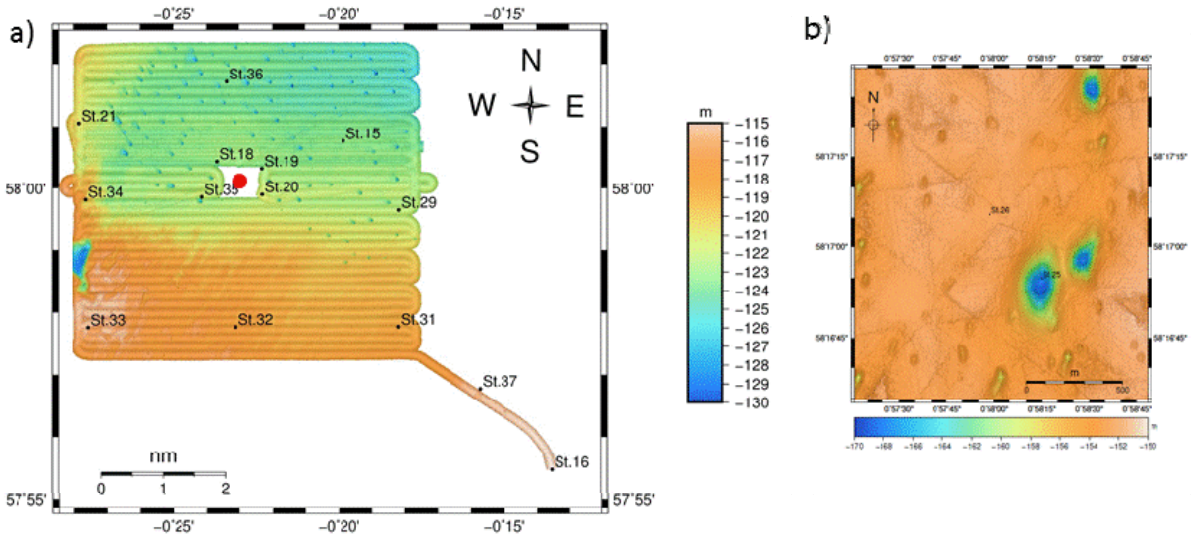

Figure 5.6.1: a) CTD sampling stations in the vicinity of the Goldeneye platform; the location of the platform is indicated by the red dot; b) CTD sampling stations inside the Scanner pockmark and at a reference site. Map: courtesy of C. Böttner (Fig. 5.4.4).

The water column was sampled at fixed depth levels: typically at 2, 10, 20 and 30 m above seafloor; one sample in the florescence peak and one surface water sample at 5 m water depth (Table 2). Samples were collected using silicone tubing with care to avoid the formation of bubbles. To minimise contact with the atmosphere at least twice the volume of the containers was allowed to overflow. Water samples were retained for dissolved inorganic carbon (DIC), total alkalinity (TA), nutrients, dissolved organic carbon (DOC), total organic carbon (TOC) and methane (CH_4). All samples were taken in duplicates (i.e. 2 different CTD bottles from the same water depth). DIC and TA samples were collected in 20 ml supra seal screw cap vials and

Figure 5.6.2: Deployment of CTD rosette. Courtesy of A. Dutrieux

methane in 20 ml glass bottles with a supra crimp seal top. To stop microbial activity 10 µL supersaturated $HgCl_2$ were added to the DIC, TA, and methane samples. TOC/DOC samples (4 ml each) were acidified with 10 µL of 6 M HCl. Nutrient samples were filtered (0.45 µm) into 20 mL plastic vials and frozen at -20°C. Samples will be analysed in the NOC/SOTON laboratories.

Table 2: Water column sampling in the Goldeneye area and the Scanner pockmark area.

station	CTD	date	time (start)	latitude	longitude	water depth (m)	sampling depth (m)	Parameters	Area
15	1	19.05.2017	12:15	58°00.763' N	0°19.850' W	124	120,109,100,90,6	CH_4, DIC, TA, DOC, TOC, nutrients	Goldeneye
16	2	19.05.2017	15:31	57°55.470' N	0°13.529' W	104	102, 92, 82, 72, 6.5	CH_4, DIC, TA, DOC, TOC, nutrients	Goldeneye
18	3	20.05.2017	07:23	58°00.430' N	0°23.676' W	124	122, 112, 102, 92, 25, 65	CH_4, DIC, TA, DOC, TOC, nutrients	Goldeneye
19	4	20.05.2017	10:32	58°00.320' N	0°22.312' W	124	118, 109, 99, 89, 25, 65	CH_4, DIC, TA, DOC, TOC, nutrients	Goldeneye
20	5	20.05.2017	12:12	57°59.902' N	0°22.304' W	122	119, 108, 98, 88, 30, 6.5	CH_4, DIC, TA, DOC, TOC, nutrients	Goldeneye
21	6	20.05.2017	14:06	58°01.047' N	0°27.837' W	121	116, 106, 96, 86, 25, 6.7	CH_4, DIC, TA, DOC, TOC, nutrients	Goldeneye
25	7	21.05.2017	12:24	58°16.914' N	0°58.248' E	169	165, 160, 155, 145, 140, 135, 20, 6.7	CH_4, DIC, TA, DOC, TOC, nutrients	Scanner pockmark
26	8	21.05.2017	13:48	58°17.091' N	0°57.983' E	154	149, 139, 128, 119, 30, 6.5	CH_4, DIC, TA, DOC, TOC, nutrients	outside Scanner pockmark
29	9	22.05.2017	07:39	57°59.654' N	0°18.148' W	123	no sampling	no sampling	Goldeneye
31	10	22.05.2017	08:49	57°57.770' N	0°18.161' W	120	114.9, 105, 95, 85, 21, 6.3	CH_4, DIC, TA, DOC, TOC, nutrients	Goldeneye
32	11	22.05.2017	10:01	57°57.767' N	0°23.101' W	119	no sampling	no sampling	Goldeneye
33	12	22.05.2017	11:11	57°57.759' N	0°27.567' W	116	111, 101, 91, 81, 18, 6.4	CH_4, DIC, TA, DOC, TOC, nutrients	Goldeneye
34	13	22.05.2017	12:19	57°59.817' N	0°27.640' W	121	no sampling	no sampling	Goldeneye
35	14	22.05.2017	13:18	57°59.860' N	0°24.126' W	122	118, 108, 98, 88, 22, 6.5	CH_4, DIC, TA, DOC, TOC, nutrients	Goldeneye
36	15	22.05.2017	14:22	58°1.715' N	0°23.389' W	124	no sampling	no sampling	Goldeneye
37	16	22.05.2017	15:27	57°56.774' N	0°15.969' W	115	no sampling	no sampling	Goldeneye

Table 3: Sensors mounted on Sea-Bird SBE9plus CTD and their specifications

Parameter	Instrument	S/N
Conductivity1	SBE4	4152
Conductivity1	SBE4	4156
Temperature 1	SBE3	5716
Temperature 1	SBE3	5719
Oxygen 1	SBE 43	2417
Oxygen 2	SBE 43	2418
Fluorescence	MSM-SPAR-20195	20195
Turbidity	FluroWetlabECO_AFL_FL_Sensor	1754
Altimeter	-	1187
Pressure	SBE9plus	0807

5.6.2 Preliminary Results

The hydrography of the northern North Sea is influenced by the inflow of warm and saline Atlantic water entering through the Orkneys-Shetland section, the Shetland shelf and the Norwegian trench. It is further influenced by inflow of less saline water from the Baltic Sea and fresh water from river discharge indicative of diverse factors influencing the composition of subsurface water in the Goldeneye region. The temperature ranged between 7.5 - 9.8 °C, salinity varied between 34.82 - 35.17. The $T_{(pot)}$-S plot (Fig. 5.6.3) and vertical section along a NW-SE transect (Fig. 5.6.3) indicates that the subsurface water originated from a similar high saline "source water" (8°C, salinity 35.1-35.17) with influence of slightly cooler, low saline water towards the eastern most stations #16 and#37.

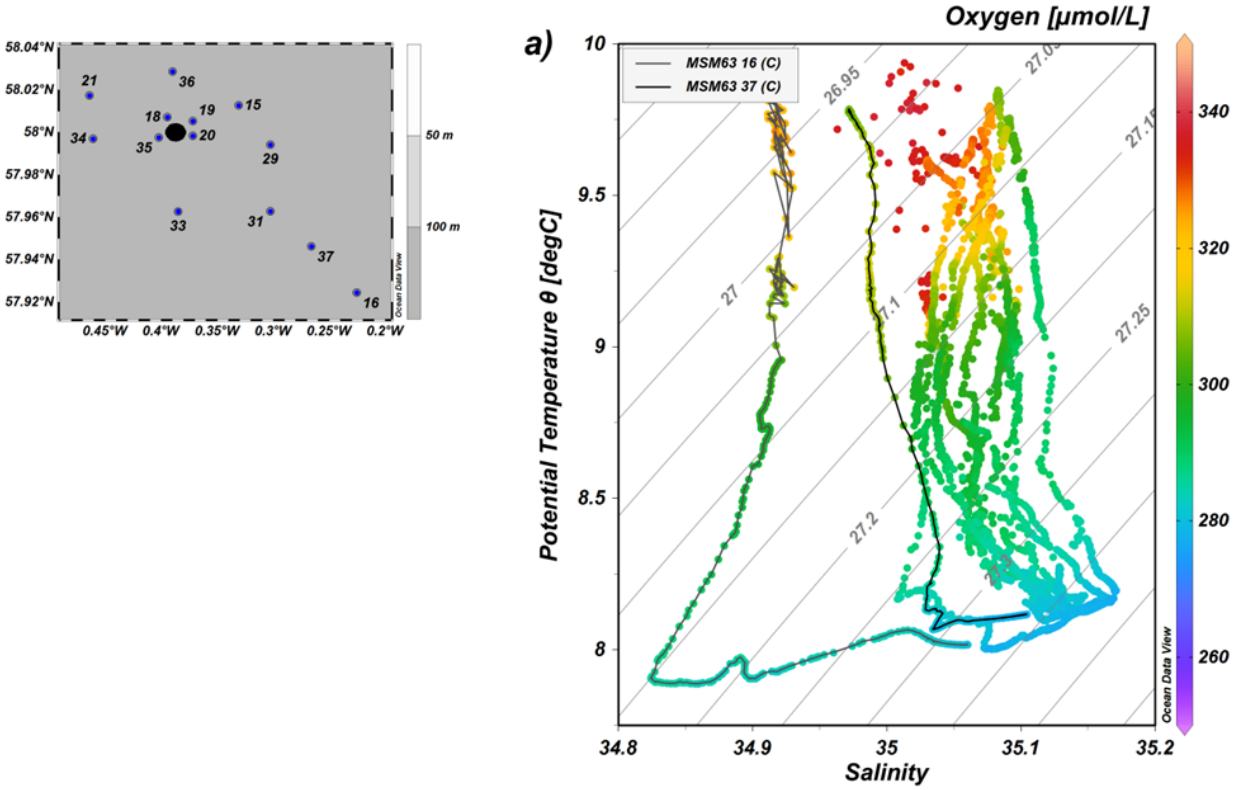

Figure 5.6.3: Map showing the CTD stations. The black circle indicates the position of the Goldeneye area. b) T(pot) -S plot with isopycnals given by grey lines and O2 concentration (µmol/L) indicated by the colour shading.

High dissolved oxygen concentrations of up to 330 µmol L-1 between 0 and 30 m water depth were associated with elevated Chla/fluorescence values. Maximum values of fluorescence/Chl a of up to 6 mg m-3 were observed between 20 and 30 m water depth.

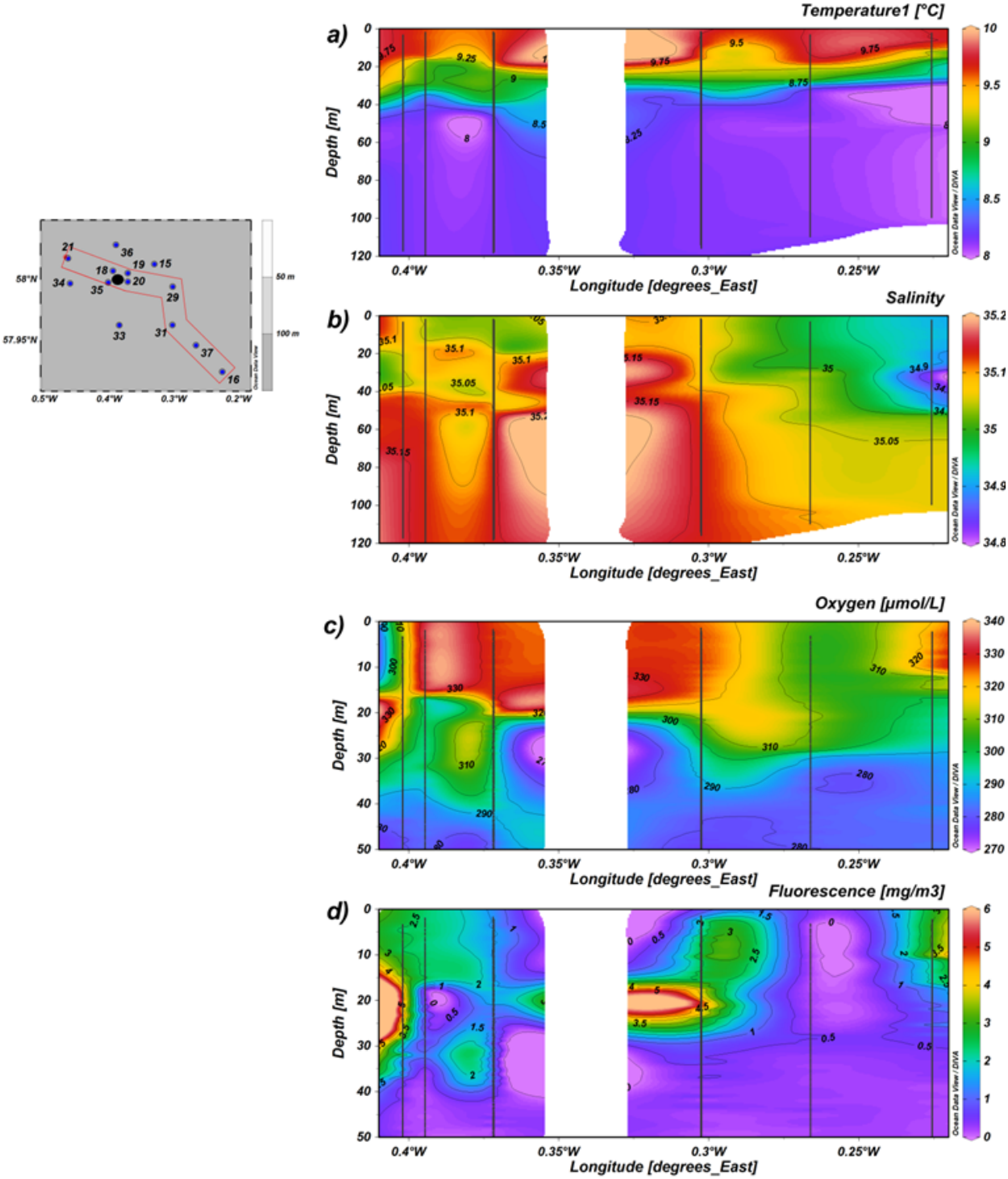

Figure 5.6.4: Vertical section of (a) temperature [°C], (b) salinity, (c) oxygen [µmol/L] and fluorescence along a NW-SE transect. Concentrations are given by colour shading. Isosurfaces are given. The stations included in the transect are indicated by the red line line in the map and by black vertical lines in the sections. Please note the different depth scales.

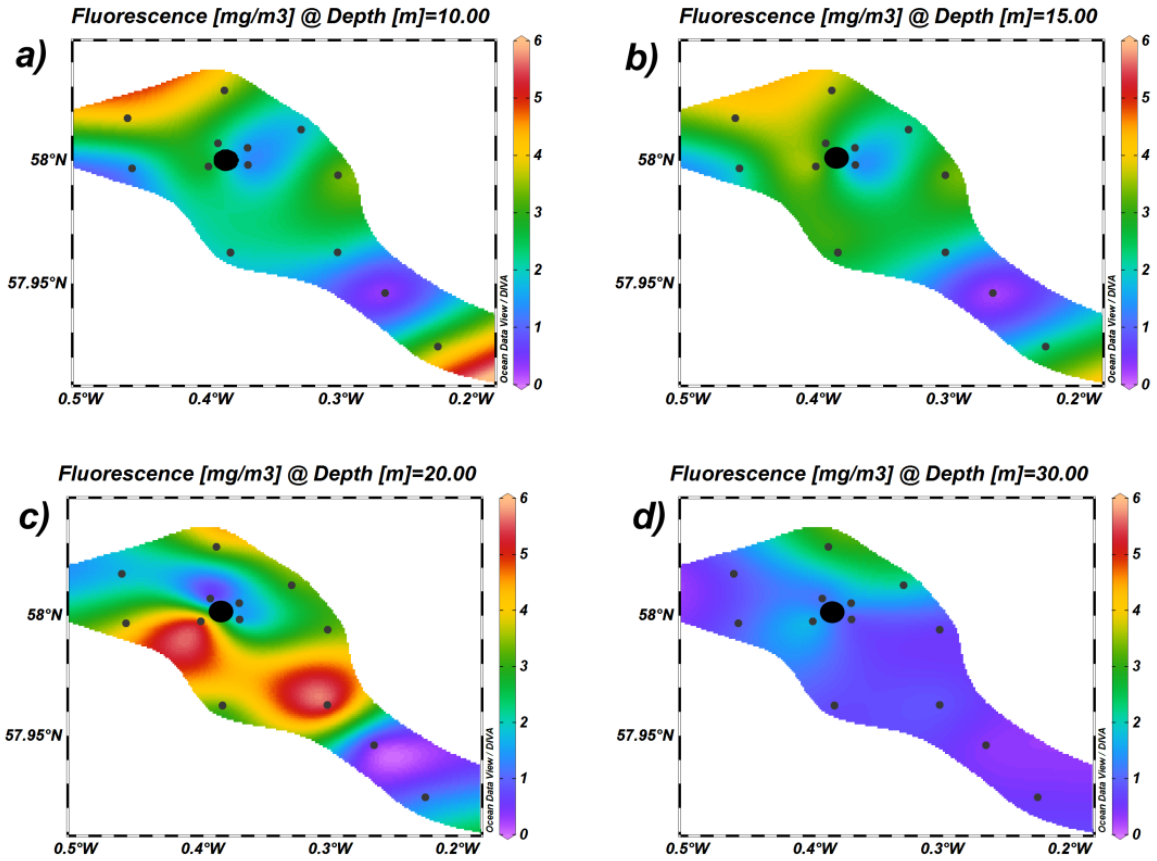

Figure 5.6.5: Surface sections of fluorescence observed at (a) 10 m, (b) 15 m, (9) 20 m and (d) 30 m water depth. The black dots indicate the CTD stations. The black filled circle marks the Goldeneye area.

6 Ship's Meterological Station

(A. Völsch)

There was no meteorologist on board during MSM63.

7 Station List MSM63

(B. Schramm, A. Völsch)

Please see Attachment A.

8 Data and Sample Storage and Availability

(C. Berndt)

The meta data for this cruise including positions, station logs from DSHIP and data types acquired will be made publicly available immediately after the cruise through GEOMAR data management. The raw data will be archived on the dedicated data server Permian at GEOMAR and will be made publicly available two years after the end of the project through GEOMAR data management.

9 Acknowledgements

(C. Berndt)

We would like to thank captain Björn Maaß, his officers and crew of RV Maria S. Merian for their professional support of our science programme and for very pleasant company on board. We also thank our technical team Gero Wetzel, Florian Beeck, Tan Yee Yuan, Laurence North, Ben Pitcairn, Martin Week and Dean Wilson for making this cruise a success.

The project STEMM-CCSS was funded by the European Commission (grant agreement 654462) and the Deutsche Forschungsgemeinschaft (project PERMO). Additional funding came from the institutions involved. We gratefully appreciate all these contributions.

10 References

Abegg, F., Bohrmann, G., Freitag, J., und Kuhs, W., 2007, Fabric of gas hydrate in sediments from Hydrate Ridge—results from ODP Leg 204 samples: Geo-Marine Letters, v. 27, 269-277.

Archer, D., und Buffett, B., 2005, Time-dependent response of the global ocean clathrate reservoir to climate und anthropogenic forcing: Geochemistry Geophysics Geosystems, v. 6, 1-13.

Archie, G.E. The electrical resistivity log as an aid in determining some reservoir characteristics, Petroleum Transactions of AIME 146, 54-62.

Berndt, C., 2005, Focused fluid flow in passive continental margins: Philosophical Transactions of the Royal Society A, v. 363, S. 2855-2871.

Berndt, C., Mienert, J., Vanneste, M., und Bünz, S., 2004, Gas hydrate dissociation und seafloor collapse in the wake of the Storegga Slide, Norway, in Wandås, B.T.G., Eide, E., Gradstein, F., und Nystuen, J.P., eds., Onshore–Offshore Relationships on the North Atlantic Margin. Norwegian Petroleum Society (NPF) Special Publication, Volume Norwegian Petroleum Society (NPF) Special Publication: Amsterdam, Netherlands, Elsevier, 285–292.

Birchwood, R., Singh, R., and Mese, A., 2006, Estimating the in situ mechanical properties of sediments containing gas hydrates, Proceedings of the 6th International Conference on Gas Hydrates) ICGH 2008, Vancouver, British Columbia, Canada, July 6-10.

Boswell, R., 2007, Resource potential of methane hydrate coming into focus, Journal of Petroleum Engineering, 56, 9-13.

Bowin, C., Lu, R.S., Lee, C.S., und Schouten, H., 1978, Plate convergence und accretion in the Taiwan-Luzon region: American Association of Petroleum Geologists Bulletin, v. 62,1645-1672.

Brown, H.E., Holbrook, W.S., Hornbach, M.J., und Nealon, J., 2006, Slide structure und role of gas hydrate at the northern boundary of the Storegga Slide, offshore Norway: Marine Geology, v. 229, S. 179-186.

Carcione, J.M. and Tinivella, U., 2000, Bottom-simulating reflectors: Seismic velocities and AVO effects, Geophysics 65, 54-67.

Chand, S., Minshull, T.A., Gei, D., und Carcione, J.M., 2004, Elastic velocity models for gas-hydrate-bearing sediments - a comparison: Geophysical Journal International, v. 159, 573-590..

Cheng, W. B.; Lin, S. S.; Wang, T. K.; Lee, C. S.; Liu, C. S., 2010. Velocity structure and gas hydrate saturation estimation on active margin off SW Taiwan inferred from seismic tomography, Marine Geophysical Researches, 31(1-2), Sp. Iss. SI .77-87.

Cheng, W.-B., Lee, C.-S., Liu, C.-S., Schnurle, P., Lin, S.-S., und Tsai, H.-R., 2006, Velocity structure in marine sediments with gas hydrate reflectors in offshore SW Taiwan, from OBS data tomography: Terrestrial, atmospheric und ocean sciences, v. 17.

Chi, W.-C., Reed, D.L., Liu, C.-S., und Lundberg, N., 1998, Distribution of the Bottom-Simulating Reflector in the Offshore Taiwan Collision Zone: Terrestrial, atmospheric und ocean sciences, v. 9, 779-794.

Chi, W.-C., Reed, D.L., und Tsai, C.-C., 2006, Gas Hydrate Stability Zone in Offshore Southern Taiwan: Terrestrial, Atmospheric and Ocean Sciences, v. 17, 829-843.

Chi, W.-C., und Reed, D.L., 2008, Evolution of shallow, crustal thermal structure from subduction to collision: An example from Taiwan: GSA Bulletin, v. 120, 679-690.

Chiu, J.-K., Tseng, W.-H., und Liu, C.-S., 2006, Distribution of gassy sediments und mud volcanoes offshore southwestern Taiwan: Terrestrial, atmospheric und ocean sciences, v. 17, 703–722.

Clennell, M.B., Hovland, M., Booth, J.S., Henry, P., and Winters, W.J., 1999, Formation of natural gas hydrates in marine sediments: 1. Conceptual model of gas hydrate growth conditioned by host sediment properties, Journal of Geophysical Research 104, 1978-2012.

Dickens, G.R., O'Neil, J.R., D. K. Rea, und Owens, R.M., 1995, Dissociation of oceanic methane hydrate as a cause of the carbon isotope excursion at the end of the Paleocene: Paleoceanography, v. 10.

Ecker, C., Dvorkin, J., and Nur, A.M., 1999, Estimating the amount of gas hydrate and free gas from marine seismic data, Geophysics 65, 565-573.

Frej-Ayoub, R., Tan, C., Clennell, B., Tohidi, B., and Yang, J., 2007, A wellbore stability model for hydrate bearing sediments, Journal of Petroleum Science and Engineering 57, 209-220.

Fyke, J.G., und Weaver, A.J., 2006, The Effect of Potential Future Climate Change on the Marine Methane Hydrate Stability Zone: Journal of Climate, v. 19, 5903-5917.

Ginsburg, G.D., and Soloviev, V.A., 1997, Methane migration within the submarine gas-hydrate stability zone under deep-water conditions: Marine Geology, v. 137, 49-57.

Golmshtok, A.Z. and Soloviev, V.A., 2006, Some remarks on the thermal nature of the double BSR, Marine Geology 229, 3-4.

Haacke, R.R., Westbrook, G.K., und Hyndman, R.D., 2007, Gas hydrate, fluid flow und free gas: Formation of the bottom-simulating reflector: Earth und Planetary Science Letters, v. 261, 407-420.

Hesslebo, S.P., Gröcke, D.R., Jenkyns, H.C., Bjerrum, C.J., Farrimond, P., Morgans-Bell, H.S., und Green, O.R., 2000, Massive dissociation of gas hydrate during a Jurassic oceanic anoxic event: Nature, v. 406.

Hirtzel, J., Chi, W.C., Reed, D., Chen, L., Liu, C.-S., und Lundberg, N., 2009, Destruction of Luzon forearc basin from subduction to Taiwan arc–continent collision Tectonophysics, v. in Druck.

Jakobsen, M., Hudson, J.A., Minshull, T.A., und Singh, S.C., 2000, Elastic properties of hydrate-bearing sediments using effective-medium theory: Journal of Geophysical Research, v. 105, 561-577.

Johnson, A.H., und Max, M.D., 2006, The path to commercial hydrate gas production: The Leading Edge, v. May, S. 648-651.

Judd, A. G. (1990, January). Shallow gas and gas seepages: a dynamic process?. In Safety in Offshore Engineering: Proceedings of an international conference. Society of Underwater Technology.

Judd, A. G., Long, D., & Sankey, M. (1994). Pockmark formation and activity, UK block 15/25, North Sea. Bulletin of the Geological Society of Denmark, 41(1), 34-49.

Judd, A. Long, D. & Sankey, M.: Pockmark formation and activity, U.K. block 15/25, North Sea. Bulletin of the Geological Society of Denmark, vol. 41, pp. 34-49, Copenhagen, 1994-03-30.

Judd, A., and Hovland, M., 2007, Seabed fluid flow: the impact on geology, biology and the marine environment. Cambridge: Cambridge University Press.

Jung, W.-Y., und Vogt, P., 2004, Effects of bottom water warming und sea level rise on Holocene hydrate dissociation und mass wasting along the Norwegian-Barents Continental Margin: Journal of Geophysical Research, v. 109, S. 1-18.

Kennett, J.P., Cannariato, K.G., Hendy, I.L., und Behl, R.J., 2003, Methane Hydrates in Quaternary Climate Change: The Clathrate Gun Hypothesis: Washington DC, American Geophysical Union Special Publication, 216.

Lin C-K., 2008, Algorithm for determining optimum sequestration depth of CO2 trapped by residual-gas and solubility trapping mechanisms in a deep saline formation. Geofluids, 8, 333–343.

Lin, C.-C., Lin, A.T.-S., Liu, C.-S., Chen, G.-Y., Liao, W.-Z., und Schnurle, P., 2009, Geological controls on BSR occurrences in the incipient arc-continent collision zone off southwest Taiwan: Marine und Petroleum Geology, v. 26, 1118-1131.

Liu, C.-S., Schnurle, P., Wang, Y., Chuang, S.-H., Chen, S.-C., und Hsiuan, T.-H., 2006, Distribution und characters of gas hydrate offshore of southwestern Taiwan: Terrestrial, atmospheric und ocean sciences, v. 17, S. 615–644.

Liu, X., und Flemings, P.B., 2006, Passing gas through the hydrate stability zone at southern Hydrate Ridge, offshore Oregon: Earth und Planetary Science Letters, v. 241, S. 211-226.

Long, D., Lovell, M.A., Rees, J.G., und Rochelle, C.A., 2009, Sediment-hosted gas hydrates: new insights on natural und synthetic systems: Geological Society, London, Special Publications, v. 319, S. 1-9.

Martin C Sinha, PD Patel, MJ Unsworth, TRE Owen, and MRG MacCormack. An active source electromagnetic sounding system for marine use. Marine Geophysical Researches, 12(1-2):59-68, 1990.

McDonnell, S.L., Max, M.D., Cherkis, N.Z., and Czarnecki, M.F., 2000, Tectono-sedimentary controls on the likelihood of gas hydrate occurrence near Taiwan, Marine and Petroleum Geology, 17, 929-936.

McQuillin, R., & Fannin, N. (1979). Explaining the North Seas lunar floor. New Scientist, 83(1163), 90-92.

Micallef, A., Masson, D.G., Berndt, C., und Stow, D.A.V., 2009, Development und mass movement processes of the north-eastern Storegga Slide: Quaternary Science Reviews, v. 28, S. 433-448.

Mienert, J., Vanneste, M., Bünz, S., Andreassen, K., Haflidason, H., und Sejrup, H.P., 2005, Ocean warming und gas hydrate stabilisty on the mid-Norwegian margin at the Storegga Slide: Marine und Petroleum Geology, v. 22, S. 233-244.

Milkov, A.V., 2004, Global estimates of hydrate-bound gas in marine sediments: how much is really out there?: Earth-Science Reviews, v. 66, S. 183-197.

Milkov, A.V., und Sassen, R., 2002, Economic geology of offshore gas hydrate accumulations und provinces: Marine und Petroleum Geology, v. 19, S. 1-11.

Nimblett, J., and Ruppel, C., 2003, Permeability evolution during the formation of gas hydrates in marine sediments: Journal of Geophysical Research, v. 108, p. 2420, doi: 10.1029/2001JB001650.

Nouzé, H., Henry, P., Noble, M., Martin, V. and Pascal, G., 2004, Large gas hydrate accumulations on the eastern Nankai Trough inferred from new high-resolution 2-D seismic data, Geophysical Research Letters 31, doi:10.1029/2004GL019848.

Oung, J.N., Lee, C.Y. Lee, C.S., and Kuo, C.L., 2006, Geochemical study on hydrocarbon gases in seafloor sediments, southwestern offshore Taiwan - implications in the potential occurrence of gas hydrates. Terr. Atmos. Ocean. Sci., 17, 921-931.

Paull, C.K., Ussler, W., und Dillon, W.P., 2000, Potential role of gas hydrate decomposition in generating submarine slope failures, in M., M., ed., Natural gas hydrate in oceanic und permafrost environments: Dordrecht, Kluwer, S. 149-156.

Pecher, I.A., Henrys, S.A., Ellis, S., Chiswell, S.M., and Kukowski, N., 2005, Erosion of the seafloor at the top of the gas hydrate stability zone on the Hikurangi Margin, New Zealand: Geophysical Research Letters, v. 32, p. L24603.

Reagan, M.T., und Moridis, G.J., 2007, Oceanic gas hydrate instability und dissociation under climate change scenarios: Geophysical Research Letters, v. 34, S. L22709.

Ruppel, C., 2007, Tapping Methane Hydrates for Unconventional Natural Gas: Elements, v. 3, S. 193-199.

Schnurle, P., Liu, C.-S., Hsiuan, T.-H., und Wang, T.-K., 2004, Characteristics of gas hydrate und free gas offshore southwestern Taiwan from a combined MCS/OBS data analysis: Marine Geophysical Researches, v. 25, S. 157-180.

Shyu, C.-T., Chen, Y.-J., Chiang, S.-T., Liu, C.-S., 2006. Heat flow measurements over bottom simulating reflectors, offshore southwestern Taiwan. Terrestrial, Atmospheric and Ocean Sciences. 17, 845–869.

Sloan, D. and Koh, C., 2007, Clathrate Hydrates of Natural Gases, 3. Ed., Taylor and Francis.

Steven Constable, PK Kannberg, and K Weitemeyer. Vulcan: A deep-towed CSEM receiver. Geochemistry, Geophysics, Geosystems, 17(3):1042-1064, 2016.

Sultan, N., 2007, Comment on "Excess pore pressure resulting from methane hydrate dissociation in marine sediments: A theoretical approach" by Wenyue Xu und Leonid N. Germanovich, Journal of Geophysical Research-Solid Earth, 112 (B2), Artikel Nr. B02103

Sultan, N., Cochonat, P., Canals, M., Cattaneo, A., Dennielou, B., Haflidason, H., Laberg, J.S., Long, D., Mienert, J., Trincardi, F., Urgeles, R., Vorren, T.O., und Wilson, C., 2004a, Triggering mechanisms of slope instability processes und sediment failures on continental margins: a geotechnical approach: Marine Geology, v. 213, S. 291-321.

Sultan, N., Cochonat, P., Foucher, J.P., und Mienert, J., 2004b, Effect of gas hydrates melting on seafloor slope instability: Marine Geology, v. 213, S. 379-401.

Suppe, J., 1984, Kinematics of arc-continent collision, flipping of subduction, und back-arc spreading near Taiwan: Memoir of the Geological Society of China, v. 6, S. 21-33.

Taylor, B., und Hayes, D.E., 1983, Origin und history of the south China Sea basin: AGU Geophysical Monograph, v. 27, S. 23-56.

Wang, Y-S (2008) Recent development of gas hydrate investigation in Taiwan. The Taiwan-Germany Joint Symposium on Marine Gas Hydrate Exploration and Carbon Sequestration Technologies Conference.

Westbrook, G.K., Thatcher, K.E., Rohling, E.J., Piotrowski, A.M., Pälike, H., Osborne, A.H., Nisbet, E.G., Minshull, T.A., Lanoisellé, M., James, R.H., Hühnerbach, V., Green, D., Fisher, R.E., Crocker, A.J., Chabert, A., Bolton, C., Beszczynska-Möller, A., Berndt, C., und Aquilina, A., 2009, Escape of methane gas from the seabed along the West Spitsbergen continental margin: Geophysical Research Letters, 36: L15608.

Winters, W.J., Pecher, I.A., Waite, W.F., and Mason, D.H., 2004, Physical properties and rock physics models of sediment containing natural and laboratory-formed methane hydrate, American Mineralogist 89, 1221-1227.

Wood, W.T., Gettrust, J.F., Chapman, N.R., Spence, G.D., und Hyndman, R.D., 2002, Decreased stability of methane hydrates in marine sediments owing to phase-boundary roughness: Nature, v. 420, S. 656-660.

Xu, W., und Germanovich, L., N., 2006, Excess pore pressure resulting from methane hydrate dissociation in marine sediments: A theoretical approach: Journal of Geophysical Research, v. 111, S. 1-12.

Yang, T., Jiang, S.Y., Yang, J.H., Ge, L., Wu, N.Y., Liu, J., und Chen, D.H., 2008, Dissolved inorganic carbon (DIC) und its carbon isotopic composition in sediment pore waters from the Shenhu area, northern South China Sea: Journal of Oceanography, v. 64, S. 303-310.

Yang, T.F., Chuang, P.-C., Lin, S., Chen, J.-C., Wang, Y., und Chung, S.-H., 2006, Methane Venting in Gas Hydrate Potential Area Offshore of SW Taiwan: Evidence of Gas Analysis of Water Column Samples: Terrestrial, atmospheric und ocean sciences, v. 17, S. 933-950.

You, C.F., J.M. Gieskes, T. Lee, T.F. Yui, and H.W. Chen, 2004. Geochemistry of mud volcano fluids in the Taiwan accretionary prism, Applied Geochemistry, 19, 695-707.

—, 2003, Preliminary assessment of resources und economic potential of individual gas hydrate accumulations in the Gulf of Mexico continental slope: Marine und Petroleum Geology, v. 20, S. 111-128.

—, 2007, Dynamic multiphase flow model of hydrate formation in marine sediments: Journal of Geophysical Research, v. 112.

Appendices

Appendix A: Station Book

MSM63-1

Activity - Device Operation	Timestamp	Device	Action	Latitude	Longitude	Depth (m)	Speed (kn)	Course	Latitude (deg)	Longitude (deg)	Wind Dir	Wind Velocity	Winch	Rope Length (m)	Comment
MSM63_0_Underway-1	01.05.2017 04:50	ADCP	information	55 °05,388' N	003° 05,277' E			350.7	55,089,802	3,087,943	103	32.00		0.0	
MSM63_0_Underway-3	01.05.2017 04:50	Multibeam Echosounder	information	55 °05,404' N	003° 05,270' E			348.6	55,090,073	3,087,840	103				
MSM63_0_Underway-2	01.05.2017 04:50	Weatherstation	information	55 °05,497' N	003° 05,234' E			344.9	55,091,614	3,087,230	103	31.40		0.0	
MSM63_0_Underway-4	01.05.2017 09:00	Parasound	information	55 °53,655' N	002° 45,558' E	80.8	12.0	348.5	55,894,250	2,759,293	109	29.20		0.0	
MSM63_3-1	02.05.2017 00:45	Parasound	profile start	58 °14,798' N	001° 49,056' E	88.0		33.6	58,246,639	1,817,595	122	20.60		0.0	v=7kn, Kurs 028°
MSM63_3-1	02.05.2017 01:33	Parasound	alter course	58 °19,685' N	001° 53,956' E	83.1		50.8	58,328,080	1,899,271	120	21.00		0.0	Kurs: 187°
MSM63_3-1	02.05.2017 02:03	Parasound	alter course	58 °17,121' N	001° 53,215' E	85.2		194.0	58,285,356	1,886,913	108	20.70		0.0	Kurs: 247°
MSM63_3-	02.05.2017	Parasound	alter	58 °15,906' N	001° 48,118' E	91.0	7.0	245.4	58,265,102	1,801,969	115	17.80		0.0	Kurs: 323°

1	02:29		course												
MSM63_3-1	02.05.2017 02:44	Parasound	alter course	58 °17,180' N	001° 45,883' E	100.0	7.0	328.9	58,286,333	1,764,716	113	15.80		0.0	Kurs: 104°
MSM63_3-1	02.05.2017 03:25	Parasound	alter course	58 °16,335' N	001° 51,984' E	86.3		104.1	58,272,247	1,866,393	108	15.80		0.0	Kurs: 319°
MSM63_3-1	02.05.2017 03:36	Parasound	profile end	58 °16,446' N	001° 50,859' E	88.0		318.9	58,274,097	1,847,651	104	14.30		0.0	
MSM63_4-1	02.05.2017 07:21	Magnetotellurics	in the water	58 °17,553' N	000° 59,199' E	152.3	0.0	182.8	58,292,545	0.986649	95	15.60	AW	-1.0	
MSM63_4-1	02.05.2017 07:44	Magnetotellurics	information	58 °17,552' N	000° 59,197' E	152.8	0.1	231.4	58,292,534	0.986613	97	15.30	AW	140.0	mit Posidonia ausgelöt
MSM63_4-1	02.05.2017 08:07	Magnetotellurics	information	58 °17,551' N	000° 59,198' E	151.5	0.1	66.0	58,292,515	0.986637	101	17.30	AW	-12.0	Gerade hat sich erst an der Oberflähe vom Draht gelöt. Releaser an Deck
MSM63_4-2	02.05.2017 08:41	Magnetotellurics	in the water	58 °17,339' N	000° 58,886' E	153.2	0.0	321.8	58,288,978	0.981436	98	16.70	AW	-3.0	
MSM63_4-2	02.05.2017 09:03	Magnetotellurics	information	58 °17,335' N	000° 58,895' E	152.8	0.1	324.9	58,288,921	0.981579	102	15.60	AW	136.0	mit Posidonia ausgelöt
MSM63_4-2	02.05.2017 09:09	Magnetotellurics	information	58 °17,336' N	000° 58,893' E	152.6	0.1	333.4	58,288,926	0.981554	101	17.50	AW	-12.0	Releaser an Deck
MSM63_4-3	02.05.2017 09:40	Magnetotellurics	in the water	58 °16,961' N	000° 58,978' E	152.5	0.0		58,282,685	0.982959	98	15.20	AW	-2.0	
MSM63_4-3	02.05.2017 10:00	Magnetotellurics	information	58 °16,956' N	000° 58,988' E	152.5	0.2	275.3	58,282,601	0.983141	101		AW	140.0	mit Posidonia ausgelöt
MSM63_4-	02.05.2017	Magnetotellurics	inform	58 °16,958' N	000° 58,990' E	152.1	0.1		58,282,628	0.983175	103	17.00	AW	-13.0	Releaser an

3	10:08		ation												Deck
MSM63_4-4	02.05.2017 10:39	Magnetotellurics	in the water	58 °17,126' N	000° 58,578' E	154.9	0.1	203.5	58,285,432	0.976300	105	17.20	AW	7.0	
MSM63_4-4	02.05.2017 10:56	Magnetotellurics	inform ation	58 °17,119' N	000° 58,582' E	155.1	0.1	228.2	58,285,318	0.976374	107	19.50	AW	140.0	mit Posidonia ausgelöt
MSM63_4-4	02.05.2017 11:05	Magnetotellurics	inform ation	58 °17,116' N	000° 58,586' E	155.9	0.1	235.3	58,285,260	0.976426	104	19.80		0.0	Releaser an Deck
MSM63_4-5	02.05.2017 11:49	Magnetotellurics	in the water	58 °17,290' N	000° 58,170' E	153.7	0.0		58,288,167	0.969493	103	17.00	AW	4.0	
MSM63_4-5	02.05.2017 12:07	Magnetotellurics	inform ation	58 °17,285' N	000° 58,179' E	154.6	0.0	314.7	58,288,089	0.969645	106	17.00	AW	140.0	mit Posidonia ausgelöt
MSM63_4-5	02.05.2017 12:14	Magnetotellurics	inform ation	58 °17,286' N	000° 58,179' E	154.0	0.1	295.5	58,288,092	0.969643	105	15.00	AW	-12.0	Releaser an Deck
MSM63_4-6	02.05.2017 12:35	Magnetotellurics	in the water	58 °17,241' N	000° 57,450' E	153.9	0.1	51.5	58,287,344	0.957505	107	15.40	AW	1.0	
MSM63_4-6	02.05.2017 12:54	Magnetotellurics	inform ation	58 °17,238' N	000° 57,464' E	154.1	0.0	357.6	58,287,305	0.957733	99		AW	140.0	mit Posidonia ausgelöt
MSM63_4-6	02.05.2017 13:02	Magnetotellurics	inform ation	58 °17,239' N	000° 57,463' E	153.5	0.1	314.8	58,287,315	0.957714	99	15.60	AW	-11.0	Releaser an Deck
MSM63_5-1	02.05.2017 13:48	Seismic Ocean Bottom Receiver	OBS deploy ed	58 °16,381' N	000° 57,480' E	153.8	0.1		58,273,019	0.958008	106	15.20		0.0	
MSM63_5-2	02.05.2017 14:08	Seismic Ocean Bottom Receiver	OBS deploy ed	58 °16,805' N	000° 58,105' E	157.2	0.1		58,280,081	0.968416	104	15.60		0.0	
MSM63_5-3	02.05.2017 14:18	Seismic Ocean Bottom Receiver	OBS deploy ed	58 °16,868' N	000° 58,197' E	167.4	0.1	142.5	58,281,130	0.969943	107	16.90		0.0	

MSM63_5-4	02.05.2017 14:26	Seismic Ocean Bottom Receiver	OBS deployed	58 °16,911' N	000° 58,261' E	164.9	0.1	153.5	58,281,848	0.971020	104	15.80	0.0
MSM63_5-5	02.05.2017 14:35	Seismic Ocean Bottom Receiver	OBS deployed	58 °16,976' N	000° 58,353' E	157.1	0.1	92.8	58,282,928	0.972558	105		0.0
MSM63_5-6	02.05.2017 14:47	Seismic Ocean Bottom Receiver	OBS deployed	58 °17,040' N	000° 58,447' E	158.1	0.0	306.7	58,284,007	0.974122	105	14.00	0.0
MSM63_5-7	02.05.2017 15:04	Seismic Ocean Bottom Receiver	OBS deployed	58 °17,446' N	000° 59,044' E	152.7	0.0	225.1	58,290,761	0.984069	98		0.0
MSM63_5-8	02.05.2017 15:19	Seismic Ocean Bottom Receiver	OBS deployed	58 °16,997' N	000° 58,570' E	154.9	0.0	347.2	58,283,290	0.976161	96		0.0
MSM63_5-9	02.05.2017 15:33	Seismic Ocean Bottom Receiver	OBS deployed	58 °16,699' N	000° 58,763' E	153.3	0.1	110.9	58,278,312	0.979376	99		0.0
MSM63_5-10	02.05.2017 16:01	Seismic Ocean Bottom Receiver	OBS deployed	58 °16,861' N	000° 58,338' E	160.4	0.1	285.6	58,281,020	0.972297	89		0.0
MSM63_5-11	02.05.2017 16:09	Seismic Ocean Bottom Receiver	OBS deployed	58 °16,885' N	000° 58,278' E	170.1	0.0	100.9	58,281,418	0.971302	94	13.00	0.0
MSM63_5-12	02.05.2017 16:58	Seismic Ocean Bottom Receiver	OBS deployed	58 °16,919' N	000° 58,195' E	159.8	0.1	301.6	58,281,991	0.969915	88		0.0
MSM63_5-	02.05.2017	Seismic Ocean	OBS	58 °16,943' N	000° 58,136' E	155.4	0.0	116.2	58,282,389	0.968933	75		0.0

13	17:54	Bottom Receiver	deployed											
MSM63_5-14	02.05.2017 18:24	Seismic Ocean Bottom Receiver	OBS deployed	58 °17,108' N	000° 57,731' E	153.8	0.1	203.1	58,285,141	0.962182	71			0.0	
MSM63_5-15	02.05.2017 18:38	Seismic Ocean Bottom Receiver	OBS deployed	58 °16,900' N	000° 58,054' E	154.9	0.3	42.8	58,281,669	0.967573	68			0.0	
MSM63_5-16	02.05.2017 18:48	Seismic Ocean Bottom Receiver	OBS deployed	58 °16,807' N	000° 58,283' E	157.3	0.1	126.1	58,280,110	0.971382	74	11.00		0.0	
MSM63_5-17	02.05.2017 19:00	Seismic Ocean Bottom Receiver	OBS deployed	58 °16,917' N	000° 58,440' E	158.5	0.1	75.7	58,281,953	0.973994	80			0.0	
MSM63_5-18	02.05.2017 19:19	Seismic Ocean Bottom Receiver	OBS deployed	58 °17,010' N	000° 58,206' E	155.4	0.0	145.0	58,283,498	0.970103	83			0.0	
MSM63_4-7	02.05.2017 21:06	Magnetotellurics	in the water	58 °17,078' N	000° 57,852' E	153.6	0.1	292.3	58,284,631	0.964195	54		AW	0.0	
MSM63_4-7	02.05.2017 21:25	Magnetotellurics	information	58 °17,075' N	000° 57,863' E	153.6	0.0	155.9	58,284,575	0.964387	49	13.00	AW	139.0	mit Posidonia ausgelöt
MSM63_4-7	02.05.2017 21:33	Magnetotellurics	information	58 °17,068' N	000° 57,868' E	153.0	0.2	159.3	58,284,471	0.964468	49	13.40		0.0	Releaser an Deck
MSM63_4-8	02.05.2017 21:48	Magnetotellurics	in the water	58 °16,746' N	000° 58,669' E	153.6	0.0	307.3	58,279,096	0.977811	52	13.60	AW	-3.0	
MSM63_4-8	02.05.2017 22:04	Magnetotellurics	information	58 °16,743' N	000° 58,672' E	153.0	0.1	176.2	58,279,054	0.977864	51	13.40	AW	140.0	mit Posidonia ausgelöt
MSM63_4-	02.05.2017	Magnetotellurics	inform	58 °16,742' N	000° 58,674' E	153.7	0.4	177.1	58,279,030	0.977896	47	13.20	AW	-6.0	Releaser an

8	22:11		ation											Deck
MSM63_4-9	02.05.2017 22:44	Magnetotellurics	inform ation	58 °16,585' N	000° 59,061' E	152.7	0.0	102.4	58,276,412	0.984355	45	11.00	AW	2.0	
MSM63_4-9	02.05.2017 23:04	Magnetotellurics	inform ation	58 °16,583' N	000° 59,070' E	152.7	0.1	124.7	58,276,387	0.984508	40	11.00	AW	140.0	mit Posidonia ausgelöt
MSM63_4-9	02.05.2017 23:12	Magnetotellurics	inform ation	58 °16,582' N	000° 59,071' E	152.5	0.1	273.9	58,276,372	0.984517	43		AW	-11.0	Releaser an Deck
MSM63_4-10	02.05.2017 23:28	Magnetotellurics	in the water	58 °16,536' N	000° 58,346' E	154.6	0.0	287.8	58,275,607	0.972428	42		AW	-2.0	
MSM63_4-10	02.05.2017 23:46	Magnetotellurics	inform ation	58 °16,533' N	000° 58,352' E	154.2	0.1	309.6	58,275,551	0.972534	49	12.00	AW	138.0	mit Posidonia ausgelöt
MSM63_4-10	02.05.2017 23:55	Magnetotellurics	inform ation	58 °16,533' N	000° 58,351' E	153.8	0.2	132.8	58,275,548	0.972520	44		AW	-12.0	Releaser an Deck
MSM63_4-11	03.05.2017 00:18	Magnetotellurics	in the water	58 °16,702' N	000° 57,937' E	154.3	0.1	174.4	58,278,361	0.965622	44		AW	8.0	
MSM63_4-11	03.05.2017 00:36	Magnetotellurics	inform ation	58 °16,699' N	000° 57,946' E	154.3	0.0	122.2	58,278,320	0.965766	38		AW	140.0	mit Posidonia ausgelöt
MSM63_4-11	03.05.2017 00:43	Magnetotellurics	inform ation	58 °16,696' N	000° 57,954' E	155.0	0.6	120.4	58,278,260	0.965907	38	13.20	AW	-5.0	Releaser an Deck
MSM63_4-12	03.05.2017 01:00	Magnetotellurics	in the water	58 °16,864' N	000° 57,540' E	154.1	0.5	297.2	58,281,074	0.958995	43		AW	17.0	
MSM63_4-12	03.05.2017 01:17	Magnetotellurics	inform ation	58 °16,864' N	000° 57,542' E	153.5	0.0	126.8	58,281,063	0.959040	44		AW	140.0	mit Posidonia ausgelöt
MSM63_4-12	03.05.2017 01:24	Magnetotellurics	inform ation	58 °16,860' N	000° 57,551' E	153.3	0.6	147.4	58,281,001	0.959180	41	13.50	AW	-4.0	Releaser an Deck
MSM63_4-13	03.05.2017 01:45	Magnetotellurics	in the water	58 °16,488' N	000° 57,629' E	153.4	0.1	143.5	58,274,794	0.960486	42	13.40	AW	-2.0	
MSM63_4-	03.05.2017	Magnetotellurics	inform	58 °16,486' N	000° 57,631' E	154.6	0.0	219.7	58,274,767	0.960522	42		AW	140.0	mit Posidona

13	02:07		ation												ausgelöt
MSM63_4-13	03.05.2017 02:14	Magnetotellurics	information	58 °16,487' N	000° 57,628' E	154.3	0.0	148.8	58,274,785	0.960464	40		AW	-10.0	Releaser an Deck
MSM63_4-14	03.05.2017 02:27	Magnetotellurics	in the water	58 °16,274' N	000° 57,316' E	154.3	0.1	202.9	58,271,237	0.955270	35		AW	2.0	
MSM63_4-14	03.05.2017 02:47	Magnetotellurics	information	58 °16,275' N	000° 57,322' E	154.5	0.1	282.2	58,271,250	0.955365	28		AW	140.0	mit Posidonia ausgelöt
MSM63_4-14	03.05.2017 02:54	Magnetotellurics	information	58 °16,274' N	000° 57,325' E	155.1	0.4	129.3	58,271,238	0.955414	28		AW	-7.0	Releaser an Deck
MSM63_6-1	03.05.2017 03:53	Controlled Source Electromagnetics	in the water	58 °16,923' N	000° 55,538' E	155.0		48.6	58,282,044	0.925633	28	13.30	F2S2	20.0	Vulcan 1
MSM63_6-1	03.05.2017 04:02	Controlled Source Electromagnetics	in the water	58 °17,003' N	000° 55,801' E	153.9	1.0	61.2	58,283,381	0.930020	28		F2S2	20.0	Vulcan 2
MSM63_6-1	03.05.2017 04:17	Controlled Source Electromagnetics	in the water	58 °17,123' N	000° 56,196' E	154.8	1.0	44.3	58,285,376	0.936602	29	13.30	F2S2	20.0	Pressure Sensor + 1 Benthos
MSM63_6-1	03.05.2017 04:19	Controlled Source Electromagnetics	in the water	58 °17,138' N	000° 56,246' E	154.8	1.0	55.4	58,285,633	0.937439	29	13.40	F2S2	20.0	Antenna + 5 Benthos
MSM63_6-1	03.05.2017 04:54	Controlled Source Electromagnetics	in the water	58 °17,434' N	000° 57,222' E	153.4	0.9	79.8	58,290,573	0.953702	24	15.40	F2S2	10.0	
MSM63_6-1	03.05.2017 05:42	Controlled Source Electromagnetics	on deck	58 °17,847' N	000° 58,584' E	153.9		63.3	58,297,450	0.976398	22	18.50	F2S2	-13.0	techn. Probleme
MSM63_6-1	03.05.2017 05:45	Controlled Source Electromagnetics	in the water	58 °17,868' N	000° 58,651' E	153.8	1.0	60.4	58,297,794	0.977510	20	17.60	F2S2	-1.0	
MSM63_6-1	03.05.2017 07:22	Controlled Source Electromagnetics	profile start	58 °18,033' N	001° 00,551' E	150.5	1.0	231.3	58,300,555	1,009,184	23	16.20	F2S2	115.0	v=1kn, Kurs 218°
MSM63_6-1	03.05.2017 10:36	Controlled Source Electromagnetics	profile end	58 °15,467' N	000° 56,786' E	153.9	1.0	218.3	58,257,784	0.946441	0	0.00	F2S2	121.0	

MSM63_6-1	03.05.2017 10:37	Controlled Source Electromagnetics	alter course	58 °15,454' N	000° 56,767' E	153.8	1.0	226.6	58,257,564	0.946111	0	0.00	F2S2	121.0	Kurs 038°
MSM63_6-1	03.05.2017 11:35	Controlled Source Electromagnetics	profile start	58 °15,226' N	000° 55,788' E	154.0	1.0	40.3	58,253,772	0.929801	0	0.00	F2S2	60.0	
MSM63_6-1	03.05.2017 15:53	Controlled Source Electromagnetics	profile end	58 °18,615' N	001° 00,757' E	150.9	1.0		58,310,247	1,012,620	25		F2S2	60.0	
MSM63_6-1	03.05.2017 15:54	Controlled Source Electromagnetics	alter course	58 °18,631' N	001° 00,770' E	150.9			58,310,511	1,012,837	32		F2S2	60.0	Kurs 218°
MSM63_6-1	03.05.2017 16:09	Controlled Source Electromagnetics	profile start	58 °18,763' N	001° 00,331' E	151.1		219.9	58,312,717	1,005,514	39		F2S2	60.0	
MSM63_6-1	03.05.2017 19:55	Controlled Source Electromagnetics	profile end	58 °15,787' N	000° 55,964' E	154.8	0.9	216.5	58,263,115	0.932733	33		F2S2	60.0	
MSM63_6-1	03.05.2017 19:55	Controlled Source Electromagnetics	alter course	58 °15,782' N	000° 55,955' E	154.8	0.9	220.1	58,263,034	0.932590	33		F2S2	60.0	Kurs 353°
MSM63_6-1	03.05.2017 21:03	Controlled Source Electromagnetics	profile start	58 °15,276' N	000° 57,918' E	153.7	1.0	357.5	58,254,599	0.965294	36	10.00	F2S2	74.0	
MSM63_6-1	04.05.2017 00:16	Controlled Source Electromagnetics	profile end	58 °18,473' N	000° 57,138' E	152.9			58,307,887	0.952302	51		F2S2	60.0	
MSM63_6-1	04.05.2017 00:16	Controlled Source Electromagnetics	alter course	58 °18,476' N	000° 57,138' E	152.6		359.5	58,307,931	0.952301	51		F2S2	60.0	Kurs 173°
MSM63_6-1	04.05.2017 00:35	Controlled Source Electromagnetics	profile start	58 °18,510' N	000° 57,859' E	152.1	1.0	170.3	58,308,499	0.964317	35	9.00	F2S2	60.0	
MSM63_6-1	04.05.2017 03:49	Controlled Source Electromagnetics	profile end	58 °15,300' N	000° 58,642' E	153.2	1.0	171.6	58,254,996	0.977362	34	11.00	F2S2	60.0	
MSM63_6-1	04.05.2017 03:49	Controlled Source Electromagnetics	alter course	58 °15,297' N	000° 58,643' E	153.0		168.3	58,254,950	0.977382	34	11.00	F2S2	60.0	Kurs 353°
MSM63_6-1	04.05.2017 04:12	Controlled Source Electromagnetics	profile start	58 °15,357' N	000° 59,354' E	153.7		345.7	58,255,945	0.989232	60		F2S2	60.0	

MSM63_6-1	04.05.2017 07:27	Controlled Source Electromagnetics	profile end	58 °18,562' N	000° 58,576' E	152.5	1.0	348.5	58,309,368	0.976259	78	F2S2	122.0	
MSM63_6-1	04.05.2017 07:31	Controlled Source Electromagnetics	alter course	58 °18,628' N	000° 58,589' E	152.5	1.0		58,310,460	0.976476	48	F2S2	79.0	Kurs 128°
MSM63_6-1	04.05.2017 08:44	Controlled Source Electromagnetics	profile start	58 °18,107' N	000° 56,133' E	154.1	1.0	131.0	58,301,780	0.935555	36	F2S2	60.0	
MSM63_6-1	04.05.2017 11:00	Controlled Source Electromagnetics	profile end	58 °16,128' N	001° 00,995' E	151.3		137.0	58,268,808	1,016,581	54	F2S2	135.0	
MSM63_6-1	04.05.2017 11:22	Controlled Source Electromagnetics	alter course	58 °15,796' N	001° 01,815' E	149.5		133.5	58,263,265	1,030,258	55	F2S2	60.0	Kurs 308°
MSM63_6-1	04.05.2017 11:39	Controlled Source Electromagnetics	profile start	58 °15,592' N	001° 01,472' E	151.1	1.0	300.6	58,259,859	1,024,538	71	F2S2	60.0	
MSM63_6-1	04.05.2017 15:58	Controlled Source Electromagnetics	profile end	58 °18,226' N	000° 55,004' E	153.6		297.7	58,303,765	0.916731	116	F2S2	60.0	
MSM63_6-1	04.05.2017 15:58	Controlled Source Electromagnetics	alter course	58 °18,228' N	000° 54,999' E	153.0		298.0	58,303,797	0.916645	116	F2S2	60.0	Kurs 128°
MSM63_6-1	04.05.2017 16:44	Controlled Source Electromagnetics	profile start	58 °17,676' N	000° 55,520' E	152.8	1.0	143.1	58,294,599	0.925329	75	F2S2	129.0	
MSM63_6-1	04.05.2017 17:32	Controlled Source Electromagnetics	on deck	58 °17,192' N	000° 56,711' E	154.0	0.7	121.1	58,286,530	0.945178	338	F2S2	-12.0	techn. Probleme - Unterbrechung Profil
MSM63_6-1	04.05.2017 17:41	Controlled Source Electromagnetics	in the water	58 °17,129' N	000° 56,865' E	154.5	1.0	131.9	58,285,490	0.947757	331	F2S2	-1.0	Fortsetzung Profil
MSM63_6-1	04.05.2017 20:02	Controlled Source Electromagnetics	profile end	58 °15,702' N	001° 00,370' E	152.0	0.8	116.4	58,261,693	1,006,165	4	F2S2	60.0	
MSM63_6-1	04.05.2017 20:02	Controlled Source Electromagnetics	alter course	58 °15,701' N	001° 00,372' E	151.7	0.8	145.8	58,261,680	1,006,195	4	F2S2	60.0	Kurs 263°

MSM63_6-1	04.05.2017 21:11	Controlled Source Electromagnetics	profile start	58 °16,726' N	001° 01,272' E	150.9	1.0	309.5	58,278,768	1,021,208	4		F2S2	60.0	
MSM63_6-1	05.05.2017 00:22	Controlled Source Electromagnetics	profile end	58 °16,322' N	000° 55,288' E	154.3	1.0	259.5	58,272,030	0.921468	9		F2S2	108.0	
MSM63_6-1	05.05.2017 00:23	Controlled Source Electromagnetics	alter course	58 °16,322' N	000° 55,263' E	154.2	1.0	278.7	58,272,030	0.921051	9		F2S2	104.0	Kurs 083°
MSM63_6-1	05.05.2017 00:46	Controlled Source Electromagnetics	profile start	58 °16,699' N	000° 55,188' E	154.0	1.0	65.6	58,278,315	0.919795	3	13.90	F2S2	60.0	
MSM63_6-1	05.05.2017 04:00	Controlled Source Electromagnetics	profile end	58 °17,112' N	001° 01,295' E	150.0		82.5	58,285,206	1,021,591	9	15.90	F2S2	60.0	
MSM63_6-1	05.05.2017 04:00	Controlled Source Electromagnetics	alter course	58 °17,113' N	001° 01,301' E	150.6		79.4	58,285,211	1,021,684	8	15.80	F2S2	60.0	Kurs 263°
MSM63_6-1	05.05.2017 04:24	Controlled Source Electromagnetics	profile start	58 °17,487' N	001° 01,180' E	151.5	1.0	249.3	58,291,457	1,019,663	22	14.60	F2S2	62.0	
MSM63_6-1	05.05.2017 07:35	Controlled Source Electromagnetics	profile end	58 °17,083' N	000° 55,199' E	154.6	1.0	269.4	58,284,714	0.919988	38		F2S2	105.0	
MSM63_6-1	05.05.2017 07:54	Controlled Source Electromagnetics	on deck	58 °17,043' N	000° 54,619' E	154.9	1.0	256.8	58,284,051	0.910312	42		F2S2	-13.0	DASI
MSM63_6-1	05.05.2017 08:10	Controlled Source Electromagnetics	on deck	58 °17,009' N	000° 54,118' E	154.6	0.9	251.6	58,283,486	0.901965	42			0.0	Antenna + 5 Benthos
MSM63_6-1	05.05.2017 08:10	Controlled Source Electromagnetics	on deck	58 °17,007' N	000° 54,097' E	154.8	0.8	269.9	58,283,456	0.901613	42			0.0	Pressure sensor
MSM63_6-1	05.05.2017 08:17	Controlled Source Electromagnetics	on deck	58 °17,006' N	000° 54,076' E	155.0	0.1	169.6	58,283,436	0.901259	56			0.0	Vulcan 2
MSM63_6-1	05.05.2017 08:20	Controlled Source Electromagnetics	on deck	58 °17,006' N	000° 54,076' E	154.2	0.0	73.8	58,283,429	0.901259	53			0.0	Vulcan 1
MSM63_4-14	05.05.2017 08:50	Magnetotellurics	information	58 °17,011' N	000° 54,161' E	154.9		41.1	58,283,520	0.902684	57			0.0	Ausgelöt

MSM63_4-14	05.05.2017 09:18	Magnetotellurics	on deck	58 °16,181' N	000° 57,145' E	155.1	0.4	327.3	58,269,679	0.952424	46	9.00	0.0	
MSM63_4-13	05.05.2017 09:21	Magnetotellurics	information	58 °16,182' N	000° 57,144' E	155.9	0.2	229.6	58,269,708	0.952399	38		0.0	Ausgelöt
MSM63_4-13	05.05.2017 09:43	Magnetotellurics	on deck	58 °16,377' N	000° 57,362' E	154.3	0.6	50.9	58,272,955	0.956039	48		0.0	
MSM63_4-11	05.05.2017 10:00	Magnetotellurics	information	58 °16,754' N	000° 57,445' E	154.4	0.1	338.5	58,279,234	0.957411	45		0.0	Ausgelöt
MSM63_4-12	05.05.2017 10:20	Magnetotellurics	on deck	58 °16,577' N	000° 57,726' E	154.6	0.9	165.0	58,276,278	0.962096	63		0.0	
MSM63_4-10	05.05.2017 10:33	Magnetotellurics	information	58 °16,476' N	000° 58,161' E	154.7	0.0	42809	58,274,594	0.969347	51		0.0	Ausgelöt
MSM63_4-11	05.05.2017 10:36	Magnetotellurics	on deck	58 °16,477' N	000° 58,161' E	154.4	0.3	339.2	58,274,609	0.969348	56		0.0	
MSM63_4-10	05.05.2017 10:37	Magnetotellurics	on deck	58 °16,484' N	000° 58,155' E	154.9		337.9	58,274,741	0.969247	46		0.0	
MSM63_4-9	05.05.2017 10:57	Magnetotellurics	on deck	58 °16,506' N	000° 58,784' E	152.8	0.0		58,275,101	0.979733	71		0.0	
MSM63_4-8	05.05.2017 11:15	Magnetotellurics	on deck	58 °16,620' N	000° 58,498' E	153.6	0.0	83.3	58,276,994	0.974968	54		0.0	
MSM63_4-7	05.05.2017 11:33	Magnetotellurics	on deck	58 °17,030' N	000° 57,676' E	153.2	0.0	341.5	58,283,841	0.961272	89		0.0	
MSM63_4-6	05.05.2017 11:46	Magnetotellurics	on deck	58 °17,154' N	000° 57,335' E	153.7	0.0	279.9	58,285,894	0.955579	77		0.0	
MSM63_4-4	05.05.2017 11:59	Magnetotellurics	information	58 °17,204' N	000° 57,927' E	153.6	0.1	117.6	58,286,738	0.965443	44	6.00	0.0	Ausgelöt
MSM63_4-5	05.05.2017 12:03	Magnetotellurics	on deck	58 °17,204' N	000° 57,927' E	153.5	0.0	54.7	58,286,741	0.965443	36		0.0	

MSM63_4-3	05.05.2017 12:18	Magnetotellurics	information	58 °17,066' N	000° 58,263' E	154.8	0.0	304.8	58,284,440	0.971055	57	0.0	Ausgelöt
MSM63_4-4	05.05.2017 12:19	Magnetotellurics	on deck	58 °17,068' N	000° 58,264' E	154.5	0.4	345.9	58,284,461	0.971059	55	0.0	
MSM63_4-2	05.05.2017 12:31	Magnetotellurics	information	58 °16,915' N	000° 58,685' E	153.4	0.4	42.2	58,281,923	0.978079	30	0.0	Ausgelöt
MSM63_4-3	05.05.2017 12:31	Magnetotellurics	on deck	58 °16,916' N	000° 58,686' E	152.9	0.4		58,281,930	0.978092	30	0.0	
MSM63_4-1	05.05.2017 12:50	Magnetotellurics	information	58 °17,204' N	000° 58,710' E	153.3	0.0	326.8	58,286,732	0.978501	44	0.0	Ausgelöt
MSM63_4-2	05.05.2017 12:52	Magnetotellurics	on deck	58 °17,204' N	000° 58,710' E	153.3	0.0		58,286,734	0.978503	43	0.0	
MSM63_4-1	05.05.2017 13:06	Magnetotellurics	on deck	58 °17,569' N	000° 59,046' E	152.0	0.5		58,292,811	0.984097	36	0.0	
MSM63_7-1	05.05.2017 14:28	Seismic Towed Receiver	in the water	58 °12,526' N	000° 50,639' E	155.3		37.8	58,208,771	0.843991	11	0.0	Stb Scheerbrett
MSM63_7-1	05.05.2017 18:45	Seismic Towed Receiver	in the water	58 °18,131' N	000° 58,342' E	153.9	0.0	35.0	58,302,176	0.972360	351	0.0	P-Cable
MSM63_7-1	05.05.2017 18:47	Seismic Towed Receiver	in the water	58 °18,159' N	000° 58,381' E	153.1	0.0	33.6	58,302,650	0.973010	350	0.0	Bb Scheerbrett
MSM63_7-1	05.05.2017 19:00	Seismic Towed Receiver	in the water	58 °18,402' N	000° 58,715' E	152.3	0.0	37.2	58,306,693	0.978579	353	0.0	Airguns
MSM63_7-1	05.05.2017 19:12	Seismic Towed Receiver	information	58 °18,635' N	000° 59,036' E	152.4	0.0	33.8	58,310,583	0.983934	355	0.0	techn. Probleme Seismik, Beginn einholen
MSM63_7-	05.05.2017	Seismic Towed	on	58 °18,804' N	000° 59,270' E	151.7	0.0	35.8	58,313,402	0.987830	346	0.0	Airguns

1	19:21	Receiver	deck											
MSM63_7-	05.05.2017	Seismic Towed	on	58 °19,318' N	000° 59,978' E	151.2	0.0	40.4	58,321,969	0.999634	345		0.0	Bb Scheerbrett
1	19:48	Receiver	deck											
MSM63_7-	05.05.2017	Seismic Towed	on	58 °19,829' N	001° 00,643' E	149.8	0.0	31.4	58,330,479	1,010,724	343		0.0	P-Cable
1	20:15	Receiver	deck											
MSM63_7-	05.05.2017	Seismic Towed	on	58 °20,057' N	001° 00,939' E	149.8	0.0	33.5	58,334,286	1,015,654	343		0.0	Stb
1	20:27	Receiver	deck											Scheerbrett
MSM63_7-	05.05.2017	Seismic Towed	in the	58 °20,318' N	001° 01,277' E	149.4	0.0	38.6	58,338,626	1,021,284	346		0.0	Airguns
2	20:40	Receiver	water											
MSM63_7-	05.05.2017	Seismic Towed	profile	58 °19,763' N	001° 01,640' E	149.8		215.0	58,329,383	1,027,329	359	13.60	0.0	v=4,5kn, Kurs
2	21:38	Receiver	start											218°
MSM63_7-	05.05.2017	Seismic Towed	profile	58 °14,333' N	000° 53,694' E	154.8		216.3	58,238,875	0.894895	351	15.20	0.0	
2	23:10	Receiver	end											
MSM63_7-	05.05.2017	Seismic Towed	alter	58 °14,310' N	000° 53,662' E	154.8		215.5	58,238,500	0.894362	353	15.50	0.0	Kurs 038°
2	23:11	Receiver	course											
MSM63_7-	05.05.2017	Seismic Towed	profile	58 °14,281' N	000° 54,198' E	155.1	5.0	42.9	58,238,013	0.903307	353	15.70	0.0	
2	23:18	Receiver	start											
MSM63_7-	06.05.2017	Seismic Towed	profile	58 °19,541' N	001° 01,939' E	149.3		37.0	58,325,677	1,032,320	353	15.20	0.0	
2	00:46	Receiver	end											
MSM63_7-	06.05.2017	Seismic Towed	alter	58 °19,560' N	001° 01,968' E	149.9		36.8	58,325,998	1,032,795	350	14.40	0.0	Kurs 218°
2	00:46	Receiver	course											
MSM63_7-	06.05.2017	Seismic Towed	profile	58 °19,544' N	001° 02,102' E	148.8		209.4	58,325,728	1,035,026	354	13.20	0.0	
2	01:02	Receiver	start											
MSM63_7-	06.05.2017	Seismic Towed	profile	58 °14,203' N	000° 54,297' E	154.7		219.4	58,236,718	0.904949	357		0.0	
2	02:34	Receiver	end											
MSM63_7-	06.05.2017	Seismic Towed	alter	58 °14,195' N	000° 54,284' E	154.5		220.5	58,236,588	0.904741	357		0.0	Kurs: 038°
2	02:34	Receiver	course											
MSM63_7-	06.05.2017	Seismic Towed	profile	58 °14,188' N	000° 54,450' E	154.3		41.0	58,236,474	0.907495	348	13.30	0.0	

2	02:49	Receiver	start											
MSM63_7-2	06.05.2017 04:18	Seismic Towed Receiver	profile end	58 °19,534' N	001° 02,295' E	147.9		37.1	58,325,573	1,038,247	2		0.0	
MSM63_7-2	06.05.2017 04:18	Seismic Towed Receiver	alter course	58 °19,545' N	001° 02,311' E	148.2		37.3	58,325,755	1,038,510	2		0.0	Kurs 218°
MSM63_7-2	06.05.2017 04:27	Seismic Towed Receiver	profile start	58 °19,357' N	001° 02,653' E	152.3	5.0	214.3	58,322,625	1,044,220	1		0.0	
MSM63_7-2	06.05.2017 05:56	Seismic Towed Receiver	profile end	58 °14,008' N	000° 54,831' E	155.1		217.6	58,233,474	0.913847	354		0.0	
MSM63_7-2	06.05.2017 06:27	Seismic Towed Receiver	alter course	58 °13,719' N	000° 58,532' E	153.8		87.5	58,228,654	0.975528	2		0.0	Kurs 353°
MSM63_7-2	06.05.2017 06:34	Seismic Towed Receiver	profile start	58 °14,095' N	000° 58,915' E	157.6		357.9	58,234,917	0.981912	355		0.0	
MSM63_7-2	06.05.2017 07:49	Seismic Towed Receiver	profile end	58 °19,684' N	000° 57,548' E	152.1		353.9	58,328,069	0.959137	8		0.0	
MSM63_7-2	06.05.2017 07:51	Seismic Towed Receiver	on deck	58 °19,832' N	000° 57,514' E	152.0		353.6	58,330,537	0.958565	3		0.0	Airguns
MSM63_8-1	06.05.2017 09:34	Seismic Towed Receiver	in the water	58 °20,627' N	000° 57,349' E	151.5	0.9		58,343,779	0.955816	5		0.0	Streamer 70m
MSM63_8-1	06.05.2017 09:48	Seismic Towed Receiver	in the water	58 °20,977' N	000° 57,436' E	151.2			58,349,620	0.957262	4		0.0	Airguns
MSM63_8-1	06.05.2017 10:44	Seismic Towed Receiver	profile start	58 °19,614' N	001° 02,004' E	149.3		219.4	58,326,896	1,033,393	17		0.0	v=4,5kn, Kurs 218°
MSM63_8-1	06.05.2017 12:13	Seismic Towed Receiver	profile end	58 °14,210' N	000° 54,084' E	155.0		240.0	58,236,837	0.901405	18		0.0	
MSM63_8-1	06.05.2017 12:14	Seismic Towed Receiver	alter course	58 °14,208' N	000° 54,078' E	154.8		238.9	58,236,806	0.901304	18		0.0	Kurs 038°
MSM63_8-	06.05.2017	Seismic Towed	profile	58 °14,216' N	000° 54,294' E	153.7		41.9	58,236,932	0.904892	3	11.00	0.0	

1	12:37	Receiver	start										
MSM63_8-1	06.05.2017 14:07	Seismic Towed Receiver	profile end	58 °19,563' N	001° 02,143' E	148.4	32.4	58,326,055	1,035,720	6		0.0	
MSM63_8-1	06.05.2017 14:08	Seismic Towed Receiver	alter course	58 °19,575' N	001° 02,157' E	148.6		58,326,254	1,035,949	8		0.0	Kurs 218°
MSM63_8-1	06.05.2017 14:35	Seismic Towed Receiver	profile start	58 °19,278' N	001° 01,922' E	149.4	216.6	58,321,306	1,032,026	347		0.0	
MSM63_8-1	06.05.2017 16:00	Seismic Towed Receiver	profile end	58 °14,437' N	000° 54,821' E	154.1	217.6	58,240,613	0.913688	353		0.0	
MSM63_8-1	06.05.2017 16:30	Seismic Towed Receiver	alter course	58 °16,235' N	000° 53,132' E	154.4	342.8	58,270,584	0.885535	17		0.0	Kurs 082°
MSM63_8-1	06.05.2017 16:35	Seismic Towed Receiver	profile start	58 °16,531' N	000° 53,389' E	150.6	73.6	58,275,508	0.889813	360		0.0	
MSM63_8-1	06.05.2017 17:43	Seismic Towed Receiver	profile end	58 °17,253' N	001° 02,952' E	149.5	84.2	58,287,556	1,049,195	8		0.0	
MSM63_8-1	06.05.2017 18:10	Seismic Towed Receiver	alter course	58 °15,391' N	001° 02,992' E	147.1	189.5	58,256,509	1,049,865	8	14.90	0.0	Kurs 308
MSM63_8-1	06.05.2017 18:16	Seismic Towed Receiver	profile start	58 °15,228' N	001° 02,422' E	150.6	297.3	58,253,795	1,040,372	21	16.80	0.0	
MSM63_8-1	06.05.2017 19:36	Seismic Towed Receiver	profile end	58 °18,830' N	000° 53,473' E	152.3	306.4	58,313,835	0.891215	14	20.30	0.0	
MSM63_8-1	06.05.2017 19:37	Seismic Towed Receiver	alter course	58 °18,871' N	000° 53,333' E	152.4	290.8	58,314,512	0.888889	20	20.80	0.0	Kurs 128°
MSM63_8-1	06.05.2017 19:58	Seismic Towed Receiver	profile start	58 °18,710' N	000° 54,326' E	152.9	127.3	58,311,831	0.905436	4	18.90	0.0	
MSM63_8-1	06.05.2017 21:11	Seismic Towed Receiver	profile end	58 °15,328' N	001° 02,589' E	150.6	129.0	58,255,471	1,043,149	6	24.90	0.0	
MSM63_8-	06.05.2017	Seismic Towed	alter	58 °15,315' N	001° 02,622' E	149.5	126.0	58,255,254	1,043,698	8	24.50	0.0	Kurs 308°

1	21:11	Receiver	course										
MSM63_8-	06.05.2017	Seismic Towed	profile	58 °15,136' N	001° 02,297' E	150.8	307.5	58,252,265	1,038,283	4	21.80	0.0	
1	21:29	Receiver	start										
MSM63_8-	06.05.2017	Seismic Towed	profile	58 °18,541' N	000° 54,011' E	153.5	311.0	58,309,018	0.900191	14	19.20	0.0	
1	22:43	Receiver	end										
MSM63_8-	06.05.2017	Seismic Towed	alter	58 °18,559' N	000° 53,970' E	153.2	303.4	58,309,319	0.899495	13		0.0	Kurs 128°
1	22:44	Receiver	course										
MSM63_8-	06.05.2017	Seismic Towed	profile	58 °18,697' N	000° 54,136' E	152.7	132.9	58,311,611	0.902274	0	18.90	0.0	
1	23:03	Receiver	start										
MSM63_8-	07.05.2017	Seismic Towed	profile	58 °15,251' N	001° 02,515' E	150.2	126.0	58,254,189	1,041,918	2		0.0	
1	00:15	Receiver	end										
MSM63_8-	07.05.2017	Seismic Towed	alter	58 °15,246' N	001° 02,532' E	151.2	120.9	58,254,092	1,042,202	3	19.30	0.0	Kurs 308°
1	00:15	Receiver	course										
MSM63_8-	07.05.2017	Seismic Towed	profile	58 °15,120' N	001° 02,194' E	150.4	308.4	58,251,994	1,036,561	6	21.50	0.0	
1	00:32	Receiver	start										
MSM63_8-	07.05.2017	Seismic Towed	profile	58 °18,507' N	000° 53,938' E	153.4	306.5	58,308,443	0.898969	5	24.60	0.0	
1	01:45	Receiver	end										
MSM63_8-	07.05.2017	Seismic Towed	alter	58 °18,536' N	000° 53,866' E	152.1	312.0	58,308,935	0.897759	12	24.90	0.0	Kurs 128°
1	01:45	Receiver	course										
MSM63_8-	07.05.2017	Seismic Towed	profile	58 °18,134' N	000° 53,209' E	152.1	130.7	58,302,238	0.886817	355	22.30	0.0	
1	01:59	Receiver	start										
MSM63_8-	07.05.2017	Seismic Towed	profile	58 °14,876' N	001° 01,133' E	151.9	125.2	58,247,939	1,018,878	358	24.90	0.0	
1	03:08	Receiver	end										
MSM63_8-	07.05.2017	Seismic Towed	alter	58 °15,577' N	001° 02,762' E	149.6	40.0	58,259,621	1,046,028	345	28.20	0.0	Kurs 308°
1	03:25	Receiver	course										
MSM63_8-	07.05.2017	Seismic Towed	profile	58 °15,865' N	001° 02,766' E	149.4	314.9	58,264,409	1,046,097	358		0.0	
1	03:29	Receiver	start										
MSM63_8-	07.05.2017	Seismic Towed	profile	58 °19,040' N	000° 55,100' E	151.4	315.1	58,317,334	0.918331	356	27.90	0.0	

1	04:38	Receiver	end										
MSM63_8-1	07.05.2017 04:39	Seismic Towed Receiver	alter course	58 °19,074' N	000° 54,999' E	150.7	301.6	58,317,897	0.916647	359	29.40	0.0	Kurs 128°
MSM63_8-1	07.05.2017 04:51	Seismic Towed Receiver	profile start	58 °18,729' N	000° 53,799' E	153.6	151.4	58,312,145	0.896651	12	27.30	0.0	
MSM63_8-1	07.05.2017 06:04	Seismic Towed Receiver	profile end	58 °15,378' N	001° 02,012' E	149.7	119.2	58,256,308	1,033,526	2	32.10	0.0	
MSM63_8-1	07.05.2017 06:18	Seismic Towed Receiver	alter course	58 °15,920' N	001° 03,317' E	149.3	34.4	58,265,327	1,055,287	359		0.0	Kurs 308°
MSM63_8-1	07.05.2017 06:23	Seismic Towed Receiver	profile start	58 °16,262' N	001° 03,148' E	150.0	305.7	58,271,032	1,052,464	1	32.10	0.0	
MSM63_8-1	07.05.2017 06:59	Seismic Towed Receiver	profile end	58 °17,883' N	000° 59,198' E	90.4	298.8	58,298,054	0.986633	11	27.70	0.0	
MSM63_8-1	07.05.2017 07:00	Seismic Towed Receiver	information	58 °17,913' N	000° 59,128' E	153.2	304.7	58,298,543	0.985471	11	30.00	0.0	techn. Probleme Airguns, Beginn einholen
MSM63_8-1	07.05.2017 07:07	Seismic Towed Receiver	on deck	58 °18,195' N	000° 59,048' E	152.8	351.0	58,303,242	0.984133	2		0.0	Streamer
MSM63_8-1	07.05.2017 07:12	Seismic Towed Receiver	on deck	58 °18,288' N	000° 59,048' E	145.2	335.9	58,304,808	0.984129	5	33.30	0.0	Airguns
MSM63_9-1	07.05.2017 07:54	Shallow-water Multibeam Echosounder	profile start	58 °17,271' N	000° 58,109' E	154.6	210.4	58,287,848	0.968479	353	30.40	0.0	v=7kn, Kurs 217°
MSM63_9-1	07.05.2017 07:59	Shallow-water Multibeam Echosounder	profile end	58 °16,830' N	000° 57,480' E	154.9	215.9	58,280,492	0.957993	356	27.70	0.0	

MSM63_9-1	07.05.2017 07:59	Shallow-water Multibeam Echosounder	alter course	58 °16,828' N	000° 57,477' E	154.7	215.9	58,280,463	0.957952	356	27.70	0.0	Kurs 037°
MSM63_9-1	07.05.2017 08:17	Shallow-water Multibeam Echosounder	profile start	58 °16,805' N	000° 57,448' E	155.7	35.9	58,280,090	0.957472	4	31.60	0.0	
MSM63_9-1	07.05.2017 08:25	Shallow-water Multibeam Echosounder	profile end	58 °17,471' N	000° 58,560' E	153.9	59.3	58,291,191	0.975998	1	33.10	0.0	
MSM63_9-1	07.05.2017 08:25	Shallow-water Multibeam Echosounder	alter course	58 °17,473' N	000° 58,563' E	152.6	54.9	58,291,211	0.976051	1	33.10	0.0	Kurs 286°
MSM63_9-1	07.05.2017 08:42	Shallow-water Multibeam Echosounder	profile start	58 °16,906' N	000° 58,978' E	155.4	268.6	58,281,762	0.982972	9	34.70	0.0	
MSM63_9-1	07.05.2017 08:49	Shallow-water Multibeam Echosounder	profile end	58 °17,119' N	000° 57,685' E	154.8	286.1	58,285,323	0.961412	8	32.80	0.0	
MSM63_9-1	07.05.2017 08:49	Shallow-water Multibeam Echosounder	alter course	58 °17,119' N	000° 57,685' E	154.2	288.6	58,285,323	0.961412	8	32.80	0.0	Kurs 106°
MSM63_9-1	07.05.2017 09:01	Shallow-water Multibeam Echosounder	profile start	58 °17,136' N	000° 57,653' E	153.5	100.4	58,285,599	0.960888	4	33.50	0.0	
MSM63_9-1	07.05.2017 09:07	Shallow-water Multibeam Echosounder	profile end	58 °16,888' N	000° 59,097' E	152.4	104.9	58,281,473	0.984958	3	34.50	0.0	
MSM63_9-	07.05.2017	Shallow-water	alter	58 °16,888' N	000° 59,102' E	153.0	108.5	58,281,462	0.985031	3	34.50	0.0	Kurs 043°

1	09:07	Multibeam Echosounder	course										
MSM63_9-1	07.05.2017 09:25	Shallow-water Multibeam Echosounder	profile start	58 °17,198' N	000° 58,079' E	153.3		47.3	58,286,641	0.967991	353	31.90	0.0	
MSM63_9-1	07.05.2017 09:32	Shallow-water Multibeam Echosounder	profile end	58 °17,724' N	000° 59,000' E	152.9		46.8	58,295,400	0.983340	357	33.70	0.0	
MSM63_9-1	07.05.2017 09:32	Shallow-water Multibeam Echosounder	alter course	58 °17,725' N	000° 59,003' E	154.2		46.4	58,295,420	0.983380	357	33.70	0.0	v=3kn, Kurs 043°
MSM63_9-1	07.05.2017 09:51	Shallow-water Multibeam Echosounder	profile start	58 °17,199' N	000° 58,063' E	152.5		41.1	58,286,645	0.967713	354	33.60	0.0	
MSM63_9-1	07.05.2017 10:04	Shallow-water Multibeam Echosounder	profile end	58 °17,707' N	000° 58,956' E	152.0		36.9	58,295,112	0.982598	350	32.20	0.0	
MSM63_10-1	07.05.2017 11:13	Shallow-water Multibeam Echosounder	profile start	58 °13,743' N	000° 54,172' E	153.2		1.0	58,229,046	0.902868	357	34.50	0.0	v=7kn; Kurs 000°
MSM63_10-1	07.05.2017 12:38	Shallow-water Multibeam Echosounder	profile end	58 °22,346' N	000° 54,161' E	140.9		358.1	58,372,432	0.902679	359	32.90	0.0	
MSM63_10-1	07.05.2017 12:38	Shallow-water Multibeam Echosounder	alter course	58 °22,382' N	000° 54,150' E	142.4		346.4	58,373,035	0.902508	0	31.60	0.0	Kurs 180°
MSM63_10-1	07.05.2017 12:51	Shallow-water Multibeam	profile start	58 °22,114' N	000° 54,281' E	141.5	7.0	172.7	58,368,559	0.904682	355	33.50	0.0	

		Echosounder												
MSM63_10-1	07.05.2017 13:59	Shallow-water Multibeam Echosounder	profile end	58 °13,607' N	000° 54,280' E	155.5		178.5	58,226,790	0.904660	2	31.90	0.0	
MSM63_10-1	07.05.2017 14:00	Shallow-water Multibeam Echosounder	alter course	58 °13,577' N	000° 54,280' E	154.8		178.9	58,226,289	0.904667	2	33.10	0.0	Kurs 000°
MSM63_10-1	07.05.2017 14:15	Shallow-water Multibeam Echosounder	profile start	58 °13,595' N	000° 54,418' E	158.0		354.1	58,226,575	0.906972	9	32.70	0.0	
MSM63_10-1	07.05.2017 15:40	Shallow-water Multibeam Echosounder	profile end	58 °22,285' N	000° 54,428' E	144.1			58,371,414	0.907125	3	36.10	0.0	
MSM63_10-1	07.05.2017 15:40	Shallow-water Multibeam Echosounder	alter course	58 °22,313' N	000° 54,425' E	143.2		349.9	58,371,889	0.907080	3	34.90	0.0	Kurs 180°
MSM63_10-1	07.05.2017 15:47	Shallow-water Multibeam Echosounder	profile start	58 °22,262' N	000° 54,604' E	142.1		179.2	58,371,038	0.910069	7	35.30	0.0	
MSM63_10-1	07.05.2017 16:54	Shallow-water Multibeam Echosounder	profile end	58 °13,556' N	000° 54,599' E	154.4		192.3	58,225,928	0.909980	3	34.60	0.0	
MSM63_10-1	07.05.2017 16:54	Shallow-water Multibeam Echosounder	alter course	58 °13,544' N	000° 54,594' E	154.8	8.0	191.6	58,225,738	0.909903	3	34.60	0.0	Kurs 000°
MSM63_10-1	07.05.2017 17:03	Shallow-water Multibeam Echosounder	profile start	58 °13,533' N	000° 54,693' E	151.5			58,225,555	0.911547	3	31.20	0.0	

MSM63_10-1	07.05.2017 18:35	Shallow-water Multibeam Echosounder	profile end	58 °22,264' N	000° 54,740' E	140.3	0.3	58,371,067	0.912334	7	36.40	0.0	
MSM63_10-1	07.05.2017 18:36	Shallow-water Multibeam Echosounder	alter course	58 °22,272' N	000° 54,741' E	143.0	2.0	58,371,205	0.912352	7	36.40	0.0	Kurs 000°
MSM63_10-1	07.05.2017 18:44	Shallow-water Multibeam Echosounder	profile start	58 °22,293' N	000° 54,951' E	142.0	184.1	58,371,552	0.915848	10	32.90	0.0	
MSM63_10-1	07.05.2017 19:51	Shallow-water Multibeam Echosounder	profile end	58 °13,410' N	000° 54,885' E	155.4	192.4	58,223,493	0.914752	2	29.70	0.0	
MSM63_10-1	07.05.2017 19:59	Shallow-water Multibeam Echosounder	alter course	58 °13,031' N	000° 54,931' E	156.0	37.5	58,217,183	0.915516	7	36.60	0.0	Kurs 000°
MSM63_10-1	07.05.2017 20:08	Shallow-water Multibeam Echosounder	profile start	58 °13,573' N	000° 55,058' E	156.6		58,226,209	0.917640	5	32.10	0.0	
MSM63_10-1	07.05.2017 22:09	Shallow-water Multibeam Echosounder	profile end	58 °22,197' N	000° 55,093' E	139.7		58,369,945	0.918220	12	34.40	0.0	
MSM63_10-1	07.05.2017 22:09	Shallow-water Multibeam Echosounder	alter course	58 °22,204' N	000° 55,091' E	143.6	351.9	58,370,062	0.918181	11	35.10	0.0	Kurs 180°
MSM63_10-1	07.05.2017 22:19	Shallow-water Multibeam Echosounder	profile start	58 °22,225' N	000° 55,251' E	142.9	179.5	58,370,415	0.920851	19	38.40	0.0	
MSM63_1	07.05.2017	Shallow-water	profile	58 °13,312' N	000° 55,160' E	155.9	215.8	58,221,864	0.919334	1	33.30	0.0	

0-1	23:32	Multibeam Echosounder	end										
MSM63_1 0-1	07.05.2017 23:32	Shallow-water Multibeam Echosounder	alter course	58 °13,294' N	000° 55,139' E	153.7	213.3	58,221,567	0.918977	359	34.70	0.0	Kurs 000°
MSM63_1 0-1	07.05.2017 23:50	Shallow-water Multibeam Echosounder	profile start	58 °13,612' N	000° 55,383' E	155.6	360.0	58,226,868	0.923042	11	33.60	0.0	
MSM63_1 0-1	08.05.2017 01:55	Shallow-water Multibeam Echosounder	profile end	58 °22,307' N	000° 55,431' E	142.8	0.9	58,371,783	0.923852	18	37.00	0.0	
MSM63_1 0-1	08.05.2017 01:55	Shallow-water Multibeam Echosounder	alter course	58 °22,319' N	000° 55,430' E	140.7	355.4	58,371,989	0.923833	18	37.00	0.0	Kurs 180°
MSM63_1 0-1	08.05.2017 02:04	Shallow-water Multibeam Echosounder	profile start	58 °22,040' N	000° 55,671' E	146.2	179.8	58,367,328	0.927848	15	35.60	0.0	
MSM63_1 0-1	08.05.2017 03:16	Shallow-water Multibeam Echosounder	profile end	58 °13,497' N	000° 55,578' E	155.0	188.4	58,224,947	0.926295	16	28.60	0.0	
MSM63_1 0-1	08.05.2017 03:16	Shallow-water Multibeam Echosounder	alter course	58 °13,456' N	000° 55,557' E	154.0	197.3	58,224,273	0.925946	13	27.90	0.0	Kurs 000°
MSM63_1 0-1	08.05.2017 03:27	Shallow-water Multibeam Echosounder	profile start	58 °13,505' N	000° 55,712' E	152.8		58,225,090	0.928526	18	32.10	0.0	
MSM63_1 0-1	08.05.2017 05:10	Shallow-water Multibeam	profile end	58 °21,688' N	000° 55,869' E	146.4		58,361,467	0.931154	21	31.80	0.0	

		Echosounder											
MSM63_10-1	08.05.2017 05:10	Shallow-water Multibeam Echosounder	alter course	58 °21,695' N	000° 55,869' E	147.8	348.1	58,361,582	0.931152	21	31.80	0.0	Kurs 180°
MSM63_10-1	08.05.2017 05:17	Shallow-water Multibeam Echosounder	profile start	58 °21,717' N	000° 55,983' E	146.1	192.2	58,361,954	0.933052	22	29.20	0.0	
MSM63_10-1	08.05.2017 06:19	Shallow-water Multibeam Echosounder	profile end	58 °13,462' N	000° 55,907' E	156.1	189.3	58,224,372	0.931787	20	31.30	0.0	
MSM63_10-1	08.05.2017 06:20	Shallow-water Multibeam Echosounder	alter course	58 °13,428' N	000° 55,897' E	156.0	193.8	58,223,803	0.931619	19	30.90	0.0	Kurs 000°
MSM63_10-1	08.05.2017 06:29	Shallow-water Multibeam Echosounder	profile start	58 °13,443' N	000° 56,074' E	151.7		58,224,045	0.934568	21	35.40	0.0	
MSM63_10-1	08.05.2017 08:25	Shallow-water Multibeam Echosounder	profile end	58 °21,710' N	000° 56,173' E	149.7	357.3	58,361,834	0.936225	21	30.80	0.0	
MSM63_10-1	08.05.2017 08:25	Shallow-water Multibeam Echosounder	alter course	58 °21,711' N	000° 56,173' E	150.5	355.9	58,361,856	0.936222	21	30.80	0.0	Kurs 181°
MSM63_10-1	08.05.2017 08:33	Shallow-water Multibeam Echosounder	profile start	58 °21,713' N	000° 56,407' E	147.4	179.1	58,361,883	0.940111	22	31.60	0.0	
MSM63_10-1	08.05.2017 09:38	Shallow-water Multibeam Echosounder	profile end	58 °13,495' N	000° 56,269' E	156.8	181.4	58,224,910	0.937817	24	26.30	0.0	

MSM63_10-1	08.05.2017 09:38	Shallow-water Multibeam Echosounder	alter course	58 °13,492' N	000° 56,269' E	156.8		179.5	58,224,870	0.937817	24	26.30	0.0	Kurs 000°
MSM63_10-1	08.05.2017 09:48	Shallow-water Multibeam Echosounder	profile start	58 °13,481' N	000° 56,379' E	155.5			58,224,680	0.939642	28	27.60	0.0	
MSM63_10-1	08.05.2017 11:25	Shallow-water Multibeam Echosounder	profile end	58 °21,858' N	000° 56,595' E	144.7		347.2	58,364,307	0.943242	37	28.80	0.0	
MSM63_10-1	08.05.2017 11:25	Shallow-water Multibeam Echosounder	alter course	58 °21,872' N	000° 56,586' E	144.9		343.1	58,364,540	0.943101	40	28.20	0.0	Kurs 000°
MSM63_10-1	08.05.2017 11:34	Shallow-water Multibeam Echosounder	profile start	58 °21,685' N	000° 56,767' E	148.8		185.8	58,361,411	0.946117	32	25.90	0.0	
MSM63_10-1	08.05.2017 12:43	Shallow-water Multibeam Echosounder	profile end	58 °13,408' N	000° 56,583' E	156.2		205.6	58,223,471	0.943047	31	22.50	0.0	
MSM63_10-1	08.05.2017 12:43	Shallow-water Multibeam Echosounder	alter course	58 °13,391' N	000° 56,566' E	154.8		209.2	58,223,176	0.942768	28	22.80	0.0	Kurs 000°
MSM63_10-1	08.05.2017 12:54	Shallow-water Multibeam Echosounder	profile start	58 °13,491' N	000° 56,757' E	155.5	6.0	356.0	58,224,855	0.945947	24	22.20	0.0	
MSM63_10-1	08.05.2017 14:17	Shallow-water Multibeam Echosounder	profile end	58 °22,222' N	000° 56,910' E	144.7		349.2	58,370,367	0.948497	13	22.80	0.0	
MSM63_1	08.05.2017	Shallow-water	alter	58 °22,240' N	000° 56,899' E	140.8		343.3	58,370,674	0.948320	13		0.0	Kurs 180°

0-1	14:18	Multibeam Echosounder	course										
MSM63_1 0-1	08.05.2017 14:25	Shallow-water Multibeam Echosounder	profile start	58 °22,150' N	000° 57,125' E	143.9	183.2	58,369,171	0.952086	3	22.40	0.0	
MSM63_1 0-1	08.05.2017 15:42	Shallow-water Multibeam Echosounder	profile end	58 °13,275' N	000° 56,930' E	154.3	175.8	58,221,249	0.948838	12	21.60	0.0	
MSM63_1 0-1	08.05.2017 15:42	Shallow-water Multibeam Echosounder	alter course	58 °13,266' N	000° 56,930' E	153.9	182.3	58,221,092	0.948839	12	21.60	0.0	Kurs 001°
MSM63_1 0-1	08.05.2017 16:00	Shallow-water Multibeam Echosounder	profile start	58 °14,320' N	000° 57,123' E	153.7	0.2	58,238,667	0.952056	6	24.30	0.0	
MSM63_1 0-1	08.05.2017 16:51	Shallow-water Multibeam Echosounder	profile end	58 °20,099' N	000° 57,249' E	149.3	357.8	58,334,989	0.954142	1	20.90	0.0	
MSM63_1 0-1	08.05.2017 16:52	Shallow-water Multibeam Echosounder	alter course	58 °20,135' N	000° 57,245' E	151.2	358.0	58,335,586	0.954081	3	20.80	0.0	Kurs 181°
MSM63_1 0-1	08.05.2017 16:56	Shallow-water Multibeam Echosounder	profile start	58 °20,226' N	000° 57,505' E	149.7	184.5	58,337,099	0.958425	1	19.90	0.0	
MSM63_1 0-1	08.05.2017 17:46	Shallow-water Multibeam Echosounder	profile end	58 °14,507' N	000° 57,413' E	152.1	178.8	58,241,786	0.956887	8	21.00	0.0	
MSM63_1 0-1	08.05.2017 17:48	Shallow-water Multibeam	alter course	58 °14,346' N	000° 57,380' E	153.1	195.3	58,239,103	0.956326	3	22.30	0.0	Kurs 000°

		Echosounder												
MSM63_10-1	08.05.2017 17:54	Shallow-water Multibeam Echosounder	profile start	58 °14,403' N	000° 57,588' E	154.0		1.0	58,240,057	0.959792	3	21.60	0.0	
MSM63_10-1	08.05.2017 18:44	Shallow-water Multibeam Echosounder	profile end	58 °20,176' N	000° 57,650' E	151.9		355.3	58,336,274	0.960831	7	21.50	0.0	
MSM63_10-1	08.05.2017 18:44	Shallow-water Multibeam Echosounder	alter course	58 °20,205' N	000° 57,646' E	151.8	7.0	352.6	58,336,758	0.960763	6	21.70	0.0	Kurs 180°
MSM63_10-1	08.05.2017 18:49	Shallow-water Multibeam Echosounder	profile start	58 °20,176' N	000° 57,883' E	151.6		175.6	58,336,264	0.964715	3	21.70	0.0	
MSM63_10-1	08.05.2017 19:40	Shallow-water Multibeam Echosounder	profile end	58 °14,426' N	000° 57,851' E	153.2		181.9	58,240,436	0.964175	8		0.0	
MSM63_10-1	08.05.2017 19:40	Shallow-water Multibeam Echosounder	alter course	58 °14,426' N	000° 57,851' E	153.2		181.9	58,240,436	0.964175	8		0.0	Kurs 000°
MSM63_10-1	08.05.2017 19:48	Shallow-water Multibeam Echosounder	profile start	58 °14,421' N	000° 58,143' E	153.7			58,240,350	0.969042	348	25.00	0.0	
MSM63_10-1	08.05.2017 20:37	Shallow-water Multibeam Echosounder	profile end	58 °20,134' N	000° 58,113' E	149.9			58,335,563	0.968551	352	22.20	0.0	
MSM63_10-1	08.05.2017 20:43	Shallow-water Multibeam Echosounder	profile start	58 °20,148' N	000° 58,426' E	152.3		191.3	58,335,795	0.973759	3	20.30	0.0	

MSM63_10-1	08.05.2017 20:43	Shallow-water Multibeam Echosounder	alter course	58 °20,145' N	000° 58,425' E	152.6	189.9	58,335,757	0.973746	3	20.30	0.0	Kurs 180°
MSM63_10-1	08.05.2017 21:32	Shallow-water Multibeam Echosounder	profile end	58 °14,420' N	000° 58,358' E	153.8	183.6	58,240,325	0.972639	359	22.60	0.0	
MSM63_10-1	08.05.2017 21:32	Shallow-water Multibeam Echosounder	alter course	58 °14,420' N	000° 58,358' E	153.8	183.6	58,240,325	0.972639	359	22.60	0.0	Kurs 000°
MSM63_10-1	08.05.2017 21:40	Shallow-water Multibeam Echosounder	profile start	58 °14,411' N	000° 58,690' E	154.6	358.5	58,240,182	0.978175	358	21.90	0.0	
MSM63_10-1	08.05.2017 22:30	Shallow-water Multibeam Echosounder	profile end	58 °20,135' N	000° 58,628' E	153.0	0.1	58,335,589	0.977127	354	23.20	0.0	
MSM63_10-1	08.05.2017 22:30	Shallow-water Multibeam Echosounder	alter course	58 °20,141' N	000° 58,628' E	151.4		58,335,689	0.977131	354	23.20	0.0	Kurs 180°
MSM63_10-1	08.05.2017 22:36	Shallow-water Multibeam Echosounder	profile start	58 °20,159' N	000° 58,939' E	151.5	184.2	58,335,976	0.982318	351	19.50	0.0	
MSM63_10-1	08.05.2017 23:25	Shallow-water Multibeam Echosounder	profile end	58 °14,298' N	000° 58,904' E	153.1	207.6	58,238,305	0.981731	352	19.80	0.0	
MSM63_10-1	08.05.2017 23:25	Shallow-water Multibeam Echosounder	alter course	58 °14,283' N	000° 58,889' E	153.2	208.1	58,238,054	0.981485	350	20.30	0.0	Kurs 000°
MSM63_1	08.05.2017	Shallow-water	profile	58 °14,457' N	000° 59,221' E	153.8	356.2	58,240,944	0.987021	4	16.90	0.0	

0-1	23:35	Multibeam Echosounder	start										
MSM63_1 0-1	09.05.2017 00:23	Shallow-water Multibeam Echosounder	profile end	58 °20,058' N	000° 59,141' E	151.0	357.7	58,334,295	0.985678	356	20.20	0.0	
MSM63_1 0-1	09.05.2017 00:23	Shallow-water Multibeam Echosounder	alter course	58 °20,073' N	000° 59,140' E	151.6	359.9	58,334,544	0.985666	356		0.0	Kurs 180°
MSM63_1 0-1	09.05.2017 00:32	Shallow-water Multibeam Echosounder	profile start	58 °20,104' N	000° 59,478' E	151.3	181.3	58,335,073	0.991295	347	15.60	0.0	
MSM63_1 0-1	09.05.2017 01:20	Shallow-water Multibeam Echosounder	profile end	58 °14,472' N	000° 59,467' E	151.9	181.7	58,241,207	0.991120	357	14.20	0.0	
MSM63_1 0-1	09.05.2017 01:21	Shallow-water Multibeam Echosounder	alter course	58 °14,463' N	000° 59,467' E	153.0	179.6	58,241,045	0.991115	357	14.20	0.0	Kurs 000°
MSM63_1 0-1	09.05.2017 01:30	Shallow-water Multibeam Echosounder	profile start	58 °14,443' N	000° 59,784' E	153.6	0.1	58,240,711	0.996397	355	19.80	0.0	
MSM63_1 0-1	09.05.2017 02:19	Shallow-water Multibeam Echosounder	profile end	58 °20,037' N	000° 59,719' E	151.8	353.6	58,333,958	0.995317	349		0.0	
MSM63_1 0-1	09.05.2017 02:19	Shallow-water Multibeam Echosounder	alter course	58 °20,041' N	000° 59,718' E	149.7	356.8	58,334,014	0.995306	348	17.50	0.0	Kurs 180°
MSM63_1 0-1	09.05.2017 02:27	Shallow-water Multibeam	profile start	58 °20,064' N	001° 00,031' E	149.8	179.5	58,334,404	1,000,511	342	20.20	0.0	

		Echosounder											
MSM63_10-1	09.05.2017 03:16	Shallow-water Multibeam Echosounder	profile end	58 °14,446' N	001° 00,007' E	152.9		180.1	58,240,767	1,000,120	350	19.90	0.0	
MSM63_10-1	09.05.2017 03:16	Shallow-water Multibeam Echosounder	alter course	58 °14,426' N	001° 00,008' E	151.8		180.8	58,240,428	1,000,134	351	19.70	0.0	Kurs 000°
MSM63_10-1	09.05.2017 03:21	Shallow-water Multibeam Echosounder	profile start	58 °14,432' N	001° 00,271' E	152.0			58,240,532	1,004,521	352	13.80	0.0	
MSM63_10-1	09.05.2017 04:11	Shallow-water Multibeam Echosounder	profile end	58 °20,059' N	001° 00,267' E	148.9			58,334,316	1,004,457	343		0.0	
MSM63_10-1	09.05.2017 04:11	Shallow-water Multibeam Echosounder	alter course	58 °20,088' N	001° 00,268' E	148.8		2.0	58,334,804	1,004,472	343	17.20	0.0	Kurs 180°
MSM63_10-1	09.05.2017 04:15	Shallow-water Multibeam Echosounder	profile start	58 °20,082' N	001° 00,516' E	148.7		174.7	58,334,692	1,008,605	341	17.30	0.0	
MSM63_10-1	09.05.2017 04:40	Shallow-water Multibeam Echosounder	profile end	58 °17,132' N	001° 00,534' E	151.4		185.2	58,285,527	1,008,898	333		0.0	
MSM63_5-1	09.05.2017 05:03	Seismic Ocean Bottom Receiver	released	58 °16,254' N	000° 57,480' E	154.1	0.1	73.8	58,270,902	0.958001	331	15.70	0.0	
MSM63_5-1	09.05.2017 05:17	Seismic Ocean Bottom Receiver	recovered	58 °16,407' N	000° 57,480' E	153.7	0.2	263.0	58,273,443	0.958001	331	18.80	0.0	
MSM63_5-2	09.05.2017 05:26	Seismic Ocean Bottom Receiver	released	58 °16,662' N	000° 58,107' E	154.4	0.6	35.4	58,277,698	0.968445	322	13.30	0.0	

MSM63_5-2	09.05.2017 05:38	Seismic Ocean Bottom Receiver	recovered	58 °16,830' N	000° 58,141' E	157.2	0.4	52.5	58,280,501	0.969012	350	16.70	0.0
MSM63_5-13	09.05.2017 05:40	Seismic Ocean Bottom Receiver	released	58 °16,837' N	000° 58,156' E	160.0	0.4	115.7	58,280,614	0.969268	349	14.50	0.0
MSM63_5-13	09.05.2017 05:49	Seismic Ocean Bottom Receiver	recovered	58 °16,931' N	000° 58,200' E	160.1		166.7	58,282,187	0.970006	351		0.0
MSM63_5-18	09.05.2017 05:52	Seismic Ocean Bottom Receiver	released	58 °16,891' N	000° 58,208' E	165.3	0.3	359.1	58,281,512	0.970128	348	16.90	0.0
MSM63_5-18	09.05.2017 06:02	Seismic Ocean Bottom Receiver	recovered	58 °17,036' N	000° 58,341' E	154.2	0.4		58,283,936	0.972345	348		0.0
MSM63_5-7	09.05.2017 06:12	Seismic Ocean Bottom Receiver	released	58 °17,299' N	000° 59,025' E	151.7	0.8	38.9	58,288,319	0.983757	341	14.70	0.0
MSM63_5-7	09.05.2017 06:24	Seismic Ocean Bottom Receiver	recovered	58 °17,470' N	000° 59,066' E	152.5		324.8	58,291,170	0.984437	337	15.20	0.0
MSM63_5-9	09.05.2017 06:38	Seismic Ocean Bottom Receiver	released	58 °16,579' N	000° 58,839' E	152.7	0.2	208.7	58,276,316	0.980643	327	16.30	0.0
MSM63_5-9	09.05.2017 06:47	Seismic Ocean Bottom Receiver	recovered	58 °16,681' N	000° 58,808' E	153.1	0.5	62.7	58,278,010	0.980125	330		0.0
MSM63_5-16	09.05.2017 06:55	Seismic Ocean Bottom Receiver	released	58 °16,668' N	000° 58,307' E	155.1	0.2	101.4	58,277,794	0.971780	331	17.90	0.0
MSM63_5-16	09.05.2017 07:07	Seismic Ocean Bottom Receiver	recovered	58 °16,762' N	000° 58,344' E	155.7		174.6	58,279,362	0.972399	322	18.20	0.0
MSM63_5-10	09.05.2017 07:14	Seismic Ocean Bottom Receiver	released	58 °16,735' N	000° 58,406' E	154.4	0.1	356.1	58,278,910	0.973431	326		0.0
MSM63_5-10	09.05.2017 07:24	Seismic Ocean Bottom Receiver	recovered	58 °16,808' N	000° 58,389' E	155.5		183.1	58,280,128	0.973151	326		0.0
MSM63_5-11	09.05.2017 07:31	Seismic Ocean Bottom Receiver	released	58 °16,755' N	000° 58,415' E	154.8	0.1		58,279,255	0.973589	321		0.0

MSM63_5-11	09.05.2017 07:42	Seismic Ocean Bottom Receiver	recovered	58 °16,817' N	000° 58,360' E	155.5		168.2	58,280,275	0.972674	326	13.60	0.0
MSM63_5-17	09.05.2017 08:02	Seismic Ocean Bottom Receiver	released	58 °16,790' N	000° 58,387' E	155.4	0.1	319.4	58,279,833	0.973110	327	15.90	0.0
MSM63_5-17	09.05.2017 08:18	Seismic Ocean Bottom Receiver	recovered	58 °16,847' N	000° 58,515' E	155.2	0.2	243.5	58,280,789	0.975253	329	14.00	0.0
MSM63_5-8	09.05.2017 08:20	Seismic Ocean Bottom Receiver	released	58 °16,845' N	000° 58,499' E	153.9	0.2	83.7	58,280,746	0.974977	338	15.60	0.0
MSM63_5-8	09.05.2017 08:31	Seismic Ocean Bottom Receiver	recovered	58 °16,916' N	000° 58,639' E	153.9		346.4	58,281,933	0.977311	344	13.80	0.0
MSM63_5-3	09.05.2017 08:39	Seismic Ocean Bottom Receiver	released	58 °16,719' N	000° 58,090' E	155.3	0.1	46.1	58,278,646	0.968164	335		0.0
MSM63_5-3	09.05.2017 08:49	Seismic Ocean Bottom Receiver	recovered	58 °16,757' N	000° 58,224' E	158.5		173.6	58,279,280	0.970402	337		0.0
MSM63_5-15	09.05.2017 08:54	Seismic Ocean Bottom Receiver	released	58 °16,743' N	000° 58,288' E	156.7	0.3	130.1	58,279,051	0.971472	331	11.00	0.0
MSM63_5-15	09.05.2017 09:04	Seismic Ocean Bottom Receiver	recovered	58 °16,788' N	000° 58,095' E	156.7		121.7	58,279,794	0.968257	316	16.00	0.0
MSM63_5-4	09.05.2017 09:06	Seismic Ocean Bottom Receiver	released	58 °16,780' N	000° 58,141' E	157.2	1.0	104.0	58,279,668	0.969018	313	17.20	0.0
MSM63_5-4	09.05.2017 09:16	Seismic Ocean Bottom Receiver	recovered	58 °16,825' N	000° 58,282' E	163.9	1.0	172.2	58,280,411	0.971361	332	16.30	0.0
MSM63_5-12	09.05.2017 09:19	Seismic Ocean Bottom Receiver	released	58 °16,790' N	000° 58,273' E	160.5	0.1	355.5	58,279,835	0.971223	329	15.60	0.0
MSM63_5-12	09.05.2017 09:30	Seismic Ocean Bottom Receiver	recovered	58 °16,817' N	000° 58,323' E	158.6	0.4	76.5	58,280,285	0.972046	324	17.00	0.0
MSM63_5-5	09.05.2017 09:31	Seismic Ocean Bottom Receiver	released	58 °16,817' N	000° 58,338' E	157.8	0.2	128.2	58,280,291	0.972299	326	15.90	0.0

MSM63_5-5	09.05.2017 09:42	Seismic Ocean Bottom Receiver	recovered	58 °16,889' N	000° 58,432' E	157.6	0.2	104.0	58,281,479	0.973875	317	14.70	0.0	
MSM63_5-6	09.05.2017 09:44	Seismic Ocean Bottom Receiver	released	58 °16,891' N	000° 58,448' E	156.8	0.7	163.0	58,281,521	0.974140	308	13.90	0.0	
MSM63_5-6	09.05.2017 09:54	Seismic Ocean Bottom Receiver	recovered	58 °16,957' N	000° 58,482' E	170.6	0.2	48.0	58,282,615	0.974707	317		0.0	
MSM63_5-14	09.05.2017 10:04	Seismic Ocean Bottom Receiver	information	58 °16,986' N	000° 57,716' E	153.4	0.1		58,283,100	0.961936	312	11.00	0.0	
MSM63_5-14	09.05.2017 10:15	Seismic Ocean Bottom Receiver	recovered	58 °17,008' N	000° 57,806' E	154.0	0.3		58,283,465	0.963440	298		0.0	
MSM63_11-1	09.05.2017 11:24	Seismic Towed Receiver	in the water	58 °12,740' N	000° 55,685' E	156.1	0.0	347.5	58,212,329	0.928091	289	15.40	0.0	Stb. Scherrbrett
MSM63_11-1	09.05.2017 12:55	Seismic Towed Receiver	PCable in water	58 °14,677' N	000° 55,151' E	155.8	0.0	350.2	58,244,620	0.919184	294	14.00	0.0	
MSM63_11-1	09.05.2017 12:57	Seismic Towed Receiver	in the water	58 °14,727' N	000° 55,138' E	154.2	0.0	356.3	58,245,443	0.918969	286	14.30	0.0	Bb. Scheerbrett
MSM63_11-1	09.05.2017 13:12	Seismic Towed Receiver	in the water	58 °15,049' N	000° 55,050' E	155.3	0.0	348.7	58,250,824	0.917500	284	14.50	0.0	GI-Guns
MSM63_11-1	09.05.2017 13:33	Seismic Towed Receiver	profile start	58 °15,915' N	000° 55,293' E	155.3	0.0		58,265,246	0.921553	294	18.20	0.0	v=3kn Kurs: 036°
MSM63_11-1	09.05.2017 13:48	Seismic Towed Receiver	information	58 °16,481' N	000° 56,068' E	154.9	0.0	36.9	58,274,688	0.934461	299	18.30	0.0	technische Probleme
MSM63_11-1	09.05.2017 13:51	Seismic Towed Receiver	on deck	58 °16,529' N	000° 56,134' E	151.6	0.0	34.7	58,275,488	0.935562	303	16.60	0.0	GI-Guns
MSM63_11-1	09.05.2017 13:54	Seismic Towed Receiver	information	58 °16,591' N	000° 56,217' E	155.4	0.0	33.4	58,276,509	0.936955	302	17.30	0.0	Scheerbrett rangeholt
MSM63_1	09.05.2017	Seismic Towed	on	58 °19,682' N	001° 00,492' E	150.8	0.0	45.4	58,328,032	1,008,197	291	17.60	0.0	Stb

1-1	16:39	Receiver	deck											Scheerbrett
MSM63_1	09.05.2017	Seismic Towed	on	58 °20,209' N	001° 00,780' E	149.2	0.0	300.3	58,336,817	1,013,006	291	20.80	0.0	Bb Scheerbrett
1-1	17:07	Receiver	deck											
MSM63_1	09.05.2017	Seismic Towed	on	58 °20,214' N	001° 00,750' E	148.6	0.0	290.2	58,336,904	1,012,495	295	21.60	0.0	P-cable
1-1	17:07	Receiver	deck											
MSM63_1	09.05.2017	Seismic Towed	in the	58 °20,417' N	001° 06,731' E	140.9	0.0	295.4	58,340,280	1,112,182	306	18.30	0.0	Streamer
2-1	20:10	Receiver	water											200m
MSM63_1	09.05.2017	Seismic Towed	in the	58 °20,652' N	001° 05,782' E	142.6	0.0	287.1	58,344,205	1,096,371	305	17.00	0.0	Airguns
2-1	20:32	Receiver	water											
MSM63_1	09.05.2017	Seismic Towed	profile	58 °21,650' N	001° 01,853' E	144.3		191.7	58,360,840	1,030,889	305	20.30	0.0	v=4,5kn, Kurs
2-1	21:25	Receiver	start											180°
MSM63_1	09.05.2017	Seismic Towed	alter	58 °11,527' N	001° 01,847' E	151.2		179.4	58,192,114	1,030,776	308	17.60	0.0	Kurs 258°
2-1	23:39	Receiver	course											
MSM63_1	10.05.2017	Seismic Towed	alter	58 °10,648' N	000° 55,786' E	156.4		286.3	58,177,459	0.929771	305	17.70	0.0	Kurs 000°
2-1	00:26	Receiver	course											
MSM63_1	10.05.2017	Seismic Towed	alter	58 °21,706' N	000° 56,083' E	147.8			58,361,762	0.934720	291	20.20	0.0	Kurs 196°
2-1	02:54	Receiver	course											
MSM63_1	10.05.2017	Seismic Towed	alter	58 °16,645' N	000° 52,731' E	154.0		190.6	58,277,418	0.878854	301	16.00	0.0	Kurs 090°
2-1	04:13	Receiver	course											
MSM63_1	10.05.2017	Seismic Towed	alter	58 °16,247' N	001° 05,741' E	146.8		89.5	58,270,788	1,095,689	299	17.50	0.0	Kurs 000°
2-1	05:46	Receiver	course											
MSM63_1	10.05.2017	Seismic Towed	alter	58 °17,244' N	001° 06,492' E	144.7		358.2	58,287,396	1,108,206	297	17.90	0.0	Kurs 270°
2-1	06:02	Receiver	course											
MSM63_1	10.05.2017	Seismic Towed	alter	58 °17,615' N	000° 51,803' E	153.8		270.7	58,293,588	0.863386	278	15.50	0.0	Kurs 000°
2-1	07:48	Receiver	course											
MSM63_1	10.05.2017	Seismic Towed	alter	58 °18,236' N	000° 51,326' E	153.6		359.9	58,303,926	0.855440	276	18.60	0.0	Kurs 088°
2-1	07:58	Receiver	course											
MSM63_1	10.05.2017	Seismic Towed	inform	58 °18,523' N	000° 52,762' E	152.5		88.0	58,308,721	0.879369	286	19.70	0.0	tech. Probleme

2-1	08:10	Receiver	ation										Streamer
MSM63_1	10.05.2017	Seismic Towed	inform	58 °18,524' N	000° 52,786' E	151.5	90.0	58,308,727	0.879768	286	19.20	0.0	Unterbrechung
2-1	08:10	Receiver	ation										Profil
MSM63_1	10.05.2017	Seismic Towed	inform	58 °19,705' N	000° 53,811' E	152.9	2.0	58,328,410	0.896855	276	17.30	0.0	Streamer-
2-1	09:07	Receiver	ation										Segment
													getauscht
MSM63_1	10.05.2017	Seismic Towed	inform	58 °18,542' N	000° 53,053' E	153.0	94.3	58,309,029	0.884213	288	17.40	0.0	Fortsetzung
2-1	09:38	Receiver	ation										Profil
MSM63_1	10.05.2017	Seismic Towed	alter	58 °18,645' N	001° 01,265' E	151.2	88.7	58,310,752	1,021,087	273	13.80	0.0	Kurs 231°
2-1	10:36	Receiver	course										
MSM63_1	10.05.2017	Seismic Towed	alter	58 °13,866' N	000° 51,195' E	157.3	236.7	58,231,092	0.853247	295	13.20	0.0	Kurs 156°
2-1	12:17	Receiver	course										
MSM63_1	10.05.2017	Seismic Towed	alter	58 °11,460' N	000° 52,709' E	156.5	155.9	58,190,999	0.878481	288		0.0	Kurs 024°
2-1	12:53	Receiver	course										
MSM63_1	10.05.2017	Seismic Towed	alter	58 °21,969' N	001° 02,441' E	148.1		58,366,150	1,040,692	278		0.0	Kurs 277°
2-1	15:35	Receiver	course										
MSM63_1	10.05.2017	Seismic Towed	alter	58 °22,559' N	000° 59,892' E	142.5	277.8	58,375,991	0.998204	278		0.0	Kurs 185°
2-1	15:58	Receiver	course										
MSM63_1	10.05.2017	Seismic Towed	alter	58 °10,879' N	000° 57,205' E	154.5	179.3	58,181,318	0.953410	268		0.0	Kurs 089°
2-1	18:40	Receiver	course										
MSM63_1	10.05.2017	Seismic Towed	alter	58 °10,600' N	000° 59,484' E	152.9	89.6	58,176,673	0.991399	267		0.0	Kurs 351°
2-1	18:58	Receiver	course										
MSM63_1	10.05.2017	Seismic Towed	alter	58 °21,461' N	000° 56,799' E	150.0	350.0	58,357,688	0.946656	67		0.0	Kurs 254°
2-1	21:28	Receiver	course										
MSM63_1	10.05.2017	Seismic Towed	alter	58 °21,526' N	000° 54,680' E	147.7	255.7	58,358,759	0.911331	60		0.0	Kurs 153°
2-1	21:45	Receiver	course										
MSM63_1	11.05.2017	Seismic Towed	alter	58 °11,601' N	001° 02,691' E	146.0	171.3	58,193,346	1,044,858	266		0.0	Kurs 346°
2-1	00:12	Receiver	course										

MSM63_1 2-1	11.05.2017 01:16	Seismic Towed Receiver	alter course	58 °15,563' N	001° 01,651' E	151.8	342.3	58,259,388	1,027,510	78	0.0	Kurs 301°
MSM63_1 2-1	11.05.2017 02:44	Seismic Towed Receiver	alter course	58 °19,387' N	000° 51,257' E	153.6	304.2	58,323,124	0.854291	84	0.0	Kurs 191°
MSM63_1 2-1	11.05.2017 03:18	Seismic Towed Receiver	alter course	58 °17,362' N	000° 49,687' E	154.3	190.3	58,289,364	0.828110	63	0.0	Kurs 091°
MSM63_1 2-1	11.05.2017 05:32	Seismic Towed Receiver	alter course	58 °16,830' N	001° 08,121' E	144.5	83.5	58,280,505	1,135,355	60	0.0	Kurs 282°
MSM63_1 2-1	11.05.2017 05:56	Seismic Towed Receiver	inform ation	58 °17,617' N	001° 06,617' E	145.0	291.4	58,293,609	1,110,285	69	0.0	Airguns an Deck - techn. Problem
MSM63_1 2-1	11.05.2017 06:43	Seismic Towed Receiver	inform ation	58 °18,111' N	001° 02,906' E	149.0	281.8	58,301,846	1,048,434	74	0.0	Airguns zu Wasser, Fortsetzung Profil
MSM63_1 2-1	11.05.2017 07:06	Seismic Towed Receiver	alter course	58 °18,297' N	000° 59,775' E	151.2	244.1	58,304,942	0.996258	82	0.0	Kurs 218°
MSM63_1 2-1	11.05.2017 08:10	Seismic Towed Receiver	alter course	58 °14,532' N	000° 54,123' E	155.4	217.2	58,242,203	0.902055	91	0.0	Kurs 353°
MSM63_1 2-1	11.05.2017 09:33	Seismic Towed Receiver	alter course	58 °18,455' N	000° 57,144' E	153.6	354.2	58,307,587	0.952406	103	0.0	Kurs 173°
MSM63_1 2-1	11.05.2017 10:33	Seismic Towed Receiver	alter course	58 °15,377' N	000° 58,640' E	153.3	170.9	58,256,283	0.977326	137	0.0	Kurs 353°
MSM63_1 2-1	11.05.2017 11:40	Seismic Towed Receiver	alter course	58 °18,508' N	000° 58,593' E	152.3	353.6	58,308,474	0.976549	137	0.0	Kurs 255°
MSM63_1 2-1	11.05.2017 11:58	Seismic Towed Receiver	alter course	58 °18,650' N	000° 56,384' E	154.6	261.9	58,310,832	0.939734	129	0.0	Kurs 128°
MSM63_1	11.05.2017	Seismic Towed	alter	58 °16,004' N	001° 01,346' E	152.2	116.4	58,266,729	1,022,432	130	0.0	Kurs 095°

2-1	12:54	Receiver	course												
MSM63_12-1	11.05.2017 13:01	Seismic Towed Receiver	alter course	58 °15,944' N	001° 02,295' E	149.8		104.7	58,265,734	1,038,248	126			0.0	Kurs 308°
MSM63_12-1	11.05.2017 14:17	Seismic Towed Receiver	profile end	58 °18,268' N	000° 54,933' E	155.0		298.9	58,304,459	0.915551	138			0.0	
MSM63_12-1	11.05.2017 14:31	Seismic Towed Receiver	on deck	58 °17,850' N	000° 54,086' E	155.5		181.9	58,297,500	0.901427	138			0.0	GI-Gun
MSM63_12-1	11.05.2017 14:31	Seismic Towed Receiver	on deck	58 °17,848' N	000° 54,085' E	153.7		182.3	58,297,470	0.901423	138			0.0	Streamer
MSM63_13-1	11.05.2017 14:46	Sound Velocity Profiler	in the water	58 °17,493' N	000° 54,057' E	154.3		182.6	58,291,554	0.900945	152	11.00		0.0	
MSM63_13-1	11.05.2017 15:06	Sound Velocity Profiler	max depth/ on ground	58 °17,474' N	000° 54,055' E	154.0	0.0	357.0	58,291,234	0.900914	142		EL1	145.0	
MSM63_13-1	11.05.2017 15:13	Sound Velocity Profiler	on deck	58 °17,474' N	000° 54,055' E	154.3	0.1		58,291,228	0.900915	147		EL1	-11.0	
MSM63_0_Underway-4	12.05.2017 01:35	Parasound	information	57 °22,524' N	001° 26,553' W	109.9		233.7	57,375,399	-1,442,544	135	17.70		0.0	
MSM63_0_Underway-3	12.05.2017 01:35	Multibeam Echosounder	information	57 °22,497' N	001° 26,619' W	109.9		231.3	57,374,943	-1,443,657	135	17.40		0.0	
MSM63_0_Underway-1	12.05.2017 01:35	ADCP	information	57 °22,485' N	001° 26,647' W	109.9		232.2	57,374,751	-1,444,114	135	17.50		0.0	

MSM63-2

Activity - Device Operation	Timestamp	Device	Action	Latitude	Longitude	Depth (m)	Speed (kn)	Course	Latitude (deg)	Longitude (deg)	Wind Dir	Wind Velocity	Winch	Rope Length (m)	Comment
MSM63_0_Underway-5	2017-05-18 19:18:00	Multibeam Echosounder	station start	57°11,269' N	001°40,217' W	78.2	12.9	78.6	57.187821	-1.670277	177	15.00		0.0	
MSM63_0_Underway-6	2017-05-18 19:18:23	ADCP	information	57°11,285' N	001°40,068' W	76.7	12.9	78.9	57.188087	-1.667795	176	14.70		0.0	
MSM63_14-1	2017-05-19 00:06:45	Parasound	profile start	57°56,136' N	000°33,169' W	111.6	7.3	91.1	57.935606	-0.552825	176	11.30		0.0	v=7kn, Kurs 090°
MSM63_14-1	2017-05-19 02:18:33	Parasound	alter course	57°56,027' N	000°04,013' W	123.3	7.0	90.3	57.933789	-0.066891	140	5.80		0.0	Kurs 000°
MSM63_14-1	2017-05-19 02:42:02	Parasound	alter course	57°58,530' N	000°03,793' W	125.2	6.9	286.9	57.975503	-0.063212	146	4.80		0.0	Kurs 270°
MSM63_14-1	2017-05-19 04:41:00	Parasound	alter course	57°58,480' N	000°30,222' W	103.5	7.1	273.3	57.974670	-0.503706	119	8.30		0.0	Kurs 000°
MSM63_14-1	2017-05-19 04:59:55	Parasound	alter course	58°00,549' N	000°30,650' W	116.9	7.2	25.0	58.009147	-0.510827	116	10.90		0.0	Kurs 090°
MSM63_14-1	2017-05-19 07:01:24	Parasound	alter course	58°00,830' N	000°04,012' W	126.0	7.0	88.8	58.013836	-0.066870	114	8.90		0.0	Kurs 359°
MSM63_14-1	2017-05-19 07:24:55	Parasound	alter course	58°03,461' N	000°03,618' W	130.4	7.1	356.6	58.057676	-0.060299	110	9.50		0.0	Kurs 269°
MSM63_14-1	2017-05-19 09:21:25	Parasound	alter course	58°03,116' N	000°29,027' W	119.8	6.8	268.9	58.051932	-0.483790	100	5.90		0.0	Kurs 059°

MSM63_14-1	2017-05-19 09:41:26	Parasound	alter course	58°04,412' N	000°26,688' W	122.6	7.2	59.6	58.073538	-0.444795	95	6.30		0.0	Kurs 180°
MSM63_14-1	2017-05-19 10:59:02	Parasound	alter course	57°55,825' N	000°25,883' W	118.1	6.8	180.0	57.930421	-0.431375	149	7.20		0.0	Kurs 090°
MSM63_14-1	2017-05-19 11:25:00	Parasound	alter course	57°55,506' N	000°20,361' W	117.0	7.1	88.9	57.925093	-0.339355	178	5.10		0.0	Kurs 000°
MSM63_14-1	2017-05-19 12:12:28	Parasound	profile end	58°00,749' N	000°19,835' W	124.4	1.2	2.5	58.012490	-0.330589	84	7.00		0.0	
MSM63_14-1	2017-05-19 12:12:29	Parasound	information	58°00,749' N	000°19,835' W	123.9	1.1	3.5	58.012490	-0.330589	84	7.00		0.0	Unterbrechung f・CTD Station
MSM63_15-1	2017-05-19 12:22:04	CTD	in the water	58°00,763' N	000°19,850' W	123.8	0.0	87.7	58.012719	-0.330829	94	7.00	EL1	-1.0	
MSM63_15-1	2017-05-19 12:35:26	CTD	max depth/ on ground	58°00,763' N	000°19,850' W	123.7	0.0	300.0	58.012724	-0.330828	89	5.60	EL1	119.0	
MSM63_15-1	2017-05-19 12:54:14	CTD	on deck	58°00,764' N	000°19,850' W	123.9	0.0	308.6	58.012726	-0.330829	86	5.10	EL1	-13.0	
MSM63_14-1	2017-05-19 12:54:34	Parasound	profile start	58°00,764' N	000°19,850' W	123.9	0.0	312.4	58.012725	-0.330830	86	5.20	EL1	-13.0	v=7kn Kurs: 000°
MSM63_14-1	2017-05-19 13:28:43	Parasound	alter course	58°04,253' N	000°19,812' W	125.7	7.1	1.4	58.070890	-0.330192	87	6.90		0.0	Kurs 090°
MSM63_14-1	2017-05-19 13:56:12	Parasound	alter course	58°04,491' N	000°14,022' W	127.7	7.1	103.5	58.074842	-0.233705	17	4.50		0.0	Kurs 180°
MSM63_14-1	2017-05-19 15:12:54	Parasound	profile end	57°55,497' N	000°13,529' W	101.5	6.2	181.2	57.924952	-0.225492	353	8.50		0.0	
MSM63_1	2017-05-19	CTD	in the	57°55,470' N	000°13,531' W	104.3	0.1	223.3	57.924502	-0.225511	2	8.80	EL1	-1.0	

6-1	15:19:48		water											
MSM63_1 6-1	2017-05-19 15:31:26	CTD	max depth/ on ground	57°55,470' N	000°13,532' W	104.3	0.0	177.8	57.924501	-0.225534	10	9.80	EL1	98.0	
MSM63_1 6-1	2017-05-19 15:40:21	CTD	on deck	57°55,470' N	000°13,532' W	104.2	0.0	240.9	57.924500	-0.225526	24	9.30	EL1	-14.0	
MSM63_1 7-1	2017-05-19 16:09:46	Shallow-water Multibeam Echosounder	profile start	57°57,308' N	000°17,636' W	118.4	6.9	280.1	57.955135	-0.293931	12	12.90		0.0	v=7kn, Kurs 270°
MSM63_1 7-1	2017-05-19 16:53:42	Shallow-water Multibeam Echosounder	alter course	57°57,306' N	000°27,478' W	118.2	7.1	269.3	57.955099	-0.457969	7	13.30		0.0	Kurs 090°
MSM63_1 7-1	2017-05-19 17:43:11	Shallow-water Multibeam Echosounder	alter course	57°57,719' N	000°17,956' W	119.2	7.0	91.0	57.961977	-0.299272	21	17.80		0.0	Kurs 270°
MSM63_1 7-1	2017-05-19 18:30:48	Shallow-water Multibeam Echosounder	alter course	57°57,448' N	000°27,502' W	117.1	7.0	270.5	57.957467	-0.458363	26	16.70		0.0	Kurs 090°
MSM63_1 7-1	2017-05-19 19:19:31	Shallow-water Multibeam Echosounder	alter course	57°57,856' N	000°17,973' W	119.7	7.0	90.1	57.964273	-0.299544	8	20.60		0.0	Kurs 270°
MSM63_1 7-1	2017-05-19 20:06:36	Shallow-water Multibeam Echosounder	alter course	57°57,586' N	000°27,555' W	117.0	7.1	273.8	57.959775	-0.459258	17	18.60		0.0	Kurs 090°
MSM63_1 7-1	2017-05-19 20:57:54	Shallow-water Multibeam Echosounder	alter course	57°58,274' N	000°17,851' W	120.4	7.0	96.7	57.971225	-0.297515	15	22.80		0.0	Kurs 270°

MSM63_17-1	2017-05-19 21:45:06	Shallow-water Multibeam Echosounder	alter course	57°57,981' N	000°27,587' W	115.7	6.9	271.6	57.966355	-0.459784	23	20.10	0.0	Kurs 090°
MSM63_17-1	2017-05-19 22:34:45	Shallow-water Multibeam Echosounder	alter course	57°58,408' N	000°17,944' W	120.2	6.9	96.9	57.973474	-0.299067	20	21.30	0.0	Kurs 270°
MSM63_17-1	2017-05-19 23:23:54	Shallow-water Multibeam Echosounder	alter course	57°58,169' N	000°27,755' W	115.4	6.5	306.4	57.969488	-0.462584	20	19.80	0.0	Kurs 090°
MSM63_17-1	2017-05-20 00:14:24	Shallow-water Multibeam Echosounder	alter course	57°58,809' N	000°17,960' W	120.5	7.1	93.0	57.980153	-0.299332	20	19.50	0.0	Kurs 270°
MSM63_17-1	2017-05-20 01:00:59	Shallow-water Multibeam Echosounder	alter course	57°58,532' N	000°27,536' W	119.0	7.0	273.7	57.975528	-0.458935	43	18.50	0.0	Kurs 090°
MSM63_17-1	2017-05-20 01:50:38	Shallow-water Multibeam Echosounder	alter course	57°58,952' N	000°17,942' W	120.9	7.1	94.5	57.982539	-0.299041	52	20.30	0.0	Kurs 270°
MSM63_17-1	2017-05-20 02:38:43	Shallow-water Multibeam Echosounder	alter course	57°58,673' N	000°27,673' W	124.1	6.7	293.0	57.977888	-0.461222	62	15.30	0.0	Kurs 090°
MSM63_17-1	2017-05-20 03:30:15	Shallow-water Multibeam Echosounder	alter course	57°59,373' N	000°17,935' W	121.9	6.9	96.1	57.989551	-0.298913	83	19.00	0.0	Kurs 270°
MSM63_17-1	2017-05-20 04:16:50	Shallow-water Multibeam Echosounder	alter course	57°59,064' N	000°27,520' W	126.3	7.0	271.1	57.984408	-0.458665	73	14.30	0.0	Kurs 090°
MSM63_1	2017-05-20	Shallow-water	alter	57°59,509' N	000°17,972' W	122.7	7.1	91.7	57.991812	-0.299535	83	15.80	0.0	Kurs 270°

7-1	05:05:20	Multibeam Echosounder	course											
MSM63_17-1	2017-05-20 05:52:51	Shallow-water Multibeam Echosounder	alter course	57°59,213' N	000°27,640' W	120.2	6.8	286.7	57.986880	-0.460666	83	14.60		0.0	Kurs 090°
MSM63_17-1	2017-05-20 06:41:22	Shallow-water Multibeam Echosounder	alter course	57°59,779' N	000°18,060' W	123.0	6.9	87.9	57.996314	-0.301007	94	16.50		0.0	Kurs 270°
MSM63_17-1	2017-05-20 07:11:30	Shallow-water Multibeam Echosounder	profile end	58°00,428' N	000°23,029' W	123.8	7.0	271.3	58.007125	-0.383809	91	16.10		0.0	
MSM63_17-1	2017-05-20 07:11:48	Shallow-water Multibeam Echosounder	information	58°00,430' N	000°23,092' W	124.3	6.6	281.3	58.007175	-0.384868	89	15.90		0.0	Unterbrechung CTD
MSM63_18-1	2017-05-20 07:23:52	CTD	in the water	58°00,428' N	000°23,676' W	124.0	0.2	20.5	58.007132	-0.394593	91	17.00	EL1	3.0	
MSM63_18-1	2017-05-20 07:37:14	CTD	max depth/ on ground	58°00,432' N	000°23,677' W	123.8	0.0	36.5	58.007199	-0.394625	93	18.00	EL1	118.0	
MSM63_18-1	2017-05-20 07:52:17	CTD	on deck	58°00,433' N	000°23,678' W	124.2	0.1	294.2	58.007210	-0.394634	90	17.30		0.0	
MSM63_17-1	2017-05-20 08:01:08	Shallow-water Multibeam Echosounder	profile start	58°00,434' N	000°22,955' W	124.2	3.0	254.9	58.007241	-0.382576	71	16.40		0.0	v=7kn, Kurs 270°
MSM63_17-1	2017-05-20 08:22:36	Shallow-water Multibeam Echosounder	alter course	58°00,428' N	000°27,480' W	122.9	6.9	273.2	58.007133	-0.458007	91	19.00		0.0	Kurs 090°

MSM63_17-1	2017-05-20 09:15:21	Shallow-water Multibeam Echosounder	alter course	57°59,646' N	000°17,916' W	122.9	6.9	91.2	57.994105	-0.298608	110	20.00		0.0	Kurs 270°
MSM63_17-1	2017-05-20 09:38:50	Shallow-water Multibeam Echosounder	alter course	58°00,164' N	000°21,912' W	123.9	7.1	268.8	58.002734	-0.365202	121	16.80		0.0	Kurs 090°
MSM63_17-1	2017-05-20 10:01:11	Shallow-water Multibeam Echosounder	alter course	57°59,912' N	000°17,988' W	122.6	7.1	86.4	57.998539	-0.299800	136	19.50		0.0	Kurs 270°
MSM63_17-1	2017-05-20 10:23:10	Shallow-water Multibeam Echosounder	profile end	58°00,303' N	000°21,742' W	123.6	6.0	272.4	58.005048	-0.362369	139	17.30		0.0	
MSM63_17-1	2017-05-20 10:23:18	Shallow-water Multibeam Echosounder	information	58°00,303' N	000°21,767' W	123.7	6.0	272.6	58.005058	-0.362777	139	17.30		0.0	Unterbrechung CTD
MSM63_19-1	2017-05-20 10:23:29	CTD	in the water	58°00,305' N	000°21,800' W	123.7	5.9	274.8	58.005076	-0.363336	139	17.30		0.0	
MSM63_19-1	2017-05-20 10:47:54	CTD	max depth/ on ground	58°00,317' N	000°22,313' W	122.9	0.1	20.6	58.005279	-0.371881	163	17.10	EL1	117.0	
MSM63_19-1	2017-05-20 11:03:51	CTD	on deck	58°00,316' N	000°22,313' W	123.4	0.0	35.4	58.005268	-0.371891	179	17.00	EL1	-14.0	
MSM63_17-1	2017-05-20 11:06:29	Shallow-water Multibeam Echosounder	profile start	58°00,318' N	000°22,294' W	123.3	1.0	103.7	58.005303	-0.371564	179	18.20		0.0	v=7kn, Kurs 090°
MSM63_17-1	2017-05-20 11:32:02	Shallow-water Multibeam	alter course	58°00,037' N	000°17,821' W	122.2	6.6	96.2	58.000617	-0.297025	175	19.60		0.0	Kurs 270°

		Echosounder												
MSM63_17-1	2017-05-20 12:00:36	Shallow-water Multibeam Echosounder	profile end	58°00,115' N	000°22,147' W	123.2	4.5	220.5	58.001921	-0.369119	176	22.40		0.0	
MSM63_17-1	2017-05-20 12:00:57	Shallow-water Multibeam Echosounder	information	58°00,095' N	000°22,175' W	122.3	4.2	210.2	58.001584	-0.369580	174	22.50		0.0	Unterbrechung f・CTD
MSM63_20-1	2017-05-20 12:12:38	CTD	in the water	57°59,902' N	000°22,304' W	122.4	0.1	324.2	57.998371	-0.371737	171	21.90	EL1	7.0	
MSM63_20-1	2017-05-20 12:25:15	CTD	max depth/ on ground	57°59,903' N	000°22,305' W	122.9	0.1	9.2	57.998388	-0.371758	178	23.80	EL1	116.0	
MSM63_20-1	2017-05-20 12:41:24	CTD	on deck	57°59,902' N	000°22,303' W	122.8	0.0	321.1	57.998370	-0.371720	190	28.20	EL1	0.0	
MSM63_17-1	2017-05-20 13:06:51	Shallow-water Multibeam Echosounder	profile start	58°00,468' N	000°17,669' W	124.2	7.7	344.8	58.007808	-0.294490	196	29.70		0.0	v= 7kn Kurs 270°
MSM63_17-1	2017-05-20 13:53:13	Shallow-water Multibeam Echosounder	profile end	58°00,588' N	000°27,709' W	122.5	8.0	282.4	58.009798	-0.461824	188	33.50		0.0	
MSM63_17-1	2017-05-20 13:53:21	Shallow-water Multibeam Echosounder	information	58°00,592' N	000°27,738' W	122.4	8.2	287.1	58.009874	-0.462306	186	32.70		0.0	Unterbrechung f・CTD
MSM63_21-1	2017-05-20 14:06:25	CTD	in the water	58°01,047' N	000°27,837' W	121.8	0.1	297.1	58.017443	-0.463946	194	29.90	EL1	1.0	
MSM63_21-1	2017-05-20 14:23:00	CTD	max depth/	58°01,047' N	000°27,838' W	121.5	0.0	98.4	58.017443	-0.463959	191	29.70	EL1	94.0	

			on ground											
MSM63_21-1	2017-05-20 14:34:12	CTD	on deck	58°01,047' N	000°27,837' W	121.3	0.1	0.8	58.017448	-0.463956	188	31.30	EL1	-14.0	
MSM63_17-1	2017-05-20 14:38:18	Shallow-water Multibeam Echosounder	profile start	58°01,009' N	000°27,814' W	121.9	3.2	124.7	58.016824	-0.463560	199	27.50		0.0	v=7kn Kurs 090°
MSM63_17-1	2017-05-20 15:23:42	Shallow-water Multibeam Echosounder	alter course	58°01,012' N	000°17,972' W	124.0	7.1	97.7	58.016861	-0.299541	191	28.40		0.0	Kurs 270°
MSM63_17-1	2017-05-20 16:11:24	Shallow-water Multibeam Echosounder	alter course	58°00,713' N	000°27,486' W	120.8	7.0	264.5	58.011877	-0.458106	182	27.70		0.0	Kurs 090°
MSM63_17-1	2017-05-20 17:00:10	Shallow-water Multibeam Echosounder	alter course	58°01,151' N	000°18,000' W	125.6	6.6	93.2	58.019184	-0.299992	184	24.60		0.0	Kurs 270°
MSM63_17-1	2017-05-20 17:47:45	Shallow-water Multibeam Echosounder	alter course	58°00,858' N	000°27,471' W	122.2	7.0	266.1	58.014301	-0.457858	175	26.60		0.0	Kurs 090°
MSM63_17-1	2017-05-20 18:37:51	Shallow-water Multibeam Echosounder	alter course	58°01,559' N	000°18,024' W	124.9	6.9	91.9	58.025976	-0.300399	178	24.40		0.0	Kurs 270°
MSM63_17-1	2017-05-20 19:25:31	Shallow-water Multibeam Echosounder	alter course	58°01,288' N	000°27,509' W	121.7	6.7	269.0	58.021468	-0.458488	172	20.90		0.0	Kurs 090°
MSM63_17-1	2017-05-20 20:13:32	Shallow-water Multibeam Echosounder	alter course	58°01,700' N	000°18,023' W	125.9	7.0	88.3	58.028336	-0.300389	166	21.70		0.0	Kurs 270°

MSM63_17-1	2017-05-20 21:01:17	Shallow-water Multibeam Echosounder	alter course	58°01,412' N	000°27,477' W	122.9	7.0	270.5	58.023534	-0.457946	165	20.10	0.0	Kurs 090°
MSM63_17-1	2017-05-20 21:52:02	Shallow-water Multibeam Echosounder	alter course	58°02,117' N	000°18,029' W	126.7	7.0	92.6	58.035289	-0.300490	164	19.80	0.0	Kurs 270°
MSM63_17-1	2017-05-20 22:40:01	Shallow-water Multibeam Echosounder	alter course	58°01,827' N	000°27,493' W	121.4	7.1	272.4	58.030447	-0.458209	160	18.40	0.0	Kurs 090°
MSM63_17-1	2017-05-20 23:29:01	Shallow-water Multibeam Echosounder	alter course	58°02,251' N	000°17,929' W	125.3	6.9	99.8	58.037513	-0.298816	166	16.60	0.0	Kurs 270°
MSM63_17-1	2017-05-21 00:16:02	Shallow-water Multibeam Echosounder	alter course	58°01,963' N	000°27,563' W	122.2	7.0	262.5	58.032721	-0.459391	170	17.30	0.0	Kurs 090°
MSM63_17-1	2017-05-21 00:48:04	Shallow-water Multibeam Echosounder	alter course	58°00,307' N	000°23,907' W	122.9	7.0	92.5	58.005113	-0.398452	184	16.70	0.0	Kurs 270°
MSM63_17-1	2017-05-21 01:08:45	Shallow-water Multibeam Echosounder	alter course	58°00,013' N	000°27,590' W	119.7	7.0	271.8	58.000217	-0.459841	174	17.30	0.0	Kurs 090°
MSM63_17-1	2017-05-21 01:32:49	Shallow-water Multibeam Echosounder	alter course	58°00,164' N	000°24,017' W	123.7	7.1	91.6	58.002726	-0.400285	181	16.50	0.0	Kurs 270°
MSM63_17-1	2017-05-21 01:55:37	Shallow-water Multibeam Echosounder	profile end	57°59,883' N	000°27,946' W	117.9	6.7	261.7	57.998057	-0.465775	172	16.50	0.0	
MSM63_1	2017-05-21	CTD	inform	57°59,880' N	000°27,981' W	117.8	6.7	253.6	57.997992	-0.466355	172	16.50	0.0	

5-1	01:55:47		ation										
MSM63_2 3-1	2017-05-21 02:03:41	Parasound	profile start	58°00,003' N	000°26,961' W	124.2	8.0	62.2	58.000048	-0.449348	178	16.00	0.0	v=7kn Kurs 073°
MSM63_2 3-1	2017-05-21 04:08:27	Parasound	profile end	58°04,305' N	000°00,701' W	133.0	7.0	71.8	58.071743	-0.011686	184	14.90	0.0	
MSM63_2 4-1	2017-05-21 07:11:01	Shallow-water Multibeam Echosounder	profile start	58°15,760' N	001°02,797' E	150.4	6.4	352.1	58.262670	1.046610	230	13.30	0.0	v=7kn, Kurs 000°
MSM63_2 4-1	2017-05-21 07:44:46	Shallow-water Multibeam Echosounder	alter course	58°19,634' N	001°02,822' E	149.3	7.0	360.0	58.327231	1.047042	195	10.20	0.0	Kurs 180°
MSM63_2 4-1	2017-05-21 08:23:08	Shallow-water Multibeam Echosounder	alter course	58°15,950' N	001°03,744' E	149.0	7.0	181.0	58.265833	1.062408	185	9.40	0.0	Kurs 000°
MSM63_2 4-1	2017-05-21 09:00:40	Shallow-water Multibeam Echosounder	alter course	58°19,710' N	001°03,057' E	148.1	7.1	0.2	58.328498	1.050953	192	12.40	0.0	Kurs 180°
MSM63_2 4-1	2017-05-21 09:38:18	Shallow-water Multibeam Echosounder	alter course	58°15,943' N	001°03,970' E	148.6	7.0	179.7	58.265715	1.066160	199	12.70	0.0	Kurs 000°
MSM63_2 4-1	2017-05-21 10:15:36	Shallow-water Multibeam Echosounder	alter course	58°19,694' N	001°03,267' E	148.2	7.0	1.4	58.328231	1.054451	207	13.60	0.0	Kurs 180°
MSM63_2 4-1	2017-05-21 10:54:24	Shallow-water Multibeam Echosounder	alter course	58°15,916' N	001°04,199' E	148.6	7.0	179.5	58.265267	1.069985	220	14.60	0.0	Kurs 000°
MSM63_2 4-1	2017-05-21 11:35:11	Shallow-water Multibeam	profile end	58°20,152' N	001°03,511' E	146.7	7.4	350.3	58.335869	1.058522	216	11.90	0.0	

		Echosounder												
MSM63_25-1	2017-05-21 12:25:25	CTD	in the water	58°16,915' N	000°58,247' E	169.3	0.1	348.4	58.281909	0.970782	201	12.70	EL1	3.0	
MSM63_25-1	2017-05-21 12:42:36	CTD	max depth/ on ground	58°16,914' N	000°58,248' E	169.5	0.0	29.0	58.281898	0.970802	204	13.80	EL1	163.0	
MSM63_25-1	2017-05-21 13:02:31	CTD	on deck	58°16,915' N	000°58,245' E	169.5	0.1	148.6	58.281914	0.970746	197	13.80	EL1	-13.0	
MSM63_26-1	2017-05-21 13:50:48	CTD	in the water	58°17,091' N	000°57,982' E	153.3	0.1	351.0	58.284856	0.966368	203	12.10	EL1	8.0	
MSM63_26-1	2017-05-21 14:04:32	CTD	max depth/ on ground	58°17,091' N	000°57,983' E	153.4	0.0	181.9	58.284848	0.966384	201	11.70	EL1	146.0	
MSM63_26-1	2017-05-21 14:23:36	CTD	on deck	58°17,091' N	000°57,982' E	153.4	0.0	94.1	58.284843	0.966371	205	11.30	EL1	-13.0	
MSM63_27-1	2017-05-21 14:43:47	Shallow-water Multibeam Echosounder	profile start	58°17,048' N	001°00,497' E	151.4	6.7	173.1	58.284134	1.008277	208	12.30		0.0	v=7kn Kurs 180°
MSM63_27-1	2017-05-21 15:07:18	Shallow-water Multibeam Echosounder	alter course	58°14,380' N	001°00,524' E	151.9	6.9	179.8	58.239661	1.008730	190	9.00		0.0	Kurs 000°
MSM63_27-1	2017-05-21 16:01:29	Shallow-water Multibeam Echosounder	alter course	58°20,061' N	001°01,426' E	148.6	6.9	0.2	58.334357	1.023763	183	10.40		0.0	Kurs 180°
MSM63_27-1	2017-05-21 16:54:56	Shallow-water Multibeam	inform ation	58°14,402' N	001°00,755' E	151.9	7.0	180.9	58.240035	1.012589	193	13.70		0.0	Kurs 000°

		Echosounder												
MSM63_27-1	2017-05-21 17:49:49	Shallow-water Multibeam Echosounder	alter course	58°20,094' N	001°01,632' E	149.0	6.8	358.2	58.334894	1.027200	188	12.80	0.0	Kurs 180°
MSM63_27-1	2017-05-21 18:43:41	Shallow-water Multibeam Echosounder	alter course	58°14,428' N	001°00,991' E	152.4	7.0	180.1	58.240463	1.016510	192	13.00	0.0	Kurs 000°
MSM63_27-1	2017-05-21 19:38:26	Shallow-water Multibeam Echosounder	alter course	58°20,069' N	001°01,847' E	148.9	7.0	0.8	58.334478	1.030780	179	10.00	0.0	Kurs 180°
MSM63_27-1	2017-05-21 20:31:05	Shallow-water Multibeam Echosounder	alter course	58°14,421' N	001°01,210' E	152.3	6.9	179.4	58.240350	1.020174	170	14.10	0.0	Kurs 000°
MSM63_27-1	2017-05-21 21:24:58	Shallow-water Multibeam Echosounder	alter course	58°20,081' N	001°02,074' E	148.6	7.0	359.0	58.334689	1.034574	173	12.80	0.0	Kurs 180°
MSM63_27-1	2017-05-21 22:05:17	Shallow-water Multibeam Echosounder	alter course	58°15,744' N	001°02,489' E	150.2	6.9	181.2	58.262407	1.041476	170	13.60	0.0	Kurs 000°
MSM63_27-1	2017-05-21 22:48:19	Shallow-water Multibeam Echosounder	alter course	58°20,077' N	001°02,277' E	148.5	7.1	0.0	58.334621	1.037951	169	12.60	0.0	Kurs 180°
MSM63_27-1	2017-05-21 23:30:08	Shallow-water Multibeam Echosounder	profile end	58°15,693' N	001°02,307' E	151.3	8.9	247.8	58.261556	1.038453	169	12.00	0.0	
MSM63_28-1	2017-05-22 03:20:16	Shallow-water Multibeam Echosounder	profile start	57°59,916' N	000°17,623' W	122.6	7.0	261.3	57.998600	-0.293723	156	16.70	0.0	v=7kn, Kurs 270°

MSM63_28-1	2017-05-22 03:39:56	Shallow-water Multibeam Echosounder	alter course	57°59,920' N	000°21,909' W	122.3	7.1	270.7	57.998671	-0.365153	162	16.30		0.0	Kurs 090°
MSM63_28-1	2017-05-22 04:03:49	Shallow-water Multibeam Echosounder	alter course	58°00,350' N	000°17,966' W	123.3	6.9	88.6	58.005834	-0.299426	161	15.80		0.0	Kurs 270°
MSM63_28-1	2017-05-22 04:53:49	Shallow-water Multibeam Echosounder	alter course	58°00,777' N	000°27,524' W	122.5	7.0	270.6	58.012955	-0.458729	159	16.80		0.0	Kurs 090°
MSM63_28-1	2017-05-22 05:44:01	Shallow-water Multibeam Echosounder	alter course	58°00,619' N	000°17,696' W	124.3	6.5	16.8	58.010323	-0.294937	171	15.60		0.0	Kurs 270°
MSM63_28-1	2017-05-22 06:31:47	Shallow-water Multibeam Echosounder	alter course	58°00,921' N	000°27,477' W	122.7	6.9	271.4	58.015352	-0.457954	160	14.80		0.0	Kurs 090°
MSM63_28-1	2017-05-22 07:22:09	Shallow-water Multibeam Echosounder	profile end	58°00,670' N	000°17,598' W	124.9	7.0	89.7	58.011162	-0.293306	166	17.80		0.0	
MSM63_29-1	2017-05-22 07:40:37	CTD	in the water	57°59,654' N	000°18,148' W	123.1	0.1	290.0	57.994234	-0.302470	159	17.20	EL1	0.0	
MSM63_29-1	2017-05-22 07:53:34	CTD	max depth/ on ground	57°59,654' N	000°18,148' W	123.2	0.0	181.7	57.994237	-0.302459	157	17.30	EL1	115.0	
MSM63_29-1	2017-05-22 08:05:52	CTD	on deck	57°59,654' N	000°18,148' W	123.0	0.0	155.6	57.994235	-0.302467	162	17.20	EL1	0.0	
MSM63_30-1	2017-05-22 08:19:51	Parasound	profile start	57°59,656' N	000°18,132' W	123.1	6.9	179.9	57.994270	-0.302201	152	17.50		0.0	v=7kn, Kurs 180°

MSM63_30-1	2017-05-22 08:36:34	Parasound	profile end	57°57,726' N	000°18,148' W	119.2	6.9	181.5	57.962101	-0.302471	146	17.00		0.0	
MSM63_30-1	2017-05-22 08:36:42	Parasound	information	57°57,711' N	000°18,149' W	119.0	6.9	181.2	57.961849	-0.302480	146	17.00		0.0	Unterbrechung CTD
MSM63_31-1	2017-05-22 08:50:20	CTD	in the water	57°57,770' N	000°18,161' W	119.6	0.1	145.2	57.962826	-0.302683	147	17.10	EL1	2.0	
MSM63_31-1	2017-05-22 09:03:28	CTD	max depth/ on ground	57°57,770' N	000°18,161' W	119.3	0.0	34.2	57.962827	-0.302692	148	18.00	EL1	113.0	
MSM63_31-1	2017-05-22 09:17:37	CTD	on deck	57°57,769' N	000°18,161' W	119.6	0.1	133.0	57.962823	-0.302689	142	18.60	EL1	-13.0	
MSM63_30-1	2017-05-22 09:29:36	Parasound	profile start	57°57,738' N	000°18,130' W	119.7	6.8	270.9	57.962297	-0.302174	153	21.90		0.0	v=7kn, Kurs 270°
MSM63_30-1	2017-05-22 09:52:00	Parasound	profile end	57°57,748' N	000°23,087' W	119.1	7.0	271.3	57.962464	-0.384787	150	20.70		0.0	
MSM63_30-1	2017-05-22 09:52:53	Parasound	information	57°57,759' N	000°23,272' W	119.3	6.0	296.6	57.962649	-0.387871	144	21.00		0.0	Unterbrechung CTD
MSM63_32-1	2017-05-22 10:01:24	CTD	in the water	57°57,767' N	000°23,100' W	119.2	0.1	129.6	57.962777	-0.384997	158	21.70	EL1	-11.0	
MSM63_32-1	2017-05-22 10:15:17	CTD	max depth/ on ground	57°57,768' N	000°23,102' W	119.1	0.0	235.1	57.962797	-0.385027	152	18.90	EL1	113.0	
MSM63_32-1	2017-05-22 10:26:49	CTD	on deck	57°57,767' N	000°23,102' W	119.1	0.0	10.7	57.962791	-0.385028	155	17.50	EL1	-13.0	
MSM63_30-1	2017-05-22 10:38:39	Parasound	profile start	57°57,747' N	000°23,057' W	119.0	6.1	268.6	57.962445	-0.384285	150	19.00		0.0	v=7kn, Kurs 270°

MSM63_30-1	2017-05-22 10:58:45	Parasound	profile end	57°57,736' N	000°27,503' W	115.1	7.2	273.4	57.962258	-0.458384	149	21.60		0.0	
MSM63_30-1	2017-05-22 10:58:55	Parasound	information	57°57,736' N	000°27,540' W	115.4	7.1	272.8	57.962270	-0.459003	149	21.50		0.0	Unterbrechung CTD
MSM63_33-1	2017-05-22 11:12:39	CTD	in the water	57°57,758' N	000°27,568' W	115.9	0.0	227.5	57.962640	-0.459459	145	20.10	EL1	10.0	
MSM63_33-1	2017-05-22 11:24:54	CTD	max depth/ on ground	57°57,758' N	000°27,566' W	115.8	0.1	70.4	57.962639	-0.459432	147	20.10	EL1	109.0	
MSM63_33-1	2017-05-22 11:38:55	CTD	on deck	57°57,758' N	000°27,566' W	115.6	0.0	194.1	57.962630	-0.459441	144	20.40	EL1	-13.0	
MSM63_30-1	2017-05-22 11:48:34	Parasound	profile start	57°57,727' N	000°27,555' W	115.3	5.8	4.0	57.962111	-0.459247	142	19.10		0.0	v=7kn Kurs:000°
MSM63_30-1	2017-05-22 12:06:40	Parasound	profile end	57°59,808' N	000°27,626' W	121.0	6.8	359.4	57.996799	-0.460438	144	18.60		0.0	
MSM63_30-1	2017-05-22 12:06:45	Parasound	information	57°59,817' N	000°27,626' W	120.9	6.9	359.6	57.996958	-0.460441	144	18.60		0.0	Unterbrechung CTD
MSM63_34-1	2017-05-22 12:20:44	CTD	in the water	57°59,816' N	000°27,641' W	121.0	0.0	32.0	57.996941	-0.460681	145	20.40	EL1	10.0	
MSM63_34-1	2017-05-22 12:32:09	CTD	max depth/ on ground	57°59,815' N	000°27,640' W	120.5	0.0	227.2	57.996922	-0.460671	153	20.70	EL1	115.0	
MSM63_34-1	2017-05-22 12:42:30	CTD	on deck	57°59,816' N	000°27,639' W	120.9	0.1	56.9	57.996934	-0.460657	152	21.40	EL1	-11.0	
MSM63_30-1	2017-05-22 12:50:11	Parasound	profile start	57°59,825' N	000°27,215' W	122.3	5.1	94.0	57.997083	-0.453583	154	21.30		0.0	v=7kn Kurs 090°

MSM63_30-1	2017-05-22 13:04:50	Parasound	profile end	57°59,831' N	000°24,109' W	122.3	7.0	88.4	57.997180	-0.401815	156	23.50		0.0	
MSM63_30-1	2017-05-22 13:17:46	Parasound	information	57°59,860' N	000°24,126' W	122.6	0.1	53.5	57.997660	-0.402099	152	21.40	EL1	-11.0	Unterbrechung CTD
MSM63_35-1	2017-05-22 13:20:27	CTD	in the water	57°59,860' N	000°24,124' W	122.7	0.0	124.9	57.997670	-0.402059	150	20.30	EL1	4.0	
MSM63_35-1	2017-05-22 13:30:59	CTD	max depth/ on ground	57°59,860' N	000°24,124' W	122.2	0.0	170.8	57.997671	-0.402060	153	20.10	EL1	116.0	
MSM63_35-1	2017-05-22 13:44:02	CTD	on deck	57°59,860' N	000°24,125' W	122.1	0.0	8.7	57.997668	-0.402076	156	19.30	EL1	-14.0	
MSM63_30-1	2017-05-22 13:53:43	Parasound	profile start	57°59,849' N	000°24,110' W	122.2	5.8	9.0	57.997489	-0.401834	156	18.70		0.0	v=7kn Kurs 012°
MSM63_30-1	2017-05-22 14:08:42	Parasound	profile end	58°01,652' N	000°23,408' W	123.7	7.3	11.0	58.027526	-0.390140	165	17.10		0.0	
MSM63_30-1	2017-05-22 14:10:50	Parasound	information	58°01,869' N	000°23,360' W	123.6	2.6	328.9	58.031153	-0.389326	176	18.80		0.0	
MSM63_36-1	2017-05-22 14:24:27	CTD	in the water	58°01,717' N	000°23,386' W	123.6	0.1	269.5	58.028615	-0.389773	160	18.60	EL1	10.0	
MSM63_36-1	2017-05-22 14:36:29	CTD	max depth/ on ground	58°01,716' N	000°23,387' W	123.7	0.0	216.0	58.028603	-0.389786	157	19.10	EL1	117.0	
MSM63_36-1	2017-05-22 14:42:09	CTD	on deck	58°01,716' N	000°23,387' W	123.7	0.0	106.8	58.028600	-0.389788	155	19.80	EL1	-12.0	
MSM63_37-1	2017-05-22 15:27:50	CTD	at surface	57°56,774' N	000°15,968' W	114.9	0.1	221.2	57.946229	-0.266131	162	18.40	EL1	-2.0	

MSM63_37-1	2017-05-22 15:38:58	CTD	max depth/ on ground	57°56,773' N	000°15,968' W	114.8	0.0	211.6	57.946217	-0.266139	153	18.50	EL1	109.0	
MSM63_37-1	2017-05-22 15:45:38	CTD	on deck	57°56,774' N	000°15,971' W	114.7	0.1	272.9	57.946226	-0.266176	162	18.50	EL1	-14.0	
MSM63_38-1	2017-05-22 16:29:16	Shallow-water Multibeam Echosounder	profile start	58°00,299' N	000°27,424' W	120.4	6.2	198.7	58.004982	-0.457065	147	24.20		0.0	v=7kn, Kurs 180°
MSM63_38-1	2017-05-22 16:47:56	Shallow-water Multibeam Echosounder	alter course	57°58,109' N	000°27,469' W	113.4	7.2	179.6	57.968483	-0.457811	148	22.70		0.0	Kurs 000°
MSM63_38-1	2017-05-22 17:10:17	Shallow-water Multibeam Echosounder	alter course	58°00,150' N	000°28,162' W	117.7	7.0	359.3	58.002501	-0.469360	147	23.20		0.0	Kurs 180°
MSM63_38-1	2017-05-22 17:32:30	Shallow-water Multibeam Echosounder	alter course	57°58,097' N	000°27,703' W	113.3	7.0	179.5	57.968284	-0.461722	145	23.80		0.0	Kurs 000°
MSM63_38-1	2017-05-22 17:54:41	Shallow-water Multibeam Echosounder	alter course	58°00,114' N	000°28,372' W	117.7	6.8	0.1	58.001904	-0.472867	149	23.80		0.0	Kurs 180°
MSM63_38-1	2017-05-22 18:17:02	Shallow-water Multibeam Echosounder	alter course	57°58,072' N	000°27,919' W	114.7	7.0	179.0	57.967871	-0.465309	153	25.10		0.0	Kurs 000°
MSM63_38-1	2017-05-22 18:41:16	Shallow-water Multibeam Echosounder	profile end	58°00,294' N	000°28,596' W	116.7	6.9	359.4	58.004905	-0.476594	149	21.10		0.0	
MSM63_3	2017-05-22	Parasound	profile	58°03,396' N	000°22,009' W	125.2	8.4	178.0	58.056603	-0.366814	141	24.30		0.0	v=7,5kn,

9-1	19:12:15		start											Kurs 180°
MSM63_3 9-1	2017-05-22 19:52:00	Parasound	alter course	57°58,432' N	000°21,928' W	120.0	7.6	176.6	57.973870	-0.365458	138	24.20	0.0	Kurs 360°
MSM63_3 9-1	2017-05-22 20:33:45	Parasound	alter course	58°03,265' N	000°21,569' W	125.4	7.5	2.6	58.054411	-0.359479	139	22.00	0.0	Kurs 180°
MSM63_3 9-1	2017-05-22 21:15:33	Parasound	alter course	57°58,467' N	000°21,032' W	120.8	7.6	181.2	57.974450	-0.350534	149	23.50	0.0	Kurs 360°
MSM63_3 9-1	2017-05-22 21:57:01	Parasound	alter course	58°03,258' N	000°20,618' W	125.9	7.5	359.3	58.054292	-0.343639	148	23.90	0.0	Kurs 180°
MSM63_3 9-1	2017-05-22 22:36:51	Parasound	alter course	57°58,744' N	000°20,099' W	121.1	7.5	180.8	57.979074	-0.334989	151	24.90	0.0	Kurs 270°
MSM63_3 9-1	2017-05-22 22:50:49	Parasound	alter course	57°58,867' N	000°22,106' W	120.3	8.6	267.9	57.981117	-0.368430	165	20.60	0.0	Kurs 090°
MSM63_3 9-1	2017-05-22 23:06:14	Parasound	alter course	57°59,404' N	000°19,785' W	122.6	7.6	89.8	57.990061	-0.329756	165	22.30	0.0	Kurs 270°
MSM63_3 9-1	2017-05-22 23:21:04	Parasound	alter course	57°59,875' N	000°22,053' W	122.2	7.3	271.7	57.997924	-0.367558	155	25.00	0.0	Kurs 359°
MSM63_3 9-1	2017-05-22 23:32:00	Parasound	alter course	58°01,178' N	000°22,372' W	124.7	7.7	357.6	58.019631	-0.372867	156	18.70	0.0	Kurs 090°
MSM63_3 9-1	2017-05-22 23:43:57	Parasound	alter course	58°01,361' N	000°19,779' W	124.8	7.5	89.2	58.022677	-0.329649	170	23.60	0.0	Kurs 270°
MSM63_3 9-1	2017-05-23 00:00:11	Parasound	alter course	58°01,912' N	000°22,209' W	125.4	7.4	291.6	58.031863	-0.370152	160	20.80	0.0	Kurs 090°
MSM63_3 9-1	2017-05-23 00:15:12	Parasound	alter course	58°02,448' N	000°19,779' W	125.9	7.5	91.6	58.040806	-0.329645	182	21.30	0.0	Kurs 270°
MSM63_3 9-1	2017-05-23 00:32:23	Parasound	profile end	58°02,919' N	000°22,512' W	124.3	7.6	261.9	58.048651	-0.375201	194	19.90	0.0	

MSM63-2

Activity - Device Operation	Timestamp	Device	Action	Latitude	Longitude	Depth (m)	Speed (kn)	Course	Latitude (deg)	Longitude (deg)	Wind Dir	Wind Velocity	Winch	Rope Length (m)	Comment
MSM63_0_Underway-5	2017-05-18 19:18:00	Multibeam Echosounder	station start	57°11,269' N	001°40,217' W	78.2	12.9	78.6	57.187821	-1.670277	177	15.00		0.0	
MSM63_0_Underway-6	2017-05-18 19:18:23	ADCP	information	57°11,285' N	001°40,068' W	76.7	12.9	78.9	57.188087	-1.667795	176	14.70		0.0	
MSM63_14-1	2017-05-19 00:06:45	Parasound	profile start	57°56,136' N	000°33,169' W	111.6	7.3	91.1	57.935606	-0.552825	176	11.30		0.0	v=7kn, Kurs 090°
MSM63_14-1	2017-05-19 02:18:33	Parasound	alter course	57°56,027' N	000°04,013' W	123.3	7.0	90.3	57.933789	-0.066891	140	5.80		0.0	Kurs 000°
MSM63_14-1	2017-05-19 02:42:02	Parasound	alter course	57°58,530' N	000°03,793' W	125.2	6.9	286.9	57.975503	-0.063212	146	4.80		0.0	Kurs 270°
MSM63_14-1	2017-05-19 04:41:00	Parasound	alter course	57°58,480' N	000°30,222' W	103.5	7.1	273.3	57.974670	-0.503706	119	8.30		0.0	Kurs 000°
MSM63_14-1	2017-05-19 04:59:55	Parasound	alter course	58°00,549' N	000°30,650' W	116.9	7.2	25.0	58.009147	-0.510827	116	10.90		0.0	Kurs 090°
MSM63_14-1	2017-05-19 07:01:24	Parasound	alter course	58°00,830' N	000°04,012' W	126.0	7.0	88.8	58.013836	-0.066870	114	8.90		0.0	Kurs 359°
MSM63_14-1	2017-05-19 07:24:55	Parasound	alter course	58°03,461' N	000°03,618' W	130.4	7.1	356.6	58.057676	-0.060299	110	9.50		0.0	Kurs 269°
MSM63_14-1	2017-05-19 09:21:25	Parasound	alter course	58°03,116' N	000°29,027' W	119.8	6.8	268.9	58.051932	-0.483790	100	5.90		0.0	Kurs 059°
MSM63_14-1	2017-05-19 09:41:26	Parasound	alter course	58°04,412' N	000°26,688' W	122.6	7.2	59.6	58.073538	-0.444795	95	6.30		0.0	Kurs 180°
MSM63_14-1	2017-05-19 10:59:02	Parasound	alter course	57°55,825' N	000°25,883' W	118.1	6.8	180.0	57.930421	-0.431375	149	7.20		0.0	Kurs 090°
MSM63_14-1	2017-05-19 11:25:00	Parasound	alter course	57°55,506' N	000°20,361' W	117.0	7.1	88.9	57.925093	-0.339355	178	5.10		0.0	Kurs 000°
MSM63_14-1	2017-05-19 12:12:28	Parasound	profile end	58°00,749' N	000°19,835' W	124.4	1.2	2.5	58.012490	-0.330589	84	7.00		0.0	
MSM63_14-1	2017-05-19 12:12:29	Parasound	information	58°00,749' N	000°19,835' W	123.9	1.1	3.5	58.012490	-0.330589	84	7.00		0.0	Unterbrechung f・CTD Station
MSM63_15-1	2017-05-19 12:22:04	CTD	in the water	58°00,763' N	000°19,850' W	123.8	0.0	87.7	58.012719	-0.330829	94	7.00	EL1	-1.0	
MSM63_15-1	2017-05-19 12:35:26	CTD	max depth/on ground	58°00,763' N	000°19,850' W	123.7	0.0	300.0	58.012724	-0.330828	89	5.60	EL1	119.0	
MSM63_15-1	2017-05-19 12:54:14	CTD	on deck	58°00,764' N	000°19,850' W	123.9	0.0	308.6	58.012726	-0.330829	86	5.10	EL1	-13.0	
MSM63_14-1	2017-05-19 12:54:34	Parasound	profile start	58°00,764' N	000°19,850' W	123.9	0.0	312.4	58.012725	-0.330830	86	5.20	EL1	-13.0	v=7kn Kurs: 000°
MSM63_14-1	2017-05-19 13:28:43	Parasound	alter course	58°04,253' N	000°19,812' W	125.7	7.1	1.4	58.070890	-0.330192	87	6.90		0.0	Kurs 090°
MSM63_14-1	2017-05-19	Parasound	alter course	58°04,491' N	000°14,022' W	127.7	7.1	103.5	58.074842	-0.233705	17	4.50		0.0	Kurs 180°

	13:56:12													
MSM63_14-1	2017-05-19 15:12:54	Parasound	profile end	57°55,497' N	000°13,529' W	101.5	6.2	181.2	57.924952	-0.225492	353	8.50		0.0	
MSM63_16-1	2017-05-19 15:19:48	CTD	in the water	57°55,470' N	000°13,531' W	104.3	0.1	223.3	57.924502	-0.225511	2	8.80	EL1	-1.0	
MSM63_16-1	2017-05-19 15:31:26	CTD	max depth/on ground	57°55,470' N	000°13,532' W	104.3	0.0	177.8	57.924501	-0.225534	10	9.80	EL1	98.0	
MSM63_16-1	2017-05-19 15:40:21	CTD	on deck	57°55,470' N	000°13,532' W	104.2	0.0	240.9	57.924500	-0.225526	24	9.30	EL1	-14.0	
MSM63_17-1	2017-05-19 16:09:46	Shallow-water Multibeam Echosounder	profile start	57°57,308' N	000°17,636' W	118.4	6.9	280.1	57.955135	-0.293931	12	12.90		0.0	v=7kn, Kurs 270°
MSM63_17-1	2017-05-19 16:53:42	Shallow-water Multibeam Echosounder	alter course	57°57,306' N	000°27,478' W	118.2	7.1	269.3	57.955099	-0.457969	7	13.30		0.0	Kurs 090°
MSM63_17-1	2017-05-19 17:43:11	Shallow-water Multibeam Echosounder	alter course	57°57,719' N	000°17,956' W	119.2	7.0	91.0	57.961977	-0.299272	21	17.80		0.0	Kurs 270°
MSM63_17-1	2017-05-19 18:30:48	Shallow-water Multibeam Echosounder	alter course	57°57,448' N	000°27,502' W	117.1	7.0	270.5	57.957467	-0.458363	26	16.70		0.0	Kurs 090°
MSM63_17-1	2017-05-19 19:19:31	Shallow-water Multibeam Echosounder	alter course	57°57,856' N	000°17,973' W	119.7	7.0	90.1	57.964273	-0.299544	8	20.60		0.0	Kurs 270°
MSM63_17-1	2017-05-19 20:06:36	Shallow-water Multibeam Echosounder	alter course	57°57,586' N	000°27,555' W	117.0	7.1	273.8	57.959775	-0.459258	17	18.60		0.0	Kurs 090°
MSM63_17-1	2017-05-19 20:57:54	Shallow-water Multibeam Echosounder	alter course	57°58,274' N	000°17,851' W	120.4	7.0	96.7	57.971225	-0.297515	15	22.80		0.0	Kurs 270°
MSM63_17-1	2017-05-19 21:45:06	Shallow-water Multibeam Echosounder	alter course	57°57,981' N	000°27,587' W	115.7	6.9	271.6	57.966355	-0.459784	23	20.10		0.0	Kurs 090°
MSM63_17-1	2017-05-19 22:34:45	Shallow-water Multibeam Echosounder	alter course	57°58,408' N	000°17,944' W	120.2	6.9	96.9	57.973474	-0.299067	20	21.30		0.0	Kurs 270°

MSM63_17-1	2017-05-19 23:23:54	Shallow-water Multibeam Echosounder	alter course	57°58,169' N	000°27,755' W	115.4	6.5	306.4	57.969488	-0.462584	20	19.80	0.0	Kurs 090°
MSM63_17-1	2017-05-20 00:14:24	Shallow-water Multibeam Echosounder	alter course	57°58,809' N	000°17,960' W	120.5	7.1	93.0	57.980153	-0.299332	20	19.50	0.0	Kurs 270°
MSM63_17-1	2017-05-20 01:00:59	Shallow-water Multibeam Echosounder	alter course	57°58,532' N	000°27,536' W	119.0	7.0	273.7	57.975528	-0.458935	43	18.50	0.0	Kurs 090°
MSM63_17-1	2017-05-20 01:50:38	Shallow-water Multibeam Echosounder	alter course	57°58,952' N	000°17,942' W	120.9	7.1	94.5	57.982539	-0.299041	52	20.30	0.0	Kurs 270°
MSM63_17-1	2017-05-20 02:38:43	Shallow-water Multibeam Echosounder	alter course	57°58,673' N	000°27,673' W	124.1	6.7	293.0	57.977888	-0.461222	62	15.30	0.0	Kurs 090°
MSM63_17-1	2017-05-20 03:30:15	Shallow-water Multibeam Echosounder	alter course	57°59,373' N	000°17,935' W	121.9	6.9	96.1	57.989551	-0.298913	83	19.00	0.0	Kurs 270°
MSM63_17-1	2017-05-20 04:16:50	Shallow-water Multibeam Echosounder	alter course	57°59,064' N	000°27,520' W	126.3	7.0	271.1	57.984408	-0.458665	73	14.30	0.0	Kurs 090°
MSM63_17-1	2017-05-20 05:05:20	Shallow-water Multibeam Echosounder	alter course	57°59,509' N	000°17,972' W	122.7	7.1	91.7	57.991812	-0.299535	83	15.80	0.0	Kurs 270°
MSM63_17-1	2017-05-20 05:52:51	Shallow-water Multibeam Echosounder	alter course	57°59,213' N	000°27,640' W	120.2	6.8	286.7	57.986880	-0.460666	83	14.60	0.0	Kurs 090°
MSM63_17-1	2017-05-20 06:41:22	Shallow-water Multibeam Echosounder	alter course	57°59,779' N	000°18,060' W	123.0	6.9	87.9	57.996314	-0.301007	94	16.50	0.0	Kurs 270°
MSM63_17-1	2017-05-20 07:11:30	Shallow-water Multibeam Echosounder	profile end	58°00,428' N	000°23,029' W	123.8	7.0	271.3	58.007125	-0.383809	91	16.10	0.0	
MSM63_17-1	2017-05-20 07:11:48	Shallow-water	information	58°00,430' N	000°23,092' W	124.3	6.6	281.3	58.007175	-0.384868	89	15.90	0.0	Unterbrechung CTD

		Multibeam Echosounder													
MSM63_18-1	2017-05-20 07:23:52	CTD	in the water	58°00,428' N	000°23,676' W	124.0	0.2	20.5	58.007132	-0.394593	91	17.00	EL1	3.0	
MSM63_18-1	2017-05-20 07:37:14	CTD	max depth/on ground	58°00,432' N	000°23,677' W	123.8	0.0	36.5	58.007199	-0.394625	93	18.00	EL1	118.0	
MSM63_18-1	2017-05-20 07:52:17	CTD	on deck	58°00,433' N	000°23,678' W	124.2	0.1	294.2	58.007210	-0.394634	90	17.30		0.0	
MSM63_17-1	2017-05-20 08:01:08	Shallow-water Multibeam Echosounder	profile start	58°00,434' N	000°22,955' W	124.2	3.0	254.9	58.007241	-0.382576	71	16.40		0.0	v=7kn, Kurs 270°
MSM63_17-1	2017-05-20 08:22:36	Shallow-water Multibeam Echosounder	alter course	58°00,428' N	000°27,480' W	122.9	6.9	273.2	58.007133	-0.458007	91	19.00		0.0	Kurs 090°
MSM63_17-1	2017-05-20 09:15:21	Shallow-water Multibeam Echosounder	alter course	57°59,646' N	000°17,916' W	122.9	6.9	91.2	57.994105	-0.298608	110	20.00		0.0	Kurs 270°
MSM63_17-1	2017-05-20 09:38:50	Shallow-water Multibeam Echosounder	alter course	58°00,164' N	000°21,912' W	123.9	7.1	268.8	58.002734	-0.365202	121	16.80		0.0	Kurs 090°
MSM63_17-1	2017-05-20 10:01:11	Shallow-water Multibeam Echosounder	alter course	57°59,912' N	000°17,988' W	122.6	7.1	86.4	57.998539	-0.299800	136	19.50		0.0	Kurs 270°
MSM63_17-1	2017-05-20 10:23:10	Shallow-water Multibeam Echosounder	profile end	58°00,303' N	000°21,742' W	123.6	6.0	272.4	58.005048	-0.362369	139	17.30		0.0	
MSM63_17-1	2017-05-20 10:23:18	Shallow-water Multibeam Echosounder	information	58°00,303' N	000°21,767' W	123.7	6.0	272.6	58.005058	-0.362777	139	17.30		0.0	Unterbrechung CTD
MSM63_19-1	2017-05-20 10:23:29	CTD	in the water	58°00,305' N	000°21,800' W	123.7	5.9	274.8	58.005076	-0.363336	139	17.30		0.0	
MSM63_19-1	2017-05-20 10:47:54	CTD	max depth/on ground	58°00,317' N	000°22,313' W	122.9	0.1	20.6	58.005279	-0.371881	163	17.10	EL1	117.0	
MSM63_19-1	2017-05-20 11:03:51	CTD	on deck	58°00,316' N	000°22,313' W	123.4	0.0	35.4	58.005268	-0.371891	179	17.00	EL1	-14.0	
MSM63_17-1	2017-05-20 11:06:29	Shallow-water Multibeam Echosounder	profile start	58°00,318' N	000°22,294' W	123.3	1.0	103.7	58.005303	-0.371564	179	18.20		0.0	v=7kn, Kurs 090°

MSM63_17-1	2017-05-20 11:32:02	Shallow-water Multibeam Echosounder	alter course	58°00,037' N	000°17,821' W	122.2	6.6	96.2	58.000617	-0.297025	175	19.60		0.0	Kurs 270°
MSM63_17-1	2017-05-20 12:00:36	Shallow-water Multibeam Echosounder	profile end	58°00,115' N	000°22,147' W	123.2	4.5	220.5	58.001921	-0.369119	176	22.40		0.0	
MSM63_17-1	2017-05-20 12:00:57	Shallow-water Multibeam Echosounder	information	58°00,095' N	000°22,175' W	122.3	4.2	210.2	58.001584	-0.369580	174	22.50		0.0	Unterbrechung f・CTD
MSM63_20-1	2017-05-20 12:12:38	CTD	in the water	57°59,902' N	000°22,304' W	122.4	0.1	324.2	57.998371	-0.371737	171	21.90	EL1	7.0	
MSM63_20-1	2017-05-20 12:25:15	CTD	max depth/on ground	57°59,903' N	000°22,305' W	122.9	0.1	9.2	57.998388	-0.371758	178	23.80	EL1	116.0	
MSM63_20-1	2017-05-20 12:41:24	CTD	on deck	57°59,902' N	000°22,303' W	122.8	0.0	321.1	57.998370	-0.371720	190	28.20	EL1	0.0	
MSM63_17-1	2017-05-20 13:06:51	Shallow-water Multibeam Echosounder	profile start	58°00,468' N	000°17,669' W	124.2	7.7	344.8	58.007808	-0.294490	196	29.70		0.0	v= 7kn Kurs 270°
MSM63_17-1	2017-05-20 13:53:13	Shallow-water Multibeam Echosounder	profile end	58°00,588' N	000°27,709' W	122.5	8.0	282.4	58.009798	-0.461824	188	33.50		0.0	
MSM63_17-1	2017-05-20 13:53:21	Shallow-water Multibeam Echosounder	information	58°00,592' N	000°27,738' W	122.4	8.2	287.1	58.009874	-0.462306	186	32.70		0.0	Unterbrechung f・CTD
MSM63_21-1	2017-05-20 14:06:25	CTD	in the water	58°01,047' N	000°27,837' W	121.8	0.1	297.1	58.017443	-0.463946	194	29.90	EL1	1.0	
MSM63_21-1	2017-05-20 14:23:00	CTD	max depth/on ground	58°01,047' N	000°27,838' W	121.5	0.0	98.4	58.017443	-0.463959	191	29.70	EL1	94.0	
MSM63_21-1	2017-05-20 14:34:12	CTD	on deck	58°01,047' N	000°27,837' W	121.3	0.1	0.8	58.017448	-0.463956	188	31.30	EL1	-14.0	
MSM63_17-1	2017-05-20 14:38:18	Shallow-water Multibeam Echosounder	profile start	58°01,009' N	000°27,814' W	121.9	3.2	124.7	58.016824	-0.463560	199	27.50		0.0	v=7kn Kurs 090°
MSM63_17-1	2017-05-20 15:23:42	Shallow-water Multibeam Echosounder	alter course	58°01,012' N	000°17,972' W	124.0	7.1	97.7	58.016861	-0.299541	191	28.40		0.0	Kurs 270°
MSM63_17-1	2017-05-20 16:11:24	Shallow-water	alter course	58°00,713' N	000°27,486' W	120.8	7.0	264.5	58.011877	-0.458106	182	27.70		0.0	Kurs 090°

		Multibeam Echosounder												
MSM63_17-1	2017-05-20 17:00:10	Shallow-water Multibeam Echosounder	alter course	58°01,151' N	000°18,000' W	125.6	6.6	93.2	58.019184	-0.299992	184	24.60	0.0	Kurs 270°
MSM63_17-1	2017-05-20 17:47:45	Shallow-water Multibeam Echosounder	alter course	58°00,858' N	000°27,471' W	122.2	7.0	266.1	58.014301	-0.457858	175	26.60	0.0	Kurs 090°
MSM63_17-1	2017-05-20 18:37:51	Shallow-water Multibeam Echosounder	alter course	58°01,559' N	000°18,024' W	124.9	6.9	91.9	58.025976	-0.300399	178	24.40	0.0	Kurs 270°
MSM63_17-1	2017-05-20 19:25:31	Shallow-water Multibeam Echosounder	alter course	58°01,288' N	000°27,509' W	121.7	6.7	269.0	58.021468	-0.458488	172	20.90	0.0	Kurs 090°
MSM63_17-1	2017-05-20 20:13:32	Shallow-water Multibeam Echosounder	alter course	58°01,700' N	000°18,023' W	125.9	7.0	88.3	58.028336	-0.300389	166	21.70	0.0	Kurs 270°
MSM63_17-1	2017-05-20 21:01:17	Shallow-water Multibeam Echosounder	alter course	58°01,412' N	000°27,477' W	122.9	7.0	270.5	58.023534	-0.457946	165	20.10	0.0	Kurs 090°
MSM63_17-1	2017-05-20 21:52:02	Shallow-water Multibeam Echosounder	alter course	58°02,117' N	000°18,029' W	126.7	7.0	92.6	58.035289	-0.300490	164	19.80	0.0	Kurs 270°
MSM63_17-1	2017-05-20 22:40:01	Shallow-water Multibeam Echosounder	alter course	58°01,827' N	000°27,493' W	121.4	7.1	272.4	58.030447	-0.458209	160	18.40	0.0	Kurs 090°
MSM63_17-1	2017-05-20 23:29:01	Shallow-water Multibeam Echosounder	alter course	58°02,251' N	000°17,929' W	125.3	6.9	99.8	58.037513	-0.298816	166	16.60	0.0	Kurs 270°
MSM63_17-1	2017-05-21 00:16:02	Shallow-water Multibeam Echosounder	alter course	58°01,963' N	000°27,563' W	122.2	7.0	262.5	58.032721	-0.459391	170	17.30	0.0	Kurs 090°
MSM63_17-1	2017-05-21 00:48:04	Shallow-water Multibeam Echosounder	alter course	58°00,307' N	000°23,907' W	122.9	7.0	92.5	58.005113	-0.398452	184	16.70	0.0	Kurs 270°

MSM63_17-1	2017-05-21 01:08:45	Shallow-water Multibeam Echosounder	alter course	58°00,013' N	000°27,590' W	119.7	7.0	271.8	58.000217	-0.459841	174	17.30	0.0	Kurs 090°
MSM63_17-1	2017-05-21 01:32:49	Shallow-water Multibeam Echosounder	alter course	58°00,164' N	000°24,017' W	123.7	7.1	91.6	58.002726	-0.400285	181	16.50	0.0	Kurs 270°
MSM63_17-1	2017-05-21 01:55:37	Shallow-water Multibeam Echosounder	profile end	57°59,883' N	000°27,946' W	117.9	6.7	261.7	57.998057	-0.465775	172	16.50	0.0	
MSM63_15-1	2017-05-21 01:55:47	CTD	information	57°59,880' N	000°27,981' W	117.8	6.7	253.6	57.997992	-0.466355	172	16.50	0.0	
MSM63_23-1	2017-05-21 02:03:41	Parasound	profile start	58°00,003' N	000°26,961' W	124.2	8.0	62.2	58.000048	-0.449348	178	16.00	0.0	v=7kn Kurs 073°
MSM63_23-1	2017-05-21 04:08:27	Parasound	profile end	58°04,305' N	000°00,701' W	133.0	7.0	71.8	58.071743	-0.011686	184	14.90	0.0	
MSM63_24-1	2017-05-21 07:11:01	Shallow-water Multibeam Echosounder	profile start	58°15,760' N	001°02,797' E	150.4	6.4	352.1	58.262670	1.046610	230	13.30	0.0	v=7kn, Kurs 000°
MSM63_24-1	2017-05-21 07:44:46	Shallow-water Multibeam Echosounder	alter course	58°19,634' N	001°02,822' E	149.3	7.0	360.0	58.327231	1.047042	195	10.20	0.0	Kurs 180°
MSM63_24-1	2017-05-21 08:23:08	Shallow-water Multibeam Echosounder	alter course	58°15,950' N	001°03,744' E	149.0	7.0	181.0	58.265833	1.062408	185	9.40	0.0	Kurs 000°
MSM63_24-1	2017-05-21 09:00:40	Shallow-water Multibeam Echosounder	alter course	58°19,710' N	001°03,057' E	148.1	7.1	0.2	58.328498	1.050953	192	12.40	0.0	Kurs 180°
MSM63_24-1	2017-05-21 09:38:18	Shallow-water Multibeam Echosounder	alter course	58°15,943' N	001°03,970' E	148.6	7.0	179.7	58.265715	1.066160	199	12.70	0.0	Kurs 000°
MSM63_24-1	2017-05-21 10:15:36	Shallow-water Multibeam Echosounder	alter course	58°19,694' N	001°03,267' E	148.2	7.0	1.4	58.328231	1.054451	207	13.60	0.0	Kurs 180°
MSM63_24-1	2017-05-21 10:54:24	Shallow-water Multibeam Echosounder	alter course	58°15,916' N	001°04,199' E	148.6	7.0	179.5	58.265267	1.069985	220	14.60	0.0	Kurs 000°

MSM63_24-1	2017-05-21 11:35:11	Shallow-water Multibeam Echosounder	profile end	58°20,152' N	001°03,511' E	146.7	7.4	350.3	58.335869	1.058522	216	11.90		0.0	
MSM63_25-1	2017-05-21 12:25:25	CTD	in the water	58°16,915' N	000°58,247' E	169.3	0.1	348.4	58.281909	0.970782	201	12.70	EL1	3.0	
MSM63_25-1	2017-05-21 12:42:36	CTD	max depth/on ground	58°16,914' N	000°58,248' E	169.5	0.0	29.0	58.281898	0.970802	204	13.80	EL1	163.0	
MSM63_25-1	2017-05-21 13:02:31	CTD	on deck	58°16,915' N	000°58,245' E	169.5	0.1	148.6	58.281914	0.970746	197	13.80	EL1	-13.0	
MSM63_26-1	2017-05-21 13:50:48	CTD	in the water	58°17,091' N	000°57,982' E	153.3	0.1	351.0	58.284856	0.966368	203	12.10	EL1	8.0	
MSM63_26-1	2017-05-21 14:04:32	CTD	max depth/on ground	58°17,091' N	000°57,983' E	153.4	0.0	181.9	58.284848	0.966384	201	11.70	EL1	146.0	
MSM63_26-1	2017-05-21 14:23:36	CTD	on deck	58°17,091' N	000°57,982' E	153.4	0.0	94.1	58.284843	0.966371	205	11.30	EL1	-13.0	
MSM63_27-1	2017-05-21 14:43:47	Shallow-water Multibeam Echosounder	profile start	58°17,048' N	001°00,497' E	151.4	6.7	173.1	58.284134	1.008277	208	12.30		0.0	v=7kn Kurs 180°
MSM63_27-1	2017-05-21 15:07:18	Shallow-water Multibeam Echosounder	alter course	58°14,380' N	001°00,524' E	151.9	6.9	179.8	58.239661	1.008730	190	9.00		0.0	Kurs 000°
MSM63_27-1	2017-05-21 16:01:29	Shallow-water Multibeam Echosounder	alter course	58°20,061' N	001°01,426' E	148.6	6.9	0.2	58.334357	1.023763	183	10.40		0.0	Kurs 180°
MSM63_27-1	2017-05-21 16:54:56	Shallow-water Multibeam Echosounder	information	58°14,402' N	001°00,755' E	151.9	7.0	180.9	58.240035	1.012589	193	13.70		0.0	Kurs 000°
MSM63_27-1	2017-05-21 17:49:49	Shallow-water Multibeam Echosounder	alter course	58°20,094' N	001°01,632' E	149.0	6.8	358.2	58.334894	1.027200	188	12.80		0.0	Kurs 180°
MSM63_27-1	2017-05-21 18:43:41	Shallow-water Multibeam Echosounder	alter course	58°14,428' N	001°00,991' E	152.4	7.0	180.1	58.240463	1.016510	192	13.00		0.0	Kurs 000°
MSM63_27-1	2017-05-21 19:38:26	Shallow-water Multibeam Echosounder	alter course	58°20,069' N	001°01,847' E	148.9	7.0	0.8	58.334478	1.030780	179	10.00		0.0	Kurs 180°
MSM63_27-1	2017-05-21 20:31:05	Shallow-water	alter course	58°14,421' N	001°01,210' E	152.3	6.9	179.4	58.240350	1.020174	170	14.10		0.0	Kurs 000°

		Multibeam Echosounder												
MSM63_27-1	2017-05-21 21:24:58	Shallow-water Multibeam Echosounder	alter course	58°20,081' N	001°02,074' E	148.6	7.0	359.0	58.334689	1.034574	173	12.80	0.0	Kurs 180°
MSM63_27-1	2017-05-21 22:05:17	Shallow-water Multibeam Echosounder	alter course	58°15,744' N	001°02,489' E	150.2	6.9	181.2	58.262407	1.041476	170	13.60	0.0	Kurs 000°
MSM63_27-1	2017-05-21 22:48:19	Shallow-water Multibeam Echosounder	alter course	58°20,077' N	001°02,277' E	148.5	7.1	0.0	58.334621	1.037951	169	12.60	0.0	Kurs 180°
MSM63_27-1	2017-05-21 23:30:08	Shallow-water Multibeam Echosounder	profile end	58°15,693' N	001°02,307' E	151.3	8.9	247.8	58.261556	1.038453	169	12.00	0.0	
MSM63_28-1	2017-05-22 03:20:16	Shallow-water Multibeam Echosounder	profile start	57°59,916' N	000°17,623' W	122.6	7.0	261.3	57.998600	-0.293723	156	16.70	0.0	v=7kn, Kurs 270°
MSM63_28-1	2017-05-22 03:39:56	Shallow-water Multibeam Echosounder	alter course	57°59,920' N	000°21,909' W	122.3	7.1	270.7	57.998671	-0.365153	162	16.30	0.0	Kurs 090°
MSM63_28-1	2017-05-22 04:03:49	Shallow-water Multibeam Echosounder	alter course	58°00,350' N	000°17,966' W	123.3	6.9	88.6	58.005834	-0.299426	161	15.80	0.0	Kurs 270°
MSM63_28-1	2017-05-22 04:53:49	Shallow-water Multibeam Echosounder	alter course	58°00,777' N	000°27,524' W	122.5	7.0	270.6	58.012955	-0.458729	159	16.80	0.0	Kurs 090°
MSM63_28-1	2017-05-22 05:44:01	Shallow-water Multibeam Echosounder	alter course	58°00,619' N	000°17,696' W	124.3	6.5	16.8	58.010323	-0.294937	171	15.60	0.0	Kurs 270°
MSM63_28-1	2017-05-22 06:31:47	Shallow-water Multibeam Echosounder	alter course	58°00,921' N	000°27,477' W	122.7	6.9	271.4	58.015352	-0.457954	160	14.80	0.0	Kurs 090°
MSM63_28-1	2017-05-22 07:22:09	Shallow-water Multibeam Echosounder	profile end	58°00,670' N	000°17,598' W	124.9	7.0	89.7	58.011162	-0.293306	166	17.80	0.0	

MSM63_29-1	2017-05-22 07:40:37	CTD	in the water	57°59,654' N	000°18,148' W	123.1	0.1	290.0	57.994234	-0.302470	159	17.20	EL1	0.0	
MSM63_29-1	2017-05-22 07:53:34	CTD	max depth/on ground	57°59,654' N	000°18,148' W	123.2	0.0	181.7	57.994237	-0.302459	157	17.30	EL1	115.0	
MSM63_29-1	2017-05-22 08:05:52	CTD	on deck	57°59,654' N	000°18,148' W	123.0	0.0	155.6	57.994235	-0.302467	162	17.20	EL1	0.0	
MSM63_30-1	2017-05-22 08:19:51	Parasound	profile start	57°59,656' N	000°18,132' W	123.1	6.9	179.9	57.994270	-0.302201	152	17.50		0.0	v=7kn, Kurs 180°
MSM63_30-1	2017-05-22 08:36:34	Parasound	profile end	57°57,726' N	000°18,148' W	119.2	6.9	181.5	57.962101	-0.302471	146	17.00		0.0	
MSM63_30-1	2017-05-22 08:36:42	Parasound	information	57°57,711' N	000°18,149' W	119.0	6.9	181.2	57.961849	-0.302480	146	17.00		0.0	Unterbrechung CTD
MSM63_31-1	2017-05-22 08:50:20	CTD	in the water	57°57,770' N	000°18,161' W	119.6	0.1	145.2	57.962826	-0.302683	147	17.10	EL1	2.0	
MSM63_31-1	2017-05-22 09:03:28	CTD	max depth/on ground	57°57,770' N	000°18,161' W	119.3	0.0	34.2	57.962827	-0.302692	148	18.00	EL1	113.0	
MSM63_31-1	2017-05-22 09:17:37	CTD	on deck	57°57,769' N	000°18,161' W	119.6	0.1	133.0	57.962823	-0.302689	142	18.60	EL1	-13.0	
MSM63_30-1	2017-05-22 09:29:36	Parasound	profile start	57°57,738' N	000°18,130' W	119.7	6.8	270.9	57.962297	-0.302174	153	21.90		0.0	v=7kn, Kurs 270°
MSM63_30-1	2017-05-22 09:52:00	Parasound	profile end	57°57,748' N	000°23,087' W	119.1	7.0	271.3	57.962464	-0.384787	150	20.70		0.0	
MSM63_30-1	2017-05-22 09:52:53	Parasound	information	57°57,759' N	000°23,272' W	119.3	6.0	296.6	57.962649	-0.387871	144	21.00		0.0	Unterbrechung CTD
MSM63_32-1	2017-05-22 10:01:24	CTD	in the water	57°57,767' N	000°23,100' W	119.2	0.1	129.6	57.962777	-0.384997	158	21.70	EL1	-11.0	
MSM63_32-1	2017-05-22 10:15:17	CTD	max depth/on ground	57°57,768' N	000°23,102' W	119.1	0.0	235.1	57.962797	-0.385027	152	18.90	EL1	113.0	
MSM63_32-1	2017-05-22 10:26:49	CTD	on deck	57°57,767' N	000°23,102' W	119.1	0.0	10.7	57.962791	-0.385028	155	17.50	EL1	-13.0	
MSM63_30-1	2017-05-22 10:38:39	Parasound	profile start	57°57,747' N	000°23,057' W	119.0	6.1	268.6	57.962445	-0.384285	150	19.00		0.0	v=7kn, Kurs 270°
MSM63_30-1	2017-05-22 10:58:45	Parasound	profile end	57°57,736' N	000°27,503' W	115.1	7.2	273.4	57.962258	-0.458384	149	21.60		0.0	
MSM63_30-1	2017-05-22 10:58:55	Parasound	information	57°57,736' N	000°27,540' W	115.4	7.1	272.8	57.962270	-0.459003	149	21.50		0.0	Unterbrechung CTD
MSM63_33-1	2017-05-22 11:12:39	CTD	in the water	57°57,758' N	000°27,568' W	115.9	0.0	227.5	57.962640	-0.459459	145	20.10	EL1	10.0	
MSM63_33-1	2017-05-22 11:24:54	CTD	max depth/on ground	57°57,758' N	000°27,566' W	115.8	0.1	70.4	57.962639	-0.459432	147	20.10	EL1	109.0	
MSM63_33-1	2017-05-22 11:38:55	CTD	on deck	57°57,758' N	000°27,566' W	115.6	0.0	194.1	57.962630	-0.459441	144	20.40	EL1	-13.0	
MSM63_30-1	2017-05-22 11:48:34	Parasound	profile start	57°57,727' N	000°27,555' W	115.3	5.8	4.0	57.962111	-0.459247	142	19.10		0.0	v=7kn Kurs:000°
MSM63_30-1	2017-05-22 12:06:40	Parasound	profile end	57°59,808' N	000°27,626' W	121.0	6.8	359.4	57.996799	-0.460438	144	18.60		0.0	

MSM63_30-1	2017-05-22 12:06:45	Parasound	information	57°59,817' N	000°27,626' W	120.9	6.9	359.6	57.996958	-0.460441	144	18.60		0.0	Unterbrechung CTD
MSM63_34-1	2017-05-22 12:20:44	CTD	in the water	57°59,816' N	000°27,641' W	121.0	0.0	32.0	57.996941	-0.460681	145	20.40	EL1	10.0	
MSM63_34-1	2017-05-22 12:32:09	CTD	max depth/on ground	57°59,815' N	000°27,640' W	120.5	0.0	227.2	57.996922	-0.460671	153	20.70	EL1	115.0	
MSM63_34-1	2017-05-22 12:42:30	CTD	on deck	57°59,816' N	000°27,639' W	120.9	0.1	56.9	57.996934	-0.460657	152	21.40	EL1	-11.0	
MSM63_30-1	2017-05-22 12:50:11	Parasound	profile start	57°59,825' N	000°27,215' W	122.3	5.1	94.0	57.997083	-0.453583	154	21.30		0.0	v=7kn Kurs 090°
MSM63_30-1	2017-05-22 13:04:50	Parasound	profile end	57°59,831' N	000°24,109' W	122.3	7.0	88.4	57.997180	-0.401815	156	23.50		0.0	
MSM63_30-1	2017-05-22 13:17:46	Parasound	information	57°59,860' N	000°24,126' W	122.6	0.1	53.5	57.997660	-0.402099	152	21.40	EL1	-11.0	Unterbrechung CTD
MSM63_35-1	2017-05-22 13:20:27	CTD	in the water	57°59,860' N	000°24,124' W	122.7	0.0	124.9	57.997670	-0.402059	150	20.30	EL1	4.0	
MSM63_35-1	2017-05-22 13:30:59	CTD	max depth/on ground	57°59,860' N	000°24,124' W	122.2	0.0	170.8	57.997671	-0.402060	153	20.10	EL1	116.0	
MSM63_35-1	2017-05-22 13:44:02	CTD	on deck	57°59,860' N	000°24,125' W	122.1	0.0	8.7	57.997668	-0.402076	156	19.30	EL1	-14.0	
MSM63_30-1	2017-05-22 13:53:43	Parasound	profile start	57°59,849' N	000°24,110' W	122.2	5.8	9.0	57.997489	-0.401834	156	18.70		0.0	v=7kn Kurs 012°
MSM63_30-1	2017-05-22 14:08:42	Parasound	profile end	58°01,652' N	000°23,408' W	123.7	7.3	11.0	58.027526	-0.390140	165	17.10		0.0	
MSM63_30-1	2017-05-22 14:10:50	Parasound	information	58°01,869' N	000°23,360' W	123.6	2.6	328.9	58.031153	-0.389326	176	18.80		0.0	
MSM63_36-1	2017-05-22 14:24:27	CTD	in the water	58°01,717' N	000°23,386' W	123.6	0.1	269.5	58.028615	-0.389773	160	18.60	EL1	10.0	
MSM63_36-1	2017-05-22 14:36:29	CTD	max depth/on ground	58°01,716' N	000°23,387' W	123.7	0.0	216.0	58.028603	-0.389786	157	19.10	EL1	117.0	
MSM63_36-1	2017-05-22 14:42:09	CTD	on deck	58°01,716' N	000°23,387' W	123.7	0.0	106.8	58.028600	-0.389788	155	19.80	EL1	-12.0	
MSM63_37-1	2017-05-22 15:27:50	CTD	at surface	57°56,774' N	000°15,968' W	114.9	0.1	221.2	57.946229	-0.266131	162	18.40	EL1	-2.0	
MSM63_37-1	2017-05-22 15:38:58	CTD	max depth/on ground	57°56,773' N	000°15,968' W	114.8	0.0	211.6	57.946217	-0.266139	153	18.50	EL1	109.0	
MSM63_37-1	2017-05-22 15:45:38	CTD	on deck	57°56,774' N	000°15,971' W	114.7	0.1	272.9	57.946226	-0.266176	162	18.50	EL1	-14.0	
MSM63_38-1	2017-05-22 16:29:16	Shallow-water Multibeam Echosounder	profile start	58°00,299' N	000°27,424' W	120.4	6.2	198.7	58.004982	-0.457065	147	24.20		0.0	v=7kn, Kurs 180°
MSM63_38-1	2017-05-22 16:47:56	Shallow-water Multibeam Echosounder	alter course	57°58,109' N	000°27,469' W	113.4	7.2	179.6	57.968483	-0.457811	148	22.70		0.0	Kurs 000°

MSM63_38-1	2017-05-22 17:10:17	Shallow-water Multibeam Echosounder	alter course	58°00,150' N	000°28,162' W	117.7	7.0	359.3	58.002501	-0.469360	147	23.20	0.0	Kurs 180°
MSM63_38-1	2017-05-22 17:32:30	Shallow-water Multibeam Echosounder	alter course	57°58,097' N	000°27,703' W	113.3	7.0	179.5	57.968284	-0.461722	145	23.80	0.0	Kurs 000°
MSM63_38-1	2017-05-22 17:54:41	Shallow-water Multibeam Echosounder	alter course	58°00,114' N	000°28,372' W	117.7	6.8	0.1	58.001904	-0.472867	149	23.80	0.0	Kurs 180°
MSM63_38-1	2017-05-22 18:17:02	Shallow-water Multibeam Echosounder	alter course	57°58,072' N	000°27,919' W	114.7	7.0	179.0	57.967871	-0.465309	153	25.10	0.0	Kurs 000°
MSM63_38-1	2017-05-22 18:41:16	Shallow-water Multibeam Echosounder	profile end	58°00,294' N	000°28,596' W	116.7	6.9	359.4	58.004905	-0.476594	149	21.10	0.0	
MSM63_39-1	2017-05-22 19:12:15	Parasound	profile start	58°03,396' N	000°22,009' W	125.2	8.4	178.0	58.056603	-0.366814	141	24.30	0.0	v=7,5kn, Kurs 180°
MSM63_39-1	2017-05-22 19:52:00	Parasound	alter course	57°58,432' N	000°21,928' W	120.0	7.6	176.6	57.973870	-0.365458	138	24.20	0.0	Kurs 360°
MSM63_39-1	2017-05-22 20:33:45	Parasound	alter course	58°03,265' N	000°21,569' W	125.4	7.5	2.6	58.054411	-0.359479	139	22.00	0.0	Kurs 180°
MSM63_39-1	2017-05-22 21:15:33	Parasound	alter course	57°58,467' N	000°21,032' W	120.8	7.6	181.2	57.974450	-0.350534	149	23.50	0.0	Kurs 360°
MSM63_39-1	2017-05-22 21:57:01	Parasound	alter course	58°03,258' N	000°20,618' W	125.9	7.5	359.3	58.054292	-0.343639	148	23.90	0.0	Kurs 180°
MSM63_39-1	2017-05-22 22:36:51	Parasound	alter course	57°58,744' N	000°20,099' W	121.1	7.5	180.8	57.979074	-0.334989	151	24.90	0.0	Kurs 270°
MSM63_39-1	2017-05-22 22:50:49	Parasound	alter course	57°58,867' N	000°22,106' W	120.3	8.6	267.9	57.981117	-0.368430	165	20.60	0.0	Kurs 090°
MSM63_39-1	2017-05-22 23:06:14	Parasound	alter course	57°59,404' N	000°19,785' W	122.6	7.6	89.8	57.990061	-0.329756	165	22.30	0.0	Kurs 270°
MSM63_39-1	2017-05-22 23:21:04	Parasound	alter course	57°59,875' N	000°22,053' W	122.2	7.3	271.7	57.997924	-0.367558	155	25.00	0.0	Kurs 359°
MSM63_39-1	2017-05-22 23:32:00	Parasound	alter course	58°01,178' N	000°22,372' W	124.7	7.7	357.6	58.019631	-0.372867	156	18.70	0.0	Kurs 090°
MSM63_39-1	2017-05-22 23:43:57	Parasound	alter course	58°01,361' N	000°19,779' W	124.8	7.5	89.2	58.022677	-0.329649	170	23.60	0.0	Kurs 270°
MSM63_39-1	2017-05-23 00:00:11	Parasound	alter course	58°01,912' N	000°22,209' W	125.4	7.4	291.6	58.031863	-0.370152	160	20.80	0.0	Kurs 090°
MSM63_39-1	2017-05-23 00:15:12	Parasound	alter course	58°02,448' N	000°19,779' W	125.9	7.5	91.6	58.040806	-0.329645	182	21.30	0.0	Kurs 270°

MSM63_39-1	2017-05-23 00:32:23	Parasound	profile end	58°02,919' N	000°22,512' W	124.3	7.6	261.9	58.048651	-0.375201	194	19.90	0.0

Appendix B: OBS stations

	Lat	Lon	Depth	Deployment	Recovery	Skew [ms]	Recorder	Battery [V]
OBS01	58°273052	0°958046	154	02.05.17	09.05.17	-13	980903	10.41
OBS02	58°280110	0°968413	157	02.05.17	09.05.17	6	020508	10.42
OBS03	58°281128	0°969944	167	02.05.17	09.05.17	-99	001001	10,50
OBS04	58°281855	0°971165	162	02.05.17	09.05.17	55	020503	11,43
OBS05	58°282932	0°972613	158	02.05.17	09.05.17	4	980908	10,46
OBS06	58°284267	0°975084	157	02.05.17	09.05.17	-252	010708	10,53
OBS07	58°290762	0°984077	153	02.05.17	09.05.17	26	020504	10,53
OBS08	58°283297	0°976139	155	02.05.17	09.05.17	Synronisation faild	000616	10,48
OBS09	58°278313	0°979366	154	02.05.17	09.05.17	27	980907	10,26
OBS10	58°281020	0°972298	160	02.05.17	09.05.17	10	990712	10,42
OBS11	58°28142	0°971293	169	02.05.17	09.05.17	-81		10,44
OBS12	58°281989	0°969917	159.7	02.05.17	09.05.17	Synronisation faild		10.21
OBS13	58°282390	0°968928	155	02.05.17	09.05.17	31	001005	10,60
OBS14	58°285142	0°962184	154	02.05.17	09.05.17	45	020509	10,55
OBS15	58°281878	0°967571	159	02.05.17	09.05.17	11	020507	10,39
OBS16	58°280107	0°91382	157	02.05.17	09.05.17	-65	000611	10,51
OBS17	58°281953	0°973995	158	02.05.17	09.05.17	-24	980403	10,66
OBS18	58°283486	0°970101	155.7	02.05.17	09.05.17	-193	000613	10,62
Trigger						-33	000614	

Appendix C: Air gun shooting for OBS

Time UTC	Latitude xx° xx.x‘	Longitude xx° xx.x‘	Course [°]	Heading [°]	Speed O.G. [kn]	Speed T.W. DoLog [kn]	Depth [m]	Geometrics FFN	Rec Len [s]	shot rate [s]	Delay (T/B)[1)] [ms]	Weather	Station No	Gun-Pressure G.I. 1 [bar]	Gun-Pressure G.I. 2 [bar]	Inline-No	Waypoint	Remarks
Friday, 05.05.2017																		
OBS Shooting																		
21:38	58.2390	02.2678	217.00	217.00	4.30	4.20	150.00			10	10	calm sea	4_1	200	200	1001	1	sol1001, wrong longitude (dship frozen)
21:58	58.3102	0.9979	217.00	217.30	4.50	4.30	152.00			10	10		4_1	200	200	1001		
22:18	58.2905	0.9700	218.00	217.40	4.50	4.30	153.00			10	10		4_1	200	200	1001		
22:38	58.2704	0.9404	217.00	216.00	4.40	4.30	151.00			10	10		4_1	200	200	1001		
22:58	58.2513	0.91234	218.00	217.60	4.40	4.10	155.10			10	10	calm sea	4_1	200	200	1001		
23:10	58.2394	0.8954	217.00	216,7	4.40	4.10	154.80			10	10		4_1	200	200	1001		end of line 1001
23:18	58.2388	0.905	39.00	34.00	4.80	4.50	155.70			10	10		4_1	200	200	1002		start of line 1002
23:38	58.2560	0.9305	38.00	34.40	4.40	4.30	154.90			10	10		4_1	200	200	1002		
23:58	58.2769	0.961	38.00	36.20	4.70	4.50	154.40			10	10		4_1	200	200	1002		
Saturday, 06.05.2017																		
0:18	58.2979	0.992	39.00	34.10	4.60	4.40	152.00			10	10		4_1	200	200	1002		
0:40	58.3194	1.0234	37.00	35.00	4.50	4.20	149.70			10	10		4_1	200	200	1002		
0:47	58.3272	1.0349	26.00	9.30	4.70	4.50	148.90			10	10		4_1	200	200	1002		end of line 1002
1:02	58.3261	1.0351	210.00	209.00	4.80	4.40	149.50			10	10		4_1	200	200	1003		start of line 1003
1:22	58.3068	1.0075	218.00	214.00	4.40	4.10	149.30			10	10		4_1	200	200	1003		
1:44	58.2884	0.9803	217.00	213.80	4.30	4.40	153.30			10	10		4_1	200	200	1003		
2:04	58.2668	0.948	218.00	215.30	4.30	4.10	154.30			10	10		4_1	200	200	1003		
2:24	58.2467	0.9191	218.00	214.50	4.60	4.50	154.20			10	10		4_1	200	200	1003		

2:34	58.2367	0.9044	225.00	232.00	4.60	4.50	154.70			10	10		4_1	200	200	1003		end of line 1003
2:49	58.2365	0.9084	38.00	34.90	5.10	4.60	154.20			10	10		4_1	200	200	1004		start of line 1004
3:11	58.2598	0.9424	38.00	36.20	4.70	4.50	154.00			10	10		4_1	200	200	1004		
3:33	58.281	0.973	37.00	35.30	4.60	4.30	161.50			10	10	calm sea	4_1	200	200	1004		
3:53	58,301	1,002	38.00	35.50	4.50	4.40	151.00			10	10	calm sea	4_1	200	200	1004		
4:13	58,321	1,031	38.00	36.60	4.50	4.30	149.10			10	10	calm sea	4_1	200	200	1004		
4:18	58,326	1,039	37.00	35.00	4.50	4.40	147.30			10	10	calm sea	4_1	200	200	1004		end of line 1004
4:27	58,322	1,044	218.00	219.30	4.80	4.70	147.60			10	10	calm sea	4_1	200	200	1005		sol 1005
4:47	58,303	1,015	217.00	215.80	4.50	4.40	150.80			10	10	calm sea	4_1	200	200	1005		
5:08	58,281	0.983	218.00	217.00	4.50	4.30	152.80			10	10	calm sea	4_1	200	200	1005		
5:19	58,270	0.967	218.00	218.30	4.50	4.70	154.30			10	10	calm sea	4_1	200	200	1005		
5:40	58,250	0.937	218.00	216.70	4.60	4.40	154.00			10	10	calm sea	4_1	200	200	1005		
5:56	58,233	0.913	217.00	217.40	4.60	4.30	153.90			10	10	calm sea	4_1	200	200	1005		eol 1005 , transit to next line
6:16	58,228	0.948	87.00	81.00	4.60	4.60	155.00			10	10	calm sea	4_1	200	200			transit
6:34	58,235	0.982	358.00	356.80	4.70	4.50	152.10			10	10	calm sea	4_1	200	200	1006		sol 1006
6:54	58° 15.567	00° 58.578	353.00	352.00	4.50	4.30	153.00			10	10	calm sea	4_1	200	200	1006		
7:14	58° 17.032	00° 58.2129	353.00	352.90	4.50	4.20	154.50			10	10	calm sea	4_1	200	200	1006		
7:34	58° 18.518	00° 57.835	352.00	353.00	4.50	4.20	152.70			10	10	calm sea	4_1	200	200	1006		
7:50	58° 19.798	00° 57.517	353.00	353.80	4.50	4.40	152.00			10	10	calm sea	4_1	200	200	1006		eol 1006
7:56	58° 20.222	00° 57.414	353.00	354.00	4.50	4.40	151.00			10	10	calm sea	4_1	200	200	1006		STOP SHOOTING, GPS Uhr rein

Appendix D: Seismic profiles

Time UTC	Latitude xx° xx.x‘	Longitude xx° xx.x‘	Course [°]	Heading [°]	Speed O.G. [kn]	Speed T.W. DoLog [kn]	Depth [m]	Geometrics FFN	Rec Len [s]	shot rate [s]	Delay (T/B)[1] [ms]	Weather	Station No	Gun-Pressure G.I. 1 [bar]	Gun-Pressure G.I. 2 [bar]	Inline-No	Waypoint	Remarks
Samstag 06.05.2017																		
2D Seismik and OBS Shooting																		
										6	10							
9:55	58°21.081	0°59.329	123.00	115.00	4.50	4.50	151.00	200	4	6	10	calm		200	200			stearing to line P2001
10:35	58° 20.1912	1° 02.2252	124.00	121.00	4.60	4.30	148.00	435	4	6	10	calm		200	200			
10:44	58° 19.588	1° 01.939	218.00	217.00	4.70	4.20	149.00	533	4	6	10	calm		200	200	2001	1	sol P2001
11:07	58° 18.160	0°59.879	218.00	217.90	4.60	4.40	151.90	773	4	6	10	calm		200	200	2001		
11:27	58° 17.022	0°58.231	218.00	217.30	4.70	4.20	157.00	954	4	6	10	calm		200	200	2001		
11:47	58° 15.756	0°56.358	216.00	215.50	4.60	4.30	154.40	1165	4	6	10	calm		200	200	2001		
12:07	58° 14.614	0°54.701	218.00	215.90	4.50	4.10	154.70	1353	4	6	10	calm		200	200	2001		
12:16	58° 14.190	0°53.737	289.00	296.00	4.20	4.10	154.00	1450	4	6	10	calm		200	200	2001	2	eol P2001 - vessel turning (log made sligtly after eol - approx. 12.12)
12:37	58° 14.227	0°54.327	37.00	33.90	4.60	4.10	154.40	1659	4	6	10	calm		200	200	2002	3	sol P2002
12:57	58° 15.360	0°56.008	38.00	36.70	4.40	4.00	154.60	1853	4	6	10	calm		200	200	2002		
13:17	58°16.551	0°57.756	38.00	38.10	4.40	4.20	153.8	2060	4	6	10	calm		20	20	200		

							0							0	0	2		
13:37	58°17.710	0°59.436	36.00	37.00	4.50	4.30	151.60	2253	4	6	10	calm		200	200	2002		
13:57	58° 18.884	01°1.157	38.00	39.00	4.60	4.50	150.00	2450	4	6	10	calm		200	200	2002		
14:07	58°19.555	01°2.145	34.00	25.00	4.60	4.30	148.20	2560	4	6	10	calm				2002	4	eol P2002
14:27	58°19.852	01°2.642	217.00	211.00	5.20	5.00	147.80	2753	4	6	10	calm		200	200			
14:32	58°19.472	1°2.189	220.00	219.00	4.50	4.20	148.60	2809	4	6	10	calm				2003	5	sol P2003
14:47	58°18.625	1°0.933	218.00	212.00	4.30	4.10	150.30	2958	4	6	10	calm		200	200	2003		
15:20	58°16.964	00°58.481	217.00	213.60	4.40	4.10	155.00	3310	4	6	10	calm		200	200	2003		
15:40	58°15.812	00°56.799	219.00	215.00	4.30	4.40	154.00	3449	4	6	10	calm		200	200	2003		
16:00	58°14.578	00°55.014	218.00	214.00	4.50	4,4	158.00	3662	4	6	10	calm		200	200	2003	6	eol P2003
16:20	58°15.165	00°53.728	343.00	342.00	4.60	4.40	155.00	3844	4	6	10	calm		200	200			transit
16:35	58°16.542	00°53.498	79.00	80.00	4.60	4.30	156.00	3991	4	6	10	calm		200	200	2004	7	sol P2004
16:59	58°16.796	00°56.870	81.00	78.00	4.50	4.50	154.00	4281	4	6	10	calm		200	200	2004		
17:29	58°17.116	01°01.158	81.00	77.00	4.40	4.40	150.00	4588	4	6	10	calm		200	200	2004		
17:45	58°17.255	001°03.11	84.00	82.00	4.30	4.20	150.00	4721	4	6	10	calm		200	200	2004	8	eol P2004
18:11	58°15.340	001°02.968	196.00	202.00	4.50	4.20	150.00	4999	4	6	10	calm		200	200			Change of course, One gun firing
18:16	58°15.245	01°02.321	303.00	308.00	4.20	4.00	150.00	5062	4	6	10	calm		200	200	2005	9	sol P2005; Two gun firing
18:37	58°16.203	00°59.938	309.00	313.00	4.60	4.40	151.00	5268	4	6	10	calm		200	200	2005		
18:57	58°17.050	00°57.835	308.00	313.00	4.50	4.50	153.00	5457	4	6	10	calm		200	200	2005		

19:17	58° 17.989	00°55.537	308.00	315.00	4.60	4.40	153.00	5660	4	6	10	calm		2000	2005			
19:37	58° 18.834	00°53.455	300.00	303.00	4.80	4.40	152.00	5846	4	6	10	calm		2000	2005	10	eol P2005	
19:58	58° 18.693	00°54.381	127.00	117.00	4.80	4.50	152.00	6066	4	6	10	calm		2000	2006	11	sol P2006	
20:18	58° 17.800	00°56.580	129.00	116.80	4.50	4.10	153.60	6262	4	6	10	calm		2000	2006			
20:38	58° 16.653	00°58.897	130.00	116.00	4.60	4.30	153.10	6467	4	6	10	calm		2000	2006			
20:58	58° 16.010	01°00.970	128.00	113.60	4.60	4.20	151.40	6652	4	6	10	calm		2000	2006			
21:11	58° 15.314	01°02.654	123.00	101.20	4.60	4.10	150.40	6801	4	6	10	calm		2000	2006	12	eol P2006	
21:30	58° 15.170	01°02.192	309.00	319.00	4.70	4.30	150.10	6990	4	6	10	calm		2000	2007	13	sol P2007	
21:50	58° 16.078	01°00.013	308.00	319.00	4.40	4.30	152.00	7183	4	6	10	calm		2000	2007			
22:10	58°17.043	01°57.637	305.00	319.00	4.50	4.30	153.90	7397	4	6	10	windy		2000	2007			
22:30	58°17.906	00°54.530	308.00	321.00	4.30	4.20	154.10	7583	4	6	10	windy		2000	2007			
22:43	58°18.554	00°53.961	307.00	312.00	4.80	4.50	153.00	7723	4	6	10	windy		2000	2007		eol P2007	
23:03	58°18.7236	00°54.1190	129.00	114.00	4.30	4..0	152.60	7916	4	6	10	windy		2000	2008		sol P2008	
23:23	58°17.7662	00°56.4337	126.00	116.00	4.90	4.80	154.10	8116	4	6	10	windy		2000	2008			
23:43	58°16.8260	00°58.7225	127.00	118.00	4.80	4.30	152.40	8316	4	6	10	windy		2000	2008			
0:05	58°15.7631	01°01.3001	127.00	117.00	4.60	4.50	151.20	8536	4	6	10	windy		2000	2008			
0:15	58°15.2460	01°02.5600	117.00	98.00	4.70	4.40	149.90	8641	4	6	10	windy		2000	2008		eol P2008	
0:32	58°15.1315	01°02.1241	305.00	312.00	4.70	4.30	150.90	8816	4	6	10	windy		2000	2009		sol P2009	
0:52	58°16.0447	00°59.8720	308.00	318.00	4.60	4.10	152.00	9011	4	6	10	windy		2000	2009			

0:18	58°17.3617	00°56.6512	308.00	316.00	4.90	4.50	154.40	9291	4	6	10	windy		2000	2000	2009	
1:38	58°18.1922	00°54.6637	308.00	317.00	4.90	4.50	153.00	9466	4	6	10	windy		2000	2000	2009	
1:43	58°18.4715	00°54.0047	308.00	318.00	4.40	4.30	151.10	9526	4	6	10	windy		2000	2000	2009	eol P2009
2:00	58°18.0655	00°53.3810	134.00	123.00	4.50	4.50	152.10	9691	4	6	10	windy		2000	2000	2010	sol P2010
2:20	58°17.0755	00°55.7980	129.00	120.00	4.70	4.50	154.00	9901	4	6	10	windy		2000	2000	2010	
2:41	58°16.1137	00°58.1609	131.00	125.70	4.60	4.30	153.50	10102	4	6	10	windy		2000	2000	2010	
3:02	58°15.1530	01°00.5087	128.00	123.70	4.70	4.50	151.40	10312	4	6	10	windy		2000	2000	2010	
3:13	58°14.854	1°1.206	123.00	113.00	4.50	4.00	150.60	10376	4	6	10	windy		2000	2000	2010	eol 2010
3:30	58°15.879	1°2.724	312.00	321.00	4.80	4.70	148.90	10585	4	6	10	windy		2000	2000	2011	sol 2011
3:50	58°16.625	1°0.487	307.00	315.60	4.70	4.40	151.70	10790	4	6	10	windy		2000	2000	2011	
4:10	58°17.719	0°58.284	308.00	17.00	4.70	4.40	153.20	10985	4	6	10	windy		2000	2000	2011	
4:31	58°18.699	0°55.915	310.00	319.00	4.70	4.30	154.00	11194	4	6	10	windy		2000	2000	2011	
4:39	58°19.056	0°55.038	302.00	311.00	4.40	4.00	151.90	11269	4	6	10	windy		2000	2000	2011	eol 2011
4:51	58°18.708	0°53.842	133.00	121.00	4.10	3.60	152.50	11388	4	6	10	windy		2000	2000	2012	sol 2012
5:11	58°17.811	0°56.076	129.00	119.00	4.50	4.30	153.70	11586	4	6	10	strong wind		2000	2000	2012	
5:34	58°16.716	0°58.734	127.00	116.00	4.50	4.20	153.80	11825	4	6	10	rough sea		2000	2000	2012	
5:55	58°15.787	1°1.092	130.00	120.00	4.70	5.30	151.40	12031	4	6	10	rough sea		2000	2000	2012	
6:04	58°15.357	1°2.081	121.00	108.00	4.50	4.20	150.30	12120	4	6	10	rough sea		2000	2000	2012	eol 2012
6:23	58°16.285	1°3.072	308.00	318.00	4.80	4.50	147.60	12312	4	6	10	rough sea		2000	2000	2013	sol 2013

6:50	58°17.481	1°0.203	311.00	320.00	4.70	4.10	150.50	12577	4	6	10	rough sea		200	200	2013		
6:59	58°17.905	0°59.120	314.00	338.00	4.10	3.80	153.30	12684	4	6	10	rough sea		200	200	2013		eol 2013 - stop shoting
07.05.2017																		
Tuesday 09.05.2017																		
P-Cable																		
14:34	58°16.027	00°55.460	35.00	37.90	2.90	2.60	154,8	25	4	5	5			200	200	3001		start of survey, sol 3001
13:41																		survey stopped
2D Survey																		
21:12	58°21.853	01°03.189	316.00	308.00	4.40	4.30	144.00	284	4	5	5	calm		200	200	3001		sol 3001
21:25	58°21.615	00°01.838	189.00	192.00	4.60	4.50	140.00	434	4	5	5	calm		200	200	3002		sol 3002 (real sol - previous is not)
21:45	58°20.155	01!01.847	179.00	186.00	4.60	4.30	148.00	667	4	5	5	calm		200	200	3002		
22:05	58°18.614	01!01.843	180.00	186.00	4.40	4.30	150.80	913	4	5	5	calm		200		3002		
22:25	58°17.184	01°01.847	179.00	184.00	4.50	4.10	151.00	1141	4	5	5							
22:29	58°18.781	01°01.851	181.00	186.00	4.50	4.10	150.20									3002		missing signal from one streamer - survey stopped
22:39	58°6.090	01°01.846	180.00	184.00	4.50	4.30	150.00	1199	4	5	5	calm		200	200	3002		Restart of survey, only two streamers getting data (:-( )
22:58	58°14.5200	01°01.844	180.00	184.00	4.50	4.10	151.00	1450	4	5	5	calm		200	200	3002		
23:16	58°13.266	01°01.853	180.00	184.00	4.60	4.10	151.90	1651	4	5	5	calm		200	200	3002		
23:37	58°11.667	01°01.842	180.00	183.20	4.50	4.50	151.60	1901	4	5	5	calm		200	200	3002		eol 3002

23:48	58°11.191	01°00.968	264.00	275.50	4.40	4.60	151.50	2030	4	5	5	calm		200	200	3003		sol 3003
23:59	58°11.026	00°59.4200	257.00	269.00	4.30	4.10	153.00	2163	4	5	5	calm		200	200	3003		
Wendsday 10.05.2017																		
0:24	58°10.635	00°55.936	271.00	285.00	4.70	4.30	155.00	2462	4	5	5	calm		200	200	3003		eol 3003
0:33	58°11.224	00°55.567	358.00	348.90	4.70	4.60	156.60	2571	4	5	5	calm		200	200	3004		sol 3004
0:53	58°12.762	00°55.530	0.00	352.90	4.70	4.40	156.00	2813	4	5	5	calm		200	200	3004		
1:13	58°14.175	00°55.534	2.00	354.00	4.30	3.90	154.00	3041	4	5	5	calm		200	200	3004		
1:33	58°15.731	00°55.554	359.00	350.00	4.50	4.30	155.40	3288	4	5	5	calm		200	200	3004		
1:55	58°17.401	00°55.555	0.00	352.00	4.50	4.30	154.00	3554	4	5	5	calm		200	200	3004		
2:15	58°18.900	00°55.572	0.00	353.00	4.40	4.40	152.00	3801	4	5	5	calm		200	200	3004		
2:34	58°20.297	00°55.605	4.00	357.00	4.70	4.50	151.00	4024	4	5	5	calm		200	200	3004		eol 3004 but we still go northeastward because the turn is too tigt otherwise
2:54	58°21.677	00°56.71	20.00	5.70	4.60	4.20	147.80	4248	4	5	5	calm		200	200	3005		sol 3005
3:16	58°20.440	00°54.758	194.00	197.00	4.50	4.40	151.00	4564	4	5	5	calm		200	200	3005		
3:39	58°19.021	00°54.018	195.00	198.00	4.50	4.40	151.00	4808	4	5	5	calm		200	200	3005		
4:08	58°16.952	00°52.884	196.00	199.00	4.40	4.30	154.00	5153	4	5	5	calm		200	200	3005		
4:12	58°16.652	00°52.722	191.00	190.00	4.50	4.60	155.00	5205	4	5	5	calm		200	200	3005		Change of course, eol 3005
4:22	58°16.296	00°53.655	95.00	100.00	4.60	4.30	154.00	5312	4	5	5	calm		200	200	3006		sol 3006
4:54	58°16.260	00°58.274	90.00	92.00	4.60	4.50	154.0	5701	4	5	5	calm		20	20	300		

							0							0	0	6		
5:19	58°16.256	01°01.995	90.00	95.00	4.70	4.40	150.0 0	6010	4	5	5	calm		20 0	20 0	300 6		
5:46	58°16.246	01°05.831	90.00	90.00	4.60	4.50	146.1 0	6324	4	5	5	calm		20 0	20 0	300 6		eol 3006, change of course
5:55	58°16.687	01°06.505	3.00	351.00	4.60	4.10	145.0 0	6433	4	5	5	calm		20 0	20 0	300 7		sol 3007
6:03	58°17.295	01°06.481	351.00	337.00	4.40	4.00	145.0 0	6530	4	5	5	calm		20 0	20 0	300 7		change of course; eol 3007
6:10	58°17.594	01°05.692	273.00	269.00	4.70	4.50	145.0 0	6618	4	5	5	calm		20 0	20 0	300 8		sol 3008
6:30	58°17.588	1°01.992	270.00	267.00	4.60	4.30	149.0 0	6939	4	5	5	calm		20 0	20 0	300 8		
7:48	58°17620	00°51.644	286.00	289.00	4.60	4.30	154.0 0	7802	4	5	5	calm		20 0	20 0	300 8		eol 3008
7:54	58°17.954	00°51.327	257.00	247.00	4.60	4.40	154.0 0	7862	4	5	5	calm		20 0	20 0	300 9		sol 3009
8:04	58°18.500	00°51.933	85.00	84.00	4.70	4.40	153.0 0	7984	4	5	5	calm		20 0	20 0	301 0		eol 3009, sol 3010
8:21								8020										survey stopped, streamer recovery
9:17								79										survey back in action
9:32	58°18.842	00°52.496	177.00	176.40	4.70	4.40	152.8 0	263	4	5	5	calm		20 0	20 0	301 1		sol 3011, strange circle during profile (end of circle FFN 371 -> real start of line)
9:52	58°18.549	00°54.965	89.00	83.80	4.60	4.50	153.0 0	493	4	5	5	calm		20 0	20 0	301 1		
10:12	58°18.594	00°57.865	89.00	84.00	4.50	4.20	153.0 0	735	4	5	5	calm		20 0	20 0	301 1		
10:32	58°18.641	01°00.785	88.00	82.60	4.40	4.10	151.0 0	984	4	5	5	calm		20 0	20 0	301 1		
10:37	58°18.645	01°01.430	98.00	101.00	4.40	4.20	151.0	1029	4	5	5	calm		20	20	301		eol 3011

							0							0	0	1		
10:46	58°18.193	01°01.381	228.00	235.00	4.40	3.90	151.00	1144	4	5	5	calm		200	200	3012		sol 3012
12:17	58°13.375	0°51.195	233.00	236.00	4.50	4.30	156.70	2238	4	5	5	calm		200	200	3012		eol 3012
12:25	58°13.323	0°51.090	159.00	158.00	4.40	4.10	158,5	2332	4	5	5	calm		200	200	3013		sol 3013
12:53	58°1.448	0°52.740	153.00	146.00	4.60	4.40	154.60	2673	4	5	5	calm		200	200	3013		eol 3013
13:06	58°11.641	0°53.945	27.00	20.50	4.60	4.30	156.20	2824	4	5	5	calm		200	200	3014		sol 3014
15:35	58°22.012	1°2.490	20.00	12.20	4.70	4.50	148.00	4604	4	5	5	calm		200	200	3014		eol 3014
15:43	58°22.432	1°02.021	277.00	273.10	4.30	4.30	146.70	4697	4	5	5	calm		200	200	3015		sol 3015
15:58	58°22.563	0°59.790	274.00	268.00	4.70	4.40	142.70	4880	4	5	5	calm		200	200	3015		eol 3015
16:05	58°22.261	0°59.148	193.00	192.00	4.60	4.50	145.60	4964	4	5	5	calm		200	200	3016		sol 3016
18:39	58°10.894	0°57.201	180.00	177.00	4.40	4.40	154.30	6813	4	5	5	calm		200	200	3016		eol 3016
18:46	58°10.602	0°57.956	95.00	104.00	4.50	4.40	153.10	6895	4	5	5	calm		200	200	3017		sol 3017
18:58	58°10,601	0°58,606	86.00	87,3	4.50	4.20	152.00	7036	4	5	5			200	200	3017		eol3017
19:07	58°11.090	01°00.091	353.00	347.20	4.50	4.20	154.00	7169	4	5	5			200	200	3018		sol 3018
21:28	58°21.488	0°56.783	347.00	342.00	4.80	4.50	149.60	8858	4	5	5			200	200	3018		eol3018, sol3019
21:35	58°21.729	0°56.063	255.00	253.00	4.60	4.30	148.00	8932	4	5	5			200	200	3019		eol3019
21:53	58°21.060	0°54.349	158.00	158.00	4.40	4.00	150.00	9156	4	5	5			200	200	3020		sol3020
0:12	58°11.611	1°002.693	170.00	166.10	4.50	4.20	150.00	10814	4	5	5	calm		200	200	3020		eol 3020
0:23	58°11.764	1°3.373	343.00	340.00	4.80	4.40	150.00	10952	4	5	5	calm		200	200	3021		sol 3021
1:17	58°15.651	1°1.560	325.00	322.00	4.90	4.70	151.7	11594	4	5	5	calm		20	20	302		eol 3021

							0							0	0	1		
1:17	58°15.651	1°1.560	325.00	322.00	4.90	4.70	151.70	11594	4	5	5	calm		200	200	3022		sol 3022
2:44	58°19.374	0°51.280	305.00	304.00	4.60	4.40	154.00	12640	4	5	5	calm		200	200	3022		eol 3022
2:53	58°19.126	0°50.353	192.00	188.00	4.50	4.20	155.00	12760	4	5	5	calm		200	200	3023		sol 3023
3:18	58°17.321	0°49.668	189.00	182.00	4.40	4.50	154.00	13040	4	5	5	calm		200	200	3023		eol 3023
3:26	58°16.954	0°50.188	91.00	92.00	4.50	4.40	154.00	13136	4	5	5	calm		200	200	3024		sol 3024
5:32	58°16.831	1°8.170	83.00	83.00	4.70	4.80	144.00	146140	4	5	5	calm		200	200	3024		eol 3024
5:47	58°17.495	1°07.615	283.00	274.00	4.40	4.10	148.00	14844	4	5	5	calm		200	200			kurz vor sol 3025, blubb platt, gun wird eingeholt
6:50	5818179	1°1.925	278.00	271.00	4.50	4.20	150.00	15595	4	5	5	calm		200	200			start survey, 15 min bis profil
7:10	58°18.106	00°59.336	213.00	208.00	4.30	4.00	151.00	15825	4	5	5	calm		200	200	3025		sol 3025
7:50	58°15.700	00°55.830	218.00	210.00	4.50	4.50	154.00	16318	4	5	5	calm		200	200	3025		eol 3025, keeping course for container work
8:50	58°15.328	00°57.817	353.00	354.00	4.40	4.40	153.00	17039	4	5	5	calm		200	200	3026		sol 3026
9:33	58°18.482	00°57.134	352.00	347.00	4.60	4.40	153.80	17551	4	5	5	calm		200	200	3026		eol 3026 - change of course
9:50	58°18.507	00°57.854	172.00	168.00	4.40	4.30	152.00	17757	4	5	5	calm		200	200	3027		sol 3027
10:34	58°15.361	00°58.641	175.00	178.00	4.50	4.30	152.00	18278	4	5	5	calm		200	200	3027		eol 3027
11:00	58°16.020	00°59.184	351.00	352.00	4.70	4.70	148.00	18562	4	5	5	calm		200	200	3028		sol 3028
11:16	58°16.725	0°59.007	352.00	354.30	4.60	4.30	154.00	18785	4	5	5	calm		200	200	3028		recognized, that one buoy is

																		missing/flat (last check was ca. 10:40)
11:40	58°18.515	0°58.090	352.00	347.00	4.50	4.10	152.30	19077	4	5	5	calm		200	200	3028		eol 3028
11:58	58°18.644	0°56.284	258.00	256.00	4.50	4.40	154.00	19282	4	5	5	calm		200	200			change of course
12:08	58°18.222	0°56.351	127.00	123.00	4.40	4.10	154.00	19400	4	5	5	calm		200	200	3029		sol 3029
12:53	58°16.025	1°1.281	119.00	108.00	4.50	4.30	151.00	19937	4	5	5	calm		200	200	3029		eol 3029
13:19	58°15.647	1°1.334	308.00	307.00	4.50	4.10	152.00	20246	4	5	5	calm		200	200	3030		sol 3030
14:15	58°18.207	0°55.044	317.00	316.00	4.50	4.30	153.00	20922	4	5	5	calm		200	200	3030		eol 3030, end of survey

GEOMAR
Helmholtz-Zentrum für Ozeanforschung Kiel

GEOMAR Reports

No.	Title
1	FS POSEIDON Fahrtbericht / Cruise Report POS421, 08. – 18.11.2011, Kiel - Las Palmas, Ed.: T.J. Müller, 26 pp, DOI: 10.3289/GEOMAR_REP_NS_1_2012
2	Nitrous Oxide Time Series Measurements off Peru – A Collaboration between SFB 754 and IMARPE –, Annual Report 2011, Eds.: Baustian, T., M. Graco, H.W. Bange, G. Flores, J. Ledesma, M. Sarmiento, V. Leon, C. Robles, O. Moron, 20 pp, DOI: 10.3289/GEOMAR_REP_NS_2_2012
3	FS POSEIDON Fahrtbericht / Cruise Report POS427 – Fluid emissions from mud volcanoes, cold seeps and fluid circulation at the Don-_Kuban deep sea fan (Kerch peninsula, Crimea, Black Sea) – 23.02. – 19.03.2012, Burgas, Bulgaria - Heraklion, Greece, Ed.: J. Bialas, 32 pp, DOI: 10.3289/GEOMAR_REP_NS_3_2012
4	RV CELTIC EXPLORER EUROFLEETS Cruise Report, CE12010 – ECO2@NorthSea, 20.07. – 06.08.2012, Bremerhaven – Hamburg, Eds.: P. Linke et al., 65 pp, DOI: 10.3289/GEOMAR_REP_NS_4_2012
5	RV PELAGIA Fahrtbericht / Cruise Report 64PE350/64PE351 – JEDDAH-TRANSECT -, 08.03. – 05.04.2012, Jeddah – Jeddah, 06.04 - 22.04.2012, Jeddah – Duba, Eds.: M. Schmidt, R. Al-Farawati, A. Al-Aidaroos, B. Kürten and the shipboard scientific party, 154 pp, DOI: 10.3289/GEOMAR_REP_NS_5_2013
6	RV SONNE Fahrtbericht / Cruise Report SO225 - MANIHIKI II Leg 2 The Manihiki Plateau - Origin, Structure and Effects of Oceanic Plateaus and Pleistocene Dynamic of the West Pacific Warm Water Pool, 19.11.2012 - 06.01.2013 Suva / Fiji – Auckland / New Zealand, Eds.: R. Werner, D. Nürnberg, and F. Hauff and the shipboard scientific party, 176 pp, DOI: 10.3289/GEOMAR_REP_NS_6_2013
7	RV SONNE Fahrtbericht / Cruise Report SO226 – CHRIMP CHatham RIse Methane Pockmarks, 07.01. - 06.02.2013 / Auckland – Lyttleton & 07.02. – 01.03.2013 / Lyttleton – Wellington, Eds.: Jörg Bialas / Ingo Klaucke / Jasmin Mögeltönder, 126 pp, DOI: 10.3289/GEOMAR_REP_NS_7_2013
8	The SUGAR Toolbox - A library of numerical algorithms and data for modelling of gas hydrate systems and marine environments, Eds.: Elke Kossel, Nikolaus Bigalke, Elena Piñero, Matthias Haeckel, 168 pp, DOI: 10.3289/GEOMAR_REP_NS_8_2013
9	RV ALKOR Fahrtbericht / Cruise Report AL412, 22.03.-08.04.2013, Kiel – Kiel. Eds: Peter Linke and the shipboard scientific party, 38 pp, DOI: 10.3289/GEOMAR_REP_NS_9_2013
10	Literaturrecherche, Aus- und Bewertung der Datenbasis zur Meerforelle (Salmo trutta trutta L.) Grundlage für ein Projekt zur Optimierung des Meerforellenmanagements in Schleswig-Holstein. Eds.: Christoph Petereit, Thorsten Reusch, Jan Dierking, Albrecht Hahn, 158 pp, DOI: 10.3289/GEOMAR_REP_NS_10_2013
11	RV SONNE Fahrtbericht / Cruise Report SO227 TAIFLUX, 02.04. – 02.05.2013, Kaohsiung – Kaohsiung (Taiwan), Christian Berndt, 105 pp, DOI: 10.3289/GEOMAR_REP_NS_11_2013
12	RV SONNE Fahrtbericht / Cruise Report SO218 SHIVA (Stratospheric Ozone: Halogens in a Varying Atmosphere), 15.-29.11.2011, Singapore - Manila, Philippines, Part 1: SO218- SHIVA Summary Report (in German), Part 2: SO218- SHIVA English reports of participating groups, Eds.: Birgit Quack & Kirstin Krüger, 119 pp, DOI: 10.3289/GEOMAR_REP_NS_12_2013
13	KIEL276 Time Series Data from Moored Current Meters. Madeira Abyssal Plain, 33°N, 22°W, 5285 m water depth, March 1980 – April 2011. Background Information and Data Compilation. Eds.: Thomas J. Müller and Joanna J. Waniek, 239 pp, DOI: 10.3289/GEOMAR_REP_NS_13_2013

GEOMAR
Helmholtz-Zentrum für Ozeanforschung Kiel

GEOMAR Reports

No.	Title
14	RV POSEIDON Fahrtbericht / Cruise Report POS457: ICELAND HAZARDS Volcanic Risks from Iceland and Climate Change:The Late Quaternary to Anthropogene Development Reykjavík / Iceland – Galway / Ireland, 7.-22. August 2013. Eds.: Reinhard Werner, Dirk Nürnberg and the shipboard scientific party, 88 pp, DOI: 10.3289/GEOMAR_REP_NS_14_2014
15	RV MARIA S. MERIAN Fahrtbericht / Cruise Report MSM-34 / 1 & 2, SUGAR Site, Varna – Varna, 06.12.13 – 16.01.14. Eds: Jörg Bialas, Ingo Klaucke, Matthias Haeckel, 111 pp, DOI: 10.3289/GEOMAR_REP_NS_15_2014
16	RV POSEIDON Fahrtbericht / Cruise Report POS 442, "AUVinTYS" High-resolution geological investigations of hydrothermal sites in the Tyrrhenian Sea using the AUV "Abyss", 31.10. – 09.11.12, Messina – Messina, Ed.: Sven Petersen, 32 pp, DOI: 10.3289/GEOMAR_REP_NS_16_2014
17	RV SONNE, Fahrtbericht / Cruise Report, SO 234/1, "SPACES": Science or the Assessment of Complex Earth System Processes, 22.06. – 06.07.2014, Walvis Bay / Namibia - Durban / South Africa, Eds.: Reinhard Werner and Hans-Joachim Wagner and the shipbord scientific party, 44 pp, DOI: 10.3289/GEOMAR_REP_NS_17_2014
18	RV POSEIDON Fahrtbericht / Cruise Report POS 453 & 458, "COMM3D", Crustal Structure and Ocean Mixing observed with 3D Seismic Measurements, 20.05. – 12.06.2013 (POS453), Galway, Ireland – Vigo, Portugal, 24.09. – 17.10.2013 (POS458), Vigo, Portugal – Vigo, Portugal, Eds.: Cord Papenberg and Dirk Klaeschen, 66 pp, DOI: 10.3289/GEOMAR_REP_NS_18_2014
19	RV POSEIDON, Fahrtbericht / Cruise Report, POS469, "PANAREA", 02. – 22.05.2014, (Bari, Italy – Malaga, Spain) & Panarea shallow-water diving campaign, 10. – 19.05.2014, Ed.: Peter Linke, 55 pp, DOI: 10.3289/GEOMAR_REP_NS_19_2014
20	RV SONNE Fahrtbericht / Cruise Report SO234-2, 08.-20.07.2014, Durban, -South Africa - Port Louis, Mauritius, Eds.: Kirstin Krüger, Birgit Quack and Christa Marandino, 95 pp, DOI: 10.3289/GEOMAR_REP_NS_20_2014
21	RV SONNE Fahrtbericht / Cruise Report SO235, 23.07.-07.08.2014, Port Louis, Mauritius to Malé, Maldives, Eds.: Kirstin Krüger, Birgit Quack and Christa Marandino, 76 pp, DOI: 10.3289/GEOMAR_REP_NS_21_2014
22	RV SONNE Fahrtbericht / Cruise Report SO233 WALVIS II, 14.05-21.06.2014, Cape Town, South Africa - Walvis Bay, Namibia, Eds.: Kaj Hoernle, Reinhard Werner, and Carsten Lüter, 153 pp, DOI: 10.3289/GEOMAR_REP_NS_22_2014
23	RV SONNE Fahrtbericht / Cruise Report SO237 Vema-TRANSIT Bathymetry of the Vema-Fracture Zone and Puerto Rico TRench and Abyssal AtlaNtic BiodiverSITy Study, Las Palmas (Spain) - Santo Domingo (Dom. Rep.) 14.12.14 - 26.01.15, Ed.: Colin W. Devey, 130 pp, DOI: 10.3289/GEOMAR_REP_NS_23_2015
24	RV POSEIDON Fahrtbericht / Cruise Report POS430, POS440, POS460 & POS467 Seismic Hazards to the Southwest of Portugal; POS430 - La-Seyne-sur-Mer - Portimao (7.4. - 14.4.2012), POS440 - Lisbon - Faro (12.10. - 19.10.2012), POS460 - Funchal - Portimao (5.10. - 14.10.2013), POS467 - Funchal - Portimao (21.3. - 27.3.2014), Ed.: Ingo Grevemeyer, 43 pp, DOI: 10.3289/GEOMAR_REP_NS_24_2015
25	RV SONNE Fahrtbericht / Cruise Report SO239, EcoResponse Assessing the Ecology, Connectivity and Resilience of Polymetallic Nodule Field Systems, Balboa (Panama) – Manzanillo (Mexico), 11.03. -30.04.2015, Eds.: Pedro Martínez Arbizu and Matthias Haeckel, 204 pp, DOI: 10.3289/GEOMAR_REP_NS_25_2015

GEOMAR
Helmholtz-Zentrum für Ozeanforschung Kiel

GEOMAR Reports

No.	Title
26	RV SONNE Fahrtbericht / Cruise Report SO242-1, JPI OCEANS Ecological Aspects of Deep-Sea Mining, DISCOL Revisited, Guayaquil - Guayaquil (Equador), 29.07.-25.08.2015, Ed.: Jens Greinert, 290 pp, DOI: 10.3289/GEOMAR_REP_NS_26_2015
27	RV SONNE Fahrtbericht / Cruise Report SO242-2, JPI OCEANS Ecological Aspects of Deep-Sea Mining DISCOL Revisited, Guayaquil - Guayaquil (Equador), 28.08.-01.10.2015, Ed.: Antje Boetius, 552 pp, DOI: 10.3289/GEOMAR_REP_NS_27_2015
28	RV POSEIDON Fahrtbericht / Cruise Report POS493, AUV DEDAVE Test Cruise, Las Palmas - Las Palmas (Spain), 26.01.-01.02.2016, Ed.: Klas Lackschewitz, 17 pp, DOI: 10.3289/GEOMAR_REP_NS_28_2016
29	Integrated German Indian Ocean Study (IGIOS) - From the seafloor to the atmosphere - A possible German contribution to the International Indian Ocean Expedition 2 (IIOE-2) programme – A Science Prospectus, Eds.: Bange, H.W. , E.P. Achterberg, W. Bach, C. Beier, C. Berndt, A. Biastoch, G. Bohrmann, R. Czeschel, M. Dengler, B. Gaye, K. Haase, H. Herrmann, J. Lelieveld, M. Mohtadi, T. Rixen, R. Schneider, U. Schwarz-Schampera, J. Segschneider, M. Visbeck, M. Voß, and J. Williams, 77pp, DOI: 10.3289/GEOMAR_REP_NS_29_2016
30	RV SONNE Fahrtbericht / Cruise Report SO249, BERING – Origin and Evolution of the Bering Sea: An Integrated Geochronological, Volcanological, Petrological and Geochemical Approach, Leg 1: Dutch Harbor (U.S.A.) - Petropavlovsk-Kamchatsky (Russia), 05.06.2016-15.07.2016, Leg 2: Petropavlovsk-Kamchatsky (Russia) - Tomakomai (Japan), 16.07.2016-14.08.2016, Eds.: Reinhard Werner, et al., DOI: 10.3289/GEOMAR_REP_NS_30_2016
31	RV POSEIDON Fahrtbericht/ Cruise Report POS494/2, HIERROSEIS Leg 2: Assessment of the Ongoing Magmatic-Hydrothermal Discharge of the El Hierro Submarine Volcano, Canary Islands by the Submersible JAGO, Valverde – Las Palmas (Spain), 07.02.-15.02.2016, Eds.: Hannington, M.D. and Shipboard Scientific Party, DOI: 10.3289/GEOMAR_REP_NS_31_2016
32	RV METEOR Fahrtbericht/ Cruise Report M127, Extended Version, Metal fluxes and Resource Potential at the Slow-spreading TAG Midocean Ridge Segment (26°N, MAR) – Blue Mining@Sea, Bridgetown (Barbados) – Ponta Delgada (Portugal) 25.05.-28.06.2016, Eds.: Petersen, S. and Shipboard Scientific Party, DOI: 10.3289/GEOMAR_REP_NS_32_2016
33	RV SONNE Fahrtbericht/Cruise Report SO244/1, GeoSEA: Geodetic Earthquake Observatory on the Seafloor, Antofagasta (Chile) – Antofagasta (Chile), 31.10.-24.11.2015, Eds.: Jan Behrmann, Ingo Klaucke, Michal Stipp, Jacob Geersen and Scientific Crew SO244/1, DOI: 10.3289/GEOMAR_REP_NS_33_2016
34	RV SONNE Fahrtbericht/Cruise Report SO244/2, GeoSEA: Geodetic Earthquake Observatory on the Seafloor, Antofagasta (Chile) – Antofagasta (Chile), 27.11.-13.12.2015, Eds.: Heidrun Kopp, Dietrich Lange, Katrin Hannemann, Anne Krabbenhoeft, Florian Petersen, Anina Timmermann and Scientific Crew SO244/2, DOI: 10.3289/GEOMAR_REP_NS_34_2016
35	RV SONNE Fahrtbericht/Cruise Report SO255, VITIAZ – The Life Cycle of the Vitiaz-Kermadec Arc / Backarc System: from Arc Initiation to Splitting and Backarc Basin Formation, Auckland (New Zealand) - Auckland (New Zealand), 02.03.-14.04.2017, Eds.: Kaj Hoernle, Folkmar Hauff, and Reinhard Werner with contributions from cruise participants, DOI: 10.3289/GEOMAR_REP_NS_35_2017

GEOMAR
Helmholtz-Zentrum für Ozeanforschung Kiel

GEOMAR Reports

No.	Title
36	RV POSEIDON Fahrtbericht/Cruise Report POS515, CALVADOS - CALabrian arc mud VolcAnoes: Deep Origin and internal Structure, Dubrovnik (Croatia) – Catania (Italy), 18.06.-13.07.2017, Eds.: M. Riedel, J. Bialas, A. Krabbenhoeft, V. Bähre, F. Beeck, O. Candoni, M. Kühn, S. Muff, J. Rindfleisch, N. Stange, DOI: 10.3289/GEOMAR_REP_NS_36_2017
37	RV MARIA S. MERIAN Fahrtbericht/Cruise Report MSM63, PERMO, Southampton – Southampton (U.K.), 29.04.-25.05.2017, Eds.: Christian Berndt and Judith Elger with contributions from cruise participants C. Böttner, R.Gehrmann, J. Karstens, S. Muff, B. Pitcairn, B. Schramm, A. Lichtschlag, A.-M. Völsch, DOI: 10.3289/GEOMAR_REP_NS_37_2017

For GEOMAR Reports, please visit:
https://oceanrep.geomar.de/view/series/GEOMAR_Report.html

Reports of the former IFM-GEOMAR series can be found under:
https://oceanrep.geomar.de/view/series/IFM-GEOMAR_Report.html

GEOMAR
Helmholtz-Zentrum für Ozeanforschung Kiel

Das GEOMAR Helmholtz-Zentrum für Ozeanforschung Kiel ist Mitglied der Helmholtz-Gemeinschaft Deutscher Forschungszentren e.V.

The GEOMAR Helmholtz Centre for Ocean Research Kiel is a member of the Helmholtz Association of German Research Centres

Helmholtz-Zentrum für Ozeanforschung Kiel / Helmholtz Centre for Ocean Research Kiel
GEOMAR
Dienstgebäude Westufer / West Shore Building
Düsternbrooker Weg 20
D-24105 Kiel
Germany

Helmholtz-Zentrum für Ozeanforschung Kiel / Helmholtz Centre for Ocean Research Kiel
GEOMAR
Dienstgebäude Ostufer / East Shore Building
Wischhofstr. 1-3
D-24148 Kiel
Germany

Tel.: +49 431 600-0
Fax: +49 431 600-2805
www.geomar.de